PB82-227695

# Smog Chamber Experiments to Test Oxidant Related Control Strategy Issues

North Carolina Univ. at Chapel Hill

Prepared for

Environmental Sciences Research Lab.
Research Triangle Park, NC

Mar 82

U.S. Department of Commerce
National Technical Information Service
NTIS

BEGIN FIRST LINE OF TEXT HERE
CENTER OF PAGE
TOP OF IMAGE AREA

EPA-600/3-82-014
March 1982

PB82-227695

DROPPED HEAD, BEGIN SECTIONS HERE

# SMOG CHAMBER EXPERIMENTS TO TEST OXIDANT RELATED CONTROL STRATEGY ISSUES

by

R.M. Kamens
H.E. Jeffries
K.G. Sexton
A.A. Gerhardt

Department of Environmental Sciences and Engineering
School of Public Health
University of North Carolina
Chapel Hill, North Carolina 27514

8 1/2"
9 1/8"

Cooperative Agreement 805726

Project Officer

Bruce Gay, Jr.
Gas Kinetics and Photochemistry Branch
Environmental Sciences Research Laboratory
Research Triangle Park, North Carolina 27711

ENVIRONMENTAL SCIENCES RESEARCH LABORATORY
OFFICE OF RESEARCH AND DEVELOPMENT
U.S. ENVIRONMENTAL PROTECTION AGENCY
RESEARCH TRIANGLE PARK, NORTH CAROLINA 27711

REPRODUCED BY
NATIONAL TECHNICAL
INFORMATION SERVICE
U.S. DEPARTMENT OF COMMERCE
SPRINGFIELD, VA. 22161

BEGIN LAST LINE OF TEXT
3/8"
BOTTOM OF IMAGE AREA; OUTSIDE DIMENSION FOR TABLES AND ILLUSTRATIONS
EPA Form 2350-4 (4-80)
(PREVIOUSLY CIN. EPA FORM 287)
TYPING GUIDE SHEET

## TECHNICAL REPORT DATA

*(Please read Instructions on the reverse before completing)*

| | | |
|---|---|---|
| 1. REPORT NO.<br>EPA-600/3-82-014 | 2.<br>ORD Report | 3. RECIPIENT'S ACCESSION NO.<br>PB82 227695 |
| 4. TITLE AND SUBTITLE<br>SMOG CHAMBER EXPERIMENTS TO TEST OXIDANT RELATED CONTROL STRATEGY ISSUES | | 5. REPORT DATE<br>March 1982 |
| | | 6. PERFORMING ORGANIZATION CODE |
| 7. AUTHOR(S)<br>R. M. Kamens, H. E. Jeffries, K. G. Sexton, and A. A. Gerhardt | | 8. PERFORMING ORGANIZATION REPORT NO. |
| 9. PERFORMING ORGANIZATION NAME AND ADDRESS<br>Department of Environmental Sciences and Engineering<br>School of Public Health<br>University of North Carolina<br>Chapel Hill, North Carolina 27514 | | 10. PROGRAM ELEMENT NO.<br>CDWA1A/01-0292 (FY-82) |
| | | 11. CONTRACT/GRANT NO.<br>CR-805726 |
| 12. SPONSORING AGENCY NAME AND ADDRESS<br>Environmental Sciences Research Laboratory-RTP, NC<br>Office of Research and Monitoring<br>U.S. Environmental Protection Agency<br>Research Triangle Park, North Carolina 27711 | | 13. TYPE OF REPORT AND PERIOD COVERED<br>Final 1978-1981 |
| | | 14. SPONSORING AGENCY CODE<br>EPA/600/09 |

15. SUPPLEMENTARY NOTES

16. ABSTRACT

Outdoor smog chamber experiments were performed to address various issues relating to ozone ($O_3$) production and oxidant control strategies. Dilute day old smog can substantially increase maximum $O_3$ yields from fresh urban type smog chamber systems. $O_3$ production from summer smog chamber systems can be reduced by at least 75% in winter conditions, with temperatures below 51-58°F. A temperature cut off below which $O_3$ will be less than some target value is different for each set of initial hydrocarbon and $NO_x$ concentrations. Temperature effects on single hydrocarbon-$NO_x$ systems were studied. Propylene-$NO_x$ systems were modeled with particular attention to peroxynitric acid chemistry. Experimental results of carbon substitution strongly suggest that substitution at the 20% level does not greatly affect the overall reactivity of an urban hydrocarbon mixture. A significant portion of the products from alpha-pinene and $O_3$ can appear in the condensed phase, particles form in the lower size ranges and grow into the optical range (i.e., greater than 0.3-0.5 μm). Dark isoprene-$O_3$ systems also appear to form homogeneously nucleated aerosol but less than 1% of the reacted isoprene is observed in the condensed phase. Mechanisms were developed to model the $O_3$ reactions with the two major isoprene daughter products, methylvinylketone and methacrolein. Chamber systems with isoprene and $O_3$ were also modeled.

17. KEY WORDS AND DOCUMENT ANALYSIS

| a. DESCRIPTORS | b. IDENTIFIERS/OPEN ENDED TERMS | c. COSATI Field/Group |
|---|---|---|
| | | |

| | | |
|---|---|---|
| 18. DISTRIBUTION STATEMENT<br>RELEASE TO PUBLIC | 19. SECURITY CLASS *(This Report)*<br>UNCLASSIFIED | 21. NO. OF PAGES<br>240 |
| | 20. SECURITY CLASS *(This page)*<br>UNCLASSIFIED | 22. PRICE |

EPA Form 2220-1 (Rev. 4-77) PREVIOUS EDITION IS OBSOLETE

NOTICE

THIS DOCUMENT HAS BEEN REPRODUCED FROM THE BEST COPY FURNISHED US BY THE SPONSORING AGENCY. ALTHOUGH IT IS RECOGNIZED THAT CERTAIN PORTIONS ARE ILLEGIBLE, IT IS BEING RELEASED IN THE INTEREST OF MAKING AVAILABLE AS MUCH INFORMATION AS POSSIBLE.

# DISCLAIMER

This report has been reviewed by the Environmental Sciences Research Laboratory, U.S. Environmental Protection Agency, and approved for publication. Approval does not signify that the contents necessarily reflect the views and policies of the U.S. Environmental Protection Agency, nor does mention of trade names or commercial products constitute endorsement or recommendation for use.

# ABSTRACT

Outdoor smog chamber experiments were performed to address various issues relating to ozone ($O_3$) production and oxidant control strategies. Dilute day old smog can substantially increase maximum $O_3$ yields from fresh urban type smog chamber systems. $O_3$ production from summer smog chamber systems can be reduced by at least 75% in winter conditions, with temperatures below 51-58$^{o}$F. A temperature cut off below which $O_3$ will be less than some target value is different for each set of initial hydrocarbon and $NO_x$ concentrations. Temperature effects on single hydrocarbon-$NO_x$ systems were studied. Propylene-$NO_x$ systems were modeled with particular attention to peroxynitric acid chemistry. Experimental results of carbon substitution strongly suggest that substitution at the 20% level does not greatly affect the overall reactivity of an urban hydrocarbon mixture.

A significant portion of the products from α-pinene and $O_3$ can appear in the condensed phase, particles form in the lower size ranges and grow into the optical range (i.e., >0.3-0.5 μm). Dark isoprene-$O_3$ systems also appear to form homogeneously nucleated aerosol but less than 1% of the reacted isoprene is observed in the condensed phase. Mechanisms were developed to model the $O_3$ reactions with the two major isoprene daughter products, methylvinylketone and methacrolein. Chamber systems with isoprene and $O_3$ were also modeled.

BEGIN FIRST LINE OF TEXT HERE
TYPING GUIDE SHEET
CENTER OF PAGE
TOP OF IMAGE AREA
DROPPED HEAD; BEGIN SECTIONS HERE

## CONTENTS

Abstract---------------------------------------------------------------- iii
List of Figures--------------------------------------------------------- vi
List of Tables---------------------------------------------------------- xiii
Acknowledgment---------------------------------------------------------- xv

1. Introduction-------------------------------------------------------- 1
2. Summary and Conclusions--------------------------------------------- 2
3. Recommendations----------------------------------------------------- 6
4. Effects of Day-old Dilute Smog on Fresh Smog Systems---------------- 8
5. Seasonal Effects on $O_3$ Production------------------------------- 24
    - For Complex Mixtures of Hydrocarbons and $NO_x$---------------- 24
    - For Single Hydrocarbon and $NO_x$ Mixtures--------------------- 37
6. Biogenic Hydrocarbon Studies--------------------------------------- 60
    - Impact of α-Pinene on Urban Smog Formation--------------------- 61
    - Ozone Isoprene Reactions, Product Formation and Aerosol Potential--------- 75
7. Changes in Initial $NO_x$ and Hydrocarbon Composition and Its Effects on $O_3$ Production--------- 96
    - Different Percentages of Starting $NO_2$----------------------- 96
    - Effect of Initial Aldehydes------------------------------------ 101
    - Addition of Propane and Butane to Reactive Smog Systems-------- 108
    - Preliminary Auto-Exhaust Experiments--------------------------- 109
    - Propylene/Butane Mixture--------------------------------------- 113
    - Hydrocarbon Substitution as a Means to Control $O_3$---------- 117
8. Other Selected Studies and Comparisons----------------------------- 123
    - Effect of Dynamic Operating Conditions on $O_3$ Formation----- 123
    - Comparison Between UNC and RTI Outdoor Chambers--------------- 126
    - Selected Chamber Characterization Results--------------------- 131
    - Characterization of Selected Single Hydrocarbon-$NO_x$ Chamber Runs for Modeling Studies--------- 142
9. Description of Measurement Techniques Implemented During This Project--------- 155

References-------------------------------------------------------------- 184

Appendices

A. Chamber and Facility Description
B. Computer Simulation of Chemical Mechanisms
C. Water Effect Experiments
D. Reproducibility of Two UNC Chambers

BOTTOM OF IMAGE AREA; OUTSIDE DIMENSION FOR TABLES AND ILLUSTRATIONS
BEGIN LAST LINE OF TEXT
3/8"

**Preceding page blank**

PAGE NUMBER
EPA-287 (Cin.)
(4-76)

BEGIN FIRST LINE OF TEXT HERE
TYPING GUIDE SHEET
CENTER OF PAGE
TOP OF IMAGE AREA
DROPPED HEAD. BEGIN SECTIONS HERE

# LIST OF FIGURES

Page

1. Two different schemata for the second day injection of fresh materials on dilute aged smog ---------------------------------- 11

2a. Effect of residual dilute smog on second day of an urban system: matched injection case. September 7, 1978 ------------ 15

2b. Effect of residual dilute smog on second day of an urban system: balanced initial conditions case. July 18, 1978 ------ 15

3. Comparision of NO, $NO_2$, and $O_3$ profiles in urban mix with (——) and without (---) additional added acetaldehyde (10% of initial NMHC). September 24, 1976 -------------------------- 18

4. Effect of injecting fresh mix and $NO_2$ to test chamber artifacts. June 18, 1979 ---------------------------------------- 18

5. Effect of air temperature at maximum nitric oxide disappearance for clear days for November 1973 and initial conditions of 0.20 ppm $NO_x$, 0.04 ppm $NO_2$ and 0.80 ppmC urban hydrocarbon mix in UNC outdoor smog chamber -------------- 26

6. Differential percentage $NO_2$ run under clear sky. Initial conditions: $NO_x$ (——) 0.364, (---) 0.366 ppm; $NO_2$ (——), 0.151, (---) 0.079 ppm; NMHC (——) 3.40, (---) 3.20 ppmC urban hydrocarbon mix in UNC outdoor smog chamber -------------- 28

7. Theoretical solar radiation on a horizontal surface as a function of month. Numbers correspond to month -------------- 28

8. Experimental data for a two day late fall run; 2.9 ppmC mix in Red plus 0.3 ppmC acetaldehyde; 2.1 ppmC mix in Blue plus 0.21 ppmC acetaldehyde ----------------------------------- 34

9. Maximum ozone as a function of the average of initial and maximum chamber air temperature for two ranges of initial propylene concentrations at approximately 0.5 ppm $NO_x$ ---------- 40

10. Maximum ozone as a function of the average of initial and maximum chamber air temperature for three ranges of initial propylene concentrations at approximately 0.5 ppm $NO_x$ ---------- 40

BEGIN LAST LINE OF TEXT
BOTTOM OF IMAGE AREA, OUTSIDE DIMENSION FOR TABLES AND ILLUSTRATIONS
3/8"

PAGE NUMBER
EPA-287 (Cin.)
(4-76)

TYPING GUIDE SHEET

Page

11a. Experimental data for October 22, 1977 ---------- 42

11b. Comparison of propylene/NO$_x$ experiments (3.8 ppmC $C_3H_6$, 0.5 ppm NO$_x$, 20% $NO_2$). October 22, 1977 (——) initial to max temperature: 35.8 to 70.2°F; January 28, 1978 (---) initial to max temperature: 18.8 to 40.1°F ---------- 43

11c. Comparison of three propylene/NO$_x$ runs with initial conditions: 3.8 ppmC propylene, 0.50 ppm NO$_x$, 20% $NO_2$. Temperature ranges: October 22, 1977, 35-70°F (——); January 28, 1978, 18-40°F (---), January 29, 1978, 8-34°F (···), January curves shifted to left to align sunrise times ---------- 43

12. Total solar radiation profiles for a fall and two winter days --- 44

13. Chamber air temperature for propylene/NO$_x$ runs ---------- 44

14. Comparison of two ethylene/NO$_x$ runs with similar initial conditions: October 18, 1977 (——): 3.84 ppmC $C_2H_4$, 0.486 ppm $NO_2$: initial T, 28.4°F; maximum T, 69.4°F; sunrise, 0730h EST; January 11, 1978 (— —): 3.8 ppmC $C_2H_4$, 0.468 ppm NO$_x$; initial T, 8.8°F; maximum T, 37.1°F; sunrise 0.830h EST. January 11 curves shifted to left to align sunrise time ---------- 46

15. Comparison of two acetaldehyde/NO$_x$ runs with initial conditions: May 18, 1977 (——): 1.87 ppmC RCHO, 0.350 ppm NO$_x$, 0.072 ppm $NO_2$; February 27, 1978 (···): 1.72 ppmC RCHO, 0.360 ppm NO$_x$, 0.087 ppm $NO_2$. May 18 temperature (69-96°F), February 22 temperature (16-49°F) ---------- 46

16a. Experimental data from August 8 and October 22, 1977 ---------- 52

16b. Experimental data from October 21, January 28, and January 29, 1978 ---------- 53

17a. Computer simulations of August 8, 1977 experiment with formation rate constant of PNA at 1,750 and 9,000 ppm$^{-1}$min$^{-1}$. Smog chamber profiles also shown (---) ---------- 54

17b. Computer simulations of October 22, 1977 experiment with formation rate constant of PNA at 1,750, 8,000, and 9,000 ppm$^{-1}$min$^{-1}$. Smog chamber profiles also shown (---) ---------- 54

18. Water effect experiments. Unless otherwise indicated, (---) represents UNC smog chamber data, (——) represents model ---------- 59

19. Effect of α-pinene carbon replacement in an urban-like hydrocarbon mix-NO$_x$ system ---------- 64

EPA-287 (Cin.)
(4-76)

TYPING GUIDE SHEET
BEGIN FIRST LINE OF TEXT HERE
CENTER OF PAGE
TOP OF IMAGE AREA
DROPPED HEAD; BEGIN SECTIONS HERE

Page

20. Effect of α-pinene carbon replacement in an urban-like hydrocarbon mix-$NO_x$ system ---------- 65

21. Effect of first reacting α-pinene and $O_3$ in matched carbon-$NO_x$ systems ---------- 68

22. Dark reaction between $O_3$ and α-pinene and resultant total aerosol number traces ---------- 70

23. EAA three-dimensional number, surface and volume plots from the reaction between 2.75 ppmC α-pinene and 0.5 ppm $O_3$, December 19, 1979 ---------- 72

24a. Reaction of isoprene and ozone on the night of October 8, 1980. Experimental data. (Temperature was approximately 65°F) ------- 79

24b. Condensation nuclei trace from a 4.90 ppmC isoprene + 0.74 ppm $O_3$ dark reaction in the UNC outdoor smog chamber ---------- 79

25a. Electrical aerosol analyzer number distribution vs. time for October 19, 1980 dark phase reaction between isoprene and ozone ---------- 80

25b. Electrical aerosol analyzer and optical particle counter total volume data for October 19, 1980 dark phase reaction between isoprene and ozone ---------- 80

26. Condensation nuclei traces for experiments of October 22 and November 1, 1980 ---------- 82

27. Dodge-Arnts chemical reaction scheme for ozone reaction with propylene ---------- 83

28. Reaction scheme for ozone reaction with methylvinylketone ----- 83

29a. UNC model of $O_3$ and MVK for November 3, 1980. 0.93 ppmV MVK slug injected at 2025 hr.; $O_3$ ramp injected (0.22 ppm/hr) at 2055. Experimental data(o o o) Model results(——)------------ 86

29b. UNC model of $O_3$ and MACR for November 3, 1980. 0.90 ppmV MACR slug injected at 1948 hr.; $O_3$ ramp injected (0.21 ppm/hr) at 2018. Experimental data(o o o) Model results(——)------------ 86

30. UNC model of $O_3$ and isoprene for November 8, 1980. 0.89 ppmV isoprene slug injected at 2000 hr.; $O_3$ ramp injected (0.46 ppm/hr) at 2020. Experimental data(o o o) Model results(——)-- 93

31. UNC model of $O_3$ and isoprene for Novmeber 9, 1980. 0.98 ppmV isoprene slug injected at 1935 hr.; $O_3$ ramp injected (0.52 ppm/hr) at 2012. Experimental data (o o o) Model results(——)--- 93

BEGIN LAST LINE OF TEXT
BOTTOM OF IMAGE AREA; OUTSIDE DIMENSION FOR TABLES AND ILLUSTRATIONS
9-1/8"
3/8"

EPA-287 (Cin.)
(4-76)

BEGIN FIRST LINE OF TEXT HERE
TYPING GUIDE SHEET
CENTER OF PAGE
TOP OF IMAGE AREA
DROPPED HEAD; BEGIN SECTIONS HERE

Page

32. Formaldehyde, carbon monoxide, and methylglyoxal product yields from October 8 and October 9, 1980 isoprene and $O_3$ experiments. Experimental data (o o o) Model results (——) -------- 94

33. Matched mix-$NO_x$ experiment with different starting percentages of $NO_2$. See Table 18 for initial conditions ----------- 99

34. Matched mix-$NO_x$ experiments with one side receiving an $O_3$ injection. See Table 19 for initial conditions ---------------- 100

35. Effect of initial aldehydes on matched mix systems. Initial conditions in Table 20 ---------------------------------- 106

36. Effect 30% extra propane carbon on urban type smog chamber systems. Initial concentrations in Table 21 ------------------- 110

37. Effect of 30% extra butane carbon on urban smog chamber systems. Initial conditions in Table 22 ---------------------- 111

38. Comparison of NO, $NO_2$ and $O_3$ profiles in dual run using auto exhaust as NMHC (——) and UNC urban mix as NMHC (---). Initial conditions: (——), $NO_x$: 0.34 ppm; NMHC: 3.1 ppmC; (---), $NO_x$: 0.33 ppm, NMHC: 3.1 ppmC -------------------------- 114

39. Experimental data for mix, auto-mix run. Initial HC: (——) 2.0 ppmC mix (auto-mix); (69% paraffin; 31% olefin). (---) 2.0 ppmC UNC mix (70% paraffin, 30% olefin) -------------------------------------------------------- 114

40. Comparisons between UNC mix and 75/25 propylene/butane mixture ------------------------------------------------------ 119

41. Experimental data for mix (with Sydney Solvent), mix-cellosolve run. Initial HC: (——) 1.12 ppmC mix, 70.7% paraffins, 29.2% olefin with 0.48 ppmC Sydney Solvent, 0.00 ppmC cellosolve mix; (---) 1.12 ppmC mix, 70.7% paraffins, 29.2% olefine with 0.24 ppmC Sydney Solvent, 0.035 ppmC cellosolve, 0.035 ppmC b-cellosolve ------------------------------------------------- 122

42. Total solar radiation and temperature data for August 14, 1979 -- 122

43. Static (——) and ramp injection (--) dual run in UNC outdoor smog chamber. Initial conditions at 0545 in static side (——): NO, 0.29 ppm; $NO_2$, 0.07 ppm; n-$C_4H_{10}$, 0.60 ppmC, 0.40 ppmC. Ramp side (--) would achieve: NO, 036 ppm; n-$C_4H_{10}$, 0.60 ppmC; $C_3H_6$, 0.40 ppmC at 1800 hours if reaction occurred ------------- 124

IMAGE AREA: OUTSIDE DIMENSION FOR TABLES AND ILLUSTRATIONS
BEGIN LAST LINE OF TEXT
3/8"

PAGE NUMBER
EPA-287 (Cin.)
(4-76)

TYPING GUIDE SHEET
BEGIN FIRST LINE OF TEXT HERE
CENTER OF PAGE
TOP OF IMAGE AREA
DROPPED HEAD; BEGIN SECTIONS HERE

Page

44. Static (——) and ramp (--) injection dual run in UNC outdoor smog chamber. Initial conditions at 0540 in static side: NO, 0.151 ppm; $NO_2$, 0.072 ppm; 1.93 ppmC urban hydrocarbon mix. Ramp side (--) would achieve: NO, 0.22 ppm, 1.93 ppmC urban hydrocarbon mix at 1800 hours if no reaction occurred ---- 124

45. Static (——) and ramp injection (0600-0900) with 50% dilution (0900-1200) and continued ramp injection (0900-1200) at rate equal to mass removal by dilution if no reaction (--). Initial conditions in static side: NO, 0.31 ppm; $NO_2$, 0.05 ppm; urban hydrocarbon mix, 4.56 ppmC. An initial condition of 0.05 ppm NO was established in ramp side (--). NO and NMHC injected in (--) so as to achieve same condition at 0900 ---------------------------------------------------------------- 127

46. Selected hydrocarbon compounds in urban hydrocarbon mix for static (——) and ramp injection (--) dual run in UNC outdoor smog chamber ---------------------------------------------------- 127

47. Selected hydrocarbon compounds in urban hydrocarbon mix for static (——) and ramp injection (--) dual run in UNC outdoor smog chamber ---------------------------------------------------- 128

48. Solar radiation for August 30, 1975 ---------------------------- 128

49. NO, $NO_2$ and $O_3$ profiles in matched dual propane run in UNC outdoor chamber. See Table 27 for initial conditions ---------- 130

50. NO, $NO_2$ and $O_3$ profiles in matched propane run in RTI outdoor chamber. See Table 27 for initial conditions ---------- 130

51. NO, $NO_2$ and $O_3$ profiles in matched propane runs in RTI outdoor chambers. See Table 27 for initial conditions --------- 130

52. Wall moisture effects on gas phase formaldehyde systems -------- 132

53a. 1979 UNC formaldehyde-$NO_x$ runs. 1979 TSR data are low by as much as 45% at the peak and another year's profile should be used to model these data ------------------------------------ 134

53b. UNC 1979 formaldehyde-$NO_x$ runs -------------------------------- 135

54. Mean $NO_2$ morning bleed (ppm) of all runs with morning $NO_2$ bleed broken down by cloud cover, humidity and temperature. Number of cases indicated in numbers over boxes ---------------------- 137

55. Estimated equilibrium profiles for $NO_x$ species versus aerosol activity ---------------------------------------------- 139

BEGIN LAST LINE OF TEXT
BOTTOM OF IMAGE AREA; OUTSIDE DIMENSION FOR TABLES AND ILLUSTRATIONS
3/8"

EPA-287 (Cin.)
(4-76)

BEGIN FIRST LINE OF TEXT HERE
TYPING GUIDE SHEET
CENTER OF PAGE
TOP OF IMAGE AREA
DROPPED HEAD; BEGIN SECTIONS HERE

Page

56. Molybedenum catalyst-chemiluminescence method for $HNO_3$ recording showing $HNO_3$ and $NO_2$ appearing on second day of a three day ethylene/$NO_x$ run ---------------------------------- 141

57. August 8, 1977, 1.5 ppmC propylene and 0.5 ppm $NO_x$ run -------- 143

58. Product, nitrogen, and carbon balance for October 8, 1977, 1.5 ppmC propylene, 0.5 ppm $NO_x$ run -------------------------- 145

59a. Experimental data for October 22, 1977 ----------------------- 146

59b. Nitrogen and carbon balances for October 22, 1977 propylene $NO_x$ run ---------------------------------------------------- 148

60. Similar propylene runs (~3.6 ppmC) conducted one year apart in UNC chamber, October 22, 1977 and October 21, 1978 --------- 149

61. Data for July 18, 1977 aldehyde-$NO_x$ smog experiment ----------- 151

62. Smog chamber data for June 3, 1977 matched propylene/$NO_x$ run in which one side had an additional injection of 0.6 ppm formaldehyde ---------------------------------------- 153

63. Effect of extra acetaldehyde on a propylene/$NO_x$ chamber run --- 154

64. Column and valve configurations for $C_1$-$C_{10}$ automatic Carle chromatograph ----------------------------------------- 157

65. Chromatogram of UNC urban type hydrocarbon mixture on Carle 211 chromatograph -------------------------------------- 158

66. Maximum sensitivity of Carle chromatograph on attenuation of X1 and gain of 2 ------------------------------- 160

67. Response of Carle 211 GC with methanizer to 1.2 ppm formaldehyde and zero air with 1.5 ppm methane. oven=73°C, HE=67 cc/min, $H_2$-80 cc/min, recorder 1 mV fs, atten.=x1, range=x1, col 1=11 ft, 1/8" ss porpack Q, 40:60 mesh, col 2=2 ft, 1/8" porpack Q, 40:60 mesh ----------------------- 162

68. Solution flow diagram for CEA automated formaldehyde instrument ---------------------------------------------------- 164

69. Response of CEA auto formaldehyde instrument to 0.5 and 1.2 ppm of HCOH injected in dry UNC chambers on August 4, 1979 and August 5, 1979 ---------------------------------------------- 165

70. An example of the response of the HPLC with DNPH method ------- 168

BEGIN LAST LINE OF TEXT
BOTTOM OF IMAGE AREA, OUTSIDE DIMENSION FOR TABLES AND ILLUSTRATIONS
9-1/8"
3/8"

PAGE NUMBER
EPA-287 (Cin.)
(4-76)

BEGIN FIRST LINE OF TEXT HERE
TYPING GUIDE SHEET
CENTER OF PAGE
TOP OF IMAGE AREA
DROPPED HEAD: BEGIN SECTIONS HERE

Page

71. Response of two UNC electron capture detectors to 0.12 ppmv PAN May 1978 ---------- 170

72. Detection of alkylnitrates with automated PAN GC, Varian 940 ECD. $N_2$ flow = 5 cc/min, oven and detector at 24°C standing current on $32x10^{-9}$ amps = 01% of full scale, chart = .1"/min, atten. = $x32x10^{-10}$ amps ---------- 173

73. Schematics of Mast electrochemical cell and configuration of entire microcoulombmetric instrument for measurement of gaseous $HNO_3$ ---------- 174

74. Example of signal trace from modified Mast microcoulombmetric method for gaseous $HNO_3$ monitoring ---------- 176

75. Example of signal trace from molybdenum catalyst chemiluminescence method for gaseous $HNO_3$ monitoring ---------- 178

76. Schematic of gaseous $HNO_3$ generator ---------- 180

77. Calibration curve for Spicer method of $HNO_3$ analysis ---------- 181

78. Response of $H_2O_2$ instrument to standard concentrations of $H_2O_2$ in dry air ---------- 183

BEGIN LAST LINE OF TEXT
BOTTOM OF IMAGE AREA OUTSIDE DIMENSION FOR TABLES AND ILLUSTRATIONS
3/8"

PAGE NUMBER
EPA-287 (Cin.)
(4-76)

BEGIN FIRST LINE OF TEXT HERE
TYPING GUIDE SHEET
CENTER OF PAGE
TOP OF IMAGE AREA
DROPPED HEAD: BEGIN SECTIONS HERE

## LIST OF TABLES

Page

1. 1979 UNC Simulated Urban Hydrocarbon Mix ---------- 9
2. Effects of Day-old Material on Ozone in Matched Injection Runs ---------- 13
3. Effects of Day-old Material on Ozone in Balanced Initial Conditions Runs ---------- 14
4. Carbon Balance at Various Times During Two Day Runs with Dilute Aged Smog ---------- 17
5. Comparison of Starting Materials for July 18, 1978 ---------- 19
6. Effects of Air Temperature on Ozone Production in Static Outdoor Chamber Runs with the Same Initial Conditions (0.8 ppmC Urban Hydrocarbon Mix, 0.20 ppm $NO_x$, and 0.04 ppm $NO_2$) ---------- 26
7. Effects of Acetaldehyde on Maximum $O_3$ Yield in Matched Dual Runs ---------- 29
8. Maximum Daily Temperature and Ozone Concentration for Two Sets of Similar Initial Conditions ---------- 30
9. Pairwise Comparison of Maximum $O_3$ Production for Winter and Summer Runs with Similar Initial Conditions of Reactants ---------- 32
10. Summary of Initial Conditions, Maximum Temperature, and Maximum Ozone for Two and Three Day Winter Outdoor Chamber Runs ---------- 36
11. Selected Propylene Runs with Clear Sky Conditions ---------- 38
12. Selected Ethylene Runs ---------- 39
13. Critical Data for Humid vs. Dry Runs ---------- 58
14. α-pinene and Urban Mix Experiments UNC Dual Smog Chamber Runs ---------- 63
15. Major Products from a 4.90 ppmC Isoprene and 0.74 Ramp Injected $O_3$ System after 4 Hours of Reaction ---------- 78

6-1/2"
BOTTOM OF IMAGE AREA; OUTSIDE DIMENSION FOR TABLES AND ILLUSTRATIONS
BEGIN LAST LINE OF TEXT
3/8"
PAGE NUMBER
EPA-287 (Cin.)
(6-78)

TYPING GUIDE SHEET
BEGIN FIRST LINE OF TEXT HERE
CENTER OF PAGE
TOP OF IMAGE AREA
DROPPED HEAD; BEGIN SECTIONS HERE

Page

16. Mechanism for Dark Phase Methylvinylketone and Ozone System ---- 85

17. Mechanism for Dark Phase Isoprene and Ozone System ------------ 92

18. Effect of Initial $NO_2$-to-$NO_x$ Ratio Maximum Ozone in UNC Urban Hydrocarbon Mix Runs ---------------------------------------- 98

19. Effect of Adding $O_3$ Initially on Maximum $O_3$ in UNC Urban Hydrocarbon Mix Runs ------------------------------------------- 98

20. Effects of Acetaldehyde on Maximum $O_3$ Yield in Matched Dual Runs ------------------------------------------------- 105

21. Effect of Additional Initial Propane on Maximum Ozone in UNC Urban Hydrocarbon Mix Runs -------------------------------- 112

22. Effect of Additional Initial Butane on Maximum Ozone in UNC Urban Hydrocarbon Mix Runs -------------------------------- 113

23. Comparison of BOM Auto Exhaust Composition with UNC Auto Exhaust and UNC Urban Mix Composition ------------------------ 115

24. UNC Mix and BOM Mix Composition -------------------------------- 116

25. Comparison of Ozone Reactivity of 25% Propylene and 75% n-butane Mixture to that of the UNC Urban Mix ----------------- 118

26. Composition of "Sydney Solvent" ------------------------------- 121

27. Ozone Formation in Static and Ramp Injected Outdoor Smog Chamber Experiments ------------------------------------------- 125

28. Summary Data September 20-22, 1976, Joint RTI & UNC Propane $NO_x$ Run ------------------------------------------------------ 129

BEGIN LAST LINE OF TEXT
BOTTOM OF IMAGE AREA; OUTSIDE DIMENSION FOR TABLES AND ILLUSTRATIONS
3/8"

PAGE NUMBER
EPA-287 (Cin.)
(4-76)

TYPING GUIDE SHEET
BEGIN FIRST LINE OF TEXT HERE
CENTER OF PAGE
TOP OF IMAGE AREA
DROPPED HEAD BEGIN SECTIONS HERE

# ACKNOWLEDGEMENTS

The authors of this document wish to express their thanks to many other people who have worked on various phases of this project. Mike Gery contributed substantially to the Biogenic Hydrocarbon Studies. Russell Weiner and Jeff Taylor worked on the day old mix and α-pinene research. Russell also implemented a method to measure hydrogen peroxide. Gary Howe did much of the PAN calibration intercomparison work. Maurice Jackson and Ed Cole conducted most of the 1980 experiments and implemented DNPH-HPLC aldehyde method. Doug Case managed the huge data processing tasks and Ken Crossen developed a much more reliable software system for the computer data acquisition system at the research facility. Donna Simmons' word processing expertise proved invaluable in compiling this report. Finally, we have received extensive support and cooperation from Mr. Bruce Gay, Jr., our EPA Project Monitor and Dr. Joe Bufalini. It was a pleasure to work with them and other researchers at the EPA Gas Kinetics and Photochemistry Branch.

BEGIN LAST LINE OF TEXT
BOTTOM OF IMAGE AREA OUTSIDE DIMENSION FOR TABLES AND ILLUSTRATIONS
3/8"
PAGE NUMBER
EPA-287 (Cin.)
(4-76)

BEGIN FIRST LINE OF TEXT HERE
TYPING GUIDE SHEET
CENTER OF PAGE
TOP OF IMAGE AREA
DROPPED HEAD: BEGIN SECTIONS HERE

## SECTION 1

## INTRODUCTION

Smog chamber investigations have been one of the ways in which scientists have tried to characterize certain chemical events which take place in the atmosphere. Many of these studies have used smog chamber data to: address control strategy issues, provide information for the further development of photochemical mechanisms and help evaluate chamber artifacts and wall problems.

In this study experiments were conducted in the University of North Carolina (UNC) outdoor smog chambers to specifically focus on selected issues relating to:

1. The impact of day old smog on fresh smog systems
2. Temperature effects on smog processes
3. Biogenic hydrocarbon smog reactions
4. Changes in initial $NO_x$ and hydrocarbon composition
5. Chamber characterization and wall reactions

The UNC dual outdoor chamber has an interior volume of 300 meters.$^3$ Its walls are composed of panels of 5 mil transparent Teflon film supported by a wooden "A frame" superstructure. The large chamber is divided into two chamber halves by an airtight 5 mil Teflon film curtain. Smog chamber experiments are conducted under natural temperature and solar conditions. Two experiments can be performed on the same day. Usually one chamber has a different initial chemical make up so that the effect of this change can be observed. Pollutants are injected before sunrise into the chambers. A sophisticated computer data acquisition system controls much of the experimental and data collection operations. The details of both of these operations are described (Appendix A) along with the analytical methods which were implemented or developed during this project (Section 7).

BEGIN LAST LINE OF TEXT
BOTTOM OF IMAGE AREA, OUTSIDE DIMENSION FOR TABLES AND ILLUSTRATIONS
3/8"

PAGE NUMBER
EPA-287 (Cin.)
(4-76)

# SECTION 2

# SUMMARY AND CONCLUSIONS

The main objective of this program was to perform outdoor chamber experiments to address various questions on ozone formation and oxidant control strategies. These included investigations into the effects of aged smog products, seasonal effects, biogenic hydrocarbons, changes in initial conditions and reactivity comparisons.

The effects of dilute day-old smog on fresh smog systems was studied in the UNC dual outdoor chamber. Smog systems which contained fresh smog precursors plus dilute residuals from the day before (0.04 parts per million (ppm) $O_3$, 0.1-0.3 ppm nonmethane hydrocarbon (NMHC) and 0.1 parts per million carbon (ppmC) aldehydes) produced almost twice the ozone as fresh systems which had the same initial NMHC and oxides of nitrogen ($NO_x$) injections. It is hypothesized that as much as 15-25% of this $O_3$ increase is due to residual first day aldehydes and that the remaining increase results from a larger morning percentage of $NO_2$ and the extra residual paraffinic hydrocarbons.

Comparison of results from static winter and summer outdoor smog chamber runs having similar initial conditions of simulated urban hydrocarbon mix and $NO_x$ shows that maximum $O_3$ concentrations in winter runs are lower than the summer ozone values by at least 75%. In many cases, the reduction was 88%. The temperature below which the ozone is less than some target value is different for each set of initial concentrations of hydrocarbon and $NO_x$. In general, at temperatures of 51 to 58$^{\circ}$F, a hydrocarbon to $NO_x$ ratio approximately equal to or greater than 10:1 was required to produce maximum $O_3$ concentrations equal to or greater than 0.1 ppm.

Single hydrocarbon $NO_x$ experiments were conducted to observe the seasonal effects on these systems. In general all simple hydrocarbons and aldehydes tested showed strong seasonal effects. The strength of these effects in roughly increasing order was seen with propylene<ethylene< acetaldehyde. A propylene mechanism was constructed to model the observed seasonal effects on propylene-$NO_x$ systems. Reasonable fits to propylene runs over a wide range of temperatures could be achieved by incorporating a water and temperature dependent peroxynitric acid (PNA) formation reaction. Experimental data and PNA model predictions indicate that humidity is not an important factor for $NO_x$ and $O_3$ behavior on warm days even for high propylene/$NO_x$ conditions. The greatest humidity-temperature effects are seen in cool systems between air with high water content and air with low water content.

Drying chamber air to dew points of 55-60$^{0}$F (ambient temperature 65$^{0}$F) permits initially injected formaldehyde to remain in the gas phase and seems to eliminate wall problems associated with formaldehyde. Nitrogen dioxide ($NO_2$) can offgas from chamber walls. The conditions for which this offgassing occurred always included very overcast, high humidity, warm conditions suggesting that a narrow range of solution strengths on the walls is required for offgassing. Chamber drying eliminates the observed $NO_2$ offgassing. Experiments conducted for the described outdoor conditions are usually not used for modeling or other comparison purposes.

UNC outdoor chamber experiments have shown that in high concentration systems of isoprene and $O_3$ (5ppmC and 1 ppm) approximately 75% of the reacted carbon can be observed in the product formation of formaldehyde (HCHO), carbon monoxide (CO), methacrolein (MACR), methylvinylketone (MVK), methylglyoxal (MGLY), acetaldehyde, and propylene. Mechanisms were developed which adequately described the data from dark experimental chamber experiments of MACR, MVK, isoprene and $O_3$. Experimental data and modeling results were used to estimate $O_3$ rates of attack on MVK and MACR. An isoprene-$O_3$ rate of $1.67\text{x}10^{-2}$ ppm$^{-13}$ min$^{-1}$ was estimated and is consistent with other rates reported in the literature. Dark isoprene-$O_3$ systems appear to form homogeneously nucleated aerosol. Most of these particles appear and remain at diameters well below the optical cutoff region (0.3-0.5 μm) as opposed to the particles from similar α-pinene-$O_3$ systems, which also form at smaller sizes but then grow into the optical size range (i.e. 0.5 μm). Lower concentrations of α-pinene and $O_3$(0.2 ppmC and 0.12 ppm) still generated substantial aerosol, but by comparison rapid condensation nuclei (CN) nucleation was not observed during a similar side-by-side system of isoprene and $O_3$.

Selected changes in initial conditions of smog chamber systems were investigated. In most cases an increase in the initial % $NO_2$ (while $NO_x$ was held constant) resulted in a 20% or greater enhancement in $O_3$ from urban mix-$NO_x$ systems. When $O_3$ was added early in the morning to simulate the increase in initial $NO_2$, the enhancement in final $O_3$ was not as great.

The addition of 10% extra acetaldehyde or formaldehyde carbon to urban mix-$NO_x$ systems did not significantly increase the initial rate of oxidation of NO to $NO_2$ but did substantially increase $O_3$ production.

The addition of 30% extra butane carbon to an eleven component urban mix suggests that this amount of extra butane can substantially increase $O_3$ formation. Similar experiments with propane usually showed only a 10-15% $O_3$ increase.

Side-by-side UNC urban mix and 25%, 75% propylene, butane carbon mixture showed these systems have similar reactivity. Dilute auto exhaust from two uncontrolled vehicles was more reactive than the UNC urban mix. A synthetic auto exhaust mixture exhibited similar reactivity to the UNC mix; it appears that aldehydes are the components in uncontrolled auto exhaust which make it more reactive than simulated mixtures which do not contain aldehydes. In a Rule 66-like substitution experiment using an actual blend of commerical solvents added to the UNC urban mixture, a 50% reduction of the solvent fraction with a small addition of cellusolves (5%), did not show any reduction of $O_3$.

TYPING GUIDE SHEET
BEGIN FIRST LINE OF TEXT HERE
CENTER OF PAGE
TOP OF IMAGE AREA
DROPPED HEAD: BEGIN SECTIONS HERE

Although α-pinene is somewhat more reactive than the hydrocarbon mixture, direct replacement of 20% carbon results in no change in overall reactivity as indicated by $NO_x$ and $O_3$ behavior. The addition of 20% extra carbon as α-pinene produces effects similar to increasing carbon concentration of the hydrocarbon mixture by 20%. If α-pinene and $O_3$ are first reacted, their products do not impart any unusual reactivity to a hydrocarbon-$NO_x$ smog system. In one experiment a loss of reactivity as measured by $O_3$ production was observed. Aerosol measurements made when α-pinene and $O_3$ reacted indicate that the majority of particles which form reside in the 0.1 μm diameter range; most of the mass, however, was in particles of 0.6 μm diameter. Carbon accountability in the product condensed phase was estimated to be 25-90%.

Most of our experimental results suggest that 20% carbon substitution of "moderately reactive" compounds like toluene or α-pinene into a simulated urban hydrocarbon mixture does not greatly affect the overall reactivity of the urban mixture. It is only when compounds of extremely high or low reactivity (like propylene, xylenes, or propane) are substituted that noticeable changes in $O_3$ production occur.

BEGIN LAST LINE OF TEXT
BOTTOM OF IMAGE AREA, OUTSIDE DIMENSION FOR TABLES AND ILLUSTRATIONS

PAGE NUMBER
EPA-287 (Cin.)
(4-76)

TYPING GUIDE SHEET
BEGIN FIRST LINE OF TEXT HERE
CENTER OF PAGE
TOP OF IMAGE AREA
DROPPED HEAD; BEGIN SECTIONS HERE

## SECTION 3

## RECOMMENDATIONS

The reactivity of single compounds should be tested within the environment of urban mixtures. This reduces questions about chamber wall problems and permits reactivity comparisons under more realistic conditions.

Further work on the α-pinene-$O_3$ systems is needed to better quantify the processes of particle formation and the amounts of reacted α-pinene which appear in the condensed phase.

To further investigate the effects of aged smog a separate chamber should be used to generate aged smog products. A portion of the day old smog should then be transferred to a clean chamber which would then receive an injection of fresh smog precursors. A third clean chamber would serve as a control and would be injected with fresh smog precursors. This feature of using three chambers would minimize uncertainties associated with wall effects.

An outdoor smog chamber database with total auto emissions (both exhaust and evaporative) should be generated for model testing. These experiments should be simultaneously performed with simulated hydrocarbon mixtures so that models can be validated on known hydrocarbon mixtures and then tested on auto emissions.

The analytical capability now exists to measure most of the major products from $C_2$-$C_3$ olefin-$O_3$ reactions. A database should be generated in either indoor or outdoor chambers to help quantify the mechanistic pathways from these reactions.

9-1/8"
BEGIN LAST LINE OF TEXT
BOTTOM OF IMAGE AREA, OUTSIDE DIMENSION FOR TABLES AND ILLUSTRATIONS
3/8"

PAGE NUMBER
EPA-287 (Cin.)
(4-76)

TYPING GUIDE SHEET

Smog chamber experiments performed for photochemical model testing should employ dynamic injection and dilution schemes. It is presently believed that different models respond differently to these conditions and these runs would provide a more realistic data set for model validation.

Outdoor smog chamber experiments should be conducted at humidities well below saturation. This will minimize formaldehyde and nitric acid wall losses and reduce other alleged chamber wall interactions. Unless humidity is specifically being studied, outdoor chamber dew points should be reduced to at least 60-50°F when ambient temperatures are above 65°F.

EPA-287 (Cin.)
(4-76)

TYPING GUIDE SHEET
BEGIN FIRST LINE OF TEXT HERE
CENTER OF PAGE
TOP OF IMAGE AREA
DROPPED HEAD; BEGIN SECTIONS HERE

# SECTION 4

# THE EFFECTS OF DAY-OLD DILUTE SMOG ON FRESH SMOG SYSTEMS

## INTRODUCTION

The effect of day-old smog materials on fresh smog systems has been of concern for more than a decade. The ability of local air pollution agencies to control their own photochemical oxidants requires more than just knowledge of their own emissions. They also need information on the kinds and amounts of smog precursors and products that are transported to their city from upwind metropolitan areas or regional sources or are recirculated from previous days' episodes. Such is the case with cities along the eastern sea coast of the United States. Unique topography and resulting meteorology, as in Los Angeles, can also give rise to a situation in which a portion of the day-old material can be retained aloft during the evening. The next morning, after these pollutants aloft have aged, they can be mixed with fresh ground level emissions as the nocturnal inversion is "burned off" by the sun and the mixing height rises.

To quantify the impact that dilute day-old smog can have, an outdoor chamber study was undertaken in which dilute residual smog products were added to a fresh smog system.

## EXPERIMENTAL

To experimentally simulate the inclusion of day-old material into fresh smog mixtures, it was necessary to run two complete days of irradiation in both compartments of the UNC outdoor chamber. The protocol for a typical experiment in the UNC chamber has been described in detail by Jeffries et al.[1] On the first day an eleven component urban-like hydrocarbon mixture (Table 1) was added during the predawn hours to both freshly purged chamber sides. This was done to generate a source of day-old smog which could be used in one of the chambers on the second day

BEGIN LAST LINE OF TEXT
BOTTOM OF IMAGE AREA; OUTSIDE DIMENSION FOR TABLES AND ILLUSTRATIONS
3/8"

PAGE NUMBER
EPA-(Cin.)
(4-76)

TABLE 1. 1979 UNC Simulated Urban Hydrocarbon Mix

| Class/Compound | Carbon Fraction<br>UNC* Analysis | <br>Matheson Analysis | Mole Fraction<br>UNC Analysis |
|---|---|---|---|
| 1. Paraffins | | | |
| isopentane | 0.1484 | .1270 | 0.1273 |
| n-pentane | 0.2531 | .2535 | 0.2411 |
| 2-methy-pentane | 0.0996 | .1027 | 0.0712 |
| 2,4-dimethyl-pentane | 0.0864 | .0791 | 0.0528 |
| 2,2,4-dimethyl-pentane | 0.1202 | .1111 | 0.0644 |
| Subtotal | 0.7077 | .6734 | 0.5568 |
| UNC Average Carbon Number = 5.89 | | | |
| 2. Olefins | | | |
| 1-butene | 0.0254 | 0.0301 | 0.0272 |
| cis-2-butene | 0.0313 | 0.0297 | 0.0335 |
| 2-methyl-butene | 0.0347 | 0.0393 | 0.0298 |
| 2-methyl-2-butene | 0.0317 | 0.0393 | 0.0272 |
| ethylene | 0.1167 | 0.1343 | 0.2504 |
| propylene | 0.0524 | 0.0539 | 0.0750 |
| Subtotal | 0.2922 | 0.3266 | 0.4431 |
| UNC Average Carbon Number = 2.78 | | | |
| TOTAL | 0.9999 | 1.0000 | 0.9999 |

---

*UNC analysis is based on an average of many determinations of what actually appears in the chamber.

of irradiation. On the evening of the first day, one of the chambers was completely purged with clean air (fresh side). The other side (residual side) remained sealed with its contents from the first day of irradiation. In the predawn hours of the second day, the residual side was opened and slowly vented so that its contents were diluted by 60-90% with clean air. Both chambers were then closed and fresh NMHC and $NO_2$ were added to both sides. Results from the second day of irradiation in the side which contained fresh smog ingredients were compared with the side with fresh plus residual material. Residual hydrocarbons usually made up 5-20% (0.1-0.5 ppmC) of the total NMHC in the residual side on the second day. Residual $NO_2$ was much lower because most of the first day $NO_x$ had reacted to form nitric acid or organic nitrates. Initial concentrations of NMHC and $NO_x$ on the first day in the residual side were selected so that when this side was diluted early the next morning only 0.02-0.08 ppm of first-day $O_3$ remained. This range was used as a guide because this amount of $O_3$ might normally be trapped above or advected into an urban center in the very early morning hours during the smog season.

Two different schemata were used in making the second day injections: a) ignore the presence of any material in the chamber and inject the same amount of mix, NO, and $NO_2$ into each side (matched injection case), and b) account for the residual $O_3$, $NO_x$, and NMHC measured in the chambers, and inject possibly different amounts of materials so as to obtain the same NO, $NO_2$, and NMHC concentrations in the two chamber halves (balanced initial conditions case).

Thus in the matched injection case on the second day, one would expect that different percentages of $NO_2$ would arise in each of the chambers immediately after the injection. This would result from the titration of residual $O_3$ with fresh NO. The residual side would also have 10-50% more initial NMHC. To eliminate the effects that different percentages of initial $NO_2$ and increased initial carbon can have on smog systems, the balanced initial conditions case was performed. Figure 1 illustrates these two different injection schemes.

Matched Injection Case: same injection of fresh, NMHC, NO and $NO_2$ on both sides

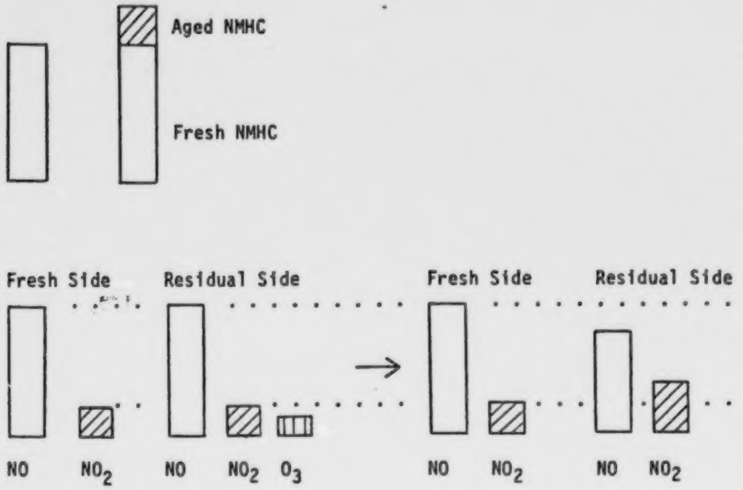
Aged NMHC
Fresh NMHC
Fresh Side
Residual Side
Fresh Side
Residual Side
NO
NO2
NO
NO2
O3
NO
NO2
NO
NO2

Balanced Injection Case

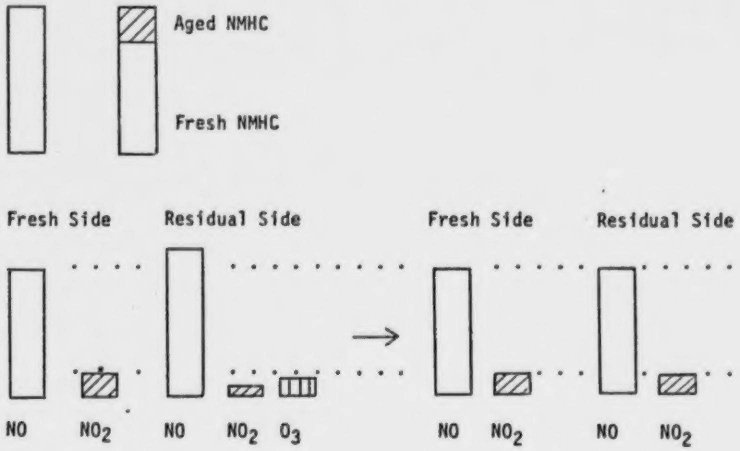
Aged NMHC
Fresh NMHC
Fresh Side
Residual Side
Fresh Side
Residual Side
NO
NO2
NO
NO2
O3
NO
NO2
NO
NO2

Figure 1. Two different schemata for the second day injection of fresh materials on dilute aged smog.

TYPING GUIDE SHEET

## RESULTS AND DISCUSSION

The runs which simulate the same emissions into "clean" and "dirty" atmospheres (matched injection case) are summarized in Table 2. A typical experiment from Table 2, September 7, 1978 is shown in Figure 2a. Note the dilution of day-old material as indicated by the early morning $O_3$ trace in the residual side. In all of these runs the day-old [NMHC] was between 0.2 and 0.5 ppmC and the residual $[O_3]$ was between 0.025 and 0.087 ppm after dilution. For systems containing about 2 ppmC of fresh mix and about 0.35 ppm $NO_x$, the total effect of the day-old material was to more than double the $[O_3]$ maximum. The experiments in Table 2 clearly demonstrate that important processes occur upon mixing old and fresh material in the chamber. These processes may be caused by:

1) extra carbon from residual NMHC,
2) higher initial percentage $NO_2$ which results from differences in initial $O_3$ concentrations, and
3) unmeasured residual materials and different hydrocarbon mixture composition.

Inspection of the NO and $NO_2$ profiles from a typical run with balanced initial concentrations (Figure 2b, July 18, 1978) shows only a slight impact of aged materials on the conversion of NO to $NO_2$ when compared to the fresh material side. For systems of this type, the effect of day-old material was to increase the $[O_3]$ maximum by 30 to 50% (Table 3 and Figure 2b). This was less than the effects illustrated in Table 2, but still demonstrated that further consideration is necessary.

### Carbon Balance and Aldehydes

To investigate the possible factors that cause dilute smog to significantly increase $O_3$ production on the second day, a carbon balance was performed on two, two day systems, on July 17-18, 1978 and September 11-12, 1979. Both of these two day systems were conducted according to the balanced injection scheme previously outlined. Table 4 shows the hydrocarbon concentrations, product concentrations, and paraffin to olefin ratios at different times during these two day runs. The detailed chromatograms of $C_2$-$C_{10}$ hydrocarbons which were taken every 30 minutes indicated that after approximately 10-12 hours of sunlight on the

EPA-287 (Cin.)
(4-76)

TYPING GUIDE SHEET

Table 2. Effects of day-old material on ozone in matched injection runs

| | HC, ppmC[a] | | NO, ppm[b] | | $NO_2$, ppm[c] | | $O_3$, ppm[d] | | |
|---|---|---|---|---|---|---|---|---|---|
| Date | Side 1[(i)] | Side 2 | Side 1 | Side 2 | Side 1 | Side 2 | Side 1 | Side 2 | Comments |
| 9/5/78 | 1.90f<br>-0.50r<br>(2.40) | 1.91f<br><br>(1.91) | 0.210<br>(0.353) | 0.239<br>(0.337) | 0.161<br>48% | 0.127<br>38% | 0.447<br>(2.07) | 0.216 | 0.047 ppm $O_3$ dil to 0.025 ppm |
| 9/6/78 | 2.13f<br><br>(2.13) | 2.13f<br>-0.30r<br>(2.43) | 0.260<br>(0.341) | 0.213<br>(0.357) | 0.081<br>24% | 0.144<br>41% | 0.163<br>(2.74) | 0.446 | 0.086 ppm $O_3$ dil to 0.028 ppm |
| 9/7/78 | 2.00f<br><br>(2.00) | 2.00f<br>-0.20r<br>(2.20) | 0.276<br>(0.358) | 0.216<br>(0.363) | 0.082<br>23% | 0.151<br>42% | 0.316<br>(2.38) | 0.753 | 0.28 ppm $O_3$ dil to 0.087 ppm |

---

[a] f ≡ fresh urban hydrocarbon mixture
r ≡ remaining day-old hydrocarbon

[b] numbers in () are total $NO_x$

[c] % express the $NO_2$-to-$NO_x$ ratio after $NO$-$O_3$ titration occurred

[d] numbers in () are the ratio of old plus fresh to fresh only ozone

[e] first number is $O_3$ concentration before dilution, second number is $O_3$ concentration after dilution, before NO injection

[i] Side 1 and 2 refer to chamber sides

EPA-287 (Cin.)
(4-70)

## Table 3. Effects of day-old material on ozone in balanced initial conditions runs

| Date | HC, ppmC[a] | | NO, ppm[b] | | $NO_2$, ppm[c] | | $O_3$, ppm[d] | | Comments |
|---|---|---|---|---|---|---|---|---|---|
| | Red | Blue | Red | Blue | Red | Blue | Red | Blue | |
| 7/18/78 | 2.05f<br>(2.05) | 1.80f<br>-0.25r<br>(2.05) | 0.301<br>(0.377) | 0.294<br>(0.370) | 0.076<br>20% | 0.076<br>20% | 0.502<br>(1.50) | 0.752 | 0.23 ppm $O_3$ diluted to 0.056 ppm |
| 7/19/78 | 1.75f<br>-0.25r<br>(2.00) | 1.95f<br>(1.95) | 0.315<br>(0.433) | 0.304<br>(0.418) | 0.118<br>27% | 0.114<br>27% | 0.783<br>(1.26) | 0.621 | 0.34 ppm $O_3$ diluted to 0.086 ppm |
| 7/20/78 | 0.90f<br>-0.17r<br>(1.07) | 1.19f<br>(1.19) | 0.228<br>(0.357) | 0.225<br>(0.359) | 0.129<br>36% | 0.134<br>37% | 0.455<br>(1.51) | 0.301 | 0.52 ppm $O_3$ diluted to 0.107 ppm |
| 9/4/79 | 1.8f<br>0<br>(1.80) | 1.7fr<br>0.1r<br>(1.80) | 0.235<br>(0.299) | 0.228<br>(0.297) | 0.064<br>21.4 | 0.069<br>23.2% | 0.054<br>(2.46) | 0.133 | This run did not go to completion; temperature limited and $\Delta O_3$ would not have been as great had more $O_3$ been made in both sides. |
| 9/12/79 | 1.95t<br>0 | 1.50f<br>.45r | 0.191<br>(0.236) | 0.182<br>0.0257) | 0.045<br>19.1% | 0.0075<br>29 | 0.330<br>(1.38) | 0.461 | 0.034 $O_3$ diluted to 0.012 ppm |
| 9/17/79 | 1.9f<br>0 | 1.65f<br>0.35r | 0.125<br>0.202 | 0.130<br>(0.201) | 0.077<br>38.1% | 0.071<br>35.3% | 0.330<br>(1.53) | 0.504 | Both sides received 0.1 ppm HCHO injections in the morning to see if aldehydes would reduce day old effect. |
| 6/18/79 | 2.0f<br>0 | 1.7f<br>0.3f | 0.214<br>(0.259) | 0.207<br>(0.255) | 0.045<br>17.3% | 0.048<br>18.8% | 0.579<br>(0.97) | 0.561 | Fresh mix and $NO_2$ injected in blue side at 10pm on June 17 and then diluted at 4am on June 18 to simulate matched initial conditions case. |
| 10/3/79 | 2.2f<br>0.2r | 2.14f<br>0.2r | 0.134<br>(0.177) | 0.134<br>(0.177) | 0.036<br>20.3% | 0.036<br>20.3% | 0.409<br>(1.19) | 0.344 | Aged materials held in red side over night and transferred to blue. Test chamber wall effects. |
| 10/4/79 | 2.77f<br>0 | 2.70f<br>0 | 0.124<br>(0.156) | 0.122<br>(0.155) | 0.026<br>16.7% | 0.027<br>17.4% | 0.400 | 0.416 | Matched system fresh materials only. |

---

[a] f ≡ fresh urban hydrocarbon mixture
r ≡ remaining day-old hydrocarbon
numbers in () are total NMHC initial conditions

[b] numbers in () are total $NO_x$

[c] % express the $NO_2$-to-$NO_x$ ratio after NO-$O_3$ titration occurred

[d] numbers in () are the ratios of old plus fresh to fresh only ozone

[e] first number is $O_3$ concentration before dilution, second number is $O_3$ concentration after dilution, before NO injection

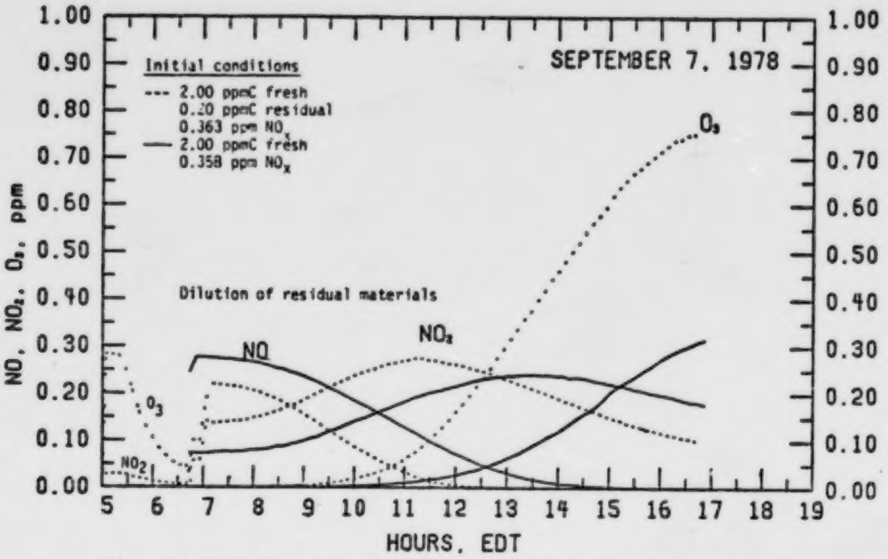

Figure 2a. Effect of residual dilute smog on second day of an urban system: matched injection case. September 7, 1978.

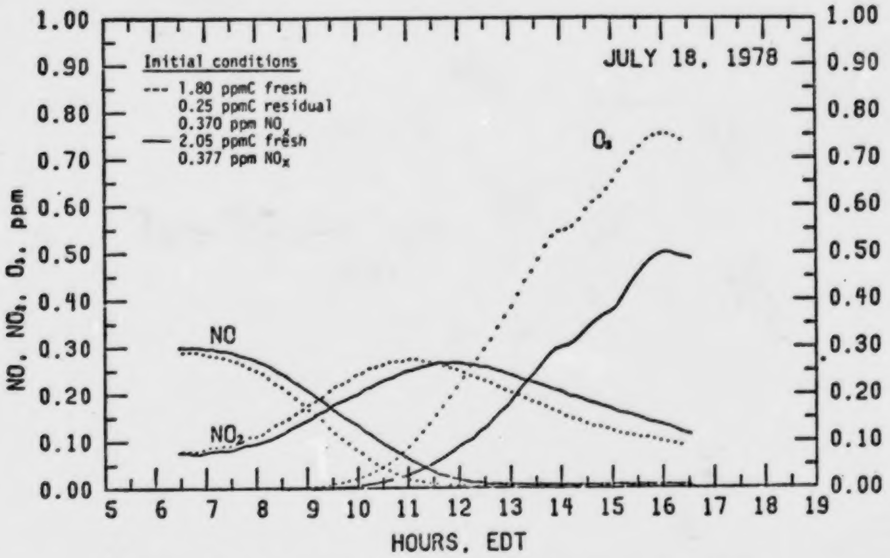

Figure 2b. Effect of residual dilute smog on second day of an urban system: balanced initial conditions case. July 18, 1978.

first day almost all of the olefins had reacted (except for ethylene) and mostly paraffins remained. By summing up all of the remaining hydrocarbons and products and comparing this to the initial NMHC (adjusted for chamber leaks and sampling losses), a carbon balance was obtained. Approximately 84 and 93% of the carbon could be accounted for in the late afternoon on the September 11 and July 17, 1978 runs. Differences in these numbers probably reside in the afternoon estimate of the dilution adjusted initial NMHC (had no reaction taken place). As the residual materials aged overnight in the July 17 run, $O_3$ had the opportunity to attack the remaining paraffinic hydrocarbons so that the carbon accountability was lower by morning. The September 11 run produced little $O_3$ and its carbon balance changed little overnight.

After the early morning dilution on the second day of both the July 17 and September 11 runs, 0.07 and 0.12 ppmC of unaccounted carbon remained in the residual side of the chamber (Table 4). Although total aldehyde MBTH bubbler samples were not taken during these experiments they were obtained during a similar run on October 3, 1979. The afternoon data show that acetaldehyde and formaldehyde make up approximately 70% of the total measured aldehydes. When the remaining 30% is translated into $C_3$ and $C_4$ aldehydes, approximately 0.17 ppmC results; this allows a sizeable portion of the "missing" afternoon carbon to be accounted for on this day.

Table 5 shows the balanced initial conditions for the second day of the two day run which began on July 17. If the unaccounted carbon on July 17, 1978 was really unmeasured higher molecular weight aldehydes and reactive ketones, the second day system on July 18 could be thought of as a matched NMHC and $NO_x$ run on both sides, with the exception that one side had an additional injection of aldehydes.

Many of these types of experiments have been conducted in previous years in the UNC chambers. (The effect of additional aldehydes is discussed in Section 7.) An example of such a run is given in Figure 3 which shows that the major effect of adding acetaldehyde is to increase $O_3$ production. Little effect is seen on the rate of NO to $NO_2$ conversion. This, of course, is similar to the day old and fresh systems with balanced NMHC, $NO_x$, and $NO_2$.

Table 4. Carbon balance at various times during two day runs with dilute aged smog

| | July 17-18, 1978 | | September 11-12, 1979 | |
|---|---|---|---|---|
| I. Initial NMHC ppmC | 1.85 | | 2.20 | |
| aldehydes | .00 | | .00 | |
| % paraffins | | 70.0 | | 70.6 |
| % olefins | | 30.0 | | 29.4 |
| II. NMHC after 10 hours of sunlight $C_2$-$C_{10}$ ppmC | 1.10 | | 1.41 | |
| % paraffins | | 93.3[b] | | 94.3[b] |
| acetaldehyde ppmC | 0.09 | | 0.08 | |
| formaldehyde ppm | 0.08 | | 0.06 | |
| carbon monoxide ppm | 0.14 | | 0.15 | |
| PAN + alkylnitrates ppm C | 0.16 | | 0.02 | |
| Sum of NMHC & products | 1.57 | (1.68)[a] | 1.72 | (2.04)[a] |
| Missing carbon ppmC | 0.11 | | 0.32 | |
| III. Early morning before dilution $C_2$-$C_{10}$ NMHC ppmC | 0.95 | | 1.30 | |
| acetaldehyde | 0.07 | | 0.07 | |
| formaldehyde | 0.06 | | 0.05 | |
| PAN + alkynitrates ppmC | 0.08 | | 0.01 | |
| CO | 0.12 | | 0.13 | |
| Sum of NMHC & products | 1.28 | (1.55)[a] | 1.56 | (1.91)[a] |
| Missing carbon ppmC | 0.27 | | 0.35 | |
| Ozone | | | 0.039 | |
| IV. After dilution dilution factor | | 4.1 | | 3.3 |
| Ozone | 0.056 | | 0.012 | |
| NMHC + CO | 0.26 | (0.39)[a,c] | 0.42 | (0.58)[a] |
| acetaldehyde | 0.01-0.02[c] | | 0.02 | |
| formaldehyde | 0.01-0.02[c] | | 0.02 | |
| PAN + alkynitrates ppmC | 0.02 | | 0.003 | |
| Sum of missing carbon | 0.07-0.09 | | 0.12 | |

---

[a] initial NMHC adjusted for chamber leaks and sampling losses

[b] the only remaining olefin at this time was ethylene

[c] estimated concentration based on dilution

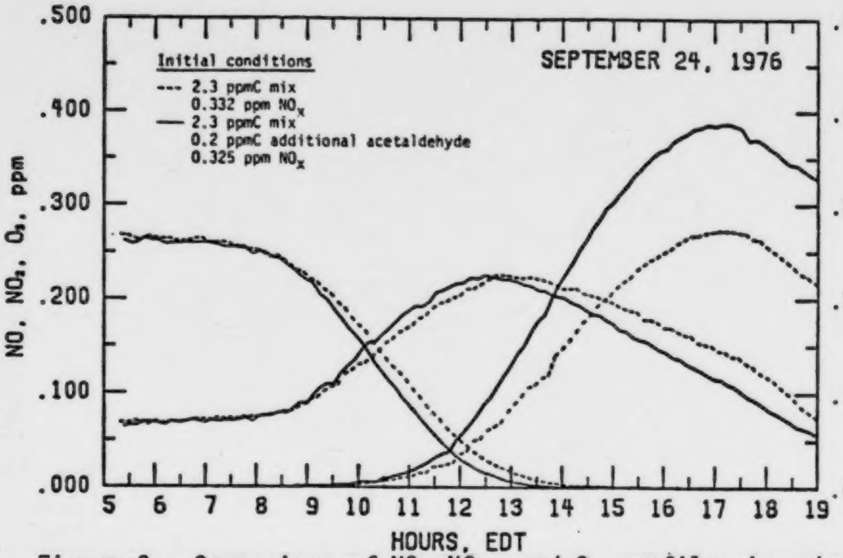

Figure 3. Comparison of NO, $NO_2$, and $O_3$ profiles in urban mix with (——) and without (---) additional added acetaldehyde (10% of initial NMHC). September 24, 1976.

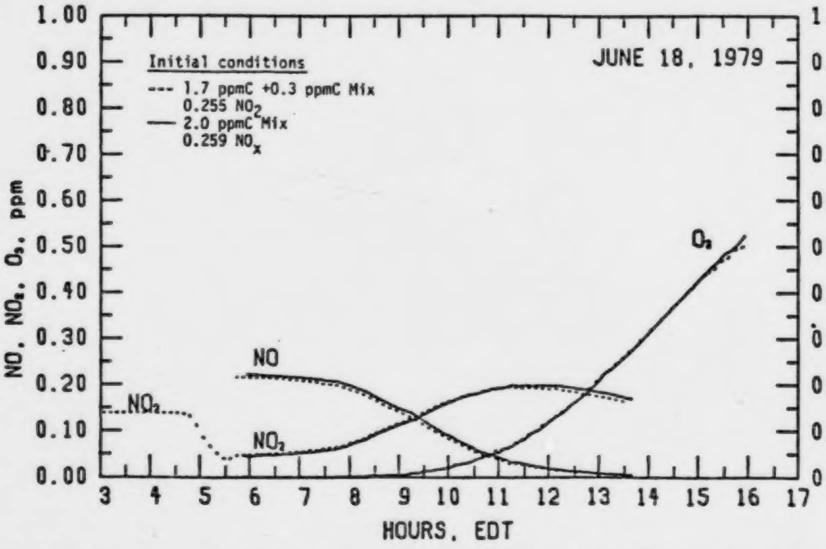

Figure 4. Effect of injecting fresh mix and $NO_2$ to test chamber artifacts. June 18, 1979.

TYPING GUIDE SHEET

Table 5. Comparison of Starting Materials for July 18, 1978

| Fresh Materials Side | Aged Plus Fresh Materials Side |
|---|---|
| 2.05 ppmC | 1.85 ppmC fresh mix |
| 30% olefins | 0.25 ppmC old paraffins |
| | 0.03 ppmC $C_1$ and $C_2$ aldehydes |
| | 0.08 ppmC unaccounted |
| 2.05 ppmC fresh | 2.10 ppmC NMHC |
| | 0.11 ppmC aldehydes |

There was the concern that the UNC mix does not contain aldehydes. Normally one might expect that 5 to 10% of the NMHC emitted from mobile sources would be formaldehyde. It could then be reasoned that if 10% additional aldehydes had been injected along with urban mix on both the aged smog and fresh mix sides, the effect of aldehydes in the dilute day old smog would be reduced if not lost. When formaldehyde was included in each side on both the first and second day of a run (beginning September 16, 1979), the side with aged materials still made 50% more $O_3$ (Table 3) and showed the same characteristic profiles as every other run with balanced NMHC, $NO_x$, and $\%NO_2$.

## Chamber Effects

Although indirect evidence has been offered which suggests that aldehydes are the ingredient which gives dilute aged smog its additional reactivity, specific $C_3$ and higher aldehydes must be identified. In addition, more experiments to test chamber wall effects (which can be most accented in two day runs) are needed so that one can separate the possible increase in second day $O_3$ from chamber wall interactions vs. day old gas phase residuals. The holding of fresh materials in the chamber the evening before a morning smog experiment was the first thing to be examined on June 18, 1979; 1.2 ppmC of fresh mix and 0.17 ppm $NO_2$ were

EPA-287 (Cin.)
(4-76)

added to a clean chamber half at 2200 EDT (10:00 pm). The other chamber was purged with clean air all night. The next morning the side with mix and $NO_2$ was diluted down so that 0.3 ppmC NMHC and 0.035 ppm $NO_2$ remained. Fresh mix and $NO_2$ were then added to both sides so that the same initial NMHC, $NO_x$ and $\%NO_2$ were measured on both sides. The result of this run was a perfect match of the NO, $NO_2$ and $O_3$ profiles (Figure 4). This demonstrated that holding fresh materials overnight in the chamber does not accelerate $O_3$ production the next day.

To further test the chamber walls a unique transfer type experiment was planned but poor weather prevented its execution on a warm day. It was successfully conducted on October 2 and 3, 1979. As in other experiments only one side was opened up and vented in the afternoon of the first day. Early the next morning 0.19 ppmC of the residual contents from the closed chamber was transferred through a connecting duct into the freshly vented chamber. This was followed by diluting the chamber half which was closed all night so that the same level (0.19 ppmC) of residual materials was observed and verified in both sides. Shortly after sunrise both sides then received the same injection of fresh mix and $NO_x$. It was anticipated that significant wall effects would show up in the smog profiles from the two chamber sides.

Unfortunately the predawn temperature on the second day of this run (October 3) was 58°F and there was concern that some of the aldehydes and other reactive materials in the unvented side might be lost in the cool transfer duct as day old smog was being pumped into the clean chamber half. Slight evidence of this was revealed after transfer and final residual hydrocarbon balance, because slightly less formaldehyde appeared in the fresh side (0.015 compared to 0.02 ppm). In any event, the side which was not vented all night made 0.408 ppm $O_3$ while the freshly vented side generated only 0.356 ppm. This suggests that as much as 19% of the $O_3$ increase in the balanced initial conditions case of left over smog was either a chamber wall artifact or an incomplete transfer of aldehydes or other reactive species.

If one were to assume for the moment that chamber artifacts were the major cause of the above noted difference, then the relative importance of

BEGIN FIRST LINE OF TEXT HERE
TYPING GUIDE SHEET
CENTER OF PAGE
TOP OF IMAGE AREA
DROPPED HEAD, BEGIN SECTIONS HERE

residual hydrocarbons would have to be revised. It is expected that any $O_3$ maximum correction to runs already presented in this paper would not be strictly linear. As an approximation, however, if the $O_3$ data in Table 2 were scaled downward by 20%, the overall influence of aged materials in the balanced initial conditions case would not be as pronounced as originally thought. Four of the six cases show an $O_3$ increase of approximately 20%; one had almost no increase, yet in another there was a strong effect. On the other hand, if one considers the matched initial injection case, even after factoring in a worst case 20% chamber effect, an $O_3$ increase of 100% was still evident. This large increase is, of course, due to the interaction of residual hydrocarbons, increased % $NO_2$ and an overall higher initial NMHC concentration.

## Photochemical Modeling Implications

The importance of aldehydes has long been of great concern to those who develop and use photochemical mechanisms and models. Modeling studies by this group[2] have very recently included comparison of several well known mechanisms. Different mechanisms were substituted into a simple trajectory model utilizing the RAPS data base of St. Louis. Ozone isopleths were generated as well as diurnal profiles of the trajectories' actual and simulated chemistry. It was found that reasonable changes in assumptions of the aldehyde fraction in emissions or morning initial HC values have considerable effects on the overall reactivity, the predicted $O_3$ maximum, and the $O_3$ isopleth diagram.

It appears therefore that both chamber and modeling studies indicate that the amount and distribution of aldehydes (and other related oxidation products) present in hydrocarbon-$NO_x$ systems should be more carefully determined and considered. The potential for a given locality to produce oxidant can be affected by the degree of photochemical activity which an old smog system has undergone, the degree and rate of mixing or incorporation of an aged air mass into the "fresh" system, and the relative contribution of "aged" products (aldehydes, etc.) to new local emissions.

BOTTOM OF IMAGE AREA, OUTSIDE DIMENSION FOR TABLES AND ILLUSTRATIONS
BEGIN LAST LINE OF TEXT
3/8"

PAGE NUMBER
EPA-287 (Cin.)
(4-76)

TYPING GUIDE SHEET
BEGIN FIRST LINE OF TEXT HERE
CENTER OF PAGE
TOP OF IMAGE AREA
DROPPED HEAD: BEGIN SECTIONS HERE

## SUMMARY AND CONCLUSION

In this study the effect of dilute day-old smog on fresh smog systems was assessed in the UNC outdoor chamber. If dilute residual smog (0.2 ppmC paraffins, 0.1 ppmC aldehydes and ketones, and 0.04 ppm $O_3$) was present at the start of the second day then one might see a doubling of $O_3$ from a 2 ppmC and 0.3 ppm $NO_x$ system. Although more chamber validation experiments are required, it is hypothesized that as much as 15-25% of this $O_3$ increase is due to residual first day aldehydes and that the remaining increase results from higher morning percentage of $NO_2$ (titration of leftover dilute $O_3$ and fresh NO) and the extra residual paraffinic hydrocarbons. Previous chamber experiments suggest that, on the average, increasing the initial percentage of $NO_2$ from 20% to 50%[2] (also see Section 7) in these types of mix-$NO_x$ runs can increase $O_3$ by 20%. Increasing NMHC by 10% with aged paraffins and a little ethylene most probably does not increase $O_3$ by more than 10%. The combined interactive effect, however, of 0.2 ppmC aged mix, 0.1-0.15 ppmC aldehydes and 40% $NO_2$ is to advance the morning conversion of NO to $NO_2$ so that by the time $O_3$ is being produced it can take place over a longer period of natural sunlight. The resulting enhancement of $O_3$ production appears to be greater than the sum of the individual changes from aldehydes, % $NO_2$ and residual paraffins and ethylene.

It is believed that the experiments discussed in this study use realistic levels of aged hydrocarbons which might be transported between cities. Since this residual level, 0.12-0.2 ppmC, is only slightly above the natural background (~0.1 ppmC) it might not ordinarily be observed by conventional environmental chromatographs. Furthermore, in the past, the measurement of aldehydes and ketones has been difficult; the needed aerometeric data to document the transport of photochemically generated aldehydes is now possible.[3,4,5] If it is suspected that aged smog is being transported from one urban center to another, it would be useful to incorporate this into our current photochemical models. Assuming that the photochemical mechanism is an adequate representation of the effects of such additions, it might be desirable as a first approximation, to rerun isopleth model surfaces with an additional 5-10% aldehydes, 5-10%

BOTTOM OF IMAGE AREA; OUTSIDE DIMENSION FOR TABLES AND ILLUSTRATIONS
BEGIN LAST LINE OF TEXT
3/8"

PAGE NUMBER
EPA-287 (Cin.)
(4-76)

paraffins and ethylene, and 0.04-0.06 ppm $O_3$. This could then be compared with the original isopleths (which do not include these representatives of dilute aged smog) in order to gain insight into the influence of an upwind city on the resulting smog in a city down wind.

## SECTION 5

## SEASONAL EFFECTS ON $O_3$ PRODUCTION

### SEASONAL EFFECTS FOR COMPLEX MIXTURES OF HYDROCARBONS AND $NO_x$

#### Introduction

In 1975 various energy audits had initially indicated that substantial quantities of natural gas were being or would potentially be used to incinerate hydrocarbon emissions as a means to control $O_3$. Preliminary information at that time suggested that oxidant formation was significantly retarded at reduced ambient temperatures. Two questions were raised: 1) to what extent was it necessary to reduce hydrocarbon emissions as an $O_3$ control strategy during the colder months in the northern portions of the U.S., and 2) was it possible to determine a temperature cut-off below which $O_3$ would not be produced in excess of some designated value (then 0.08 ppm).

It is well known that maximum $O_3$ production in a photochemical smog system is strongly related to NMHC, NO, and $NO_2$ available for reaction. In static smog chamber experiments, these are the initial conditions. It is also known that maximum $O_3$ production is related to the light intensity (and perhaps total light history) at the time $O_3$ forms. It is only recently that we are beginning to have some insights into the exact dependence of maximum $O_3$ production on air temperature and temperature history in complex photochemical systems. Five years ago the temperature dependence of rate constants for many important reactions was either unknown or only poorly known. Although our understanding has increased in recent years much uncertainty still exists and it was felt that static outdoor smog chamber experiments under winter time conditions could provide useful information regarding this question.

In a previous study,[6] we were able to perform a number of similar, low concentration, simulated urban hydrocarbon-$NO_x$ runs over a range of maximum air temperatures. These runs demonstrated that as the air temperature decreased, so did the maximum NO oxidation rate and the maximum $O_3$ produced. Figure 5 shows the NO rate as a function of temperature, and indicates a 50% decrease in NO oxidation rate for a $14^{o}F$ decrease in temperature at the maximum rate. Table 6 gives the maximum $O_3$ produced and the temperature at $O_3$ maximum for two runs in June and six runs in November. The maximum $O_3$ is clearly related to both the solar radiation conditions and the air temperature at which it forms. These runs, however were performed at relatively low initial concentrations; it would be difficult to precisely predict the effect of temperature at other HC or $NO_x$ ratios and concentrations.

Due to interest in winter oxidant formation potential and its associated energy and air monitoring implications for northern cities in the United States, EPA support was provided to perform outdoor smog chamber experiments under winter conditions. Of special interest was the relationship between hydrocarbon control and winter oxidant formation potential. The objectives of this study were:

1. To determine the oxidant potential of urban atmospheres during the late fall and winter months (ambient maximum temperature in the range $45\text{-}60^{o}F$) in a statically operated smog chamber. Hydrocarbon and $NO_x$ concentrations and ratios should reflect real urban conditions and reflect possible increases in hydrocarbon emissions.
2. To investigate the winter oxidant potential of three-day systems with and without continual injection and dilution.
3. To simulate lower tropospheric oxidant production of winter air masses with very low initial $NO_x$ and hydrocarbons.

## Experimental

Winter smog chamber experiments began on November 29, 1975. The experiments were designed so that some of the winter runs would have initial conditions similar to previously conducted summer experiments in

**TABLE 6.** Effects of Air Temperature on Ozone Production in Static Outdoor Chamber Runs with the Same Initial Conditions (0.8 ppmC urban hydrocarbon mix, 0.20 ppm $NO_x$, and 0.04 ppm $NO_2$)

| Month | Temp. at $O_3$ Max., °F | Maximum $O_3$, ppm |
|---|---|---|
| June | 90 | 0.17 |
| June | 84 | 0.10 |
| November | 80 | 0.06 |
| November | 80 | 0.05 |
| November | 70 | 0.03 |
| November | 69 | 0.03 |
| November | 53.8 | 0.014 |
| November | 53.4 | 0.012 |

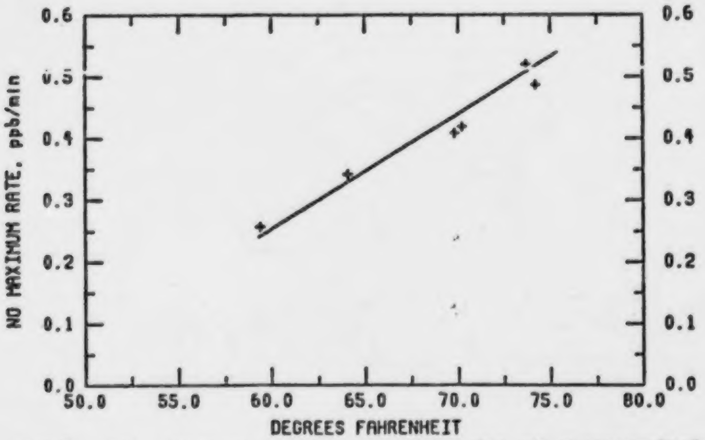

Figure 5. Effect of air temperature at maximum rate on maximum nitric oxide disappearance for clear days for November 1973 and initial conditions of 0.20 ppm $NO_x$, 0.04 ppm $NO_2$ and 0.80 ppmC urban hydrocarbon mix in UNC outdoor smog chamber.

the UNC chambers. A total of 38 individual experiments were carried out of which 20 were 2 and 3 day runs.

Almost all of the winter experiments began with 30-40% of the initial $NO_x$ as $NO_2$. By comparison, summer runs began with only 20% initial $NO_2$. To increase the reactivity of the simulated urban hydrocarbon mix and more quickly initiate the chemical processes, an additional injection of acetaldehyde was made. This injection was 10% of the initial NMHC and is not reflected in the reported initial hydrocarbon conditions. Summer runs used in this report for comparisons did not have any initial acetaldehyde. Hence from the standpoint of initial conditions, oxidant yields from the winter experiments were biased toward maximum values and therefore represented a worst case condition. The composition of the urban hydrocarbon mix used in these experiments was basically the same as that reported in Section 4, Table 1 of this report.

## Results and Discussion

### Effects of Adding Acetaldehyde--

Two dual wintertime experiments were performed to test the effect of 10% extra acetaldehyde carbon on $O_3$ formation (Table 7). The initial hydrocarbon and $NO_x$ concentrations were the same on both sides of the chamber except that one side received an additional injection of acetaldehyde. Inspection of the experimental data shows that morning NO and $NO_2$ behavior is not greatly influenced by additional acetaldehyde. The major impact appears in the afternoon; the side with acetaldehyde made 20% more $O_3$. The effects of additional acetaldehyde during summertime conditions will be discussed in detail in Section 7.

### Effect of Increasing Initial $NO_2$--

As Figure 6 indicates, varying the initial $NO_2$ from 20% to 40% of the initial $NO_x$ in summer experiments could cause an increase in maximum oxidant of 20%. We did not test different initial $NO_2$ effects in winter runs. It is assumed, however, that increasing the initial percentage $NO_2$ from 20 to 30% or 45% would almost certainly increase maximum $O_3$ yields. This is also discussed in greater detail in Section 7.

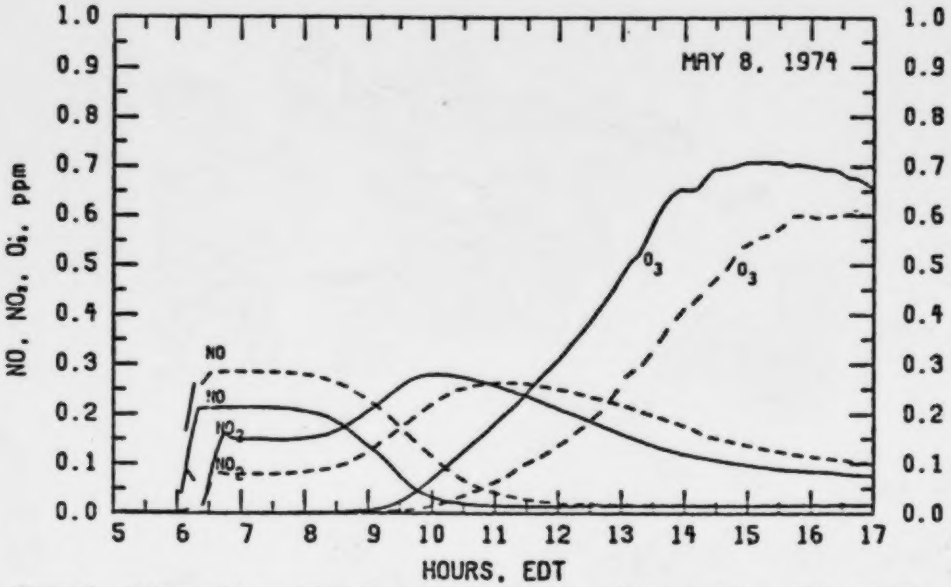

**Figure 6.** Differential percentage $NO_2$ run under clear sky. Initial conditions: $NO_x$(—) 0.364, (---) 0.366 ppm; $NO_2$(—) 0.151, (---) 0.079 ppm; NMHC(—) 3.40, (---) 3.20 ppmC urban hydrocarbon mix in UNC outdoor smog chamber.

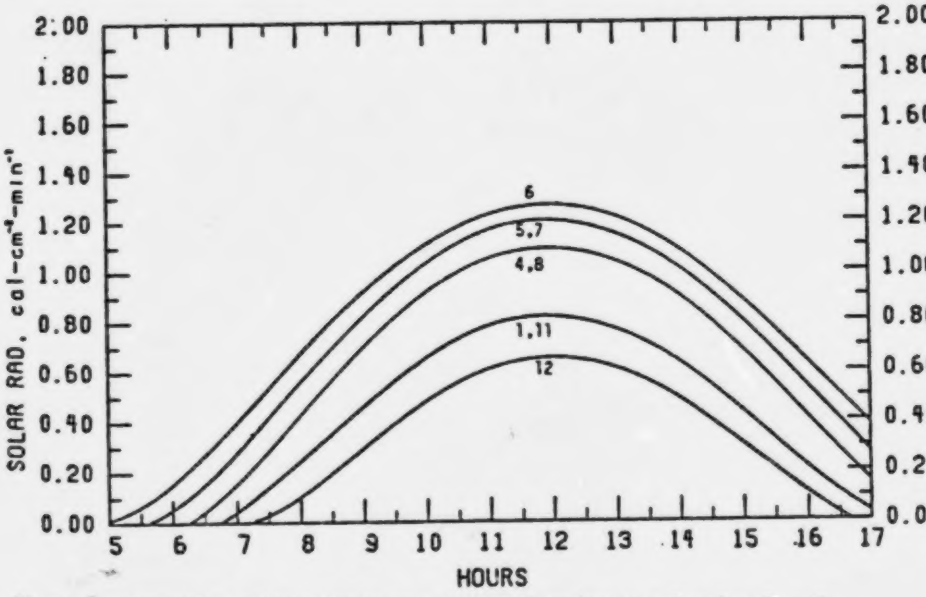

**Figure 7.** Theoretical solar radiation on a horizontal surface as a function of month. Numbers correspond to month.

TABLE 7. Effects of Acetaldehyde on Maximum $O_3$ Yield in Matched Dual Runs

| | Initial Conditions | | | | | | | |
|---|---|---|---|---|---|---|---|---|
| Date | HC,[a] ppmC | Aldehyde,[b] ppmC | $NO_x$, ppm | $NO_2$, % of $NO_x$ | Temp., °F | Maximum Temp., °F | Maximum $O_3$, ppm | Ratio[c] |
| 1/31/76 | 1.88 | 0.0 | 0.218 | 43 | 19.8 | 57.8 | 0.074 | 1.16 |
| 1/31/76 | 1.98 | 0.2 | 0.202 | 43 | 19.8 | 57.8 | 0.086 | |
| 3/7/76 | 3.13 | 0.0 | 0.211 | 25 | 31.2 | 62.0 | 0.171 | 1.23 |
| 3/7/76 | 3.13 | 0.3 | 0.214 | 25 | 31.2 | 62.0 | 0.210 | |

---

[a] Nonmethane hydrocarbon concentration for simulated urban mixture. Reported value does not include acetaldehyde concentration.

[b] Acetaldehyde concentration was approximately 10% of initial HC

[c] Ratio of maximum $O_3$ in run with added acetaldehyde to maximum $O_3$ in run without added acetaldehyde.

Direct Temperature Effects at Constant Initial Conditions--

It is suggested in Table 6, that at a constant set of initial conditions, the maximum $O_3$ decreases as the daily maximum temperature decreases. This trend was further confirmed by additional experiments in 1976. Table 8 presents data for three runs at different temperatures, and at each of two sets of initial conditions. These runs have relatively low initial HC and $NO_x$ conditions and therefore do not have a very large $O_3$ formation potential. The data do strongly suggest that a decrease in maximum temperature leads to a decrease in $O_3$ formation at these initial conditions. There does not appear to be a "cut-off" temperature, but rather a gradient effect, that is, a continuous association between temperature and $O_3$ production. It also appears that if a target concentration for $O_3$ is chosen, then a choice of a specific temperature below which $O_3$ will not exceed this target value becomes a function of initial conditions.

Comparison of Winter and Summer Outdoor Chamber Experiments--

A group of winter experiments were performed with initial urban mix HC and $NO_x$ concentrations closely matching previously performed summer

TABLE 8. Maximum Daily Temperature and Ozone Concentration for Two Sets of Similar Initial Conditions

| Initial Conditions | | | | | |
|---|---|---|---|---|---|
| HC ≃ 1 ppmC, $NO_x$ ≃ 0.1 ppm | | | HC ≃ 1 ppmC, $NO_x$ ≃ 0.2 ppm | | |
| | Maximum Value | | | Maximum Value | |
| Date | Temp., °F | $O_3$, ppm | Date | Temp., °F | $O_3$, ppm |
| 1/22/76[a] | 45.7 | 0.039 | 1/22/76[d] | 45.7 | 0.020 |
| 1/20/76[b] | 51.3 | 0.048 | 1/29/76[e] | 56.0 | 0.037 |
| 2/13/76[c] | 70.0 | 0.085 | 2/11/76[f] | 68.1 | 0.054 |

---

[a] IHC = 1.1 ppmC, $INO_x$ = 0.102 ppm, 44% $NO_2$, initial Temp. = 30.0°F, good sun, run started at 0900 EDT, appeared to reach $O_3$ potential. 100% maximum possible sunshine.

[b] IHC = 1.0 ppmC, $INO_x$ = 0.101 ppm, 43% $NO_2$, initial Temp. = 35.2°F, good morning sun, clouding up 1100-1200 EDT, clear afternoon, 67% maximum possible sunshine.

[c] IHC = 0.9 ppmC, $INO_x$ = 0.078 ppm, 58% $NO_2$, initial Temp. = 48.7°F, good morning sun, partial overcast after 1100 EDT. 29% maximum possible sunshine.

[d] IHC = 1.1 ppmC, $INO_x$ = 0.185 ppm, 31% $NO_2$, see note a.

[e] IHC = 1.07 ppmC, $INO_x$ = 0.194 ppm, 33% $NO_2$, initial Temp. = 39.5°F, run started at 1000 EDT, good sun. (3/10 sky cover).

[f] IHC = 0.9 ppmC, $INO_x$ = 0.2 ppm, 35% $NO_2$, initial Temp. = 56°F, partial overcast.

TYPING GUIDE SHEET

runs. As mentioned before, these winter runs did have additional acetaldehyde and a higher percentage of initial $NO_2$ which biases them toward higher $O_3$. They therefore represent a type of worst case winter condition for $O_3$ production.

The eleven runs of this type are paired with their summer and later summer-early fall counterparts in Table 9, which is arranged in the order of increasing HC to $NO_x$ ratio.

The results in Table 9 fall into two major categories: the runs in which the winter $O_3$ was 10-20% of the summer $O_3$ (first 6 pairs), and those in which the winter $O_3$ was 23-32% of the summer $O_3$ (last 5 pairs). Figure 7 shows theoretical total solar radiation profiles for the outdoor chamber site. These calculated curves include the seasonal effects of average dust concentration, water vapor concentration, and ozone aloft. Although a curve does not appear for September, its line can be interpolated between the line for month 8 and month 11. The curves indicate that the solar day in September is about 11 hours long, compared with 14 hours in June. In addition, the maximum value in June is approximately 1.23 $cal\text{-}cm^{-2}\text{-}min^{-1}$ compared with approximately 0.88 $cal\text{-}cm^{-2}\text{-}min^{-1}$ for September. At the UNC facility a detailed study by Saeger[7,8] shows that the specific photolysis rate for $NO_2$, the driving force for photochemical smog, is highly correlated to the shape of the total solar radiation curve, but does not correlate as well with UV measurements. All of this suggests that a September run will produce less $O_3$ than a June run at similar initial conditions. It is worth mentioning that regions more northern than North Carolina will have shorter solar days and less solar radiation during the winter months than in the runs reported here. This implies that northern cities would show a greater difference in $O_3$ maxima in winter vs summertime conditions.

The winter run conditions covered in Table 9 include: a HC concentration range of 1.07 to 4.3 ppmC, a $NO_x$ concentration range of 0.116 to 0.39 ppm, a HC to $NO_x$ ratio range of 5.5 to 24, and a maximum temperature range of 51.3 to 57.8°F.

The highest $O_3$ in all winter runs was only 0.183 ppm; for approximately the same range of conditions in summer, it was 0.66 ppm. This suggests at least a 72% reduction in $O_3$ maximum associated with

EPA-287 (Cin.)
(4-76)

## Table 9. Pairwise Comparison of Maximum $O_3$ Production for Winter and Summer Runs with Similar Initial Conditions of Reactants.[a]

| | Initial Conditions | | | | | | | |
|---|---|---|---|---|---|---|---|---|
| Date | HC, ppmC | $NO_x$, ppm | Ratio HC to $NO_x$ | Maximum Temp., °F | Maximum Solar Radiation, $ly\text{-}min^{-1}$ | Maximum $O_3$, ppm | Ratio of $O_3$, Winter to Summer | Percent[b] $O_3$ Reduction |
| 1/29/76 | 1.07 | 0.194 | 5.5 | 56.2 | 0.841 | 0.037 | 0.21 | 79 |
| 6/22/74 | 0.85 | 0.259 | 3.3 | 91.7 | 1.26 | 0.177 | | |
| 1/23/76 | 2.30 | 0.391 | 5.9 | 51.7 | 0.80 | 0.045 | 0.18 | 82 |
| 6/29/74 | 2.10 | 0.362 | 5.8 | 83.6 | 1.09 | 0.247 | | |
| 2/12/76 | 2.20 | 0.310 | 7.1 | 56.1 | 0.788 | 0.039 | 0.10 | 90 |
| 6/11/74 | 2.90 | 0.381 | 7.6 | 88.1 | 1.10 | 0.391 | | |
| 1/31/76 | 2.0 | 0.202 | 9.8 | 57.8 | - | 0.086 | 0.13 | 87 |
| 6/22/74 | 1.87 | 0.250 | 7.5 | 91.1 | 1.21 | 0.660 | | |
| 2/23/76 | 3.70 | 0.385 | 9.8 | 51.7 | 1.04 | 0.083 | 0.12 | 88 |
| 5/8/74 | 3.20 | 0.366 | 8.7 | 80.5 | 1.18 | 0.605 | | |
| 1/12/76 | 3.4 | 0.311 | 10.8 | 56.1 | 0.788 | 0.070 | 0.12 | 88 |
| 5/8/74 | 3.20 | 0.366 | 8.7 | 80.5 | 1.18 | 0.605 | | |
| 1/15/76 | 2.63 | 0.210 | 12.3 | 51.3 | 0.801 | 0.108 | 0.24[c] | 76 |
| 9/13/74 | 2.48 | 0.188 | 13.2 | 88.1 | 0.906 | 0.453 | | |
| 1/29/76 | 2.10 | 0.124 | 16.9 | 57.4 | 0.75 | 0.107 | 0.24[c] | 76 |
| 9/11/74 | 1.78 | 0.125 | 14.2 | 88.9 | 0.89 | 0.443 | | |
| 1/23/76 | 1.90 | 0.116 | 18.9 | 55.8 | 0.80 | 0.101 | 0.23[c] | 77 |
| 9/11/74 | 1.78 | 0.125 | 14.2 | 88.9 | 0.89 | 0.443 | | |
| 1/29/76 | 2.90 | 0.120 | 24.2 | 57.4 | 0.75 | 0.140 | 0.32[c] | 68 |
| 9/11/74 | 4.22 | 0.121 | 34.9 | 89.6 | 0.88 | 0.437 | | |
| 2/3/76 | 4.30 | 0.201 | 21.6 | 54.1 | 0.807 | 0.183 | 0.27[c] | 73 |
| estimated[d] | 4.00 | 0.200 | 20.0 | 90 | 1.10 | 0.7-0.8 | | |

---

[a] All winter runs had an additional 10% nonmethane HC acetaldehyde which is not included in the reported initial HC concentration. No acetaldehyde was used for summer runs. In addition, winter runs had 30-45% of the initial $NO_x$ as $NO_2$ while the summer runs had only 20% of initial $NO_x$ as $NO_2$.

[b] Computed by 100% ((max $O_3$ summer-max $O_3$ winter)/(max $O_3$ summer))

[c] September runs have shorter solar day, lower maximum solar radiation, and lower initial temperatures, all of which lead to lower $O_3$ yields than mid-summer conditions.

[d] Estimated outcome for given initial conditions based on experience with other runs at different conditions.

winter conditions of solar radiation and temperature. The lowest $O_3$ in winter runs in Table 9 was 0.037 ppm, whereas the lowest $O_3$ in all summer runs used for comparison was 0.177 ppm (and this summer run had a lower HC and a lower HC to $NO_x$ ratio than its paired winter counterpart). Here at least a 79% reduction in $O_3$ maximum at lower HC concentrations is indicated.

Individual winter and summer reductions in $O_3$ indicate that, for mid-summer comparison, the reductions are approximately 88%, while for late summer or early fall comparisons, the reductions are approximately 75%. It therefore appears that winter conditions similar to those reported in Table 9 will result in at least a 75% reduction in maximum $O_3$. Depending upon the season in which the comparison is made, there may be greater than 75% reduction. This minimum 75% reduction suggests that if mid-summer northern ambient $O_3$ values were greater than 0.4-0.48 ppm, the $O_3$ in winter may be above 0.12 ppm (assuming that maximum temperatures did not exceed $55^{\circ}$F).

It has been our experience that there is sufficient variation in natural conditions of temperature and solar radiation from day to day that replicate initial conditions on different days can lead to variation in $O_3$ yields of ±20%. All comparisons made so far should be tempered by this experimental variability.

### Extended Two and Three Day Experiments--

Two and three day irradiations were conducted by injecting smog precursors into the outdoor chambers during the first day and leaving the chambers closed (static grade) for the next 36-48 hours. A sample run is shown in Figure 8. The runs were intended to be static, but after three and one-half years of outdoor exposure, the wooden exterior frame which supports the chamber film had fatigued. This allowed leaks to develop under high wind stress, so that on windy days the intense pumping action of the wind on the Teflon would cause chamber dilution with background air. Since unreactive tracers were not used in these experiments, the actual amount of dilution is difficult to quantify. N-butane, which does exhibit some reaction, was used as an estimator of the dilution. Approximately 75% of the initial n-butane was left at the end of the first

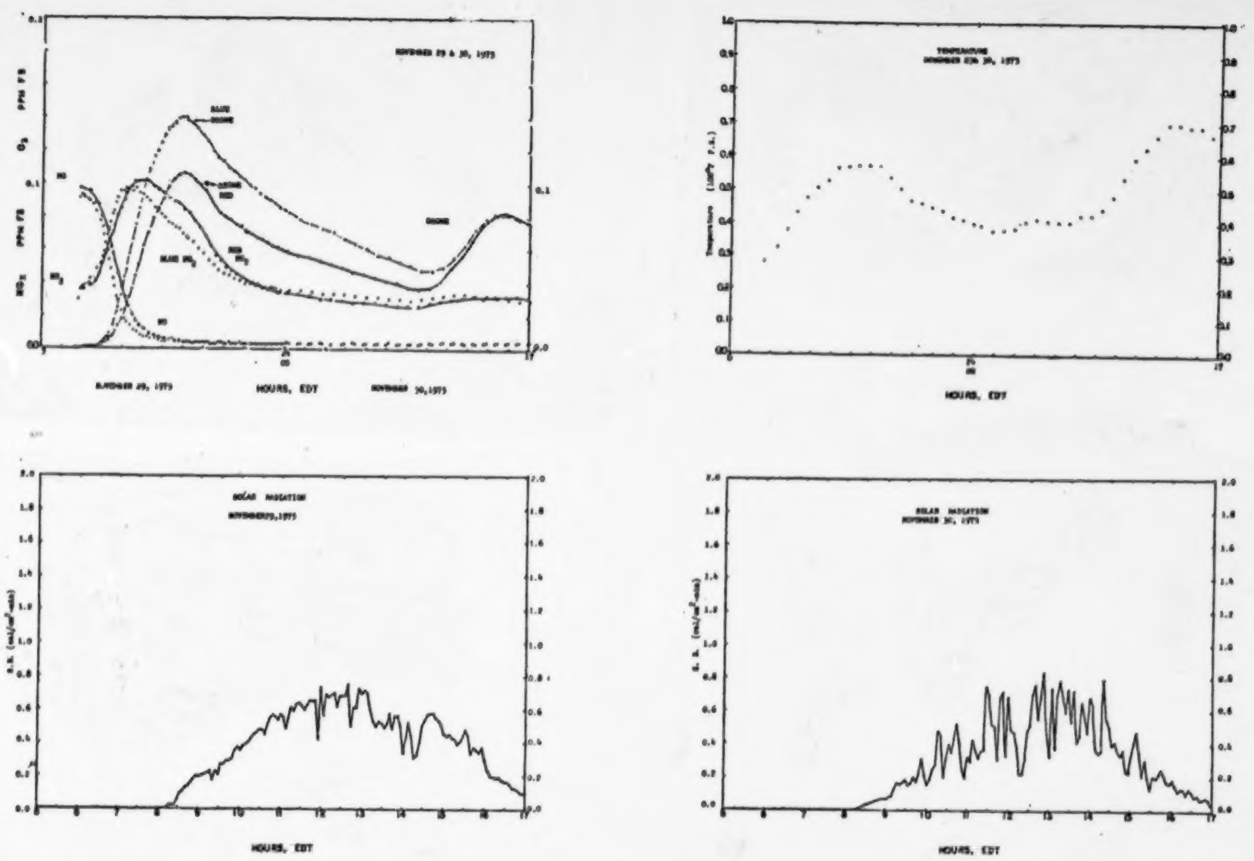

Figure 8. Experimental data for a two day late fall run; 2.9 ppmC mix in Red plus 0.3 ppmC acetaldehyde; 2.1 ppmC mix in Blue plus 0.21 ppmC acetaldehyde.

12 hour exposure. By 1200 EDT on the second day, approximately 50% of the n-butane remained, and only 25 to 30% remained by mid-afternoon of the third day. These dilution rates are lower than estimates of urban plume dilution down wind of metropolitan areas. Studies by UNC[9] and the Research Triangle Institute[10] suggest that $O_3$ in photochemical systems does not decrease in proportion to dilution.

In Table 10, 13 runs had initial $NO_x$ less than 0.3 ppm and produced less $O_3$ on the second and third days. The three runs (January 1 and 12, 1976 and February 3, 1976) which had higher initial $NO_x$ produced more, or very nearly the same, $O_3$ on the second day irradiation. In batch systems, whether the second day $O_3$ is higher or lower than the first day $O_3$ appears to be a function of first day initial conditions.[10] In particular, systems with initial $NO_x$ near 0.3 ppm and greater than 2 ppmC initial HC seem to produce second day $O_3$ nearly equal to, or greater than, first day $O_3$.

## Conclusions

Comparison of results from static winter and summer outdoor smog chamber runs having similar initial conditions of simulated urban hydrocarbon mix and $NO_x$ shows that maximum $O_3$ concentration and one hour average $O_3$ concentration in winter runs is lower than the summer $O_3$ values by at least 75%. In many cases, the reduction was 88%.

The temperature below which the $O_3$ is less than some target value is different for each set of initial concentrations of hydrocarbon and $NO_x$. In general, at temperatures of 51 to 58$^0$F, a hydrocarbon to $NO_x$ ratio approximately equal to or greater than 10 to 1 was required to produce maximum $O_3$ concentrations approximately equal to or greater than 0.1 ppm.

These winter runs were biased toward higher $O_3$ yields by adding acetaldehyde to the initial hydrocarbon and by adjusting the initial $NO_2$ to NO ratio to values higher than those used in summer runs. The results reported are therefore considered conservative.

Table 10. Summary of Initial Conditions, Maximum Temperature, and Maximum Ozone for Two and Three Day Winter Outdoor Chamber Runs.

| | Initial Conditions | | | | Maximum Temp. | | | Maximum Ozone | | | |
|---|---|---|---|---|---|---|---|---|---|---|---|
| Date | HC, ppmC | $NO_x$, ppm | $NO_2$, % of $NO_x$ | Temp., °F | Day 1, °F | Day 2, °F | Day 3, °F | Day 1, ppm | Day 2, ppm | Day 3, ppm | Comment |
| 11/29/76 | 2.9 | 0.120 | 24 | 32.2 | 57.4 | 70.4 | — | 0.140 | 0.082 | - | |
| 11/29/76 | 2.1 | 0.124 | 25 | 32.2 | 57.4 | 70.4 | -- | 0.107 | 0.081 | - | |
| 1/12/76 | 3.35 | 0.311 | 31 | 39.8 | 56.1 | 61.8 | -- | 0.069 | 0.088 | - | a |
| 1/12/76 | 2.17 | 0.310 | 32 | 39.8 | 56.1 | 61.8 | -- | 0.039 | 0.071 | - | a |
| 1/15/76 | 4.35 | 0.213 | 32 | 17.2 | 51.7 | 55.2 | -- | 9.182 | 0.072 | - | b |
| 1/15/76 | 2.63 | 0.210 | 32 | 17.2 | 51.7 | 55.2 | — | 0.108 | 0.096 | - | b |
| 1/17/76 | 1.10 | 0.130 | 42 | 40.0 | 32.2 | 32.0 | 35.8 | 0.011 | 0.039 | 0.044 | c |
| 1/17/76 | 1.10 | 0.210 | 42 | 40.0 | 32.2 | 32.0 | 35.8 | 0.007 | 0.038 | 0.047 | c |
| 1/31/76 | 1.98 | 0.202 | 42 | 19.8 | 57.8 | 32.0 | 45.1 | 0.086 | 0.046 | 0.025 | d,e |
| 1/31/76 | 1.88 | 0.218 | 43 | 19.8 | 57.8 | 32.0 | 45.1 | 0.074 | 0.045 | 0.036 | d |
| 2/3/76 | 5.45 | 0.316 | 32 | 25.0 | 54.1 | 68.8 | 67.0 | 0.110 | 0.105 | 0.082 | f |
| 2/3/76 | 4.34 | 0.201 | 30 | 25.0 | 54.1 | 68.8 | 67.0 | 0.201 | 0.141 | 0.106 | g |
| 2/13/76 | 1.15 | 0.085 | 52 | 48.7 | 70.6 | 68.0 | -- | 0.093 | 0.093 | - | |
| 2/13/76 | 0.90 | 0.078 | 58 | 48.7 | 70.6 | 68.0 | — | 0.084 | 0.083 | - | |
| 12/3/76 | 0.50 | 0.050 | 90 | 31.1 | 65.4 | 62.0 | 70.0 | 0.051 | 0.036 | 0.036 | h |
| 12/3/76 | 0.30 | 0.040 | 90 | 31.1 | 65.4 | 62.0 | 70.0 | 0.057 | 0.059 | 0.072 | |

---

[a] $O_3$ did not reach full potential because of overcast on afternoon of 1/13/76

[b] Good sun on 1/15/76, slight choppiness in solar radiation on 1/16/76. Some dilution occurred in 4.35 ppmC run.

[c] Snow on 1/17/76, clear on 1/18/76 and 1/19/76

[d] Rained on 1/1/76, dilution and reaction (as determined by n-butane concentration) left 30% of initial material at end of 1/2/76.

[e] Run with 1.98 ppmC NMHC had an additional injection of acetaldehyde equal to 10% of reported initial HC but not included in HC initial condition value reported here.

[f] Dilution and reaction (as determined by n-butane concentration) left 34% of initial material on second day, 15% on third day.

[g] Dilution and reaction (as determined by n-butane concentration) left 50% of initial material on second day, 30% on third day.

[h] Dilution and reaction (as determined by n-butane concentration) left 50% of initial material on second day, 30% on third day.

# SEASONAL EFFECTS FOR SINGLE HYDROCARBON AND $NO_x$ MIXTURES

## Introduction

It is clear from the experimental work presented in the previous section that different seasonal conditions can have a profound effect on $O_3$ production from a given smog chamber mixture. To gain additional insight into the various ways that changes in outdoor physical conditions can affect $O_3$ production, simpler rather than more complex smog systems were investigated. In this study single hydrocarbon-$NO_x$ systems with propylene, ethylene, acetaldehyde, and butane were examined. Experimental work for this program formally began in mid-October 1977 and continued through March 1978. Detailed comparisons of runs with similar initial chemical conditions were made and a modeling study initiated to simulate and help explain the seasonal effects observed on propylene and smog systems.

## Results

### General--

A total of 29 dual experiments (58 conditions) were performed. From these, experiments with clear sky conditions were selected; these are summarized in Table 11 and 12.

The maximum $O_3$ concentration for propylene runs in Table 11 was plotted against the average run temperature (Figure 9). Note that the data were first divided into two classes depending upon initial hydrocarbon (HC). These were: HC between 3 and 4 ppmC, and HC between 1.6 and 2.2 ppmC. A similar procedure was used for ethylene-$NO_x$ runs. The selected ethylene runs are given in Table 12 and a plot of maximum $O_3$ vs temperature is shown as Figure 10. The three hydrocarbon classes for Figure 2 were: HC between 3 and 4 ppmC, HC between 1.4 and 1.9 ppmC, and HC less than 1 ppmC.

Comparing Figures 9 and 10 suggests that ethylene-$NO_x$ systems at certain concentration regimes may be more temperature sensitive in terms of $O_3$ production than propylene-$NO_x$ systems.

Table 11. SELECTED PROPYLENE RUNS WITH CLEAR SKY CONDITIONS

| Date | Initial $NO_x$, ppm | Initial HC, ppmC | Temperature, °F | | Maximum $O_3$, ppm |
|---|---|---|---|---|---|
| | | | initial | final | |
| 10/22/77 | 0.5 | 3.73 | 36 | 75.6 | 0.702 |
| 11/09/77 | 0.520 | 3.76 | 51 | 65 | 0.679 |
| 1/27/78 | ~0.50 | ~3.8 | 23 | 44 | 0.520 |
| 1/28/78 | 0.501 | 4.04 | 19 | 41 | 0.545 |
| 1/29/78 | 0.481 | 3.99 | 9 | 37 | 0.467 |
| 5/07/74 | 0.503 | 2.09* | 52 | 77 | 0.715 |
| 11/09/77 | 0.524 | 1.92 | 51 | 65 | 0.408 |
| 8/08/77 | 0.495 | 1.56 | 75 | 100 | 0.884 |
| 1/11/78 | 0.482 | 3.85 | 9 | 36 | 0.482 |
| 1/10/78 | 0.481 | 3.25 | 10 | 30 | 0.361 |
| 12/29/77 | 0.430 | 3.38 | 15 | 39 | 0.360 |
| 1/04/78 | 0.415 | 2.92 | 18 | 42 | 0.431 |
| 12/29/77 | 0.425 | 1.63 | 12 | 41 | 0.032 |
| 12/26/77 | 0.395 | 2.96 | 18 | 33 | 0.384 |
| 12/22/77 | 0.381 | 3.22 | 29 | 91 | 0.468 |
| 12/22/77 | 0.389 | 1.69 | 29 | 41 | 0.102 |

*10% initial $NO_2$

Table 12. Selected Ethylene Runs

| | Initial | Initial | Temperature, °F | | Maximum |
|---|---|---|---|---|---|
| Date | HC, ppmC | $HO_x$,ppm | Initial | Maximum | $O_3$, ppm |
| 10/18/77 | 3.84 | 0.486 | 28.4 | 69.4 | 0.916 |
| 11/20/77 | 3.49 | 0.444 | 27.6 | 64.3 | 0.751 |
| 1/17/78 | 3.8 | 0.468 | 8.8 | 37.1 | 0.206 |
| 8/11/77 | 1.49 | 0.520 | 66.7 | 100.3 | 0.863 |
| 11/12/77 | ~1.90 | 0.430 | 2.61 | 52.0 | 0.038 |
| 10/18/77 | 1.88 | 0.489 | 28.4 | 69.4 | 0.467 |
| 10/19/77 | 1.97 | 0.485 | 42.2 | 75 | 0.587 |
| 8/11/77 | 0.74 | 0.556 | 66.7 | 98.25 | 0.169 |
| 10/19/77 | 0.99 | 0.489 | 41.0 | 75.1 | 0.080 |

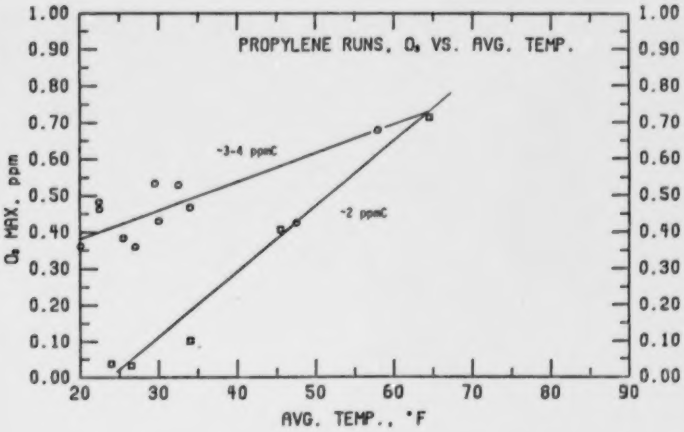

Figure 9. Maximum ozone as a function of the average of initial and maximum chamber air temperature for two ranges of initial propylene concentrations at approximately 0.5 ppm $NO_x$.

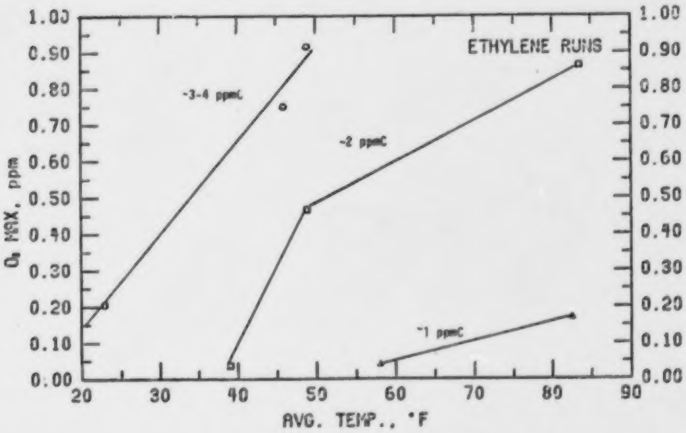

Figure 10. Maximum ozone as a function of the average of initial and maximum chamber air temperature for three ranges of initial propylene concentrations at approximately 0.5 ppm $NO_x$.

### Detailed Examination of Propylene Runs--

Table 11 lists several runs that had essentially the same initial chemical conditions but were performed under a wide range of temperature conditions. One of the runs listed, October 22, 1977, is described in detail in Section 7. This run was selected as a "baseline" run because it had fairly complete product data (Figure 11a) and it was the highest temperature, high concentration propylene run in the data set.

The first propylene smog system comparison between runs with similar initial chemical conditions is shown in Figure 11b. This figure shows the results of the October 22, 1977 propylene experiment and those of January 28, 1978. The target concentrations for both runs were 3.8 ppmC propylene and 0.5 ppm $NO_x$. Plots of both runs were adjusted to the same sunrise time so that $NO$-$NO_2$ crossover times could be compared (sunrise on October 22 was 0728 and on January 28, 0802 EDT) (Figure 12). The morning temperatures at sunrise for the October and January runs were 35.8°F and 18.8°F. The afternoon maxima were 70.2°F and 40.1°F (Figure 13).

Little change can be seen in the shape of the morning profiles. $NO_2$-$NO$ crossover time differs only by 28 minutes (after aligning sunrise times) and, in general, one is led to believe that this 20 to 30°F temperature difference did not greatly affect the important parts of the morning smog chemistry. If these two days were replotted with the same $NO_2$-$NO$ crossover time, both sets of profiles would almost coincide until the $O_3$ concentrations began to exceed 0.1 ppm. Beyond this point, the warmer October day produced a much faster rise in $O_3$. Figure 11c shows the two days of Figure 11b (October 22, 1977 and January 28, 1978) and a third propylene/$NO_x$ experiment (January 29, 1978) with nearly identical initial conditions. It would be expected that the light intensity conditions for January 28 and January 29 would be very similar (Figure 12). The air temperatures for January 29, however, were much lower than January 28; the sunrise temperature for January 29 was 9°F compared to 19°F for January 28 and the afternoon maximum temperature was only 36°F compared to 40°F (Figure 13). The morning conversion of $NO$-to-$NO_2$ for January 29 was slower than on January 28. The afternoon $O_3$ production rate on the 29th was slower; resulting in a lower maximum $O_3$ than the previous day.

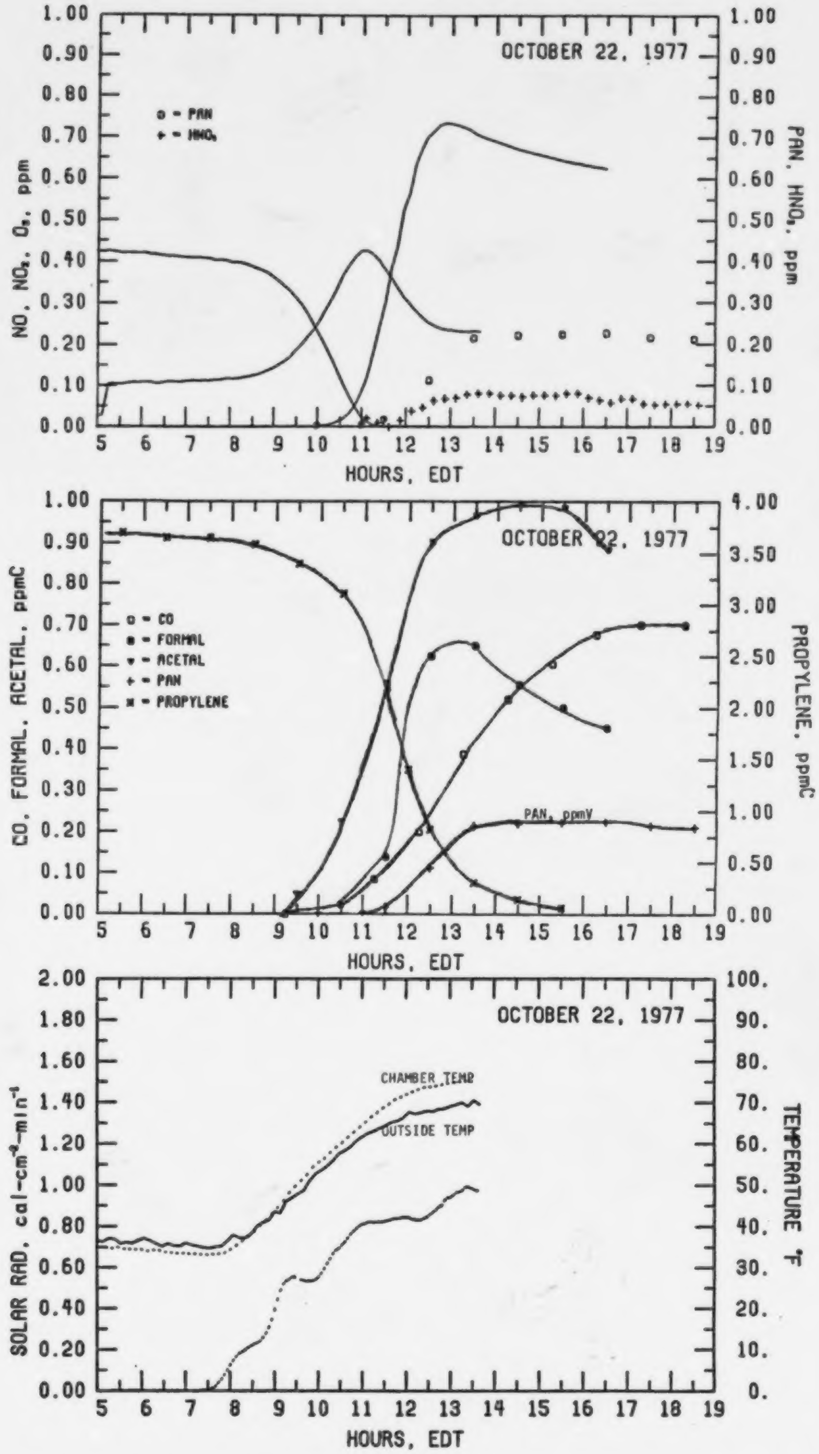

Figure 11a. Experimental data for October 22, 1977.

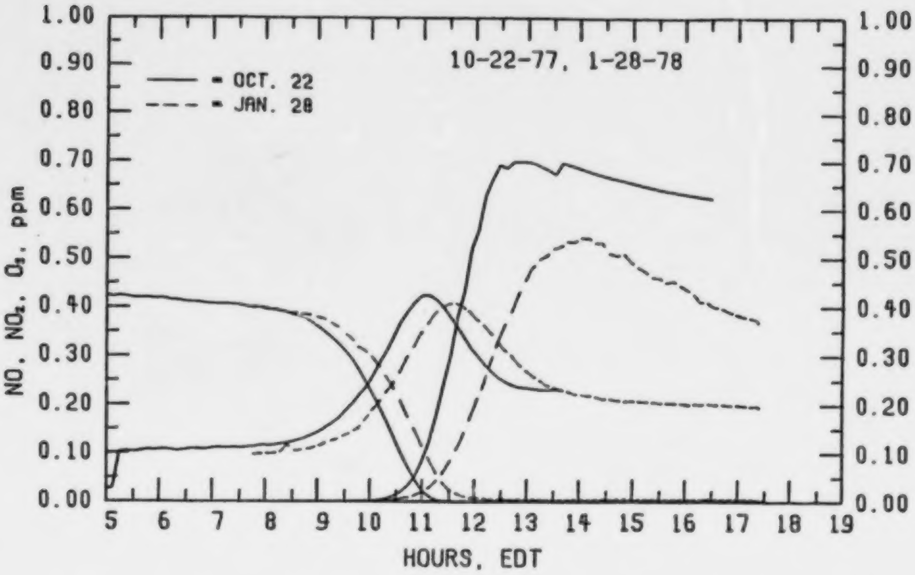

Figure 11 b. Comparison of propylene/$NO_x$ experiments (3.8 ppmC $C_3H_6$, 0.5 ppm $NO_x$, 20% $NO_2$). October 22, 1977 (——) initial to max temperature: 35.8 to 70.2°F; January 28, 1978 (– – –) initial to max temperature: 18.8 to 40.1°F.

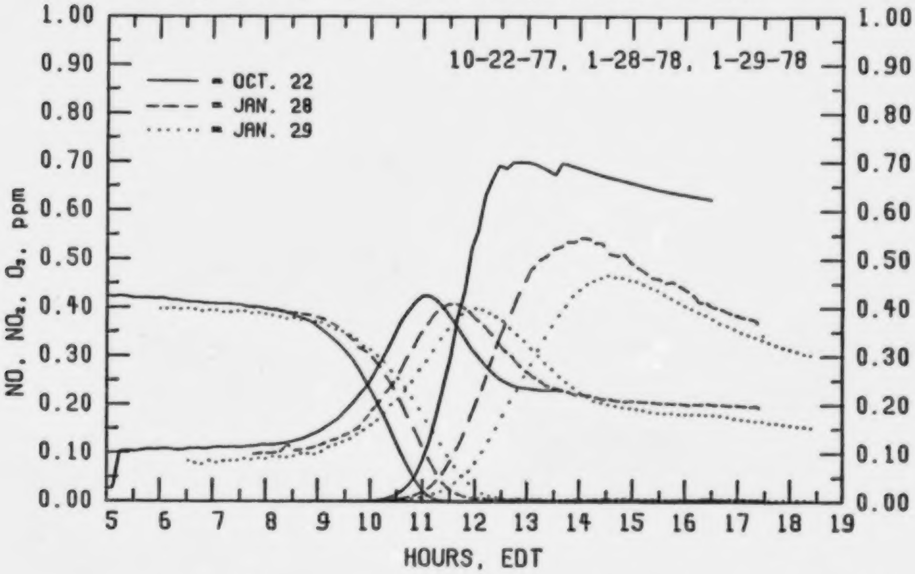

Figure 11 c. Comparison of three propylene/$NO_x$ runs with initial conditions: 3.8 ppmC propylene, 0.50 ppm$^1$ $NO_x$, 20% $NO_2$. Temperature ranges: October 22, 1977, 35-70°F (——); Jan. 28, 1978, 18-40°F (– – –); Jan. 29, 1978, 8-34°F (·····). Jan. curves shifted to left to align sunrise times.

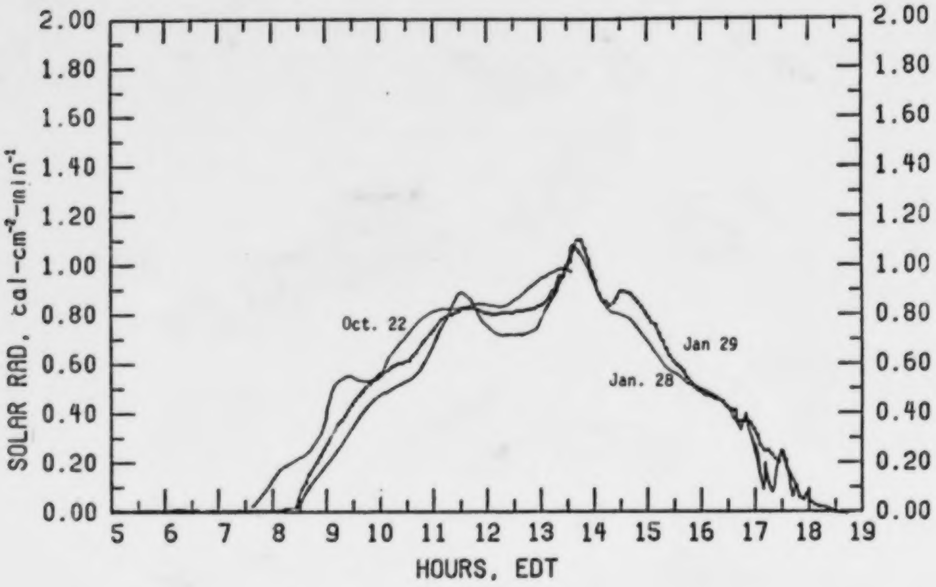

Figure 12. Total Solar Radiation profiles for a fall and two winter days.

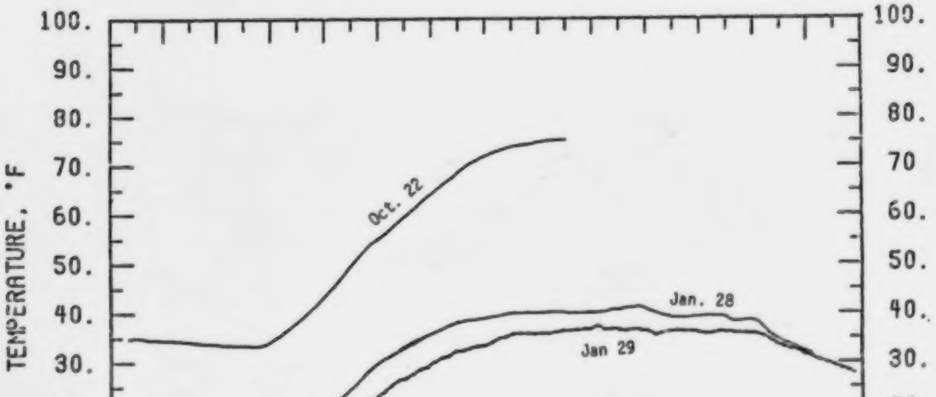

Figure 13. Chamber air temperature for propylene/$NO_x$ runs.

A similar examination of other runs listed in Table 11 (making appropriate allowances for small differences in initial $NO_x$) supports the above conclusion. The January 11, 1978 run, for example, had a crossover time approximately 45 minutes later than October 22, 1977 when adjusted for sunrise time and slight differences in initial $NO_x$. This compares very well with the difference in crossover between the January 28 and October 22 runs (Figure 11b). The difference in initial temperature between the October 22 and January 11 days was 27°F. At the time crossovers were reached, the difference was still 28°F. Table 11 shows that the $O_3$ maximum for January 11 was 0.482 ppm compared with October 22's 0.702 ppm. It thus appears that in propylene-$NO_x$ runs, lower temperatures slightly inhibit the NO-to-$NO_2$ oxidation rate but can significantly alter the amount of $O_3$ produced. Potential causes of these effects of temperature on $O_3$ will be discussed in the modeling section.

### Examination of Ethylene Runs--

Figure 14 compares the two highest concentration ethylene runs with the largest temperature difference. Although the initial NO concentrations were not as well matched in these runs as in other runs, the carbon concentrations and temperature ranges were almost identical to the October 22, 1977 and January 29, 1978 propylene runs shown in Figure 12. This allows not only a comparison of results for temperature ranges for ethylene, but also a relative comparison of ethylene and propylene at two different temperatures.

As seen in Figure 14, even allowing for the difference in sunrise (curves are already shifted) and initial NO concentrations, the cold (9-37°F) January 11 ethylene run was approximately one hour slower than its counterpart run on October 18, 1977. The $NO_2$ peak was even more delayed in the lower temperature run than in the comparable propylene runs in Figure 11. Ozone suppression was much greater during the cold ethylene compared to the cold propylene runs.

### Examination of Acetaldehyde Runs--

An examination of acetaldehyde-$NO_x$ runs shows temperature effects

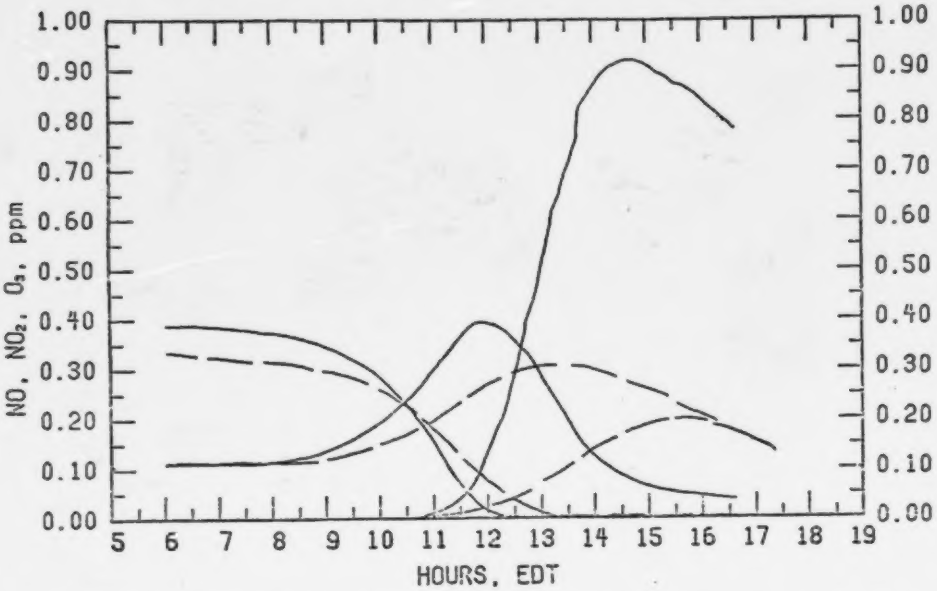

Figure 14. Comparison of two ethylene/$NO_x$ runs with similar initial conditions: October 18, 1977 (——): 3.84 ppmC $C_2H_4$, 0.486 ppm $NO_2$: initial T, 28.4°F; maximum T, 69.4°F; sunrise, 0730h EST; Jan. 11, 1978 (– –): 3.8 ppmC $C_2H_4$, 0.468 ppm $NO_x$; initial T, 8.8°F; maximum T, 37.1°F; sunrise 0830h EST. Jan 11 curves shifted to left to align sunrise times.

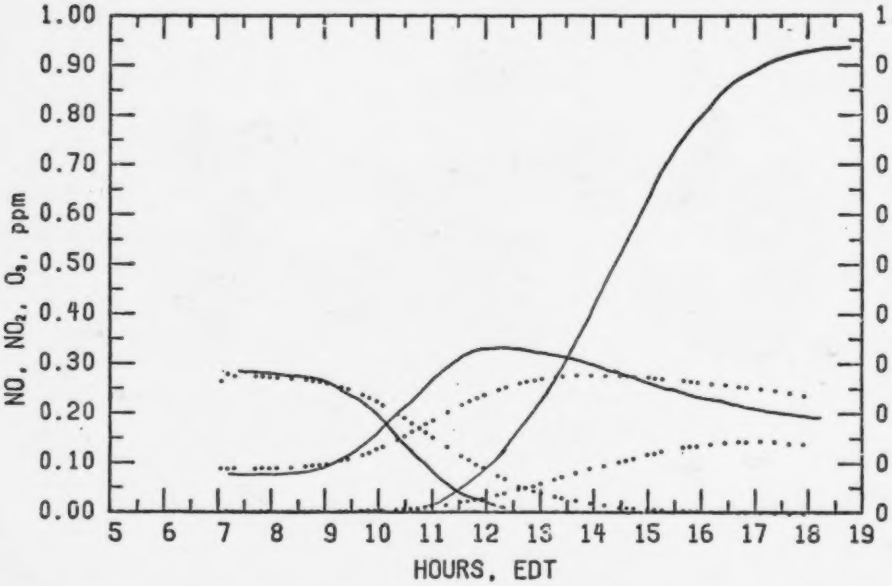

Figure 15. Comparison of two acetaldehyde/$NO_x$ runs with initial conditions: May 18, 1977 (——): 1.87 ppmC RCHO, 0.350 ppm $NO_x$, 0.072 ppm $NO_2$; Feb. 27, 1978 (····): 1.72 ppmC RCHO, 0.360 ppm $NO_x$, 0.087 ppm $NO_2$. May 18 temperature (69-96°F), February 27 temperature (16-49°F).

similar to those of propylene and ethylene. To illustrate these effects in detail a warm run (May 18, 1977, initial temperature 69°F, maximum temperature 96°F), and a cold run (February 27, 1978, initial temperature 16.4°F, maximum temperature 49.4°F) were plotted together in Figure 15. As in the propylene plots, the curves have been aligned at sunrise (0604 hr for May 18, 1977; 0744 hr for February 27, 1978). Once again, the winter run required more time to reach $NO_2$-NO crossover and produced substantially less maximum $O_3$; $NO_2$ concentration profiles, however, appear to be more affected for acetaldehyde than for propylene.

## Discussion of Experimental Results

Although total light intensity, spectral changes, and air temperature all change with season, air temperature is the factor that changes the most. The chemical conditions for the runs presented were selected so that the systems would be primarily $NO_x$ limited and not time or light limited. That is, HC concentrations were high enough that usually $NO_2$ was either nearly or totally consumed in early afternoon and $O_3$ reached a maximum primarily because $NO_2$ was consumed and not because the sun was setting. This choice reduced the impact of a shorter solar day and a lower maximum light intensity for winter runs. To some extent, the choice of initial conditions would also lessen the effects of shifts in short wavelength solar spectrum as a result of seasonal changes. Based on System Application, Inc.'s (SAI) modeling results for the University of California at Riverside (UCR) chamber, such shifts would probably affect the initiation time of a system. Since the runs essentially "went to completion" in the early afternoon, such shifts in the speed of the systems would be visible in the data, but would probably not be a major factor controlling maximum $O_3$. This suggests that air temperature was the principal cause of the observed effects on $O_3$ maxima.

All single hydrocarbons and aldehydes tested showed strong seasonal effects. The strength of these effects, in roughly increasing order, was propylene < ethylene < acetaldehyde on a ppmC basis.

The fact that each individual hydrocarbon or aldehyde system exhibited seasonal effects suggests that the origin of the effect would be in some common aspect of the organic portions. That the effect also differs in strength for each organic compound suggests that the process may, in part, be dependent upon organic structure (i.e. some "reactivity"-type factor). Such a dependency, however, does not exempt some temperature dependent inorganic process from partial responsibility.

Additional discussion will be presented after the modeling results have been described.

Sources of Kinetic Information Used

Major advancements in both radical and nitrogen chemistry have been made since 1977. Much interest has been given to the formation of nitric acid by either reaction 1 or 2.

$$NO_2 + OH \rightarrow HNO_3 \qquad (1)$$

$$N_2O_5 + H_2O \rightarrow 2\ HNO_3 \qquad (2)$$

Some researchers had assumed that the reaction between OH and $NO_2$ was unimportant because: 1) a low third order rate constant had been determined by Niki (1970, in Gay et al. 1971)[11] and 2) the belief that OH concentrations were high only in the initial phase of the irradiations, and 3) that the OH would be consumed by the much faster reactions with hydrocarbons (olefins). The assumption was that $HNO_3$ was formed principally from hydrolysis of $N_2O_5$. It was later demonstrated that OH concentrations are considerable late in the irradiation experiments. Furthermore, the rate constant for the OH + $NO_2$ reaction was greatly underestimated. A new value of 14,000 ppm$^{-1}$ (almost three times the earlier value) was utilized (NASA 1977).[12]

Chameides (1978),[13] Cox (1978),[14] and Fishman (1978)[15] all discussed the importance of two reactions whose rates have increased significantly through reevaluation. Howard's (1977)[16] new direct determination of $HO_2 + NO \rightarrow OH + NO_2$ is six times faster than earlier estimates. Second, the rate of $CO + OH \rightarrow CO_2 + HO_2$ has been redetermined to be faster than previously accepted. This and other similar mechanistic sequences allow greater than previously accepted $HO_2$

and OH pathways, consistent with a greater generation of $HNO_3$ by OH + $NO_2$.

Another important discovery was that PAN chemistry (Reaction Scheme 3) is very similar to $N_2O_5$ chemistry (Hendry 1977[17] Cox and Roffey 1977),[18] (Reaction Scheme 4) with PAN decomposition more temperature dependent than that of $N_2O_5$. An important aspect of this sequence is that PAN decomposes to the original reactants.

$$\begin{aligned} CH_3C(O)O_2 + NO &\rightleftarrows NO_2 + CH_3C(O)O \\ CH_3C(O)O_2 + NO_2 &\rightleftarrows PAN \\ PAN &\rightleftarrows CH_3C(O)O_2 + NO_2 \end{aligned} \qquad (3)$$

$$\begin{aligned} NO_3 + NO &\rightleftarrows 2NO_2 \\ NO_3 + NO_2 &\rightleftarrows N_2O_5 \\ N_2O_5 &\rightleftarrows NO_3 + NO_2 \end{aligned} \qquad (4)$$

Another new addition is the kinetics surrounding the discovery of gaseous $HO_2NO_2$ (pernitric acid or PNA) formed via $HO_2$ + $NO_2$ (Niki 1977).[19] Graham et al. (1977),[20] Simonaitis (1977).[21] Hanst and Gay (1977),[22] Levine et al. (1977),[23] Baldwin et al. (1977),[24] and Uselman et al. (1978)[25] have all discussed the significance of this compound and the effect it has on the photochemical smog mechanism. Graham et al. (1977)[20] and Hanst and Gay (1977)[22] have shown that the half-life of $HO_2NO_2$ (PNA) is short and temperature dependent, and that it thermally decomposes back to $HO_2$ and $NO_2$. Previous studies had reported that HONO was the principal product of the $HO_2$ + $NO_2$ reaction (Cox and Derwent 1975)[26]. Grahman et al. (1977)[20] and Hanst and Gay (1977)[22] showed that no HONO (nor peroxyformylnitrate) could be detected.

TYPING GUIDE SHEET

HONO has played an important role in the development of nitrogen chemistry. Since the OH radical is believed to be one of the most important active free radicals, HONO has been investigated and treated by many as a major intermediate of this radical. Photolysis of HONO yields OH and NO. Cox and Derwent (1975)[26] among others, had concluded earlier that the major source of HONO was the reaction of $HO_2$ with $NO_2$. It has already been mentioned that this reaction is now known to produce predominantly PNA. Chan et al. (1976)[27] showed that other reactions, namely $NO + NO_2 + H_2O \rightarrow 2$ HONO, proceed very slowly and questioned whether it is measurable in the atmosphere. It has been postulated that HONO might form to a small extent in concentrated tail pipe auto exhaust concentrations (Demerjian et al. 1974),[28] and have a role as an initiating source of OH radicals in the morning hours. Direct measurement for OH + NO   HONO by Howard[16] resulted in a rate constant three times greater than previous estimates; photolysis rates however, have also been increased by a factor of three based on new data (Cox and Derwent 1976;[29] Stockwell and Calvert 1978)[30]. These measurements plus Howard's higher rate for $HO_2 + NO \rightarrow OH + NO_2$ and the new PNA mechanism minimize the importance of HONO and make PNA more important.

Niki (1978)[31] presented spectroscopic evidence for the formation of $RO_2NO_2$ type compounds via $RO_2 + NO_2$ for carbons 1-6. It has been speculated that these compounds behave similarly to PAN type compounds and PNA, in that they exhibit a strong temperature dependence on decomposition. These species therefore become another temporary $NO_2$ "storage" mechanism. The kinetic data, other than the expected activation energy, are unknown and must be estimated. Values are expected to be intermediate to PAN and $HO_2NO_2$.

## Assumptions in Mechanism Construction

Before the seasonal study, the mechanism used for computer simulation of UNC smog chamber experiments was the result of modeling mostly summer-type experiments. The organic chemistry (OH + olefin, $O_3$ + olefin) was fairly well established and will be presented in Appendix B. The formation rate of $HNO_3$ utilized ranged from 5,000-9,000 ppm$^{-1}$ min$^{-1}$ from theoretical estimates. Either Cox's or Hendry's rates

EPA-287 (Cin.)
(6-76)

TYPING GUIDE SHEET
BEGIN FIRST LINE OF TEXT HERE
CENTER OF PAGE
TOP OF IMAGE AREA
DROPPED HEAD; BEGIN SECTIONS HERE

for PAN formation and decomposition were used. A low rate for hydrolysis of $N_2O_5$ was used. Methyl peroxynitrate ($CH_3OONO_2$) was formed in small quantities, and the formation of PNA with decomposition back to $HO_2$ and $NO_2$ was not always included (rates from theoretical estimates).

Modeling has concentrated mainly on the results of the propylene smog chamber runs of August 8, 1977, October 21, 1978, and the previously discussed October 22, 1977, January 28, 29, 1978. Time vs concentration plots of the critical data from these runs are shown in Figure 16a and 16b. In all of these experiments, the initial $NO_x$ was about 0.5 ppm (20% $NO_2$) and all were $NO_x$ limited. The initial propylene concentration was about 1.5 ppmC in the August run and about 3.5 ppmC in all of the cooler experiments. The experiment of October 21, 1978 had matched initial conditions in each side of the chamber. However, one side had been dried with molecular sieve.

In 1977, Howard published rates (determined by direct measurements) for the formation and decomposition of PNA, concluding that the decomposition of PNA yielded predominantly $HO_2$ and $NO_2$ as others had suggested. His temperature dependent decomposition rate indicated that PNA might form to appreciable amounts in cooler conditions such as the October 22, 1977 experiment. Therefore Howard's rates were included in the first modeling effort of the August 8, 1977 and October 22, 1977 experiments.

The optimum fitting of both of these experiments could be achieved with the same model by 1) setting the formation rate of $HNO_3$ at 12,000 $ppm^{-1} min^{-1}$, 2) utilizing Cox's PAN rates, and 3) forming PNA at 9,000 $ppm^{-1} min^{-1}$ with an adjusted decomposition rate (while maintaining a low rate of hydrolyzed $N_2O_5$ lost to the walls). These fits (Figure 17a and 17b) were less than perfect but considered successful in view of the range of temperature and magnitude of initial conditions. A description of the mechanism as developed by Jeffries and Sexton is given in Appendix B.

The results obtained from the runs performed on January 28 and 29, 1978 presented another challenge to the model. The profiles of these runs have already been presented and compared with October 22, 1977, an experiment with similar initial conditions (Figure 11a-c and Figures 12

BEGIN LAST LINE OF TEXT
BOTTOM OF IMAGE AREA; OUTSIDE DIMENSION FOR TABLES AND ILLUSTRATIONS

PAGE NUMBER
EPA-287 (Cin.)
(4-76)

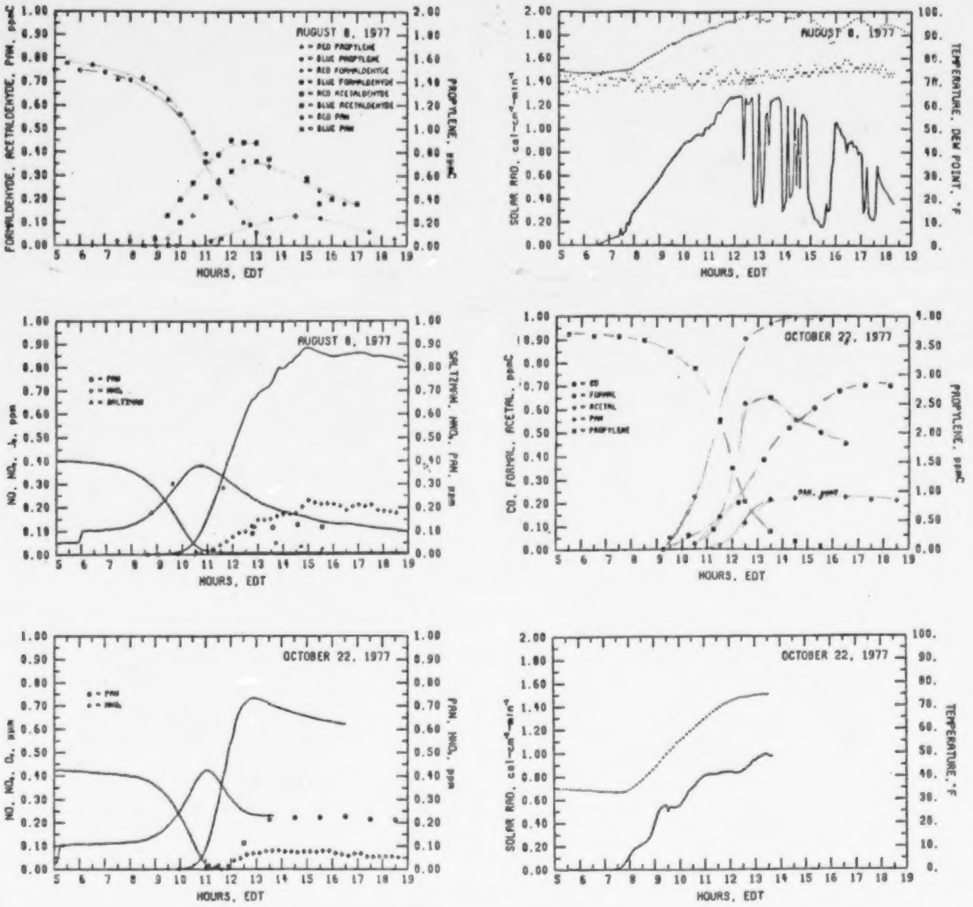

Figure 16a. Experimental data from August 8 and October 22, 1977.

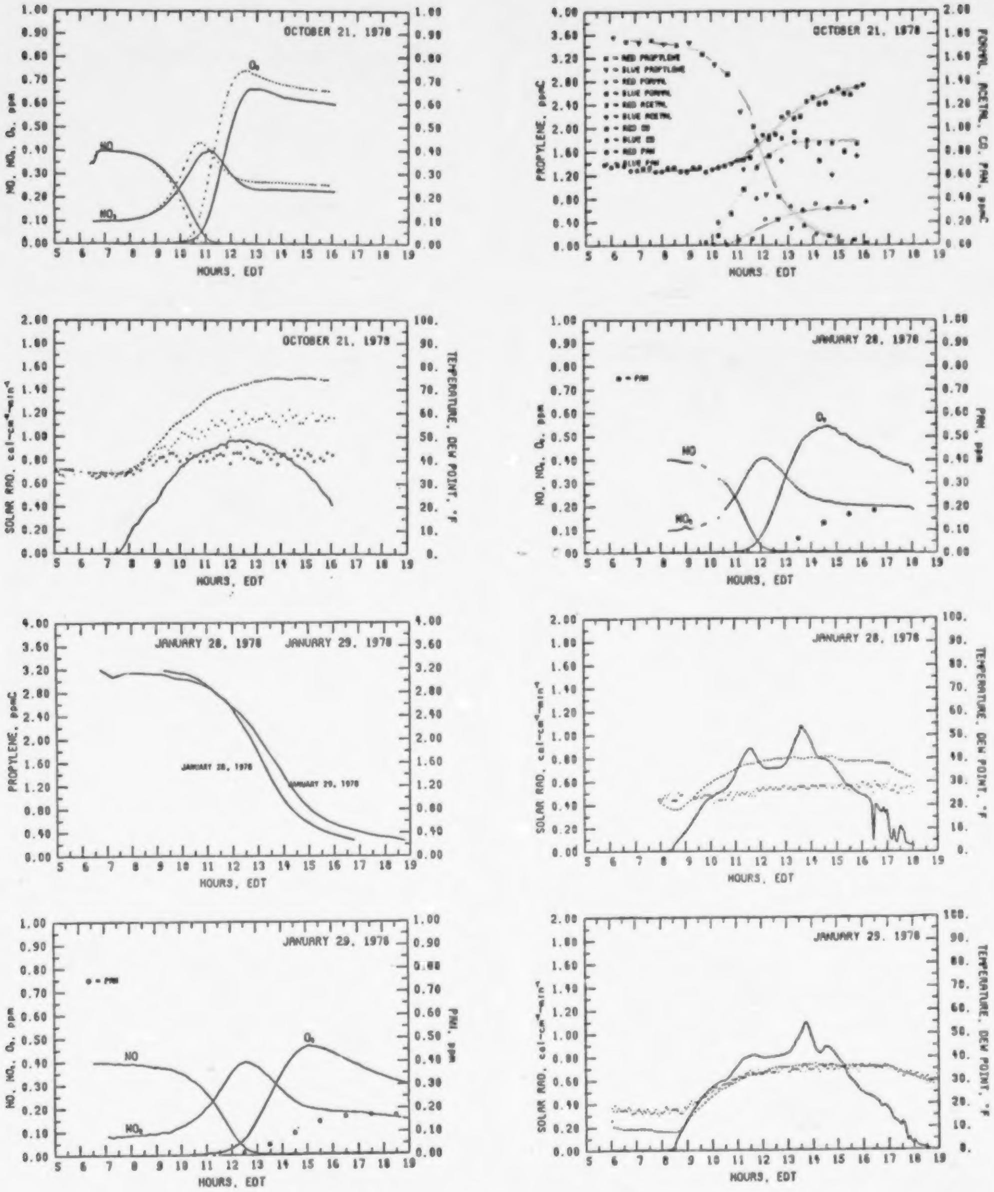

Figure 16b. Experimental data from October 21, January 28, and January 29, 1978.

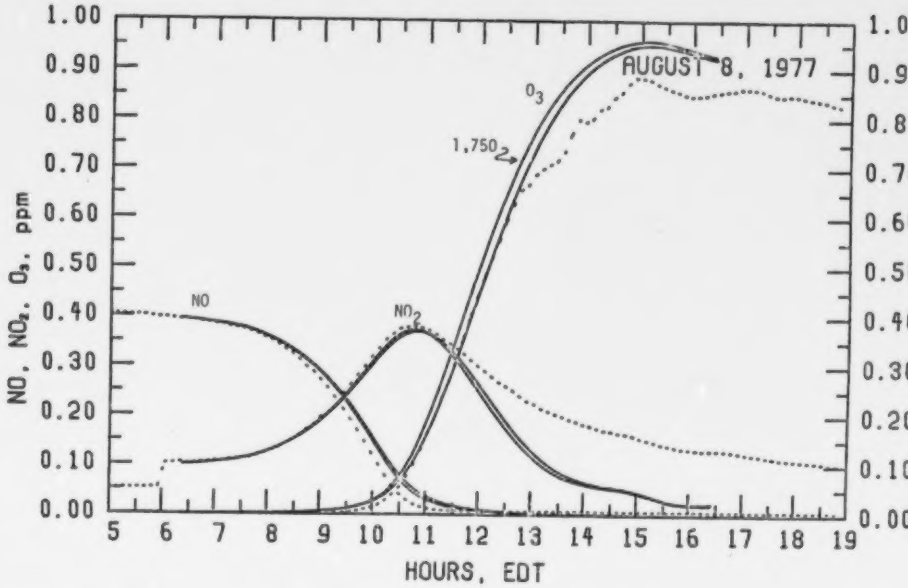

FIGURE 17a. Computer simulations of August 8, 1977 experiment with formation rate constant of PNA at 1,750 and 9,000 ppm$^{-1}$min$^{-1}$. Smog chamber profiles also shown (---).

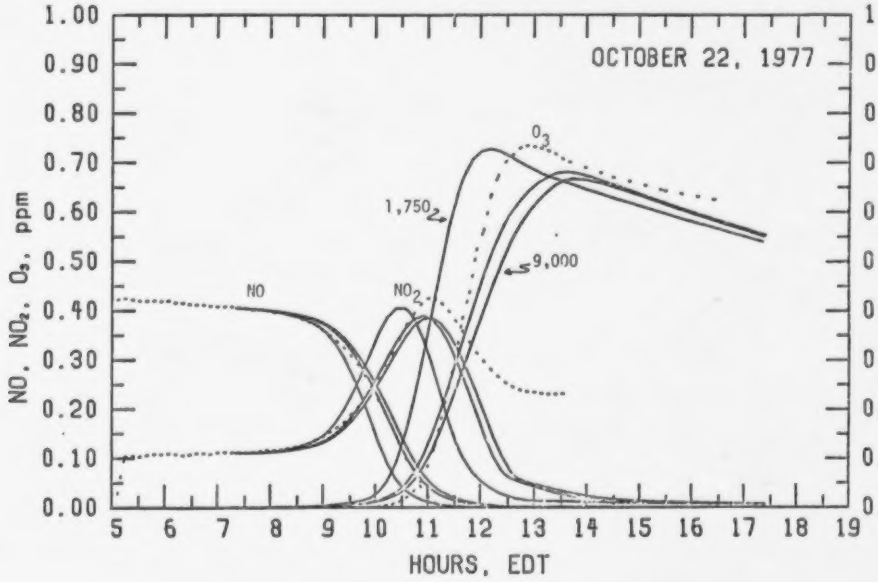

FIGURE 17b. Computer simulations of October 22, 1977 experiment with formation rate constant of PNA at 1,750, 8,000, and 9,000 ppm$^{-1}$min$^{-1}$. Smog chamber profiles also shown (---).

and 13). The effect of temperature was apparent. The same model, however, given the temperature and light profiles and initial conditions of the cold January experiments, resulted in very low $O_3$ production and high final PNA concentrations. Kinetic rate parameters (activation energies, frequency factors, and rate constants) were adjusted within acceptable uncertainty limits for many reactions capable of accounting for seasonal effects. The formation of PNA (peroxynitric acid) had been incorporated into the earlier version of the model with a rate constant of 9,000 $ppm^{-1} min^{-1}$. Empirically it was found that a fair to good simulation for the January runs could be obtained if the rate constant was lowered to about 2,000 $ppm^{-1} min^{-1}$. Not only were the $O_3$ concentrations predicted, but the trends and magnitudes of the other important timing events were also simulated. It was also discovered that a better fit for the October 22, 1977 experiment was obtained when the formation rate of PNA was set at 7,000, that the August simulation was insensitive to the formation rate, and that a value as high as 9,000 (as the earlier model version used) could be accommodated. These results seemed to indicate that the formation rate should increase with temperature or, that the decomposition rate should be decreased at higher temperatures and increased at lower temperatures.

Several estimates for a new activation energy (and frequency factor) were tried. The resulting simulations had about the right $O_3$ maximum but had grossly misshapen profiles. More important, the timing of the events of the October 21, 1978 simulations (one side air dried) were different even though the initial conditions were carefully matched; each side was subject to the same temperature. The difference in events and timing could not be simulated with our model even by having inordinately high formaldehyde concentrations go to the walls in the wet side.

Therefore, the formation rate must vary proportionally with some other parameter associated with temperature. In 1977 Hamilton[32] presented experimental results showing a positive water vapor effect on the formation of $H_2O_2$ from the reaction of two hydroperoxy radicals. He suggested that one radical hydrates and reacts with another unhydrated $HO_2$ radical. Water vapor is proportional to dew point which is limited by temperature.

This approach was tested in the model. By analogy the formation of PNA was made water vapor dependent (Reaction 5-11). Remarkably, multiplying the concentration of water vapor (obtained from dew point measurement) by a new constant provided the desired rates and enabled the model to simulate the full range of these experiments without any rate constant changes. This mechanism also modeled the "wet and dry" sides of October 21, 1978.

$$HO_2 + H_2O \rightleftarrows H_2O{\cdot}HO_2 \qquad (5)$$

$$HO_2 + NO \rightarrow NO_2 + OH \qquad (6)$$

$$HO_2 + NO_2 \rightarrow HO_2NO_2 \qquad (7)$$

$$H_2O{\cdot}HO_2 + NO \rightarrow NO_2 + OH + H_2O \qquad (8)$$

$$H_2O{\cdot}HO_2 + NO_2 \rightarrow HO_2NO_2 + H_2O \qquad (9)$$

$$H_2O{\cdot}HO_2 + HO_2 \rightarrow H_2O_2 + O_2 + H_2O \qquad (10)$$

$$HO_2 + HO_2 \rightarrow H_2O_2 + O_2 \qquad (11)$$

The role of PNA in the UNC model for propylene and ethylene is similar to the role of PAN in the propylene mechanism. PNA forms from the reaction of $HO_2$ and $NO_2$ (proportional to water concentration) and thermally decomposes back to the same reactants. At $298^{\circ}$K PNA decomposes about a hundred times faster than PAN. Therefore, PAN and PNA provide a mechanism to temporarily store $NO_2$ and a radical. Like PAN, the amount of PNA that accumulates is dependent on the ratio of the formation rate to the decomposition rate. This ratio therefore is dependent on the concentrations of $HO_2$, $NO_2$, $H_2O$ and temperature. The accumulation of PNA seems to delay the photochemical system by taking $NO_2$ and an important radical out of the system and then releasing it later. This causes lower $NO_2$ and $O_3$ maximum concentrations. Most important is the fact that this mechanism seems *necessary* to model experimental $HC/NO_x$ systems in colder environments where the air is naturally drier (Figure 18). We have found that temperature dependent reactions alone cannot account for the observed results. Finally, seasonal effects of water vapor and temperature changes may be important considerations for cities and states in cooler and drier climates, where modeling will be utilized in determining control strategies for photochemical oxidants.

On the basis of the proposed PNA chemistry we would predict 1) that summer, dry vs. humid, matched propylene experiments would not show strong "PNA effects", 2) high temperatures would prevent significant PNA accumulation at any period during a run, 3) in runs with low propylene/$NO_2$ ratios, reactant concentrations would be less sensitive to this mechanism and 4) cooler and more humid conditions would tend to show the most dramatic "PNA effects".

More experiments were needed with matched initial conditions on each side but with drier air on one side, to test the mechanism's success. Table 13 lists these experiments and some of the more important results. Each run will be briefly discussed in Appendix C.

With a few exceptions, the general conclusions are that water vapor does have an effect on these hydrocarbon and $NO_x$ systems and on $O_3$ production. Humidity is unimportant on warm days as the model suggests, even for high [propylene]/[$NO_x$] conditions. The greatest effects will be seen in *cool* systems between air with high water content and air with low water content.

Table 13. Critical Data for Humid VS. Dry Runs

| Date | Run Type | $[NO_2]_o$ | | $[NO_x]_o$ | | $[HC]_o^{ppmC}$ | | $[D.P.]_F$ | | $[T°]_I$ | $[T°]_F$ | Time Cross | | $[NO_2]$ Max | | Time $NO_2$ Max | | $[O_3]$ max | | Time $O_3$ max | | Sun |
|---|---|---|---|---|---|---|---|---|---|---|---|---|---|---|---|---|---|---|---|---|---|---|
| | | Blue | Red | Blue | Red | Blue | Red | Blue | Red | | | Blue | Red | Blue | Red | Blue | Red | Blue | Red | Blue | Red | |
| 10/21/78 | Match propylene<br>Blue dried | 0.110 | 0.111 | 0.503 | 0.505 | 3.45 | 3.48 | 43 | 58 | 34.7 | 72.4 | 9:41 | 9:50 | 0.484 | 0.461 | 10:48 | 11:05 | 0.743 | +11%<br>0.670 | 12:30 | 12:42 | 90% |
| 6/29/79 | Match propylene<br>Blue dried | 0.085 | 0.094 | 0.458 | 0.464 | 3.504 | 3.553 | 57 | 69 | 58 | 79.2 | 8:32 | 8:31 | 0.396 | 0.387 | 9:26 | 9:24 | 0.891 | 0.893 | 13:35 | 12:32 | 23% |
| 10/16/79 | Match propylene<br>Blue dried | 0.085 | 0.083 | 0.371 | 0.371 | 3.126 | 3.172 | 32 | 48 | 40.8 | 74.5 | 9:55 | 9:46 | 0.341 | 0.342 | 10:58 | 10:52 | 0.822 | +1.9%<br>0.807 | 13:01 | 12:47 | 80% |
| 10/26/79 | Match propylene<br>Blue dried<br>Red misted | 0.081 | 0.092 | 0.494 | 0.496 | 4.765 | 4.839 | 28 | 58 | 35 | 61 | 9:54 | 10:00 | 0.472 | 0.452 | 10:43 | 10:59 | 0.822 | +41%<br>0.582 | 12:16 | 12:24 | 100% |
| 10/29/79 | Match ethylene<br>Blue dried | 0.087 | 0.086 | 0.476 | 0.474 | 3.189 | 3.212 | 58.5 | 68.4 | 44 | 75 | 10:47 | 10:58 | 0.411 | 0.403 | 12:06 | 12:27 | 0.760 | +24%<br>0.613 | 14:25 | 14:59 | 55% |
| 10/31/79 | Match ethylene<br>Blue dried | 0.097 | 0.098 | 0.497 | 0.498 | 3.706 | 3.743 | 28 | 62.5 | 50 | 72 | 11:08 | 10:49 | 0.43 | 0.416 | 12:26 | 12:19 | 0.887 | +7.3%<br>0.827 | 3:30 | 3:02 | Clear |
| 11/8/79 | Match ethylene<br>Blue dried<br>Red misted | 0.096 | 0.097 | 0.492 | 0.494 | 3.818 | 3.79 | 27.4 | 47.6 | 31.2 | 60.3 | 12:03 | 11:42 | 0.387 | 0.366 | 14:34 | 14:34 | 0.31 | +>100%<br>0.15 | 16:23 | | Cloudy |

a. All dewpoints and temperatures are in °F.

b. $[D.P.]_F$ is dew point at $O_3$ maximum.

c. $[T°]_I$ and $[T°]_F$ are temperatures at time of sunrise and $O_3$ maximum

d. "Misted" means ~400 ml of distilled water added to inside of vertical walls of undried side.

e. 11/8/79 run - $O_3$ data missing until end of run on Red side. $O_3$ max concentration is estimated.

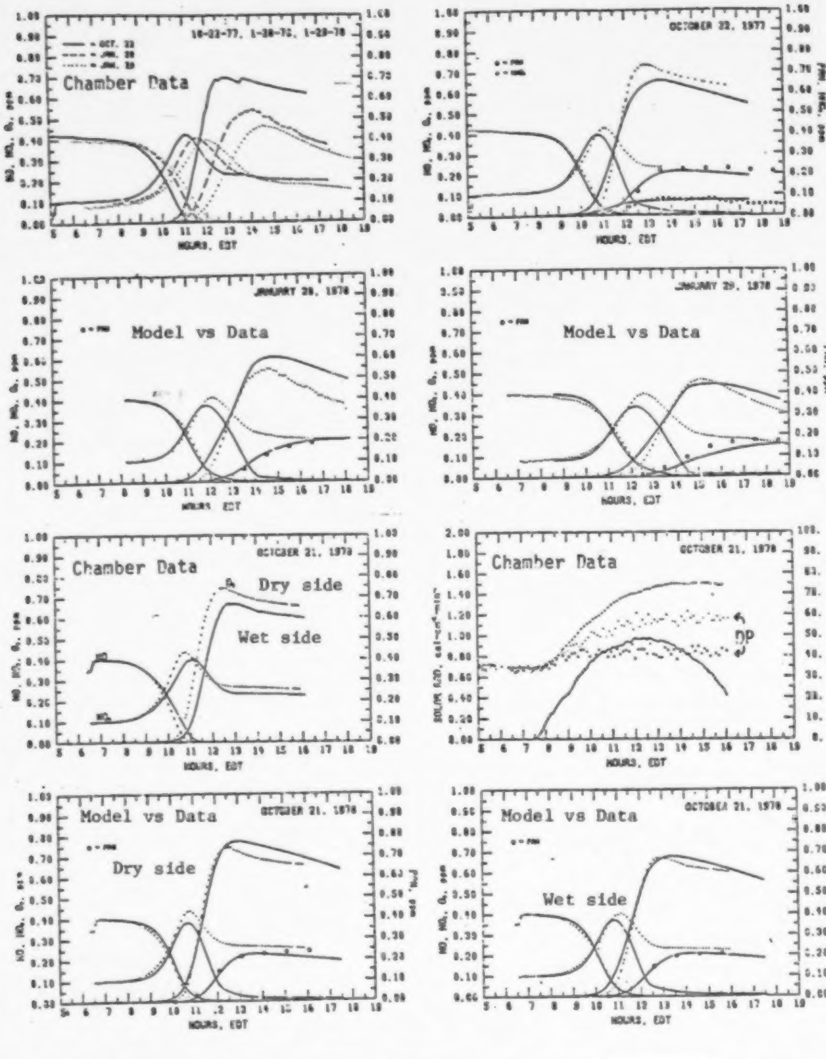

Figure 18. Water effect experiments. Unless otherwise indicated, (---) represents UNC smog chamber data, (——) represents model.

# SECTION 6

# BIOGENIC HYDROCARBON STUDIES

## INTRODUCTION

In recent years there has been controversy about the relative importance of natural hydrocarbons in both urban and rural smog formation. Attempts to relate natural hydrocarbon emission rates with natural hydrocarbon ambient levels have met wth varying degrees of success. For example, Westberg and Holdren (1976),[33] using Zimmerman's (1977)[34] experimentally determined plant specific emission rates, were able to predict an average terpene concentration of 16 ppbC within a 20 meter high pine forest. This figure was compatible with the ambient values measured during the Westberg-Holdren study (1976).[33] When Zimmerman's specific plant emission rates were later used in conjunction with biomass factors, etc. (1978)[35] for the Tampa Bay-St. Petersburg area, the final computation suggested that 68% of all hydrocarbon emissions were of natural origin. These estimates appeared to be at variance with EPA measurements (Lonneman et al., 1978)[36] which showed that almost all hydrocarbons in the Tampa Bay-St. Petersburg plume come from anthropogenic sources. Although much discussion and debate has resulted from the apparent irreconcilability between the Tampa Bay emissions and ambient measurements, one is forced to consider that experimentally determined plant emissions and biomass estimates may produce calculated overall regional emission estimates which are somewhat high. At the same time, anthropogenic emission estimates for the same day may be optimistically low. Given the many assumptions which are used to calculate both natural and anthropogenic emissions, this explanation (Lonneman and Bufalini, 1979)[37] is certainly possible.

To further complicate matters, a statistical analysis (Sandberg, et al., 1978)[38] of total hydrocarbon (THC) and $O_3$ data from the San

Francisco Bay area attempted to relate increased natural hydrocarbon emissions to increased summer $O_3$ concentrations. The increase in THC allegedly was the result of abnormally wet winters which would cause greater plant growth, higher emissions, and subsequently more $O_3$. Unfortunately, the THC data did not have any accompanying methane or detailed natural hydrocarbon information. It is plausible that extremely wet winters could cause an increase in biogenic decay and, hence, produce greater local methane emissions. This would be directly reflected in THC readings. Such an increase in methane concentrations is not expected to cause a significant increase in $O_3$ production. Furthermore, Miller et al. (1979)[39] analyzed similar San Francisco Bay data sets and could not verify the correlations in the original Sandberg study.

In any event, since the issue of natural hydrocarbon emissions has not been completely resolved, and because certain urban emission inventories used by photochemical modelers still contain large fractions of natural hydrocarbons, it was proposed that some relevant questions about the photochemical activity of natural hydrocarbons could be addressed through experiments conducted in a large outdoor smog chamber. In 1979, experiments were focused on the possible effect that natural hydrocarbons could have on urban $O_3$ formation and the photochemical reactivity of the products formed from α-pinene and $O_3$. During 1980 research was directed to isoprene, its products, and aerosol potential.

## IMPACT OF α-PINENE ON URBAN SMOG FORMATION

### Experimental

The experimental protocol employed for conducting runs in the UNC dual outdoor chamber has been described in detail by Jeffries et al. (1975).[36] In this study α-pinene was used to represent natural terpenoid hydrocarbons. It was injected at predawn hours into only one compartment of the outdoor chamber. An eleven component urban-like hydrocarbon mix (70% paraffins and 30% olefins, by carbon, (see Table 1) was then added to both chamber halves such that the effect of α-pinene on $O_3$ formation could be observed. In most of the runs α-pinene did not make up more than 20% of the total nonmethane hydrocarbon mix (NMHC);

α-pinene was either substituted for carbon in the mix so that both sides had the same initial carbon concentrations, or it was added to the mix so one side had about 20% more carbon than the other. Comparisons with mix on one side and just α-pinene on the other were also performed. In all cases the injected morning levels of NO and $NO_2$ were the same. On a few occasions early morning α-pinene was allowed to react in the dark for approximately 2 hours with low levels of $O_3$. Hydrocarbon mix and $NO_x$ were then added and the experiments carried out in the sun in a fashion similar to that described above. Summary data for the experiments of interest are given in Table 14 and sample smog profiles for both an α-pinene carbon substitution and addition to the mix are given in Figures 19 and 20.

Results and Discussion--

It is useful in discussing the reactivity of α-pinene within an urban-like mix environment to compare the $O_3$ yields from similar carbon concentrations of mix and α-pinene with the same initial $NO_x$. Such an experiment occurred on August 18, 1979. Approximately 1.3 ppmC of mix was added to one chamber half and 1.3 ppmC α-pinene to the other. Both sides started with 0.19 and 0.05 ppm of NO and $NO_2$. The side with α-pinene produced a little more $O_3$ (0.39 ppm) than the side with mix (0.32 ppm $O_3$) and did have a somewhat faster rate of oxidation of NO to $NO_2$. On the other hand Arnts and Gay (1979)[40] compared the $O_3$ yields from various terpenes and $O_3$ in an indoor chamber with constant light. The most favorable conditions for $O_3$ formation at a constant $NO_x$ of 0.33 ppm occurred at an α-pinene/$NO_x$ ratio of 10:1 (carbon/$NO_x$). Interestingly, α-pinene had a maximum $O_3$ which was 70% of a similar propylene/$NO_x$ system. As one moved to higher or lower ratios, however, the propylene systems would generate substantially more $O_3$ than similar α-pinene/$NO_x$ experiments. From the standpoint of NO oxidation and $O_3$ production, the photochemical reactivity of α-pinene by itself is slightly greater than that of the UNC mix and generally much lower than that of propylene.

### Table 14. α-pinene and Urban Mix Experiments UNC Dual Smog Chamber Runs.

| Date | Initial HC, ppm | $NO_x$, ppm[b] | $O_3$ max, ppm |
|---|---|---|---|
| **Substitution of α-pinene for mix** | | | |
| 8/18/79 | 1.31 α-pinene | 0.241 | 0.391 |
| | 1.33 mix | 0.240 | 0.323 |
| 8/31/79[c] | 1.26 mix | 0.351 | 0.063 |
| | 1.24 α-pinene | 0.354 | 0.160 |
| 9/1/79 | 0.67 mix+0.55 α-pinene | 0.219 | 0.287 |
| | 1.22 mix | 0.208 | 0.258 |
| 6/10/79 | 1.60 mix+0.34 α-pinene | 0.302 | 0.252 |
| | 2.03 mix | 0.299 | 0.248 |
| 7/6/79 | 2.09 mix+(0.2 α-pinene crossover) | 0.350 | 0.192 |
| | 2.08 mix+(0.2 mix crossover) | 0.345 | 0.223 |
| **Addition of α-pinene to mix** | | | |
| 6/9/79 | 2.12 mix 0.43 α-pinene | 0.301 | 0.467 |
| | 2.14 mix | 0.300 | 0.388 |
| 7/5/79 | 2.13 mix+0.30 α-pinene | 0.359 | 0.468 |
| | 2.15 mix | 0.354 | 0.371 |
| **Increased carbon effect of mix** | | | |
| 7/14/79 | 2.24 mix | 0.315 | 0.340 |
| | 2.65 mix | 0.309 | 0.462 |
| 7/4/79[c] | 2.22 mix | 0.348 | 0.201 |
| | 2.73 mix | 0.342 | 0.257 |
| **Early morning reaction of $O_3$ and α-pinene** | | | |
| 9/11/79 | 1.62 mix+(0.07 $O_3$+0.42 α-pinene) | 0.392 | 0.094 |
| | 2.02 mix | 0.392 | 0.145 |
| 10/2/79 | 1.93 mix | 0.201 | 0.264 |
| | 1.51 mix+(0.06 $O_3$+0.52 α-pinene) | 0.205 | 0.265 |
| 7/24/79 | 1.62 mix (0.08 $O_3$+0.41 α-pinene) | 0.414 | 0.663 |
| | 2.03 mix | 0.420 | 0.670 |
| 7/13/79 | 2.25 mix | 0.357 | 0.41 |
| | 2.25 mix (0.18 $O_3$+0.38 α-pinene) | 0.355 | 0.57 |
| **Matched mix and $NO_x$** | | | |
| 7/3/79 | 1.82 mix | 0.337 | 0.411 |
| | 1.82 mix | 0.333 | 0.422 |
| 7/28/79 | 2.36 mix | 0.436 | 0.241 |
| | 2.28 mix | 0.428 | 0.226 |
| 6/19/79 | 2.26 mix | 0.307 | 0.304 |
| | 2.26 mix | 0.301 | 0.320 |
| 6/5/79 | 4.73 mix | 0.403 | 0.863 |
| | 4.71 mix | 0.400 | 0.86[illegible] |
| 10/4/79 | 2.72 mix | 0.165 | 0.294 |
| | 2.74 mix | 0.165 | 0.287 |

---

[a] Each date shows initial conditions and $O_3$ max for both chambers

[b] 20% $NO_2$

[c] Overcast

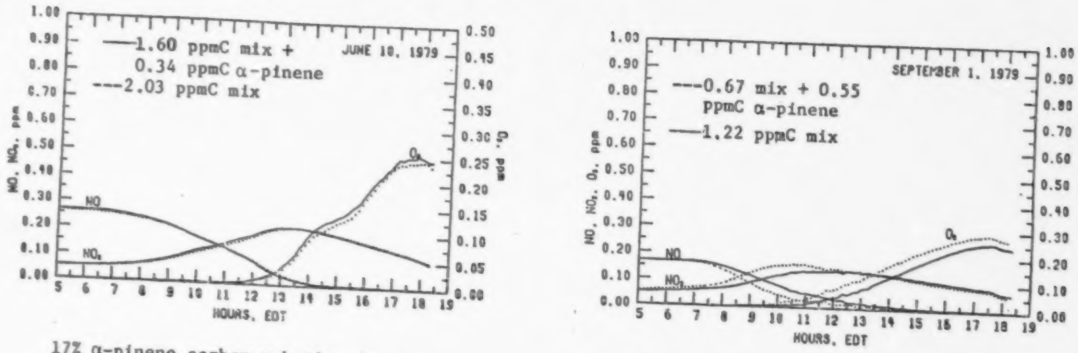

17% α-pinene carbon substitution

45% α-pinene carbon substitution

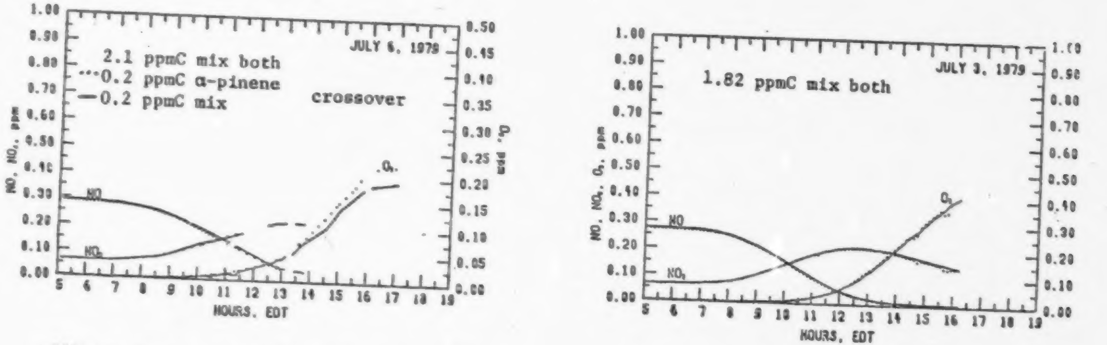

addition of mix and α-pinene after crossover

matched mix-$NO_x$ system

Figure 19. Effect of α-pinene carbon substitution in an urban-like hydrocarbon mix-$NO_x$ system.

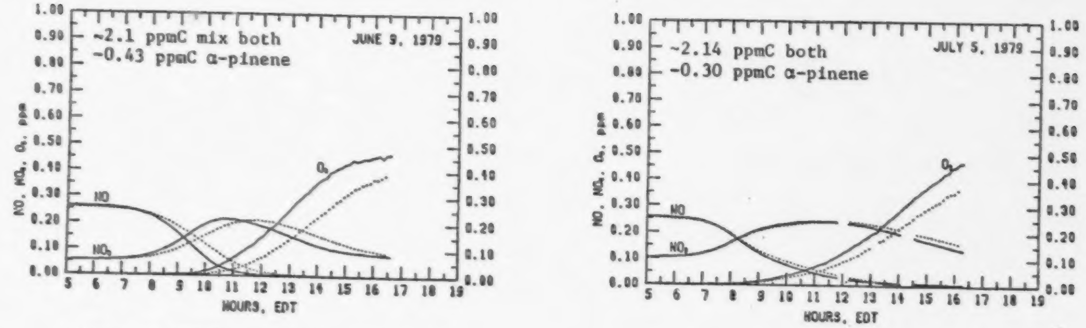

Effect of 20% Extra α-pinene carbon

Effect of 14% Extra α-pinene carbon

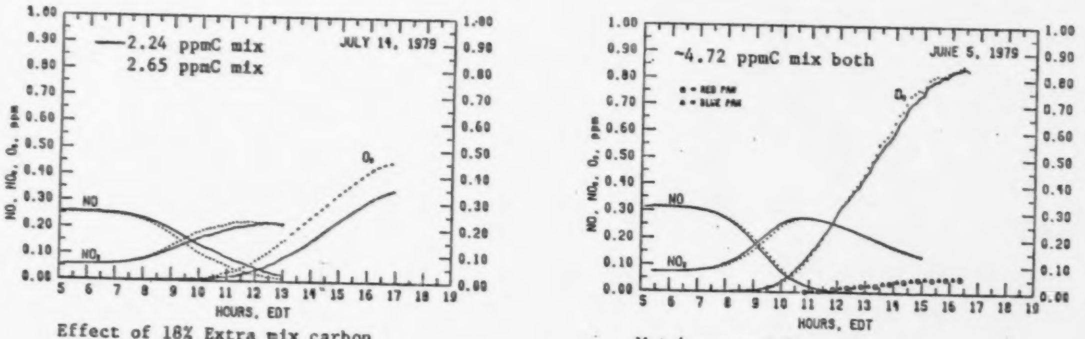

Effect of 18% Extra mix carbon

Match mix and $NO_x$ system

Figure 20. Effect of α-pinene carbon addition to an urban-like hydrocarbon mix-$NO_x$ system.

## Substitution of α-pinene Carbon for Mix Carbon

Replacement of hydrocarbon mix carbon with α-pinene was performed to see if any changes in $NO_x$ or $O_3$ behavior could be observed. Direct substitution with 45% α-pinene (by carbon) was performed on September 1, 1979 (Table 14). The α-pinene plus mix side made a little more $O_3$ (0.28 ppm compared to 0.25 ppm) and reached NO-$NO_2$ crossover about 1 hour sooner than the 100% mix side. When replacement was lowered to 17% (June 10, Figure 19) the impact of the slightly more reactive α-pinene was almost completely lost; both sides had nearly identical NO, $NO_2$ and $O_3$ time profiles. It was suggested (Dodge, 1979)[41] that if α-pinene was added after crossover to a dual run which had the same mix and $NO_x$ in both sides, then an α-pinene effect might be observed. This was done on July 6; 0.2 ppmC of α-pinene were added to one side of a 2.1 ppmC, 0.35 ppm $NO_x$ matched run and 0.2 ppmC mix to the other at crossover. As shown in Table 14 and Figure 19 a slight but negligible reduction in $O_3$ production was observed in the α-pinene side.

It has been previously proposed (Kamens et al., 1980;[42] Jeffries, 1980[43]) that 20% carbon substitution of most hydrocarbons into a complex urban-like hydrocarbon mixture does not greatly alter the resultant $NO_x$ or $O_3$ behavior. Data have been presented for aromatic substitution (Jeffries et al., 1975)[6] as well as more involved replacement of various hydrocarbons within a mixture. All of these experiments lend support to the above hypothesis; it is only when compounds of extremely low or high reactivity are substituted in the mix that noticeable changes in the overall mix reactivity occur. The implications of these findings may be of value to control agencies which consider hydrocarbon substitution as a way to lower the reactivity of urban emissions and thereby a means for oxidant control.

## Addition of Extra α-pinene Carbon to a Hydrocarbon Mixture

When 20% extra α-pinene carbon was added to a matched mix dual chamber run, the side with α-pinene generated about 20% more $O_3$. Similar experiments (Table 14) were then run with mix, except that one chamber side had 20% more mix than the other. As can be seen (Figure 20) both of these systems exhibit similar behavior and, hence, the changes associated with the addition of 20% extra α-pinene carbon seems to be mostly that of an increased carbon effect.

### Reaction of Ozone and α-Pinene Prior to the Injection of Mix--

In some experiments a low concentration of $O_3$ (0.068 ppm) and α-pinene (0.4 ppmC) were added to the chamber and allowed to react for 1-2 hours in the dark before the addition of either mix or $NO_x$. These tests were designed to determine if the product of this reaction in either the vapor or aerosol phase would influence the net $O_3$ production from a carbon mix-$NO_x$ system. An experiment of this type was conducted on September 11, 1979 (Figure 21). Condensation nuclei formation was observed about fifteen minutes after the addition of $O_3$ in the dark to α-pinene.

When mix and $NO_x$ were finally added to both sides of this experiment it was done so that each side had the same total carbon (i.e., initial [α-pinene] +[mix] = [mix]) and the same initial NO and $NO_2$ (after $O_3$ had been titrated by the NO injection). This run was similar to the one on July 10 except that $O_3$ and α-pinene had an opportunity to react before the addition of either mix or $NO_x$. Recall that in the June 10 experiment (Figure 19) both sides generated the same $O_3$. In this experiment, however, the side with reacted α-pinene generated less $O_3$ (Figure 21).

Two other runs in which α-pinene and $O_3$ were first added to the chamber had missing data or were performed in poor meteorological conditions; the results of these experiments are not very certain. They do tend to support the results of the September 11 run. Furthermore, runs on July 24, 1979, and October 2, 1979, (Figure 21) did not show the reduced $O_3$ effect of first reacting $O_3$ and α-pinene. These experiments behave in the same way as the substitution and addition runs in Figures 19 and 20. All of the runs in which $O_3$ and α-pinene were first reacted do not show any more reactivity than those in which α-pinene was not first reacted, and in certain cases do show less $O_3$ production.

If reacting $O_3$ and α-pinene first leads to less $O_3$ production, then the products of α-pinene and $O_3$ may be stabilizing in the dark (that is, would not be available for reaction) and losing some of their

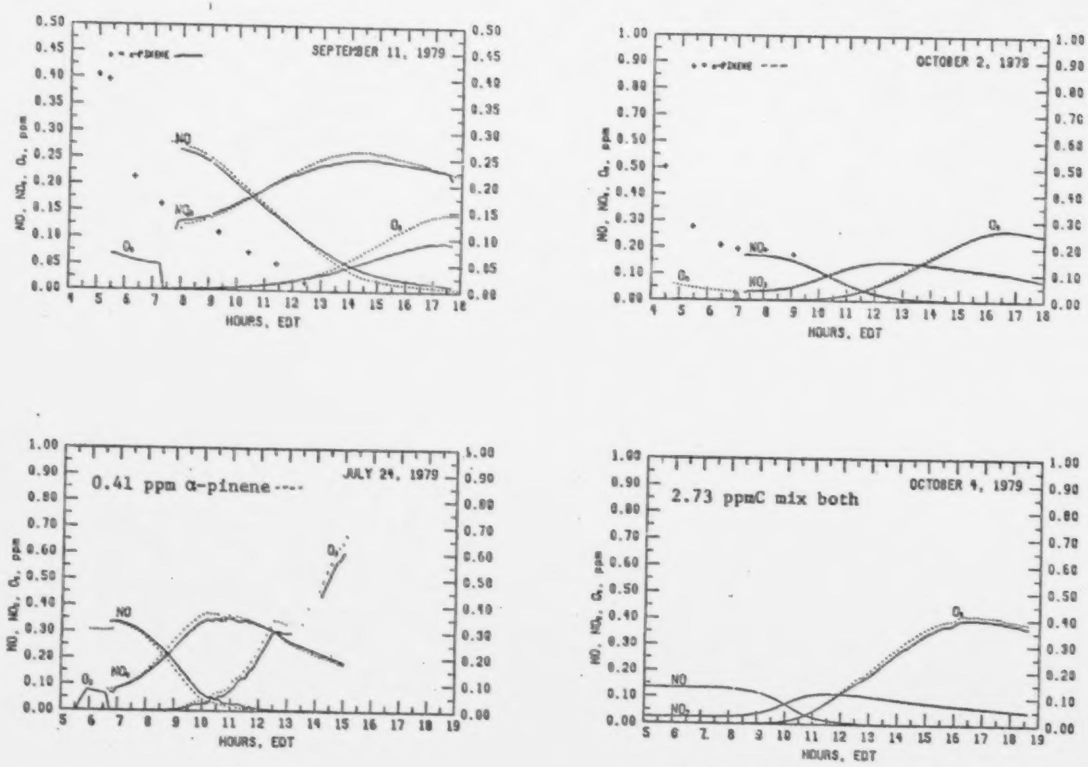

Matched mix-NO$_x$ system

Figure 21. Effect of first reacting α-pinene and O$_3$ in matched carbon-NO$_x$ systems.

photochemical activity. On the other hand, when α-pinene is not first reacted with $O_3$, it participates as does any hydrocarbon in a morning smog system; that is, the products which result from either OH or $O_3$ attack will subsequently lead to NO oxidation before these products have an opportunity to stabilize. Further, the nature and amount of aerosol vs. vapor phase products may also influence the $O_3$ yield from the subsequent smog system. If different amounts of aerosol and products were generated in the above experiment, then perhaps the relative importance of other reactions, like aerosol radical scavenging, could also have been shifted. This could partially account for the apparent inconsistencies of the experiments in Figure 21. Unfortunately, chemical characterization of the products from ppm levels of α-pinene and $O_3$ is very difficult and only recently (Hull, 1980)[44] has reasonable success at high concentrations been achieved. In two selected experiments physical measurements of the aerosol were made in the UNC chambers. These will be discussed in the next section.

### Dark Experiments between $O_3$ and α-pinene--

As noted before, in the September 11, 1979 run, condensation nuclei (CN) were detected approximately 15 minutes after the addition of 0.06 ppm $O_3$ and 0.4 ppmC of α-pinene. The CN trace is shown in Figure 22. Note the return to zero of the CN response when the monitor was momentarily switched to the chamber half which did not contain either α-pinene or $O_3$. A maximum number of 3000 nuclei per cc was recorded. Given the length of the sampling manifold (~40 ft), nucleation may have begun sooner than it was observed. This is because there is a high potential for diffusion losses to the manifold walls of the smallest particles in the CN range prior to entering the CN counter. If one assumes, however, based on the more detailed particle information given in the next experiment, that the average detected particle was about 0.1 μm, then approximately 1% of the reacted carbon could be accounted for as CN aerosol. Doubling the particle diameter to 0.2 μm would give approximately a 10% carbon accountability.

After one hour of reacting 0.068 ppm of $O_3$ with 0.41 ppmC α-pinene, only 0.21 ppmC (0.021 ppmV) of α-pinene remained in the gas phase; 0.019

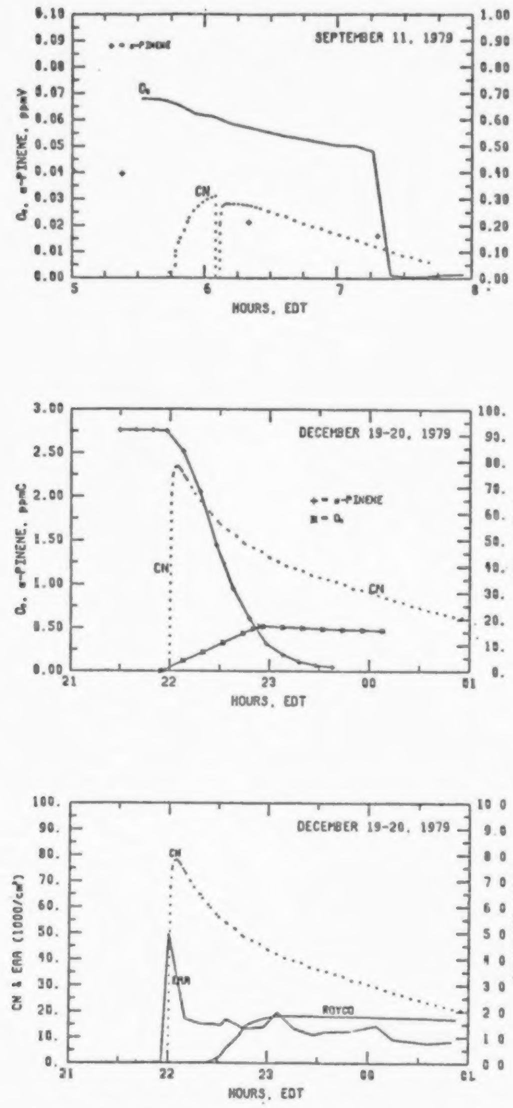

Figure 22. Dark reaction between $O_3$ and α-pinene and resultant total aerosol number traces.

ppmV had gone into gas phase products and aerosols. During this time 0.014 ppm $O_3$ had disappeared. Of this amount, a previously determined low concentration, dark-phase $O_3$, decay rate calculation could account for a wall loss of only 0.003 ppmV/hour. Hence, during the first hour, 0.02 ppmV of α-pinene and 0.01 ppm of $O_3$ had reacted. This is within the lower end of the reaction stoichiometry previously cited by Ripperton et al., (1972)[45] but higher than the 1.3 to 1 stoichiometry recently suggested by Hull (1980).[44] A rate constant for the reaction between $O_3$ and α-pinene of $3.6 \times 10^4$ $l\ mol^{-1}\ sec^{-1}$ was calculated from the net $O_3$ disappearance data. This number is slightly lower, but similar to other literature values.

On the night of December 19, 1979, α-pinene and $O_3$ were reacted in the large UNC aerosol chamber (Fox et al., 1975)[46] so that the aerosol instruments located in the laboratory beneath the chamber could be utilized to study the changing aerosol size distribution. Aerosol data were collected with an Environment/One condensation nuclei counter (CNC), a Thermo Systems, Inc. 3030 electrical aerosol analyzer (EAA), and a Royco 220 optical particle counter (OPC). These types of instruments are often used for aerosol measurements. The operating characteristics of our instruments are not unique and will not be discussed here. Further information concerning the operation of the aerosol instrumentation during this experiment may be found in Kamens et al., 1980.[42]

After sunset on December 19, 2.75 ppmC equivalent liquid α-pinene was gently vaporized into the chamber at 2100 hours; 0.5 ppm of $O_3$ was then ramp injected from 2155 to 2252 hours. The concentrations of α-pinene and $O_3$, along with the total particle counts from each aerosol instrument are shown in Figure 22. Within five minutes after the addition of $O_3$, aerosol was observed by the CNC and EAA monitors. The slight difference in response between both of these instruments is due to differences in data acquisition periods.

Inspection of the EAA number distribution vs. time plot (Figure 23) shows a large burst of particles with diameters near 0.01 μm immediately after the start of $O_3$ injection. Growth into the larger size ranges of the EAA (0.05 to 0.4 μm) took place over the next thirty minutes, with the greatest numbers appearing in the 0.07-0.13 m range. The surface and

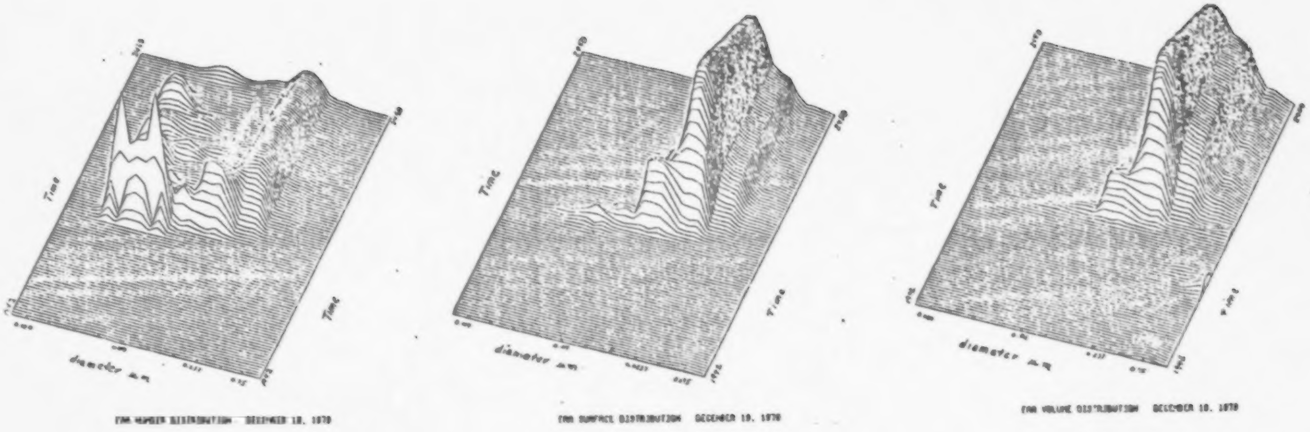

Figure 23. EAA three-dimensional number, surface and volume plots from the reaction between 2.75 ppmC α-pinene and 0.5 ppm $O_3$, December 19, 1979.

volume distributions vs. time that are associated with the EAA detectable particles are shown in Figure 23. Coincidental with the later stage of EAA growth, OPC particles began to accumulate (Figure 22) approximately thirty minutes after the start of the $O_3$ injection. Some of these particles have diameters within the EAA detection limits for the last channel (0.56 to 1.0 μm), even though no EAA counts were recorded there. This result is due to the lack of sensitivity in the last channels caused by the high counts in the middle channels. Unfortunately, since these are the largest EAA particles, a great deal of volume is not accounted for even though only a small percentage of the overall particle count is lost.

Because the EAA actually responded only to particles below 0.56 μm, the EAA and OPC have detected relatively exclusive sets of particles and the data sets are effectively isolated from each other. The volumes calculated from these two sets of data can be added to give an estimate of the total aerosol volume in both regions. The actual volume is expected to be slightly greater than that calculated since particles in the next to last EAA channel may also unaccounted for. Thus, even though most of the particles occur in the middle of the EAA region, due to the larger size of the OPC particles, most of the total volume will reside in the optical region. An estimate of the total aerosol volume based on different calibration procedures ranged from 500-2000 $\mu m^3/cm^3$. Of this, 97-99% were OPC detected particles.

Assuming that the liquid aerosol product has a density of 1 g/cc, a crude conversion to aerosol mass loading can be made; this is to compare percent carbon of α-pinene reacted with the percent detected as aerosol. Our estimates suggest that the aerosol yield for this experiment was between 25% and 90%. Again, these numbers are highly uncertain. It was suggested by Hull (1980)[44] that some of the α-pinene $O_3$ reaction products have vapor pressures of 1 ppm. This experiment started with 0.3 ppmV of α-pinene. If 10-40% of the products existed in the gas phase, then an upper limit on the total concentration of these compounds would be 0.1 ppmV. This would permit many of these products to exist in the gas phase as long as critical aerosol surfaces did not form and aid in the condensation of these compounds.

## Summary and Conclusions

If α-pinene and $O_3$ reaction products are photochemically inert then there would be no need to consider natural terpene emissions in any control strategy for $O_3$. This would follow because ambient levels of reacted terpenes are very low and because the products of $O_3$ and terpenes would not significantly participate in the critical reactions of $O_3$ production.

On the other hand, if these products are as reactive as α-pinene or an urban mix then continued refinement of natural emissions inventories and product measurements would be needed to determine to what extent natural emissions should be used in urban or regional photochemical models.

The substitution of 20% α-pinene carbon into a complex urban-like hydrocarbon-$NO_x$ system does not lead to discernible changes in $NO_x$ or $O_3$ concentration rates and times. In the case of 20% α-pinene carbon addition, increases in $O_3$ concentrations and rates were similar to the expected increases from the same carbon addition in the hydrocarbon mix concentration.

From the experiments performed in this study, it is not clear how the products of terpene-$O_3$ reactions should be treated. Data has been presented which suggest that the prior formation of these products may reduce $O_3$ yields from urban-$NO_x$ smog systems, when compared to the $O_3$ yields from unreacted terpenes within similar urban smog-type mixtures. Other experiments do not confirm these results but indicate that the reacted products do not impart any "unusual" reactivity to the smog system.

Aerosol measurements made during the dark reaction of $O_3$ and α-pinene indicate that the majority of the number of particles resulting from this process reside in the 0.1 μm diameter range. Most of the mass, however, is in particles >0.6 μm in diameter. Carbon accountability of reacted α-pinene in the product condensed phase was estimated to be 25-90%.

## OZONE ISOPRENE REACTIONS, PRODUCT FORMATION AND AEROSOL POTENTIAL

### Introduction

Isoprene is one of the major non-terpenoid compounds emitted by vegetation. Indoor smog chamber experiments suggest that isoprene-$NO_x$ smog systems are somewhat less reactive than propylene systems in terms of maximum $O_3$ yields.[40] UNC outdoor chamber experiments indicate that isoprene is similar in reactivity to propylene and much more reactive than either $\alpha$-pinene or an urban hydrocarbon mixture.[47] The potential for natural aerosol formation from terpene-$O_3$ systems has long been demonstrated. The atmospheric reactions of isoprene and its potential for aerosol production, however, have not been extensively explored.

Over two decades ago Schuck and Doyle (1959)[48] reported on the irradiation of isoprene and $NO_x$, accounting for 87 percent of the reacted isoprene as observed products. The reaction products reported were formaldehyde (HCHO), acetaldehyde ($CH_3CHO$), acrolein, peroxyacetyl nitrate (PAN) and carbon monoxide (CO). Arnts and Gay (1979)[40] published a report on similar experiments but were able to show only a 30-45 percent carbon accountability. Their products included methylvinylketone (MVK), methacrolein (MACR), CO, $CO_2$, HCHO, $CH_3CHO$, formic acid (HCOOH), PAN and nitric acid. Acrolein was not observed. A mechanism for $O_3$ attack on isoprene to produce MVK and MACR was proposed.[42]

As shown in Reaction 12, attack by $O_3$ on the 1,2 carbon double bond of isoprene could lead to MVK, while attack on the 3,4 double bond (Reaction 13) could similarly produce methacrolein.

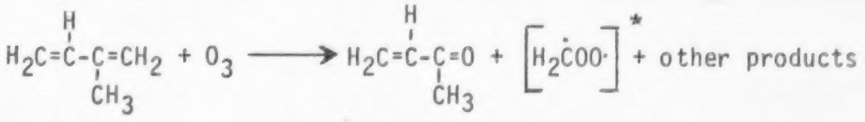

$$H_2C{=}\overset{H}{C}{-}\underset{CH_3}{C}{=}CH_2 + O_3 \longrightarrow H_2C{=}\overset{H}{C}{-}\underset{CH_3}{C}{=}O + \left[H_2\dot{C}OO\cdot\right]^{*} + \text{other products} \tag{12}$$

Isoprene MVK

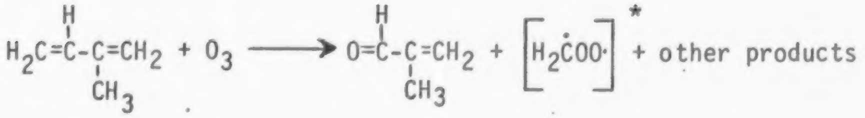

$$H_2C{=}\overset{H}{C}{-}\underset{CH_3}{C}{=}CH_2 + O_3 \longrightarrow O{=}\overset{H}{C}{-}\underset{CH_3}{C}{=}CH_2 + \left[H_2\dot{C}OO\cdot\right]^{*} + \text{other products} \tag{13}$$

Isoprene MACR

It was further hypothesized by Arnts and Gay,[40] (Reactions 14 and 15) that $O_3$ could continue to react with either MVK or MACR to produce methylglyoxal (MGLY) (pyruvic aldehyde). This product was not observed in their smog chamber experiments. This may have occurred because MGLY is photochemically reactive, and appreciable concentrations did not appear in the gas phase.

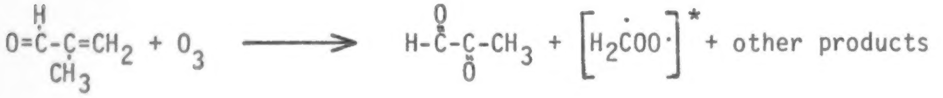

$$O{=}\overset{H}{C}-\underset{CH_3}{C}{=}CH_2 + O_3 \longrightarrow H-\overset{O}{\overset{\|}{C}}-\underset{\overset{\|}{O}}{C}-CH_3 + \left[H_2\dot{C}OO\cdot\right]^* + \text{other products} \quad (14)$$

MACR MGLY

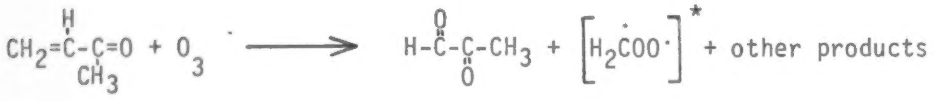

$$CH_2{=}\overset{H}{C}-\underset{CH_3}{C}{=}O + O_3 \longrightarrow H-\overset{O}{\overset{\|}{C}}-\underset{\overset{\|}{O}}{C}-CH_3 + \left[H_2\dot{C}OO\cdot\right]^* + \text{other products} \quad (15)$$

MVK MGLY

In the present study isoprene and $O_3$ were added to the UNC outdoor chambers in the dark. The intent of these experiments was twofold: (1) to examine the potential for aerosol formation from these systems, and (2) to construct a mechanism that would be consistent with the formation of the observed products.

## Experimental

Eight to twelve hours before the start of an experiment the chambers were purged with clean rural air. During the last hour of this period, the chamber air humidity was reduced by circulation through isolated air conditioner cooling coils. Desired starting concentrations of isoprene, MVK or MACR were generated in the outdoor Teflon chambers[49] by vaporizing measured volumes of the pure liquids into a warm air injection manifold. Hydrocarbon injections were usually made about 2 hours after sundown and concentrations were confirmed chromatographically before the addition of $O_3$. Background $O_3$ at approximately 0.02 ppm was not titrated with NO. Ozone was injected at a predetermined rate over periods of 120 to 250 minutes into the chambers using an oxygen supplied, ultraviolet, $O_3$ generator.

Dilution in the chambers, due to both sampling and leak losses, was determined by adding ppb levels of carbon tetrachloride and monitoring its concentration with the chromatographic system used to measure PAN.[50] The $C_2$-$C_5$ aldehydes and ketone concentrations, including those of MVK and MACR, were obtained by use of an automatically injected gas chromatograph equipped with an 8 foot x 1/8 inch stainless steel column packed with 10 percent Carbowax 20M on Supelcoport 60-80 mesh and operated at 63°C; detection was by flame ionization detector (FID). Isoprene elutes very sharply on this column and was also measured using a 6 foot stainless steel, n-octane/Poracil C column and FID. Qualitative aldehyde measurements were made using the dinitrophenylhydrozone technique recently reported by Hull[4] and Kuntz et al.[5] Formaldehyde data also were taken with an automated, colorimetric instrument manufactured by CEA Corporation using the reverse West-Gaeke method. A Beckman 6800 environmental chromatograph operated in the chromatographic mode was used to monitor CO. Ozone was measured with a Bendix chemiluminescent analyzer that was calibrated by gas phase titration (GPT) and UV photometry. In our laboratory GPT calibrated measurements are generally 3-8 percent higher than those acquired with a UV photometry calibrated instrument. GPT $O_3$ values have been reported in this study because this is the procedure by which our $O_3$ monitors have been calibrated for the past eight years.

Aerosol measurements were conducted with an Environment/One CN counter during each experiment. Since this technique is not size discriminatory, a Royco 220 optical particle counter (OPC) and a Thermo Systems Inc. Model 3030 electrical aerosol analyzer (EAA) were utilized in selected experiments to describe the aerosol size distribution. In addition, filter samples were pulled for one high-concentration experiment and subjected to gravimetric and mass spectroscopic analyses.

## Discussion

### Major Gas Phase Products and Aerosol Production--

Approximately 70 percent of the reacted isoprene carbon appeared as product MVK, MACR, HCHO or CO. For example, Table 15 shows the product concentrations that were measured in a dark experiment on October 9, 1980 (which started with 4.90 ppmC of isoprene and had 0.74 ppm of $O_3$ ramp injected over 1.38 hrs). Data for this run are shown in Figure 24a. In addition to the products noted in Table 15, approximately 5 percent of the reacted carbon appeared as a product which had the same elution time as acetone. Trace amounts of acetaldehyde and propylene were also observed as the isoprene-$O_3$ reaction proceeded.

Table 15. Major Products from a 4.90 ppmC Isoprene and 0.74 Ramp Injected $O_3$ System after 4 Hours of Reaction

| Reactants | ppmV | Products | ppmV | % Yield |
|---|---|---|---|---|
| Initial isoprene* | 0.93 | HCHO | 0.53 | 19.3 |
| Reacted isoprene | 0.55 | CO | 0.16 | 5.8 |
| Initial $O_3$* | 0.70 | MVK | 0.10 | 14.6 |
| Reacted $O_3$ | 0.58 | MACR | 0.23 | 33.5 |
|  |  | Total | 1.02 | 73.2 |

*Exponentially adjusted for dilution loss over four hours ($k=0.0127\ hr^{-1}$) assuming that no chemical sinks occurred.

In the October 9, 1980 experiment, CN formation (Figure 24b) was observed immediately after the addition of $O_3$ began. This system generated almost the same level of CN aerosol as did a previously reported $\alpha$-pinene-$O_3$ experiment which started with almost half the carbon concentration of $\alpha$-pinene.[51] Size specific particle analysis (Figure 25a) shows that most of the particles from the isoprene system form and remain at diameters well below the optical cutoff region ($d_p$ = 0.3-0.5 μm). This appears to be contrary to particle formation trends in similar $\alpha$-pinene systems, where aerosol forms at smaller sizes, but then grows into the optical size range (ie. $d_p$ is greater than 0.5 μm). Mass calculations based on OPC and EAA volume measurements (Figure 25b) suggest that very little of the reacted isoprene mass appeared in the condensed phase. On the other hand, particle measurements and resulting estimates from an $\alpha$-pinene-$O_3$ system suggest that a substantial portion of the reacted carbon can show up in the condensed phase.[51]

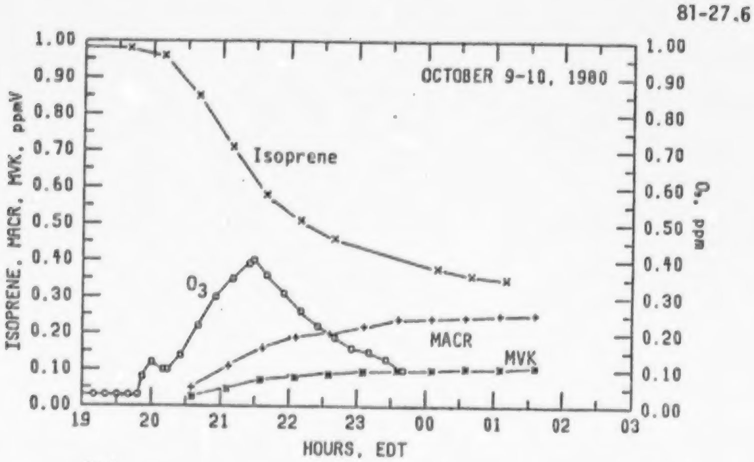

Figure 24a. Reaction of isoprene and ozone on the night of October 9, 1980; experimental data (Temperature was approximately 65°F).

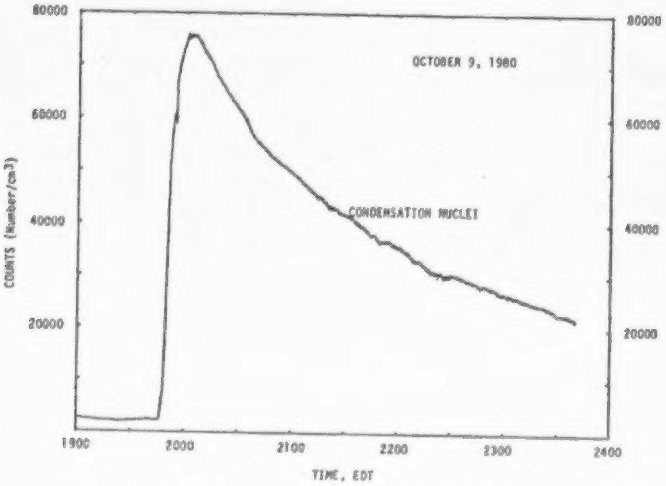

Figure 24b. Condensation nuclei trace from a 4.90 ppmC isoprene + 0.74 ppm $O_3$ dark reaction in the UNC outdoor smog chamber.

81-27.6

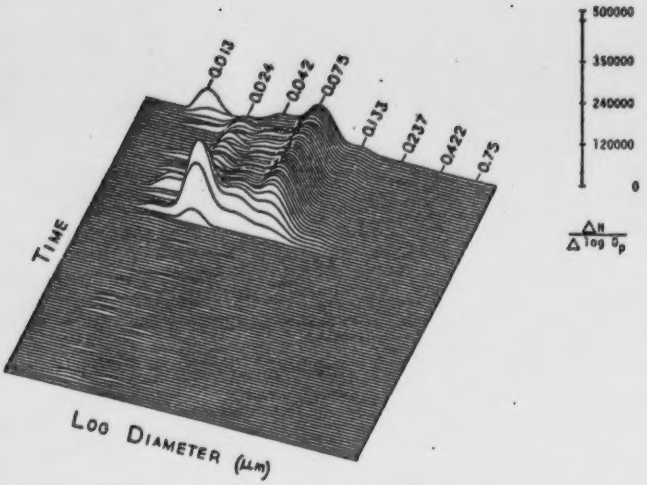

Figure 25a. Electrical Aerosol Analyzer number distribution vs. time for October 19, 1980 dark phase reaction between Isoprene and Ozone.

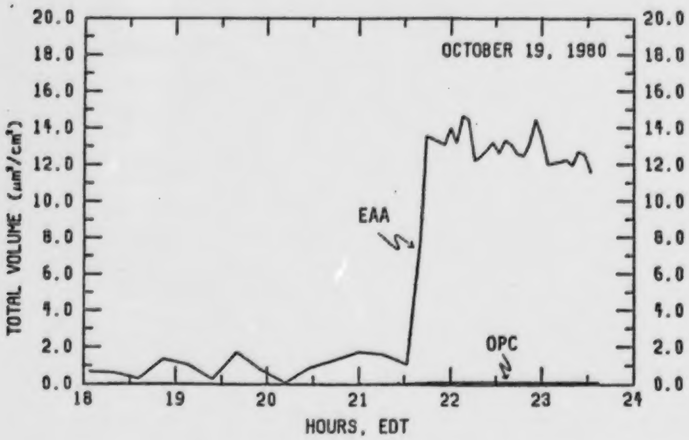

Figure 25b. Electrical Aerosol Analyzer and Optical Particle Counter Total Volume data for October 19, 1980 dark phase reaction between Isoprene and Ozone.

Gravimetric determinations from Teflon filter samples during a higher concentration isoprene-$O_3$ experiment ( 20 ppmC and 5 ppm ) indicate that less than 1 percent of the reacted isoprene mass was captured on the filter. The post-experimental filter material was light brown in color, while a chamber blank filter sample did not show any discoloration. Both filters were sonically extracted with methylene chloride. The blank filtrate remained clear while that of the suspected reaction products took on a yellow color. The filters were not removed from the extract and a few drops of diazomethane[52] in ethyl ether were added to both samples. This was done to derivitize organic acids to their methyl esters, which can be more easily chromatographed and further analyzed by mass spectroscopy. The technique may derivitize other oxygenated organic compounds. The addition of diazomethane to the isoprene-$O_3$ sample generated visible bubbling, which is a indicator of positive reaction. The blank did not show a positive response when diazomethane was added. Analysis by GCMS of the diazomethane samples from the isoprene-$O_3$ filter did not show any methyl esters.

Lower concentrations of isoprene and $O_3$ and $\alpha$-pinene and $O_3$ were also run during the day in both halves of the dual outdoor chamber. This was done to observe aerosol formation at more realistic initial concentrations. With 0.2 ppmC $\alpha$-pinene and 0.12 ppm $O_3$, substantial CN aerosol was formed (Figure 26). At this concentration in a similar system of isoprene and $O_3$ no CN was observed. In another experiment 0.2 ppmC of isoprene and 0.15 ppm $O_3$ were reacted in the afternoon with no observable CN formation. After 30 minutes, 0.2 ppmC of $\alpha$-pinene was added. Approximately 4 times the CN number were observed after $\alpha$-pinene addition as were observed in the similar system initially containing 0.2 ppmC $\alpha$-pinene and having 0.12 ppm $O_3$ added (Figure 26).

Finally, CN aerosol generation ( 600 particles per cc) has been observed from reaction of 50 ppbC of $\alpha$-pinene and 0.05 ppm of $O_3$. This level is within the hydrocarbon concentration range observed under pine forest canopies.[53] Subsequent additions of 50 ppbC of $\alpha$-pinene to the above system did not produce additional bursts of CN aerosol. It is possible that the products from $O_3$ oxidation condensed on the previously generated $\alpha$-pinene-$O_3$ aerosol. Since homogeneous nucleation would not

TYPING GUIDE SHEET
BEGIN FIRST LINE OF TEXT HERE
CENTER OF PAGE
TOP OF IMAGE AREA
DROPPED HEAD; BEGIN SECTIONS HERE

necessarily be required under natural conditions, it is possible that isoprene products under similar conditions could condense on pre-existing nuclei and hence contribute to the aerocolloidal mass found in rural atmospheres.

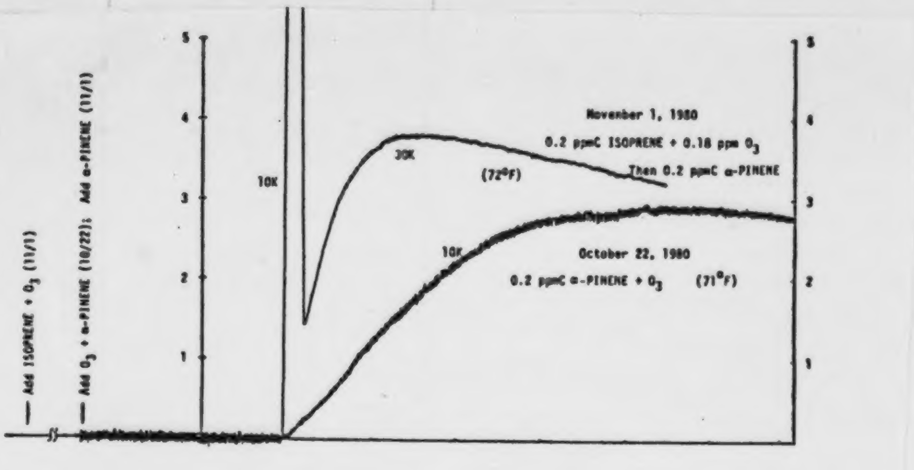

Figure 26. Condensation nuclei traces for experiments on October 22 and November 1, 1980.

Modeling Gas Phase Reactions of Isoprene and $O_3$--

It was decided that an understanding of the chemical mechanisms for $O_3$ attack on the two isoprene daughter products, MACR and MVK, would be necessary before a model for isoprene and $O_3$ could be developed. The approach used by Dodge and Arnts[54] to model propylene-$O_3$ systems was selected to describe the MVK-$O_3$ and MACR-$O_3$ reactions and products. By using the analogs of a "hot" formic acid and "hot" ester and the resulting Dodge-Arnts type products (Figure 27), a scheme for $O_3$ attack on MVK and its resulting products was developed (Figure 28).

BEGIN LAST LINE OF TEXT
BOTTOM OF IMAGE AREA, OUTSIDE DIMENSION FOR TABLES AND ILLUSTRATIONS
3/8"
PAGE NUMBER

EPA-287 (Cin.)
(4-76)

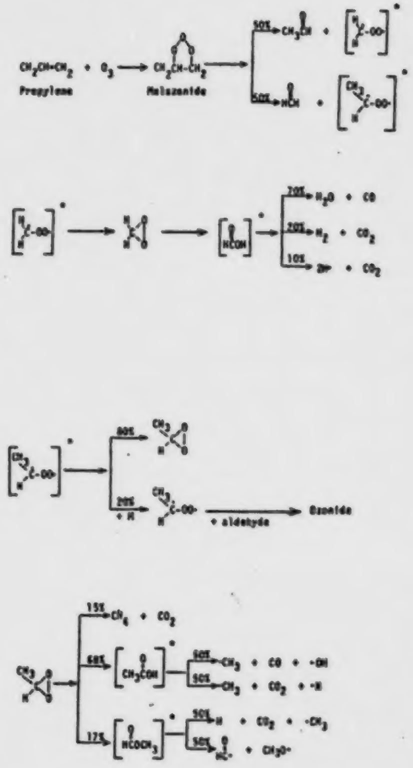
Propylene
Malozonide
+ aldehyde
Ozonide

Figure 27. Dodge-Arnts chemical reaction scheme for ozone reaction with propylene.

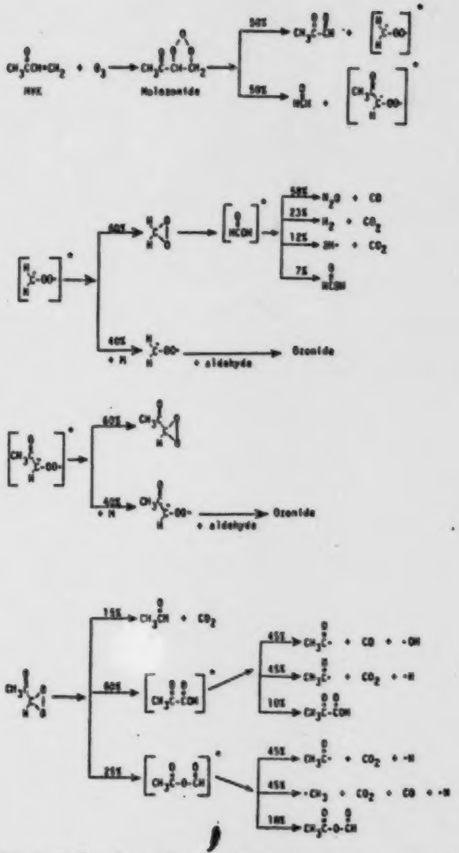
MVK
Malozonide
+ aldehyde
Ozonide

Figure 28. Reaction scheme for ozone reaction with methylvinylketone.

TYPING GUIDE SHEET
BEGIN FIRST LINE OF TEXT HERE
CENTER OF PAGE
TOP OF IMAGE AREA
DROPPED HEAD. BEGIN SECTIONS HERE

The newer decomposition pathway fractions suggested by Niki et al.[55] and Su, Calvert and Shaw[56] were used for "hot" formic acid. Note that the decomposition of the dioxirane compound of MVK suggests the formation of small quantities of acetaldehyde. This would be analogous to the formation of $CH_4$ from C-2-butene and $O_3$ (as noted by Niki et al.[55]) and can be seen in Figure 27. Low concentrations of acetaldehyde were evident in the chromatograms from the MVK and $O_3$ experiment. From the reaction scheme outlined in Figure 27, a mechanism for MVK and $O_3$ was constructed and is shown in Table 16. A similar mechanism was developed for MACR.

The MVK mechanism was tested against a dark chamber experiment in which 0.93 ppmV of MVK were reacted with $O_3$, which was added to the chamber at a rate of 0.22 ppm/hr. In this November 3, 1980 MVK-$O_3$ run, an $O_3$ attack rate on MVK of $6.0 \times 10^{-3}$ $ppm^{-1} min^{-1}$ was found to give the best fit in the simulations. A comparison between the experimental data and the model predictions is shown in Figure 29a. The best fit for $O_3$ attack rate on MACR turned out to be much less than that for MVK. A rate of $1.6 \times 10^{-3}$ $ppm^{-1} min^{-1}$ provided the best fit for the MACR-$O_3$ simulation (Figure 29b). The assumption of a 1:1 split between the formation of methylglyoxal and what will be referred to as a "hot" biradical intermediate was utilized for both the MACR and MVK oxidation pathways (Reaction 16).

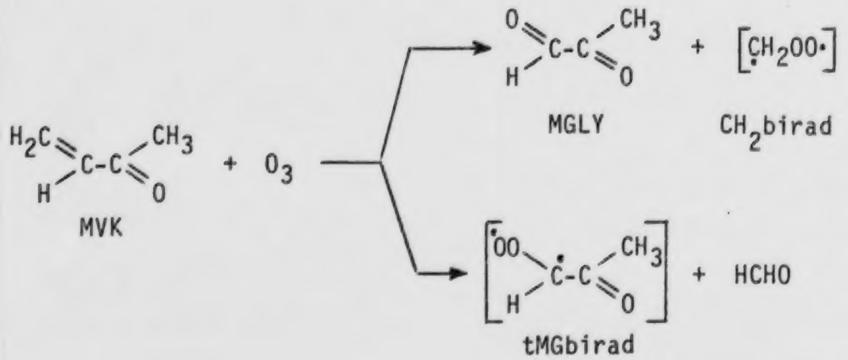

(16)

BOTTOM OF IMAGE AREA; OUTSIDE DIMENSION FOR TABLES AND ILLUSTRATIONS
BEGIN LAST LINE OF TEXT

EPA-287 (Cin.)
(4-76)

TYPING GUIDE SHEET
BEGIN FIRST LINE OF TEXT HERE
DROPPED HEAD, BEGIN SECTIONS HERE
CENTER OF PAGE
TOP OF IMAGE AREA

| **Reaction** | **Reactants** | | | **Products** | | | **Rate Constant** |
|---|---|---|---|---|---|---|---|
| 1 | | | ------> | 1.00 $O_3$ | | | 3.66 x 10-3 |
| 2 | MVK | + $O_3$ | ------> | 1.00 MGLY | + 0.60 $CH_2$diox | + 0.40 $CH_2$birad | 3.00 x 10-3 |
| 3 | MVK | + $O_3$ | ------> | 1.00 HCHO | + 0.60 tMGdiox | + 0.40 tMGbirad | 3.00 x 10-3 |
| 4 | | $CH_2$diox | ------> | 0.58 CO | + 0.23 $HO_2$ | + 0.35 $CO_2$ | 1.00 x 10+6 |
| 5 | | tMGdiox | ------> | 1.96 $CH_3CO_3$ | + 1.49 $HO_2$ | + 0.81 OH | 1.00 x 10+6 |
| 6 | | tMGdiox | ------> | 0.34 $CH_3OO$ | + 0.18 Pyruvic | + 0.08 Anhidrid | 1.00 x 10+6 |
| 7 | | tMGdiox | ------> | 0.45 $CH_3CHO$ | + 1.15 CO | + 1.94 $CO_2$ | 1.00 x 10+6 |
| 8 | MVK | + OH | ------> | 1.00 OH*Prod2 | | | 4.00 x 10+4 |
| 9 | OH*Prod2 | + OH*Prod2 | ------> | | | | 2.50 x 10+2 |
| 10 | OH*Prod2 | + OH*Prod2 | ------> | 2.00 $HO_2$ | + 2.00 HCHO | + 2.00 MGLY | 2.50 x 10+2 |
| 11 | OH*Prod2 | + $HO_2$ | ------> | | | | 8.00 x 10+3 |
| 12 | $CH_2$birad | + $CH_2$birad | ------> | 2.00 HCHO | | | 1.00 x 10+4 |
| 13 | $CH_2$birad | + $HO_2$ | ------> | | | | 8.00 x 10+3 |
| 14 | $CH_2$birad | + HCHO | ------> | 1.00 Ozonide | | | 1.00 |
| 15 | tMGbirad | + tMGbirad | ------> | 2.00 MGLY | | | 1.00 x 10+4 |
| 16 | tMGbirad | + $HO_2$ | ------> | | | | 8.00 x 10+3 |
| 17 | tMGbirad | + HCHO | ------> | 1.00 Ozonide | | | 1.00 |
| 18 | OH | + HCHO | ------> | 1.00 $HO_2$ | + 1.00 CO | | 1.40 x 10+4 |
| 19 | OH | + $CH_3CHO$ | ------> | 1.00 $CH_3CO_3$ | | | 2.40 x 10+4 |
| 20 | $O_3$ | + OH | ------> | 1.00 $HO_2$ | | | 2.365 x 10+3 x $e^{-1000/T}$ |
| 21 | $O_3$ | + $HO_2$ | ------> | 1.00 OH | | | 1.478 x 10+2 x $e^{-1250/T}$ |
| 22 | $HO_2$ | + $HO_2$ | ------> | 1.00 $H_2O_2$ | | | 4.894 x 10+4 x $e^{-541/T}$ |
| 23 | OH | + CO | ------> | 1.00 $HO_2$ | | | 4.43 x 10+2 |
| 24 | $CH_3OO$ | + $CH_3OO$ | ------> | 1.50 HCHO | + 1.50 $HO_2$ | | 6.00 x 10+2 |
| 25 | $CH_3OO$ | + $HO_2$ | ------> | | | | 8.00 x 10+3 |
| 26 | $CH_3CO_3$ | + $CH_3CO_3$ | ------> | 2.00 HCHO | + 2.00 $HO_2$ | | 2.40 x 10+3 |
| 27 | $CH_3CO_3$ | + $HO_2$ | ------> | | | | 8.00 x 10+3 |

Table 16. Mechanism for dark phase methylvinylketone and ozone system.

BEGIN LAST LINE OF TEXT
BOTTOM OF IMAGE AREA, OUTSIDE DIMENSION FOR TABLES AND ILLUSTRATIONS
3/8"
PAGE NUMBER
EPA-287 (Cin.)
(4-76)

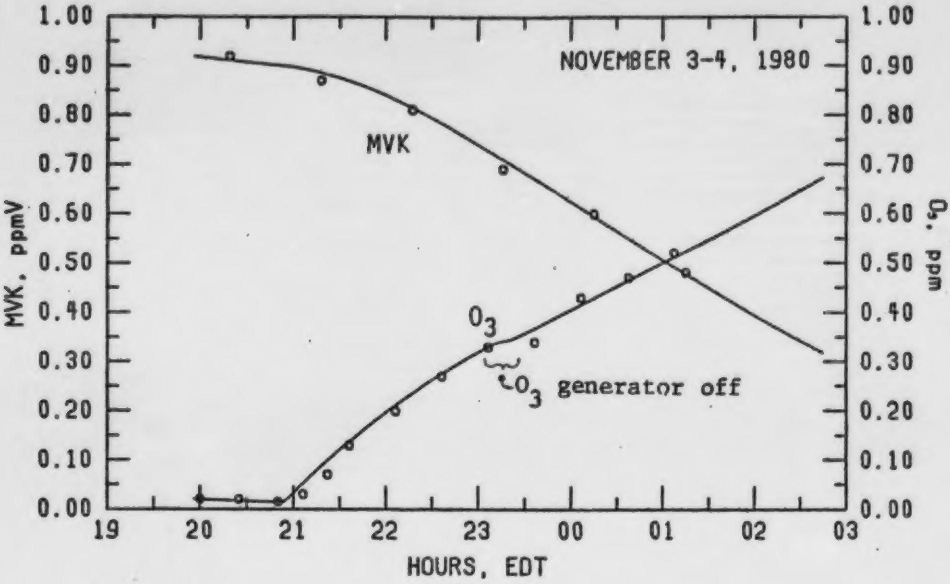

Figure 29a. UNC model of $O_3$ and MVK for November 3, 1980. 0.93 ppmV MVK slug injected at 2025 hr.; $O_3$ ramp injected (0.22 ppm/hr) at 2055. Experimental data o o o . Model results ——— .

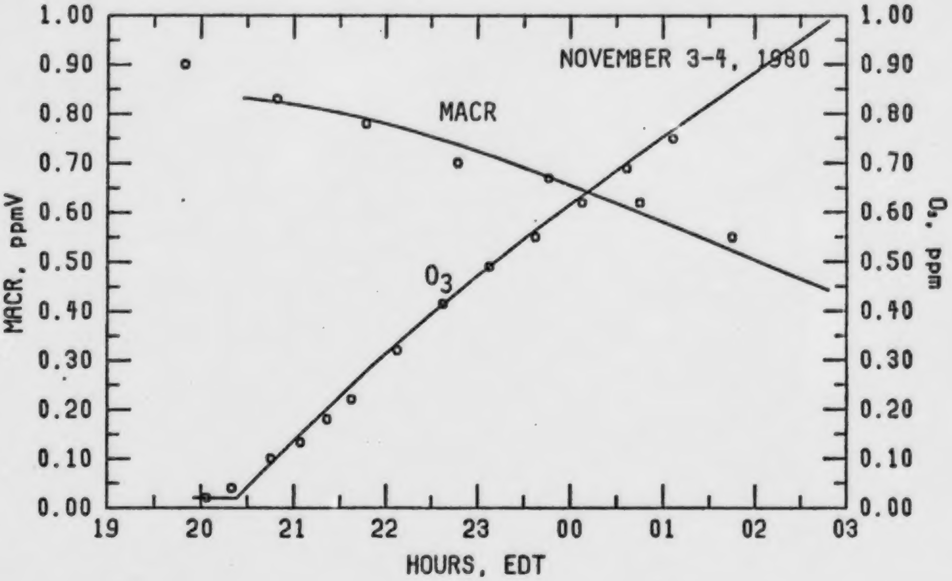

Figure 29b. UNC model of $O_3$ amd MACR for November 3, 1980. 0.90 ppmV MACR slug injected at 1948 hr.; $O_3$ ramp injected (0.21 ppm/hr) at 2018. Experimental data o o o . Model results ——— .

TYPING GUIDE SHEET

Methylglyoxal was qualitatively identified as a product by DNPH technique. Because there was an extended period between sampling and HPLC analysis, however, these data were not used to calculate the aldehyde/biradical split from $O_3$ attack on either MVK or MACR.

Expansion of the above mechanism to include isoprene required that attack on both carbon double bonds of isoprene be considered. MVK and MACR product data from the October 9-10 isoprene-$O_3$ experiment were used as initial estimates of the various chemical split ratios. This was possible because, in this experiment, computations indicated that subsequent reaction of either MVK or MACR with $O_3$ was not significant.

It was shown in Table 1 that the reaction of 0.55 ppm of isoprene formed 0.23 ppmV of MACR and 0.10 ppmV of MVK on October 9-10. To satisfy the experimental yields of MVK and MACR, split ratios of $O_3$ attack on either the 1,2 or 3,4 carbon double bond and subsequent splits of the molozonides from Reaction 17 (as shown in Reactions 7 and 8) were needed. Because of the similarity in structure it was assumed that the molozonides splits for both MVK and MACR in Reactions 7 and 8 were approximately equal. This assumption and observed product yields of MVK and MACR required a 35:65 split between the 1,2 and 3,4 carbon double bonds of isoprene in Reaction 17. Subsequently, approximately 65% of the molozonides in Reactions 18 and 19 would have to decompose to MVK and MACR and 35% to complement hot biradicals and formaldehyde. In the final mechanism these splits were optimized slightly (see actual splits in Reactions 18 and 19) and then held constant to model two different dark isoprene-$O_3$ experiments.

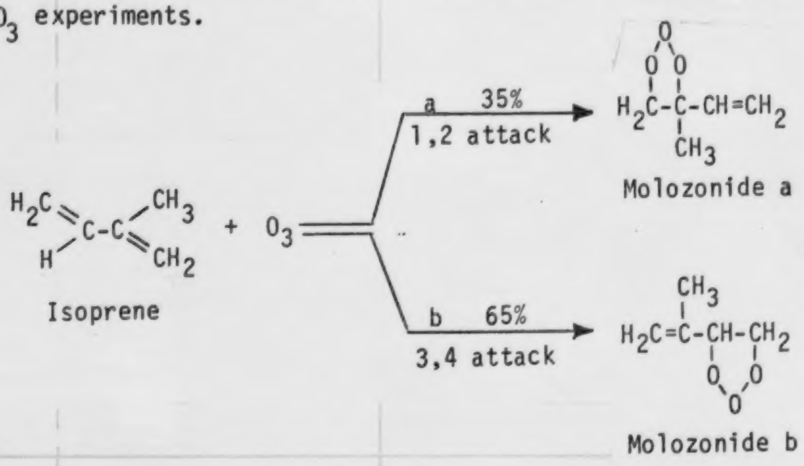

(17)

EPA-287 (Cin.)
(4-76)

BEGIN FIRST LINE OF TEXT HERE
TYPING GUIDE SHEET
CENTER OF PAGE
TOP OF IMAGE AREA
DROPPED HEAD, BEGIN SECTIONS HERE

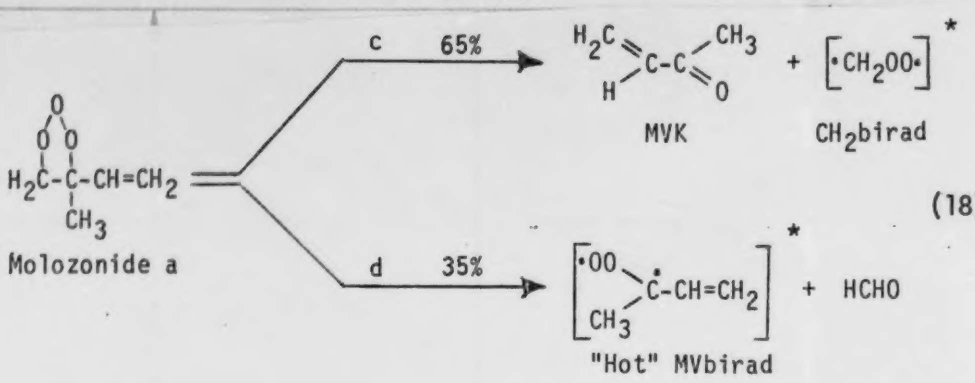

(18)

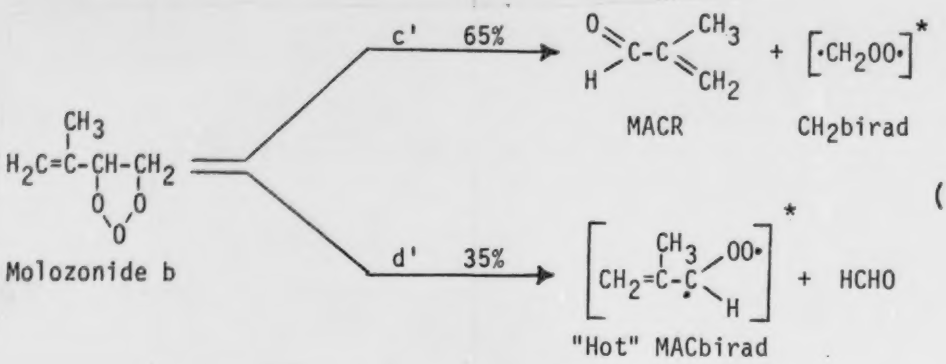

(19)

The selection of similar split ratios for Reactions 18 and 19 was somewhat arbitrary and other choices and approaches are possible. For example, with simple olefins, the $O_3$ attack rate increases as methyl groups are substituted onto a carbon participating in a double bond (i.e., trans-2-butene>propylene>ethylene). The applicability of this trend to conjugated diolefins is not clear. One might assume however, that the preferential site of initial $O_3$ attack on isoprene is the 1,2 carbon bond, possibly, indicating use of a 60:40 split for path a vs path b in Reaction 17. To comply with the experimental yields of the October 9-10 isoprene experiment a 33:67 split would then be required in Reaction 18 for MVK and better than a 100:0 split for MACR in Reaction 19. Hence this approach was abandoned and we relied on empirical information to arrive at the chemical split ratios. Once again, note that the split ratios and reaction rates used in this study are quite speculative and should only be utilized with this in mind. Further experimental and theoretical information is needed.

BEGIN LAST LINE OF TEXT
BOTTOM OF IMAGE AREA OUTSIDE DIMENSION FOR TABLES AND ILLUSTRATIONS
3/8"

PAGE NUMBER
EPA-287 (Cin.)
(4-76)

Rearrangement of the "hot" biradical complement of MACR to form a dioxirane intermediate or a stable biradical, which can further react to form an ozonide, is shown in Reaction 20.

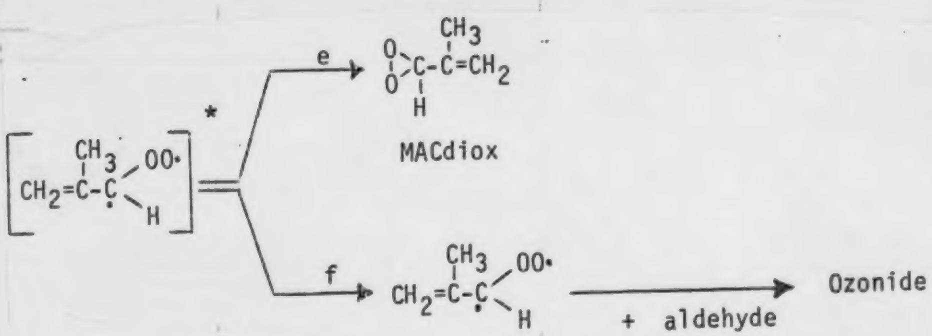

(20)

Su, Calvert and Shaw[56] and Niki et al.[51] have recently suggested that 35-38 percent of "hot" dioxirane intermediates from ethylene-$O_3$ systems form stable biradicals and are available to form ozonides. Given the level of CO production from the isoprene-$O_3$ system and the various ways CO is made in the mechanism (i.e., decomposition of hot formic acid and products in Reactions 18 and 19), this shift toward higher biradical stabilization (path f) in Reaction 20 seems to be indicated.

If the same processes used by Dodge and Arnts (Figure 27) are applied to the dioxirane compound in Reaction 20, it should rearrange and decompose according to the scheme shown in Reaction 21. Decomposition of the dioxirane compound by path g should lead to low concentrations of propylene; indeed, in the October 9, 1980 system 0.04 ppmC of propylene was measured.

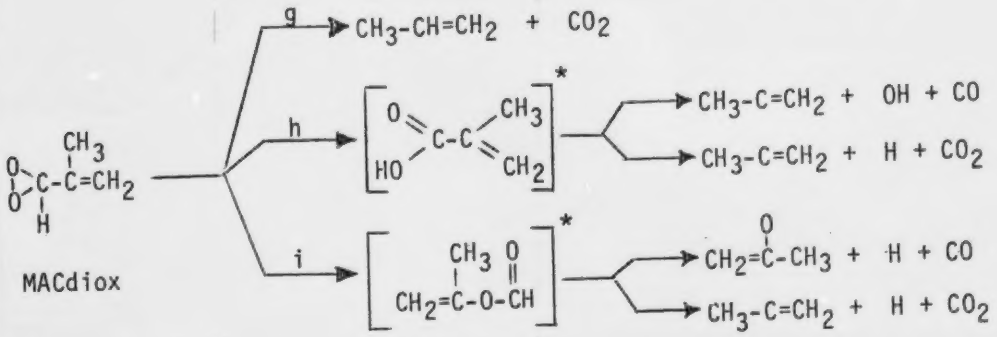
g
h
i
MACdiox
$CH_3$-CH=$CH_2$ + $CO_2$
$CH_3$-C=$CH_2$ + OH + CO
$CH_3$-C=$CH_2$ + H + $CO_2$
$CH_2$=C-$CH_3$ + H + CO
$CH_3$-C=$CH_2$ + H + $CO_2$

(21)

EPA-287 (Cin.)
(4-76)

TYPING GUIDE SHEET

Approximately 10-20 percent of the dioxirane compound would have to decompose by path g to satisfy the propylene yields. This is similar to the percentage suggested by Dodge and Arnts[54] for the $CH_4$ analog propylene-$O_3$ systems. Herron and Huie[57] estimated 20 percent for the analogous formation of $H_2$ molecules from ethylene-$O_3$. The absolute yield through path g will depend on the extent to which stable biradicals are formed in Reaction 20 vs. the formation of a dioxirane type compound.

Inspection of the final products in Reaction 21 indicates that ketene may be a possible product. In the initial discussion of the major gas phase products, approximately 5 percent of the reacted isoprene carbon appeared as a product which had the same retention time as acetone. On the Carbowax 20M column, which was used to analyze MACR and MVK, ketene would have an elution time similar to that of acetone. Clearly, additional analytical work is needed.

In the dark, radical chain reactions are effectively suppressed. Under such conditions, formaldehyde is a non-reactive product. This simplifies, to some extent, analysis of the methods of formaldehyde production. It can be seen from the isoprene reactions presented that the primary source of formaldehyde should be path d of Reactions 18 and 19. By adding the concentration of HCHO that would be produced in those reactions, a maximum of only 0.20 ppm was expected from the initial isoprene of October 9. Experimentally, we observed 0.53 ppm of HCHO produced. Although another formaldehyde source would be through MVK and MACR reactions with $O_3$, these were unimportant in the October 8 and 9 experiments. The obvious discrepancy led us to consider that a large part of the initial product carbon appears in $C_3$ and $C_4$ radical and biradical reaction products; possibly, the additional HCHO production results from reactions of these species. Because the chemistry of these species is unknown, further reactions can only be predicted through analogy to simpler species. This was done in our modeling effort, not in an attempt to confirm these reactions, but to see if it was possible to account for the HCHO data through secondary reactions without affecting our ability to simulate the chemistry of the measurable species.

EPA-287 (Cin.)
(4-76)

The mechanism used to model the dark phase isoprene-$O_3$ experiments is shown in Table 17. A best fit rate of ozone attack on isoprene of 1.67 $10^{-2}$ $ppm^{-1}$ $min^{-1}$ ($65^{0}F$) was used and is consistent with other published values.[40,58] Results for the October 8 and 9 experiments are presented in Figures 31-33. Reactions 2 through 28 are explicit descriptions for the $O_3$ and OH oxidation schemes of isoprene, MVK and MACR. Although the OH reactions are minor at night, they were included to optimize the fits of the major species. After Reactions 29 through 34, which are the important dark phase, inorganic reactions, a simplified set of reactions was utilized for the chemistry of secondary species as described above. In this scheme, radical and biradical products reacted only with themselves or $HO_2$, usually forming stable products. Biradicals also react with HCHO to form ozonides. Reactions with low mass flux had products omitted for mechanism simplicity (i.e., Reactions 43, 44, and 45). Also, some reactions were not included because their importance is not known. An example of such a step would be the $H_2O$ catalized reaction which yields formic acid from H-containing peroxy biradicals, as suggested by Calvert and recently studied by Hatakeyoma et al.

The modeling results shown in Figure 32 indicate that it is possible to approximate the HCHO buildup with this mechanism. Less than half of the HCHO is produced directly from $O_3$ oxidation of isoprene, MVK and MACR. Although we do not hold that the secondary radical and biradical reactions as shown in the mechanism are exclusively correct, more than half of the HCHO produced in these dark phase systems comes from this segment of the chemistry. The results indicate that HCHO buildup can be simulated without affecting the modeling of all major indicator species. Further elementary kinetic experiments are needed to discern the major secondary species involved and their respective chemistries before this system or a more complicated photooxidation system can be completely understood.

## Summary and Conclusions

UNC outdoor chamber experiments have shown that in high concentration systems of isoprene and $O_3$ (5 ppmC and 1 ppmC), approximately 75 percent of the reacted carbon can be observed in the product formation of HCHO, CO, methacrolein, and methylvinylketone. Other $C_2$-$C_5$ carbonyl

BEGIN FIRST LINE OF TEXT HERE
TYPING GUIDE SHEET
CENTER OF PAGE
TOP OF IMAGE AREA
DROPPED HEAD; BEGIN SECTIONS HERE

| Reaction | Reactants | | | Products | | | Rate Constant |
|---|---|---|---|---|---|---|---|
| 1 | | | ------> | 1.00 $O_3$ | | | $7.00 \times 10^{-3}$ |
| 2 | Isoprene | + $O_3$ | ------> | 1.00 MACR | + 0.60 $CH_2$diox | + 0.40 $CH_2$birad | $7.06 \times 10^{-3}$ |
| 3 | Isoprene | + $O_3$ | ------> | 1.00 HCHO | + 0.60 MACdiox | + 0.40 MACbirad | $3.80 \times 10^{-3}$ |
| 4 | Isoprene | + $O_3$ | ------> | 1.00 MVK | + 0.60 $CH_2$diox | + 0.40 $CH_2$birad | $3.50 \times 10^{-3}$ |
| 5 | Isoprene | + $O_3$ | ------> | 1.00 HCHO | + 0.60 MVdiox | + 0.40 MVbirad | $2.34 \times 10^{-3}$ |
| 6 | MACR | + $O_3$ | ------> | 1.00 MGLY | + 0.60 $CH_2$diox | + 0.40 $CH_2$birad | $8.00 \times 10^{-4}$ |
| 7 | MACR | + $O_3$ | ------> | 1.00 HCHO | + 0.60 aMGdiox | + 0.40 aMGbirad | $8.00 \times 10^{-4}$ |
| 8 | MVK | + $O_3$ | ------> | 1.00 MGLY | + 0.60 $CH_2$diox | + 0.40 $CH_2$birad | $3.00 \times 10^{-3}$ |
| 9 | MVK | + $O_3$ | ------> | 1.00 HCHO | + 0.60 tMGdiox | + 0.40 tMGbirad | $3.00 \times 10^{-3}$ |
| 10 | | $CH_2$diox | ------> | 0.58 CO | + 0.23 $HO_2$ | + 0.35 $CO_2$ | $1.00 \times 10^{+6}$ |
| 11 | Isoprene | + OH | ------> | 1.00 OH*Prod | | | $5.00 \times 10^{+4}$ |
| 12 | OH*Prod | + OH*Prod | ------> | 2.00 $HO_2$ | + 2.00 MACR | + 2.00 HCHO | $2.50 \times 10^{+2}$ |
| 13 | OH*Prod | + OH*Prod | ------> | 2.00 $HO_2$ | + 2.00 MVK | + 2.00 HCHO | $2.50 \times 10^{+2}$ |
| 14 | OH*Prod | + $HO_2$ | ------> | | | | $8.00 \times 10^{+3}$ |
| 15 | MACR | + OH | ------> | | | | $4.00 \times 10^{+4}$ |
| 16 | MVK | + OH | ------> | | | | $4.00 \times 10^{+4}$ |
| 17 | | MVdiox | ------> | 0.15 Propene | + 1.58 $CO_2$ | + 1.43 $CH_3OO$ | $1.00 \times 10^{+6}$ |
| 18 | | MVdiox | ------> | 0.90 CO | + 0.90 HCHO | + 1.43 $HO_2$ | $1.00 \times 10^{+6}$ |
| 19 | | MVdiox | ------> | 0.53 $CH_3CO_3$ | + 0.53 Ketene | + 2.33 EthenOO | $1.00 \times 10^{+6}$ |
| 20 | | MACdiox | ------> | 0.45 Propene | + 2.30 $CO_2$ | | $1.00 \times 10^{+6}$ |
| 21 | | MACdiox | ------> | 1.80 $HO_2$ | + 1.60 OH | + 1.70 CO | $1.00 \times 10^{+6}$ |
| 22 | | MACdiox | ------> | 3.30 PropenOO | + 0.10 $CH_3OO$ | + 0.10 Ketene | $1.00 \times 10^{+6}$ |
| 23 | | aMGdiox | ------> | 0.61 HCHO | + 1.15 $CH_3OO$ | + 2.90 $HO_2$ | $1.00 \times 10^{+6}$ |
| 24 | | aMGdiox | ------> | 0.54 $CH_3CO_3$ | + 0.12 Anhidrid | + 2.36 CO | $1.00 \times 10^{+6}$ |
| 25 | | aMGdiox | ------> | 0.45 $CH_3CHO$ | + 2.14 $CO_2$ | + 0.14 Ester | $1.00 \times 10^{+6}$ |
| 26 | | tMGdiox | ------> | 1.96 $CH_3CO_3$ | + 1.49 $HO_2$ | + 0.81 OH | $1.00 \times 10^{+6}$ |
| 27 | | tMGdiox | ------> | 0.34 $CH_3OO$ | + 0.18 Pyruvic | + 0.08 Anhidrid | $1.00 \times 10^{+6}$ |
| 28 | | tMGdiox | ------> | 0.45 $CH_3CHO$ | + 1.15 CO | + 1.94 $CO_2$ | $1.00 \times 10^{+6}$ |
| 29 | OH | + HCHO | ------> | 1.00 $HO_2$ | + 1.00 CO | | $1.40 \times 10^{+4}$ |
| 30 | OH | + $CH_3CHO$ | ------> | 1.00 $CH_3CO_3$ | | | $2.40 \times 10^{+4}$ |
| 31 | $O_3$ | + OH | ------> | 1.00 $HO_2$ | | | $2.365 \times 10^{+3} \times e^{-1000/T}$ |
| 32 | $O_3$ | + $HO_2$ | ------> | 1.00 OH | | | $1.478 \times 10^{+2} \times e^{-1250/T}$ |
| 33 | $HO_2$ | + $HO_2$ | ------> | 1.00 $H_2O_2$ | | | $4.894 \times 10^{+4} \times e^{-581/T}$ |
| 34 | OH | + CO | ------> | 1.00 $HO_2$ | | | $4.43 \times 10^{+2}$ |
| 35 | PropenOO | + PropenOO | ------> | 2.00 Ketene | + 2.00 HCHO | + 2.00 $HO_2$ | $1.00 \times 10^{+4}$ |
| 36 | PropenOO | + $HO_2$ | ------> | | | | 8.00 c $10^{+3}$ |
| 37 | $CH_3OO$ | + $CH_3OO$ | ------> | 1.50 HCHO | + 1.50 $HO_2$ | | $6.00 \times 10^{+2}$ |
| 38 | $CH_3OO$ | + $HO_2$ | ------> | | | | $8.00 \times 10^{+3}$ |
| 39 | EthenOO | + EthenOO | ------> | 2.00 Ketene | + 2.00 $HO_2$ | | $1.00 \times 10^{+4}$ |
| 40 | EthenOO | + $HO_2$ | ------> | | | | $8.00 \times 10^{+3}$ |
| 41 | $CH_3CO_3$ | + $CH_3CO_3$ | ------> | 2.00 HCHO | + 2.00 $HO_2$ | | $2.40 \times 10^{+3}$ |
| 42 | $CH_3CO_3$ | + $HO_2$ | ------> | | | | $8.00 \times 10^{+3}$ |
| 43 | Propene | + $O_3$ | ------> | 1.00 $CH_3CHO$ | + 0.60 $CH_2$diox | + 0.40 $CH_2$birad | $8.50 \times 10^{-3}$ |
| 44 | Propene | + $O_3$ | ------> | 1.00 HCHO | | | $8.50 \times 10^{-3}$ |
| 45 | Propene | + OH | ------> | | | | $3.80 \times 10^{+4}$ |
| 46 | Ketene | + $O_3$ | ------> | 0.60 $CH_2$diox | + 0.40 $CH_2$birad | | $1.70 \times 10^{-2}$ |
| 47 | Ketene | + OH | ------> | 1.00 Keten*OH | | | $3.80 \times 10^{+4}$ |
| 48 | Keten*OH | + Keten*OH | ------> | 2.00 HCHO | + 2.00 $HO_2$ | | $8.00 \times 10^{+3}$ |
| 49 | Keten*OH | + $HO_2$ | ------> | | | | $8.00 \times 10^{+3}$ |
| 50 | $CH_2$birad | + $CH_2$birad | ------> | 2.00 HCHO | | | $1.00 \times 10^{+4}$ |
| 51 | $CH_2$birad | + $HO_2$ | ------> | | | | $8.00 \times 10^{+3}$ |
| 52 | $CH_2$birad | + HCHO | ------> | 1.00 Ozonide | | | 1.00 |
| 53 | MVbirad | + MVbirad | ------> | 2.00 MVK | | | $1.00 \times 10^{+4}$ |
| 54 | MVbirad | + $HO_2$ | ------> | | | | $8.00 \times 10^{+3}$ |
| 55 | MVbirad | + HCHO | ------> | 1.00 Ozonide | | | 1.00 |
| 56 | MACbirad | + MACbirad | ------> | 2.00 MACR | | | $1.00 \times 10^{+4}$ |
| 57 | MACbirad | + $HO_2$ | ------> | | | | $8.00 \times 10^{+3}$ |
| 58 | MACbirad | + HCHO | ------> | 1.00 Ozonide | | | 1.00 |

Table 17. Mechanism for Dark Phase Isoprene and Ozone System

BEGIN LAST LINE OF TEXT
BOTTOM OF IMAGE AREA, OUTSIDE DIMENSION FOR TABLES AND ILLUSTRATIONS
3/8"
PAGE NUMBER
EPA-287 (Cin.)
(4-76)

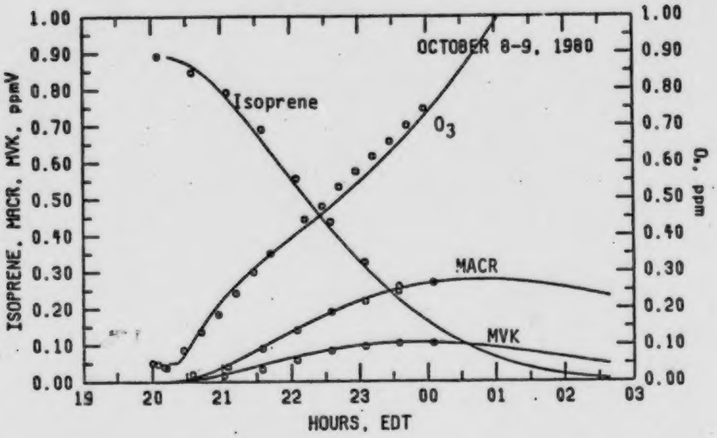

Figure 30. UNC model of $O_3$ and Isoprene for November 8, 1980. 0.89 ppmV Isoprene slug injected at 2000 hr.; $O_3$ ramp injected (0.46 ppm/hr) at 2020. Experimental data o o o . Model results ——— .

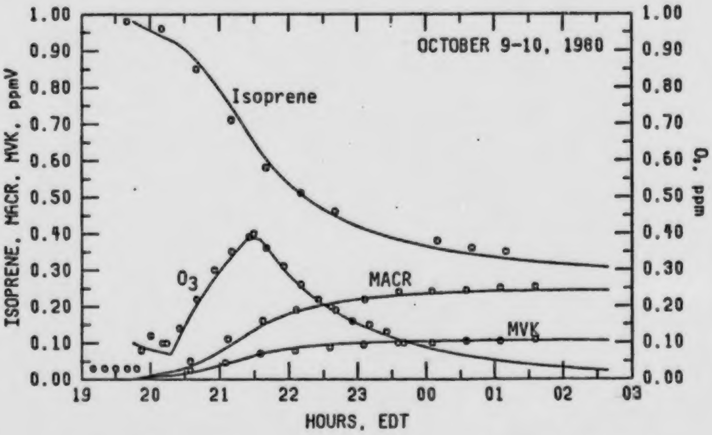

Figure 31. UNC model of $O_3$ and Isoprene for November 9, 1980. 0.98 ppmV Isoprene slug injected at 1935 hr.; $O_3$ ramp injected (0.52 ppm/hr) at 2012. Experimental data o o o . Model results ———.

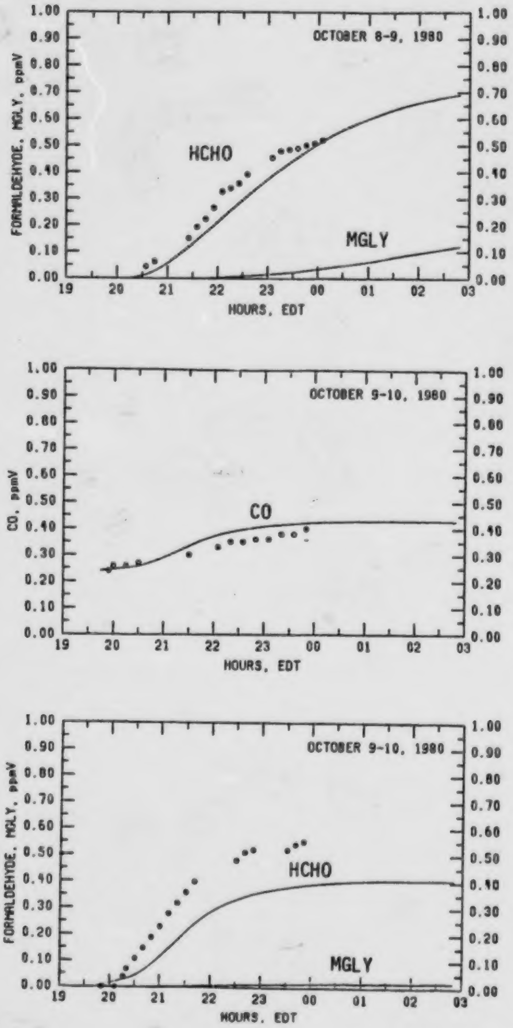

Figure 32. Formaldehyde, Carbon Monoxide, and Methylglyoxal product yields from October 8 and October 9, 1980 isoprene and $O_3$ experiments. Experimental data ∘∘∘. Model Results ——.

compounds including methylglyoxal were tentatively identified by chromatographic analysis. Measurements did not include $CO_2$ and HCOOH and once estimated yields are included even a greater portion of the reacted carbon can be accounted for.

Dark isoprene-$O_3$ systems appear to form homogeneously nucleated aerosol. Most of these particles remain at diameters well below the optical cutoff region ($d_p$ = 0.3-0.5 μm) as opposed to the particles from similar α-pinene-$O_3$ systems, which also form at smaller sizes but then grow into the optical size range ($d_p$ = 0.5 μm). On a qualitative basis isoprene, for the above noted system, generated almost the same level of CN or EAA aerosol as did half the initial carbon from a similar α-pinene-$O_3$ system. Lower concentrations of α-pinene and $O_3$ (0.2 ppmC and 0.12 ppm) still generated substantial aerosol, but by comparison, rapid CN nucleation was not observed during a similar side-by-side system of isoprene and $O_3$. CN aerosol generation did occur from the reaction of 50 ppbC of α-pinene and 0.05 ppm of $O_3$. This level is within the hydrocarbon concentration range observed under pine forest canopies. Subsequent additions of 50 ppbC of α-pinene to this system did not produce additional bursts of CN aerosol. Experimental results suggest that, since homogeneous nucleation would not necessarily be required under natural conditions, isoprene products could condense on existing nuclei and contribute to the aerocolloidal mass found in rural atmospheres.

A mechanism for $O_3$ attack on methylvinylketone, methacrolein and isoprene was proposed. Best fits to experimental data were otained when $O_3$ rates for MVK and MACR of $6.0 \times 10^{-3}$ and $1.6 \times 10^{-3}$ $ppm^{-1}$ $min^{-1}$ were used. An $O_3$ attack rate on isoprene of $1.67 \times 10^{-2}$ $ppm^{-1}$ $min^{-1}$ was used and is consistent with other literature values. The product yields of methacrolein and methylvinylketone provided some insight into the possible chemical pathways for an isoprene-$O_3$ mechanism. The mechanism used, however, accounted for only about 1/2 of the formaldehyde observed. Radical recombination and decomposition chemistry must be elucidated to accurately describe HCHO production. The formation, however, of other products like acetaldehyde and propylene suggests that the original approach taken by Herron and Huie[57] for ethylene-$O_3$ systems and Dodge and Arnts[54] for propylene-$O_3$ systems might be applicable to larger olefin molecules.

BEGIN FIRST LINE OF TEXT HERE
TYPING GUIDE SHEET
CENTER OF PAGE
TOP OF IMAGE AREA
DROPPED HEAD BEGIN SECTIONS HERE

## SECTION 7

## CHANGES IN INITIAL $NO_x$ AND HYDROCARBON COMPOSITION AND ITS EFFECTS ON $O_3$ PRODUCTION

### INTRODUCTION

In this section experiments are discussed which tested the effect of a single variable on the reactivity of an urban type mix-$NO_x$ system. Changes in initial starting conditions which were investigated include: a) effects of different starting percentages of $NO_2$ b) the addition of $O_3$ to mix-$NO_x$ smog systems at sunrise or during the morning hours c) the effects of extra initial aldehydes and d) the addition of 25-40 percent more NMHC to an atmospheric mixture in the form of propane or n-butane. In addition, the UNC 11 component mixture (Table 1) was compared in matched $NO_x$ smog systems to a 75:25 carbon mixture of butane and propylene. Simulated and real auto exhaust comparisons are also discussed.

### EFFECT OF DIFFERENT PERCENTAGES OF STARTING $NO_2$

Smog chamber data have been historically used to test photochemical mechanisms. In a computer sensitivity study of the EKMA procedure[2] it was reported that computed $O_3$ control requirements were not very sensitive to initial changes in $NO_2$. It was not known, at the time EKMA was published, the extent to which the photochemical mechanism employed within EKMA could respond to initial changes in percent $NO_2$. Therefore it was felt that a set of runs was needed using different starting percentages of $NO_2$. These experiments could then be used for further model validation studies.

All of the experiments to test the effects of different percentage $NO_2$ began with the same initial hydrocarbon concentration and total

BOTTOM OF IMAGE AREA, OUTSIDE DIMENSION FOR TABLES AND ILLUSTRATIONS
BEGIN LAST LINE OF TEXT
3/8"

PAGE NUMBER
EPA-287 (Cin.)
(4-76)

$NO_x$ on both sides of the chamber. The only difference was that the initial $NO_2$ to $NO_x$ ratio (%$NO_2$) was varied from side to side. The effect that this change can have on matched systems is shown in Table 18. Many of these runs can also be seen in Figure 33. Although there is an increase in $O_3$ maximum for an increase in initial %$NO_2$, the magnitude of the effect varies in a manner which is not clear from the presented information. The 1974 runs show a 16-20% increase in $O_3$ when the initial $NO_2$ is changed from 20 to 40%. These runs were on clear days. The 1977 runs were conducted under poor sky conditions having only 64, 70, and 66% possible sunshine for the August 28, 29, and 30 runs. In the matched August 29, 1977 run,the $O_3$ on both sides crossed once and exhibited rapid fluctuations in rate of formation; this small difference could be due to solar radiation changes. From an examination of the plots for these experiments, it may be speculated that the effect of increasing %$NO_2$ is greater for slow systems than fast ones. For example, the September 2, 1977 experiment which made only 0.1 ppm $O_3$ at 20% initial $NO_2$, showed a 25% increase in $O_3$ at 57% $NO_2$. If this run had been "slowed down" by decreasing the NMHC, then the $O_3$ maximum would have been less by sunset. This would cause the relative difference in the $O_3$ maxima to be much greater than 20%. On the other hand, runs which get closer to completion, that is, runs which are not light or hydrocarbon limited seem to exhibit less of a %$NO_2$ effect.

A second way to have different initial $NO_2$ to $NO_x$ ratios in the two chamber sides is by injecting $O_3$. It has been speculated that mixing down of residual $O_3$ trapped aloft may be a significant process in producing $O_3$ later in the day. Table 19 gives the initial conditions and $O_3$ maxima for two experiments in which $O_3$ was injected in one side only. In the September 27, 1978 experiment, the $O_3$ was slowly injected from 0730 to 1100 EDT, resulting in a total of 0.077 ppm $O_3$ being added. In the September 28, 1978 experiment, 0.08 ppm $O_3$ was slug injected at 0700 EDT. In both experiments (Figure 34) the amount of $O_3$ injected was approximately 20% of the $NO_x$. Both days were totally clear with maximum temperatures of 80 to 85°F.

The injection of $O_3$ in the morning increased the $O_3$ maximum by 9-10%. Data for the slug injected run indicate that $NO = NO_2 = 0.08$

Table 18. Effect of initial $NO_2$-to-$NO_x$ ratio maximum ozone in UNC urban hydrocarbon mix runs

| Date | HC, ppmC | | $NO_x$, ppm | | NO, ppm | | $NO_2$, ppm | | $O_3$, ppm | |
|---|---|---|---|---|---|---|---|---|---|---|
| | Red | Blue | Red | Blue | Red | Blue | Red | Blue | Red | Blue |
| 5/8/74 | 3.4 | 3.2 | 0.364 | 0.366 | 0.214 | 0.286 | 0.151<br>41.5% | 0.079<br>21.6% | 0.720<br>(1.19) | 0.606 |
| 7/15/74 | 1.48 | 1.52 | 0.363 | 0.360 | 0.239 | 0.291 | 0.130<br>35.8% | 0.076<br>21.1% | 0.686<br>(1.16) | 0.592 |
| 8/28/77 | 1.48 | 1.46 | 0.313 | 0.303 | 0.122 | 0.237 | 0.182<br>59.9% | 0.066<br>21.8% | 0.419<br>(1.08) | 0.387 |
| 8/29/77 | 1.49 | 1.49 | 0.383 | 0.376 | 0.309 | 0.303 | 0.074<br>19.3% | 0.073<br>19.7% | 0.285<br>(1.05) | 0.300 |
| 8/30/77 | 1.65 | 1.66 | 0.367 | 0.358 | 0.017 | 0.285 | 0.350<br>95.4% | 0.073<br>20.4% | 0.493<br>(1.43) | 0.346 |
| 9/2/77 | 0.95 | 0.95 | 0.349 | 0.359 | 0.151 | 0.296 | 0.199<br>57.0% | 0.071<br>19.8% | 0.178<br>(1.25) | 0.142 |
| 9/17/78 | 2.03 | 2.12 | 0.355 | 0.356 | 0.283 | 0.182 | 0.074<br>20.8% | 0.177<br>44.7% | 0.333<br>(1.44) | 0.481 |

Table 19. Effect of adding $O_3$ initially on maximum $O_3$ in UNC urban hydrocarbon mix runs

| Date | HC, ppmC | | NO, ppm | | NO, ppm | | $NO_2$, ppm [c] | | $O_3$, ppm | | Comments |
|---|---|---|---|---|---|---|---|---|---|---|---|
| | Red | Blue | Red | Blue | Red | Blue | Red | Blue | Red | Blue | |
| 9/27/78 | 2.8 | 2.8 | 0.357 | 0.350 | 0.275<br>(0.198)[a] | 0.269 | 0.081<br>(0.158)[a]<br>44.4% | 0.081<br>23.1% | 0.397<br>(1.11)[d]<br>(Δ 0.039)[e] | 0.358 | 0.077 ppm $O_3$ added Red 8:30-11:00 |
| 9/28/78 | 2.8 | 2.8 | 0.354 | 0.356 | 0.280<br>(0.208)[b] | 0.276 | 0.074<br>(0.153)[b]<br>42.4% | 0.078<br>22.0% | 0.450<br>(1.09)[d]<br>(Δ 0.038)[e] | 0.412 | 0.08 ppm $O_3$ added to Red as slug 7:01 |

---

[a] numbers in ( ) are the calculated NO and $NO_2$ concentration assuming 100% reaction of $O_3$ with NO

[b] numbers in ( ) are the measured NO and $NO_2$ concentrations after $O_3$ injection

[c] the % are $NO_2$ to $NO_x$ ratios after $O_3$ injection assuming conditions in footnote a

[d] the ratio of $O_3$ in Red side to $O_3$ in Blue side

[e] the change in $[O_3]$ between sides in ppm

*"Red" and "Blue" are names for the two chamber sides.

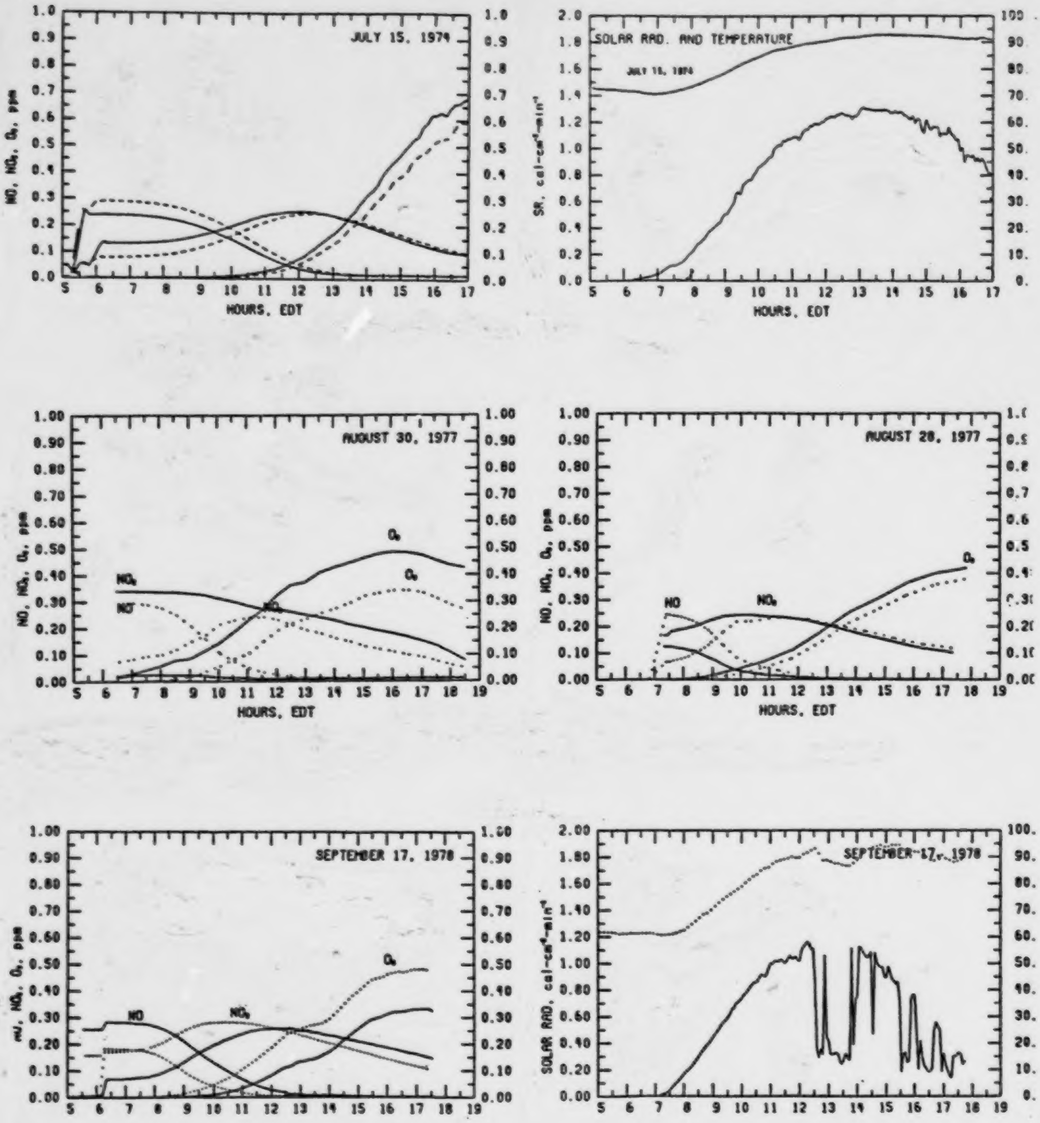

Figure 33. Matched mix-$NO_x$ experiment with different starting percentages of $NO_2$. See Table 18 for initial conditions.

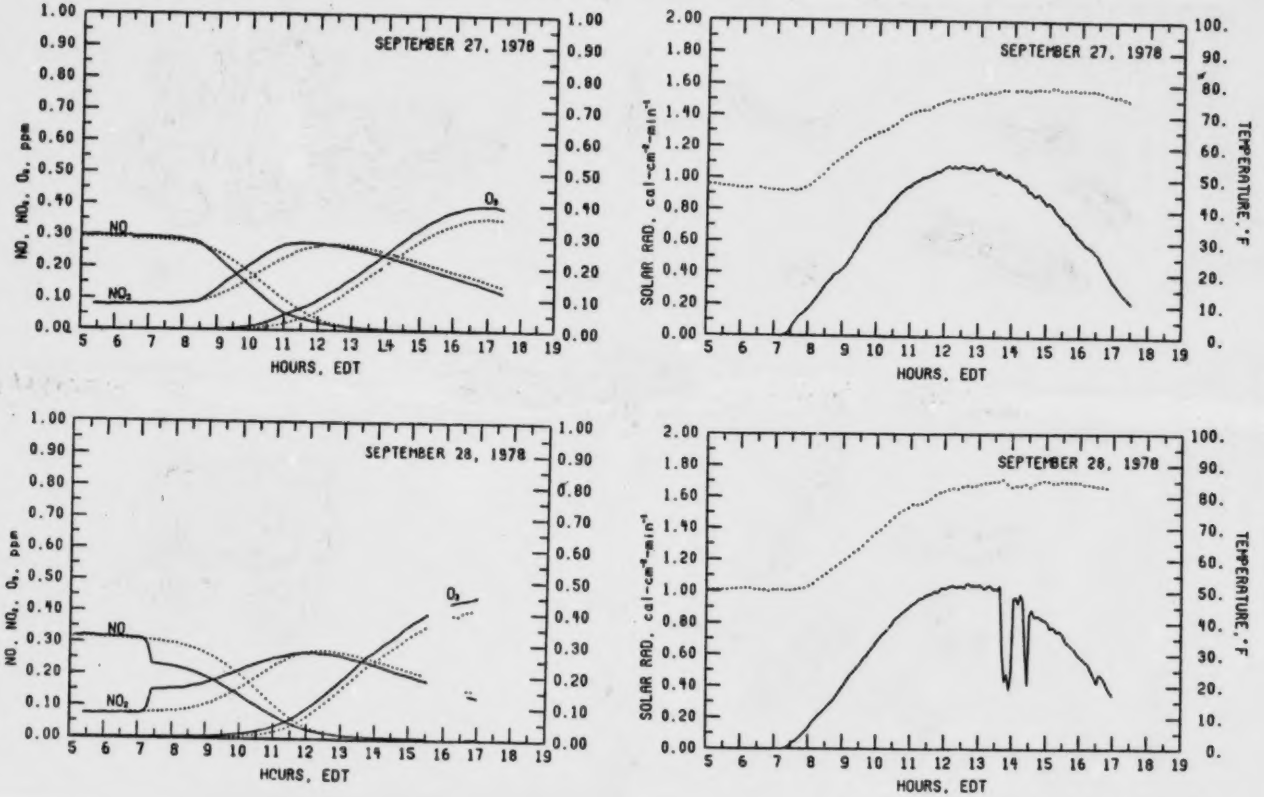

Figure 34. Matched mix-$NO_X$ experiments with one side receiving an O3 injection. See Table 19 for initial conditions.

TYPING GUIDE SHEET
BEGIN FIRST LINE OF TEXT HERE
CENTER OF PAGE
TOP OF IMAGE AREA
DROPPED HEAD; BEGIN SECTIONS HERE

ppm suggesting only a simple $O_3$-NO titration reaction occurred. Assuming that all the injected $O_3$ reacted with NO to yield $NO_2$, these runs would be approximately equivalent to different initial $\%NO_2$ runs having 40 vs. 0% $NO_2$. Table 18, however, suggests that this increase in initial $NO_2$ enhances $O_3$ maxima by 20 to 40%. It is not clear why the runs with added $O_3$ did not show the same increase in $O_3$ maxima as their counterpart experiments with similar initial $NO_2$. More experiments of this type are needed and modeling of these runs should be undertaken.

THE EFFECT OF INITIAL ALDEHYDES

Aldehyde atmospheric chemistry plays a major role in photochemical smog. If aldehydes are not present initially in a hydrocarbon-$NO_x$ system, they soon appear as some of the first oxidation products of hydrocarbons. Several oxidation schemes for hydrocarbons have been posed and tested in photochemical models. A typical example is shown below for OH attack on propylene.

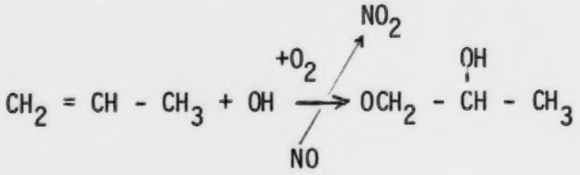

$$CH_2 = CH - CH_3 + OH \xrightarrow[NO]{+O_2 \ \nearrow NO_2} OCH_2 - \overset{OH}{CH} - CH_3 \qquad (22)$$

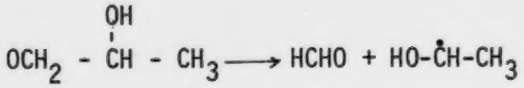

$$OCH_2 - \overset{OH}{CH} - CH_3 \longrightarrow HCHO + HO\text{-}\dot{C}H\text{-}CH_3 \qquad (23)$$

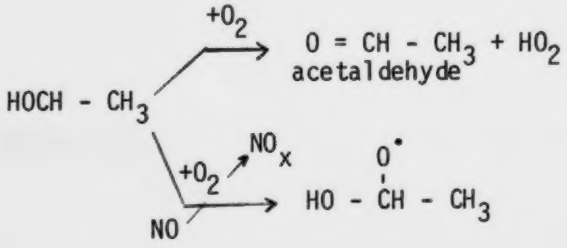

$$HOCH - CH_3 \xrightarrow{+O_2} \underset{\text{acetaldehyde}}{O = CH - CH_3} + HO_2 \qquad (24)$$
$$HOCH - CH_3 \xrightarrow[NO]{+O_2 \ \nearrow NO_x} HO - \overset{O^\bullet}{CH} - CH_3$$

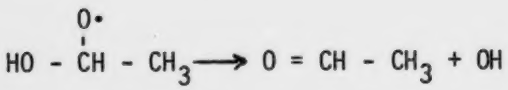

$$HO - \overset{O\bullet}{CH} - CH_3 \longrightarrow O = CH - CH_3 + OH \qquad (25)$$

BEGIN LAST LINE OF TEXT
BOTTOM OF IMAGE AREA, OUTSIDE DIMENSION FOR TABLES AND ILLUSTRATIONS
PAGE NUMBER
EPA-287 (Cin.)
(4-76)

Ozone-olefin reactions (as discussed in Section 4) also lead to aldehyde production.

$$C_3H_6 + O_3 \xrightarrow{O_2} \underset{\text{acetaldehyde}}{CH_3CHO} + [CH_2OO]^{**} \qquad (26)$$

$$C_3H_6 + O_3 \rightarrow \underset{\text{formaldehyde}}{HCHO} + [CH_3CHOO]^{*} \qquad (27)$$

If present initially, or once formed in the system, aldehydes are themselves subject to further oxidation:

$$\dot{O}H + HCHO \rightarrow H_2O + \dot{C}HO \xrightarrow{O_2} HO_2 + CO \qquad (28)$$

$$\dot{O}H + CH_3CHO \rightarrow H_2O + CH_3\dot{C}(O) \xrightarrow{O_2} CH_3C(O)\dot{O}_2 \qquad (29)$$

The radical, $CH_3C(O)O_2$, is the peroxyacetyl radical and it can either oxidize NO to $NO_2$:

$$CH_3C(O)\dot{O}_2 + NO \rightarrow NO_2 + CH_3C\dot{O}_2 \xrightarrow{O_2} CH_3O_2 + CO_2 \qquad (30)$$

$$CH_2\dot{O}_2 + NO \rightarrow NO_2 + \underline{HCHO} + H\dot{O}_2 \qquad (31)$$

TYPING GUIDE SHEET
EPA-287 (Cin.)
(4-76)

or it can react with $NO_2$ to form peroxyacetylnitrate (PAN):

$$CH_3C(O)O_2^{\bullet} + NO_2 \rightarrow CH_3C(O)O_2NO_2(PAN) \qquad (32)$$

The rates of OH attack on aldehydes are reasonably high yet are slightly less than for propylene. Thus, once the initial hydrocarbon is attacked, its subsequent oxidation (and the conversion of NO to $NO_2$) proceeds relatively quickly.

Aldehydes photolyze upon absorption of ultraviolet radiation in the short end of the spectrum beginning at around 345 nm and extending downward. The natural solar cutoff at 290 nm limits the photolysis to wavelengths between 290-345 nm. In this region, solar intensity is highly dependent on wavelength; slight attenuations in the solar spectrum can result in large variations in aldehyde photolysis rates. A 20 nm shift upward in the spectrum can decrease the photolysis rate by almost a factor of two (Durbin et al., 1975).[59] There are also indications that aldehyde photolysis rates may exhibit temperature dependence.[60]

Two photolysis processes are possible-

for formaldehyde:

$$HCHO \xrightarrow{h\nu} H_2 + CO \qquad (33)$$

$$HCHO \xrightarrow{h\nu} H\cdot + H\dot{C}O \rightarrow 2\ HO_2^{\bullet} + CO \qquad (34)$$

TYPING GUIDE SHEET
BEGIN FIRST LINE OF TEXT HERE
CENTER OF PAGE
TOP OF IMAGE AREA
DROPPED HEAD BEGIN SECTIONS HERE
BEGIN LAST LINE OF TEXT
BOTTOM OF IMAGE AREA; OUTSIDE DIMENSION FOR TABLES AND ILLUSTRATIONS
PAGE NUMBER
EPA-287 (Cin.)
(4-76)

TYPING GUIDE SHEET

for acetaldehyde:

$$CH_3CHO \xrightarrow{h\nu} CH_4 + CO \qquad (35)$$

$$CH_3CHO \xrightarrow{h\nu} \dot{C}H_3 + H\dot{C}O \xrightarrow{O_2} CH_3 + HO_2^{\cdot} + CO \qquad (36)$$

Each process has a different dependence on wavelength, and the quantum yields of each process are uncertain by about a factor of two.

These photolysis processes are critical in that they provide a continuous source of new radicals to help maintain the oxidizing system. In systems lacking major initial sources of nitrous acid (HONO), one would expect the photolysis of aldehydes could potentially provide a major impetus to starting or accelerating the NO and hydrocarbon oxidizing process.

The experiments performed during the course of this study compared chemical profiles from hydrocarbon mix-$NO_x$ systems with and without initial aldehydes. All experiments began with the same initial NMHC and $NO_x$ concentrations. An extra "spike" of 10% aldehyde carbon was then added to one side. Critical data from acetaldehyde additions are given in Table 20. In general, the addition of an extra 10% acetaldehyde carbon to a mix-$NO_x$ system did not substantially change the initial rate of NO oxidation. As mentioned before however, significant $O_3$ enhancement is possible. From the comparison profiles shown in Figure 35 one may conjecture that reaction of acetaldehyde molecules contributed more radicals during the afternoon than the morning. In the experiments described, photolysis of acetaldehyde should lead to morning radical production and hence a more rapid conversion of NO to $NO_x$. There is evidence that aldehyde photolysis is somewhat temperature dependent. The

EPA-287 (4-76)

### Table 20. Effects of Acetaldehyde on Maximum $O_3$ Yield in Matched Dual Runs

|  | Initial Conditions |  |  |  |  |  |  |  |
|---|---|---|---|---|---|---|---|---|
| Date | HC,[a] ppmC | Aldehyde, ppmC | $NO_x$, ppm | $NO_2$, % of $NO_x$ | Time $NO = NO_2$, EDT | Maximum Temp., °F | Maximum $O_3$ | Ratio[d] |
| 1/31/76 | 1.88 | 0.0 | 0.218 | 43 | 10:35 | 57.8 | 0.074 | 1.16 |
| 1/31/76 | 1.98 | 0.2[b] | 0.202 | 42 | 10:10 | 57.8 | 0.086 |  |
| 3/7/76 | 3.13 | 0.0 | 0.211 | 25 | 10:20 | 62.0 | 0.171 | 1.23 |
| 3/7/76 | 3.13 | 0.3[b] | 0.214 | 25 | 10:05 | 62.0 | 0.210 |  |
| 9/24/76 | 2.45 | 0.00 | 0.332 | 20 | 10:24 | 83.0 | 0.273 | 1.41 |
| 9/24/76 | 2.32 | 0.20[b] | 0.325 | 20 | 10:04 | 83.0 | 0.385 |  |
| 8/20/77 | 2.0 | 0.20[b] | 0.35 | 20 | 13:07 | - | 0.39 | 1.05 |
| 8/20/77 | 2.0 | 0.25[c] | 0.35 | 20 | 13:00 | - | 0.41 |  |
| 9/12/77 | 1.5 | 0.00 | 0.35 | 20 | - | 80.0 | 0.146 | 1.90 |
| 9/12/77 | 1.5 | 0.15[b] | 0.35 | 20 | - | 80.0 | 0.278 |  |
| 9/13/77 | 1.50 | 0.19[c] | 0.361 | 24 | 10:15 | 85.0 | 0.302 | 1.20 |
| 9/13/77 | 1.51 | 0.15[b] | 0.350 | 23 | 10:10 | 85.0 | 0.252 |  |
| 9/17/77 | 1.98 | 0.00 | 0.362 | 27 | - | 87.0 | 0.260 | 1.60 |
| 9/17/77 | 1.96 | 0.17[b] | 0.357 | 25 | - | 87.0 | 0.400 |  |
| 9/18/77 | 2.99 | 0.26[b] | 0.346 | 22 | - | 90.0 | 0.72 | 1.07 |
| 9/18/77 | 3.00 | 0.00 | 0.351 | 24 | - | 90.0 | 0.67 |  |

---

[a] Nonmethane hydrocarbon concentration for simulated urban mixture. Reported value does not include acetaldehyde concentration.

[b] Acetaldehyde concentration was approximately 10% of initial HC.

[c] Formaldehyde injected as solid paraformaldehyde.

[d] Ratio of maximum $O_3$ in run with added acetaldehyde to maximum $O_3$ in run without added acetaldehyde.

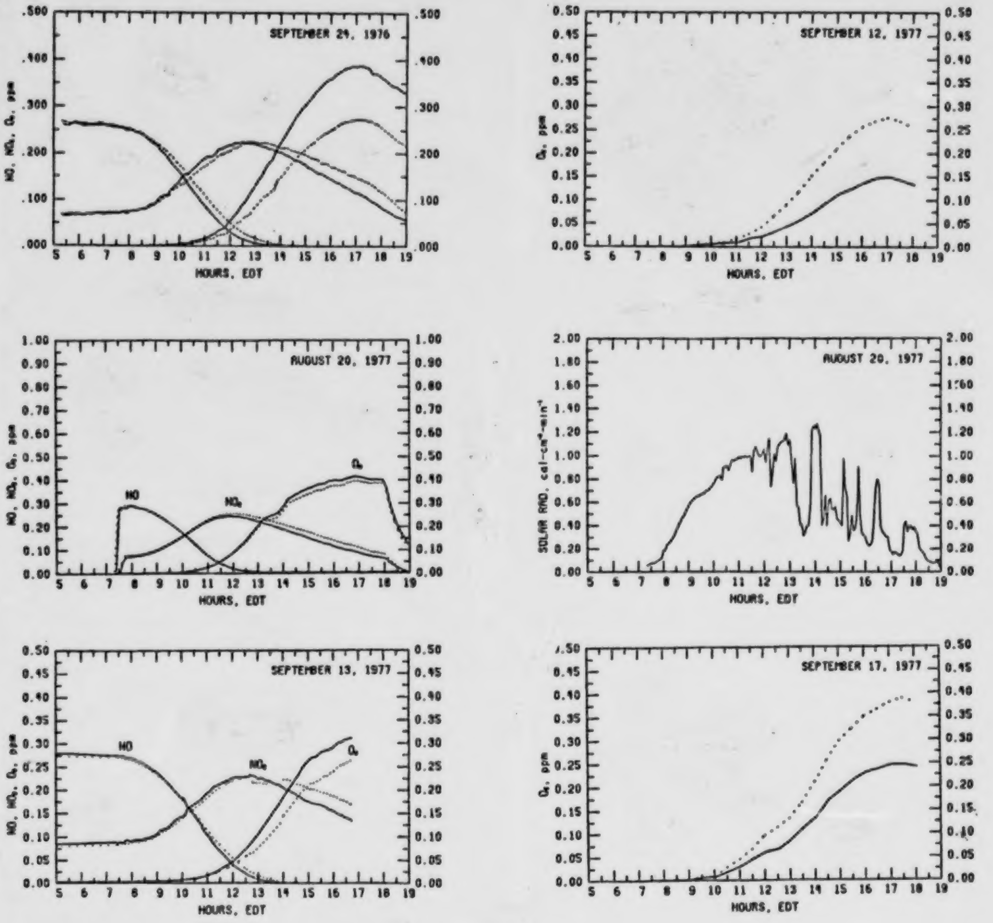

Figure 35. Effect of initial aldehydes on matched mix systems. Initial conditions in Table 20.

net result may be that morning reactions of acetaldehyde take place primarily through OH attack rather than photolytic destruction.

Analysis of the acetaldehyde chromatographic data from these runs indicates that observable acetaldehyde formation in the mix only side does not take place until 30-45 minutes before $O_3$ begins to rise. Until this time, acetaldehyde concentrations remain relatively constant at the injected level in the side with injected acetaldehyde. This suggests that significant concentrations of acetaldehyde are not reacting during the period when almost half of the NO is being oxidized to $NO_2$.

A propylene-$NO_x$ mechanism was used to model some preliminary tests of the effect of making the acetaldehyde photolysis rate highly temperature dependent over the range of 273-300$^{\circ}$K. As a very rough approximation of the mix-acetaldehyde experiments, a 0.5 ppmC propylene and 0.35 ppmC $NO_x$ system was modeled both with and without extra acetaldehyde.

By making the acetaldehyde photolysis rate highly temperature dependent, $K \text{ photolysis} = 1 \times 10^{+13} e^{-\frac{10723}{T}} \times K_1$, we could reduce the impact of extra acetaldehyde on the apparent conversion of NO to $NO_2$ and still show a faster rise in afternoon $O_3$ production. This did not completely reproduce the above noted experimental observations; additional experimental and mechanistic work is needed.

A few runs were conducted with additional formaldehyde. In one case a matched mix-matched $NO_x$ system had 13% extra injected formaldehyde in one side and 10% extra acetaldehyde in the other side. While a small enhancement in $O_3$ production can be seen in Figure 34, a substantially more rapid conversion of NO to $NO_2$ is not evident in the side with initial formaldehyde. A possible explanation is that all of the injected formaldehyde did not stay in the gas phase. Injected HCHO wall losses will be discussed in detail in Section 8. Briefly, the UNC outdoor chambers sometimes have humid walls during the morning hours of a smog run. Although film condensation is not necessarily visible, we have observed that under these humid morning conditions a portion of the injected formaldehyde can be lost to the walls and released later in the day as chamber temperatures increase. During these runs, an automatic GC (with a HCHO methanizer) was used to measure formaldehyde. With this system, it was difficult to quantify formaldehyde concentrations below 0.15-0.2 ppm in humid air samples because water generated a "ghost peak" interference in the region of formaldehyde elution; in these runs injected formaldehyde was observed but not quantitatively measured. Such measurement interferences and chamber losses do not exist with acetaldehyde and its injected concentration was verified.

Thus at this time the results of the formaldehyde additions are not conclusive; additional runs should be made in which the chambers are dried and formaldehyde is carefully monitored. One may conclude that formaldehyde additions do lend reactivity to mix-$NO_x$ smog systems and that $O_3$ enhancements on an added carbon basis are at least as great as that observed for acetaldehyde.

## ADDITION OF PROPANE AND BUTANE TO REACTIVE SMOG SYSTEMS

It was argued by Jeffries[61] that perhaps the best way to test the reactivity of a single compound in a smog chamber was to add that specie to an urban mix-$NO_x$ system which already had some demonstrated reactivity. The reason for suggesting this was twofold. First, if control decisions were to be made on a particular compound, their decisions should be made in light of the atmospheric environment in which these compounds were likely to be emitted and reacted. Secondly, much debate and discussion has centered on artifact chamber influences that may occur when a compound of low reactivity is tested in the chamber. If under certain conditions chambers do provide a source of artifact radicals, the compound in question would experimentally appear to be more reactive than it really is. A way to accommodate the issue is to have a mix-$NO_x$ smog system act as the prime generator of radicals. Then if a compound adds to mix reactivity (i.e. rate of NO oxidation and $O_3$ maximum) certain statements can be made about its reactivity within the context of an urban smog mix.

Two compounds were initially chosen for reactivity testing by this method. The question was, would additional emissions of either propane or butane enhance the reactivity of an urban smog chamber system. A corollary question was, what is the effect of substituting either propane or butane for some other hydrocarbons. In this case, either propane or butane would be used to replace a certain portion of the carbon in the urban mixture.

The effects of increasing the initial paraffin content of the UNC urban mix by the addition of either propane or butane are shown in Tables 21 and 22 and Figures 36 and 37. The May 11, 1978 matched mix run is shown in both tables as a reference for side-to-side reproducibility. The June 22, 1978 run in Table 21 compares the reactivity of 1 ppmC of propane with the reference mix system. This amount of propane did not drive the conversion of NO to $NO_2$ to crossover. For carbon mixtures of one part propane to two parts mix compared with only two parts mix, the $O_3$ maximum was increased by 10-29%, with 14% being typical. Thus, propane participates in the $O_3$ forming process to a small extent.

In Table 22, data similar to that in Table 21 are given, except that butane was the added paraffin. Ozone maxima increased by 30 to 83%. The May 14, 1978 experiment was continued an additional day, and the $O_3$ forming difference was also shown on the second day. The results suggest a substantial participation of butane in the $O_3$ forming process.

Thus, for an urban-type situation, our results clearly indicate that butane sources could contribute substantially to oxidant formation; propane sources could also make a small contribution to oxidant formation. The effect of propane, when added on a second day, has not been tested. Continued work along these lines is currently in progress under a new reactivity grant from EPA, Washington.

## PRELIMINARY AUTO EXHAUST EXPERIMENTS

Two comparisons between dilute automobile exhaust and our standard atmospheric mix were conducted in the fall of 1976. The injections were adjusted so that both the auto exhaust and the mix side started with similar $[NO_x]$, $[NO_2]$, and [NMHC]. Aldehydes were not added to the mix side.

In the first experiment, a 1972 Dodge van (8 cylinder) was used to supply the dilute auto exhaust. The raw exhaust was first pulled into a flask to remove condensed water and then pumped (with a metal diaphragm pump) through a glass fiber filter before injection into the chamber. The engine was set at a slow idle. As would be expected, very low $NO_x$

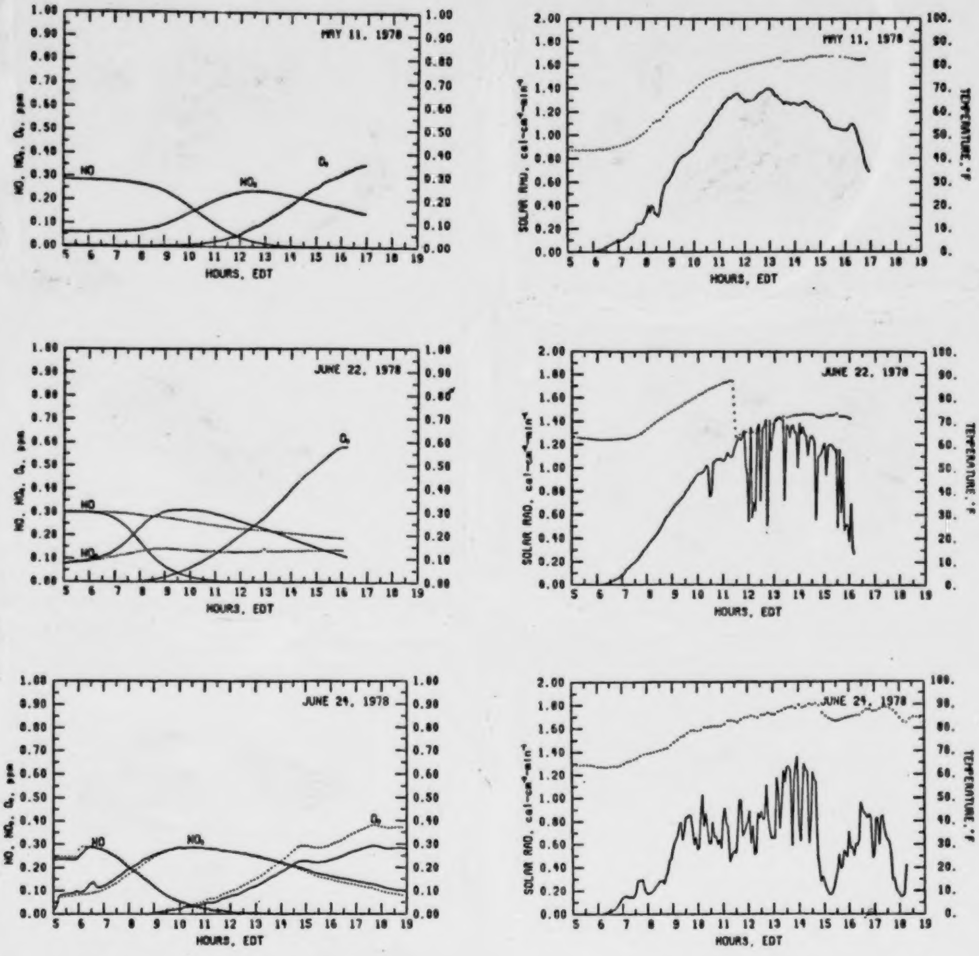

Figure 36. Effect 30% extra propane carbon on urban type smog chamber systems. Initial concentrations in Table 21.

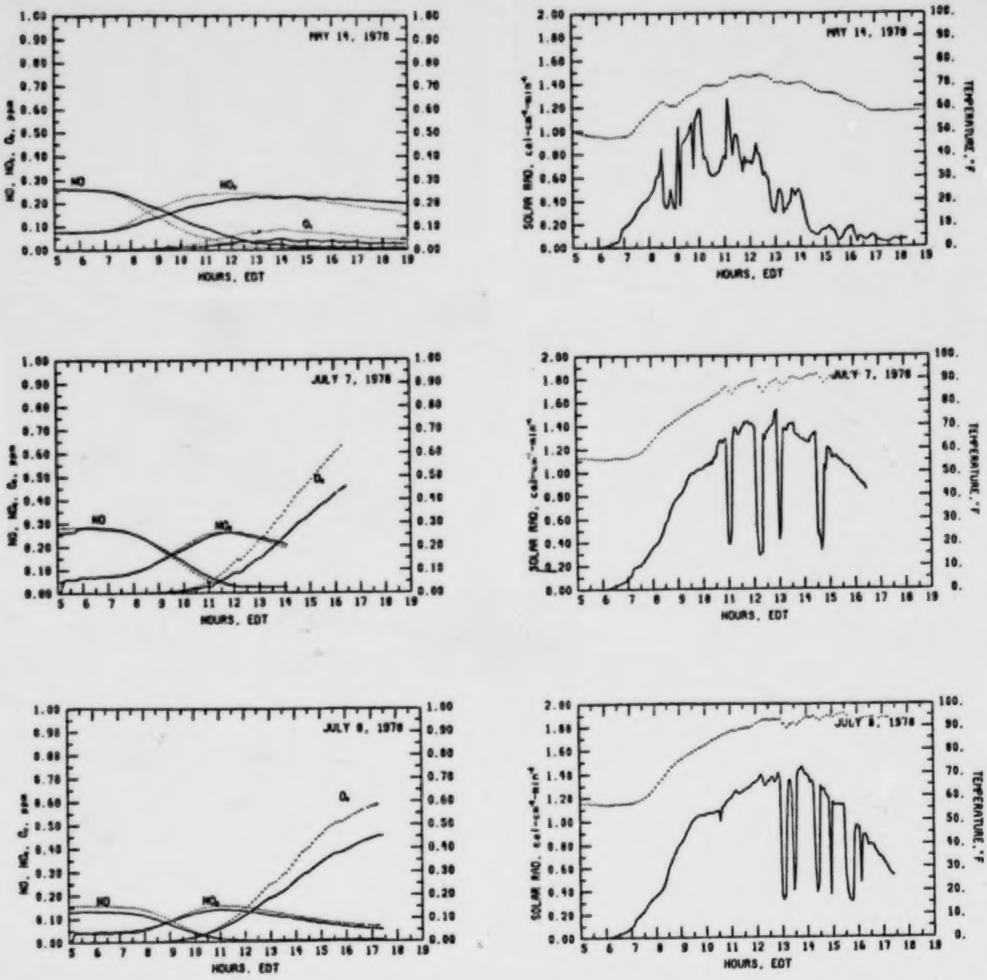

Figure 37. Effect of 30% extra butane carbon on urban smog chamber systems. Initial conditions in Table 22.

Table 21. Effect of additional initial propane on maximum ozone in UNC urban hydrocarbon mix runs

| Date | HC, ppmC [a] | | $NO_2$, ppm | | $NO_2$, ppm | | $O_3$ max, ppm [b] | |
|---|---|---|---|---|---|---|---|---|
| | Red | Blue | Red | Blue | Red | Blue | Red | Blue |
| 5/11/78 | 2.10m<br>(2.10) | 2.05m<br>(2.05) | 0.354 | 0.354 | 0.059 | 0.057 | 0.358<br>(1.006) | 0.360 |
| 6/22/78 | 2.00m<br>(2.00) | 0.00m<br>1.06p<br>(1.06) | 0.396 | 0.395 | 0.097 | 0.092 | 0.579 | 0.001 |
| 6/24/78 | 1.93m<br>(1.93) | 1.90m<br>0.93p<br>(2.83) | 0.380 | 0.373 | 0.092 | 0.080 | 0.295<br>(1.298) | 0.383 |
| 6/26/78 | 1.70m<br>(1.70) | 1.70m<br>0.80p<br>(2.50) | 0.295 | 0.300 | 0.081 | 0.077 | 0.199<br>(1.141) | 0.227 |
| 6/29/78 | 2.06m<br>0.93p<br>(2.99) | 2.10m<br>(2.10) | 0.310 | 0.309 | 0.068 | 0.073 | 0.794<br>(1.149) | 0.691 |
| 7/16/78 | 1.79m<br>0.80p<br>(2.59) | 1.72m<br>(1.72) | 0.32 | 0.34 | 0.128 | 0.128 | 0.301<br>(1.103) | 0.273 |
| 7/17/78 | 1.77<br>0.84 | 1.84 | 0.354 | 0.352 | 0.083 | 0.084 | 0.390<br>(1.066) | 0.366 |

---

[a] m = mix concentration
p = propane concentration
numbers in ( ) are total non methane hydrocarbon concentration

[b] numbers in ( ) are ratio of high $O_3$ to low $O_3$

Table 22. Effect of additional initial butane on maximum ozone in UNC urban hydrocarbon mix runs

| Date | HC, ppmC [a] | | $NO_x$, ppm | | $NO_2$, ppm | | $O_3$ max, ppm [b] | |
|---|---|---|---|---|---|---|---|---|
| | Red | Blue | Red | Blue | Red | Blue | Red | Blue |
| 5/11/78 | 2.10m<br>(2.10) | 2.05m<br>(2.05) | 0.354 | 0.354 | 0.059 | 0.057 | 0.358<br>(1.006) | 0.360 |
| 5/12/78 | 2.16<br>(2.16) | 2.17m<br>4.60b<br>(6.77) | 0.350 | 0.348 | 0.069 | 0.065 | 0.286<br>(1.832) | 0.524 |
| 5/14/78 | 2.00m<br>(2.00) | 2.00m<br>1.00b<br>(3.00) | 0.350 | 0.399 | 0.080 | 0.078 | 0.048<br>(1.833)<br>[0.083<br>(1.759) | 0.088<br><br>0.146] [c] |
| 7/7/78 | 2.28m<br>(2.28) | 2.32m<br>0.98b<br>(3.30) | 0.355 | 0.349 | 0.069 | 0.066 | 0.460<br>(1.391) | 0.640 |
| 7/8/78 | 1.10m<br>(1.10) | 1.00m<br>0.85b<br>(1.85) | 0.198 | 0.218 | 0.043 | 0.038 | 0.454<br>(1.302) | 0.591 |

---

[a] m = mix concentrations
b - butane concentration
numbers in ( ) are total non methane hydrocarbon concentration

[b] numbers in ( ) are ratio of high $O_3$ to low $O_3$

[c] these values are for a second day of irradiation with no additional materials added

concentrations were observed from the exhaust under these conditions. The second experiment (Figure 38) was performed with controlled exhaust from a 1969 Oldsmobile station wagon (8 cylinder). The engine was run at a faster idle than in the previous experiment. While somewhat more $NO_x$ was observed in this exhaust, both exhaust runs had the same general distribution of hydrocarbon compounds. Comparisons between the UNC urban mix, the Bureau of Mines (BOM) auto exhaust and UNC auto exhaust are shown in Table 23. As can be seen, the olefin content of the UNC urban mix is the highest.

In both experiments the exhaust side reached $NO_x$ maximum faster than the urban mix side. Chromatographic data show that very little toluene (or octane) in the auto exhaust reacted from 0900 to 1400 EDT. The disappearance rate for ethylene, cis-butene, and trans-2-butene for the auto exhaust and the mix were very similar. There was some indication that the xylenes reacted, but this was difficult to quantify because of the small, broad peaks for these compounds. As indicated in Table 23 however, xylenes composed only 5% by carbon of the exhaust hydrocarbons under these operating conditions.

It therefore seems difficult to account for the high reactivity of this auto exhaust based on the measured paraffin, olefin, and aromatic hydrocarbon disappearance. Aldehydes were not measured in the auto exhaust. Based on the aldehyde comparisons already presented it is entirely possible that formaldehyde in auto exhaust was responsible for the observed reactivity of auto exhaust compared to UNC mix.

To further compare auto exhaust with the UNC mix, a simulated BOM auto exhaust mixture (Table 24) was prepared for UNC by Matheson Research Gas Company. Although the total olefin to paraffin ratios for these mixtures were similar, the propylene to ethylene ratios were different. Side-by-side comparison with the same carbon concentration of UNC mix and auto mix showed very little difference in NO, $NO_2$ or $O_3$ behavior (Figure 39).

## PROPYLENE/BUTANE MIXTURE

Dodge[62] found in her modeling studies that a 25/75 propylene/butane carbon mixture was equivalent in reactivity to the dilute BOM auto exhaust

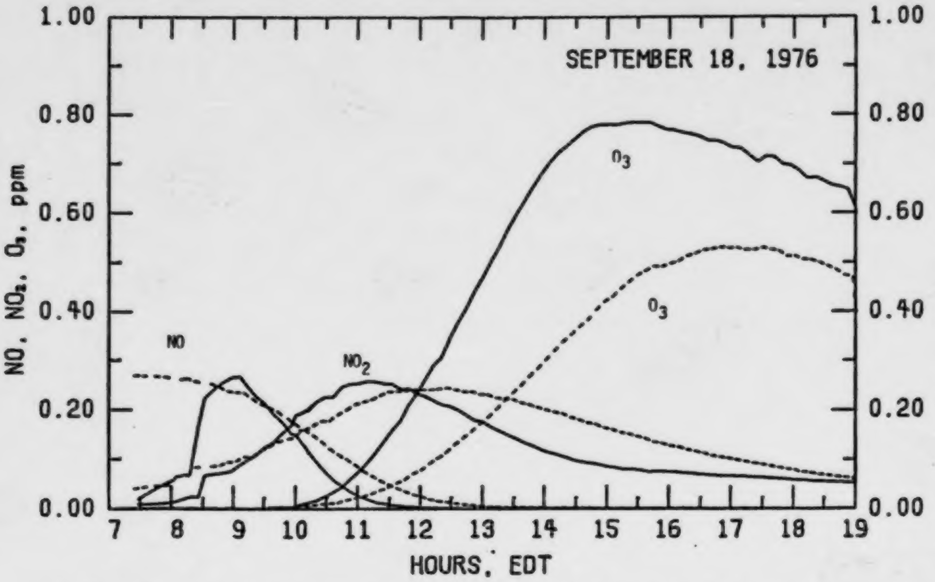

Figure 38. Comparison of NO, $NO_2$ and $O_3$ profiles indual run using auto exhaust as NMHC (___) and UNC urban mix as NMHC (---). Initial conditions: (___), $NO_x$: 0.34 ppm; NMHC: 3.1 ppmC; (---) , $NO_x$: 0.33 ppm, NMHC: 3.1 ppmC.

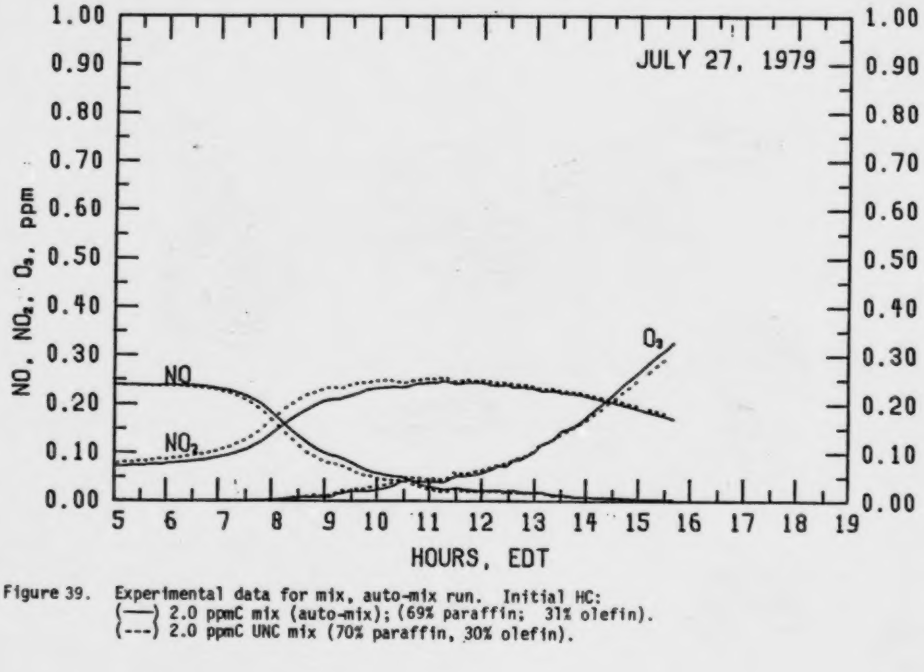

Figure 39. Experimental data for mix, auto-mix run. Initial HC:
(——) 2.0 ppmC mix (auto-mix); (69% paraffin; 31% olefin).
(---) 2.0 ppmC UNC mix (70% paraffin, 30% olefin).

TABLE 23. Comparison of BOM Auto Exhaust Composition with UNC Auto Exhaust and UNC Urban Mix Composition

| | Carbon Mole Fraction | | |
|---|---|---|---|
| Cmp | BOM Auto Exhaust[a] | UNC Auto Exhaust[b] | UNC Urban Mix[c] |
| Acetylene | 0.063 | 0.139[d] | 0.088 |
| Subtotal | 0.063 | 0.139 | 0.088 |
| ethane | 0.007 | 0.0 | |
| $C_5$-$C_8$ paraffins | 0.417 | 0.255 | 0.643 |
| Subtotal | 0.424 | 0.255 | 0.643 |
| ethylene | 0.0720 | 0.184 | 0.119 |
| propylene | 0.0457 | 0.105[d] | 0.048 |
| butenes | 0.0419 | 0.059 | 0.055 |
| pentenes + | 0.0137 | 0.018 | 0.048 |
| Subtotal | 0.173 | 0.366 | 0.270 |
| benzene | 0.035 | 0.018 | 0.0 |
| toluene/n-octane | 0.1131 | 0.143 | 0.0 |
| xylenes | 0.051 | 0.054 | 0.0 |
| High Alkyl Ø | 0.123 | 0 | 0.0 |
| Subtotal | 0.322 | 0.215 | 0.0 |
| Total | 0.982 | 0.975 | 1.000 |

---

[a] Based on Dermerjian's analysis of BOM gas chromatographic data

[b] Based on Carle automatic gas chromatographic analysis of chamber contents. See text for injection method from 1969 Oldsmobile (8 cylinder).

[c] Based on Carle automatic gas chromatographic analysis of high concentration injection tanks and chamber contents.

[d] Carle automatic chromatograph not able to separate acetylene and propylene. Total fused peak accounts for 24.4% of detected carbon. This percentage was apportioned according to a ethylene acetylene ratio of 0.18 to 0.137 as determined by Mayrsohn.

Table 24. UNC Mix and BOM Mix Composition

| | Carbon fraction | |
|---|---|---|
| | UNC Urban mix | UNC Auto mix |
| Ethane | - | 0.012 |
| n-butane | - | 0.065 |
| Isopentane | 0.137 | 0.051 |
| n-pentane | 0.252 | 0.106 |
| 2 me-pentane | 0.113 | 0.087 |
| 2,4 dime-pentane | 0.089 | 0.063 |
| 2,2,4 trime-pentane | 0.118 | 0.152 |
| Octane | - | 0.166 |
| subtotal | 0.709 | 0.692 |
| | | |
| Ethylene | 0.117 | 0.117 |
| Propylene | 0.052 | 0.089 |
| 1-butene | 0.025 | 0.018 |
| Cis-2-butene | 0.031 | - |
| Trans-2-butene | - | 0.048 |
| 2 me-1-butene | 0.035 | 0.016 |
| 2 me-2-butene | 0.032 | 0.023 |
| subtotal | 0.292 | 0.311 |

mixture. As was just discussed, comparisons of auto exhaust and simulated BOM auto exhaust with the UNC urban mixture had shown that the real auto exhaust was more reactive on a ppmC basis, but the difference was attributed to the presence of aldehydes in the real auto exhaust. A tank simulated BOM auto exhaust mixture (without aldehydes) exhibited identical reactivity to that of the UNC mix. It was expected, therefore, that the Dodge propylene/butane mixture would closely agree with the UNC mix.

The results of the side-by-side experiments with UNC mix and a 25-75% propylene/n-butane mixture are shown in Table 25. The first three runs indicate that for each mix that gave a unity ratio for $O_3$, the ratio of concentrations of propylene/butane to mix was between approximately 0.9 and 1.3. That the UNC mix was more reactive was confirmed by the June 18 and June 19 runs. The June 21 and July 13 runs have nearly identical NO, $NO_2$, and $O_3$ time profiles, and $O_3$ maxima very near 1.0. Thus, the 25% propylene/75% butane, Dodge type mixture is slightly less reactive but a reasonable estimator of the current UNC mix. Chemical profiles for selected runs are shown in Figure 40.

Selected smog chamber runs from the propylene/butane mixture and auto exhaust experiments were used in another study to test and compare five different photochemical mechanisms. The details of this research by Jeffries and Sexton[63] are too lengthy to summarize here; the reader is referred to this report for further information.

## HYDROCARBON SUBSTITUTION AS A MEANS TO CONTROL $O_3$

Throughout the course of this entire research project various experiments have been conducted in which the composition of the hydrocarbon mixture was changed. The biogenic hydrocarbon section of this report discussed experiments in which 20% of the UNC mix carbon was replaced with α-pinene on one side only; that is, 1.6 ppmC mix and 0.4 ppmC α-pinene was used on one side and 2.0 ppmC mix was used on the other. Very small differences resulted from this replacement. Other experiments of this type with toluene substitution confirmed these results.

The lack of compositional effects on $O_3$ production was also illustrated by the simulated auto exhaust-UNC mix experiments.

TYPING GUIDE SHEET

Table 25. Comparison of ozone reactivity of 25% propylene and 75% n-butane mixture to that of the UNC urban mix.

| Date | HC, ppmC[a] |  |  | $NO_x$, ppm |  | $NO_2$, ppm |  | $O_3$, ppm[b] |  |  |
|---|---|---|---|---|---|---|---|---|---|---|
|  | Red | Blue |  | Red | Blue | Red | Blue | Red | Blue |  |
| 6/8/78 | 2.15<br>m | 2.07<br>p&b | (0.96) | 0.425 | 0.424 | 0.143 | 0.137 | 0.529 | 0.432 | (0.82) |
| 6/12/78 | 1.30<br>p&b | 1.00<br>m | (1.3) | 0.336 | 0.345 | 0.059 | 0.058 | 0.159 | 0.110 | (1.45) |
| 6/15/78 | 0.92<br>p&b | 1.06<br>m | (0.87) | 0.379 | 0.382 | 0.069 | 0.065 | 0.039 | 0.060 | (0.65) |
| 6/18/78 | 3.01<br>p&b | 3.28<br>m | (0.92) | 0.358 | 0.358 | 0.084 | 0.085 | 0.728 | 0.851 | (0.86) |
| 6/19/78 | 2.17<br>m | 2.02<br>p&b | (0.93) | 0.355 | 0.355 | 0.091 | 0.088 | 0.491 | 0.437 | (0.89) |
| 6/21/78 | 1.85<br>m | 2.07<br>p&b | (1.12) | 0.358 | 0.355 | 0.068 | 0.062 | 0.313 | 0.321 | (1.03) |
| 7/13/78 | 1.15<br>p&b | 1.00<br>m | (1.15) | 0.219 | 0.217 | 0.040 | 0.040 | 0.178 | 0.165 | (1.08) |

---

[a] m ≡ mix
p&b ≡ 25% propylene + 75% n-butane

[b] numbers in ( ) are ratio of $O_3$ in p&b run to $O_3$ in m run.

EPA-287 (Cin.)
(4-76)

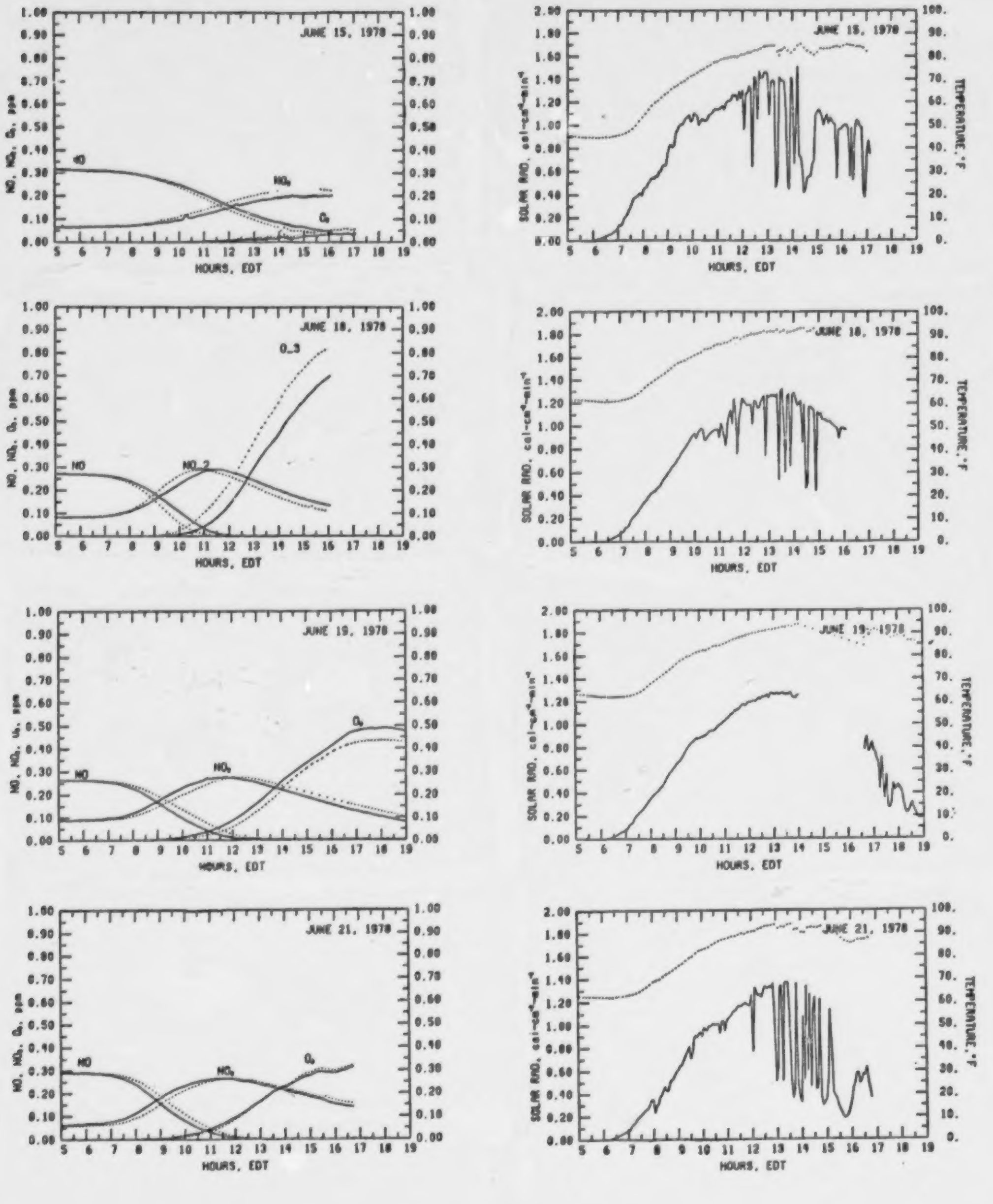

Figure 40. Comparisons between UNC mix and 25/75 propylene/butane mixture.

A final experiment of this type was conducted by UNC at the request of the State Pollution Control Commission (SPCC) of New South Wales, Australia. The Australians were considering a reactivity-based, substitution control policy for solvents and wanted some direct measure of the expected benefits. Members of the SPCC had generated a solvent mixture in which the various solvents were proportional to actual usage in the Sydney air basin. An analysis of the major components of this mixture is shown in Table 26.

Members of the SPCC estimated that a 50% reduction in solvent emissions was the maximum possible and that emissions of cellosolves would be expected to increase as a result of the necessary shift to water-based paint techology. Therefore, the experiment was to illustrate the benefits of a 50% reduction in solvent emissions accompanied by a slight increase in cellosolve emissions while the other urban HC sources remained constant. The exact experimental conditions are given in the caption of Figure 41. The results are shown in Figures 41 and 42. These results indicate that there probably are no significant benefits to be obtained from any practical substitution strategies.

Table 26. Composition of "Sydney Solvent"

| Compound | Weight % |
|---|---|
| Toluene | 17.89 |
| Ethanol | 13.4 |
| m,p-Xylenes | 7.68 |
| $C_{10}$ aromatics and alkanes | 5.02 |
| 1,2,4,-Trimethylbenzene | 3.09 |
| Methyl ethyl ketone | 2.[illegible]0 |
| n-Nonane | 2.76 |
| o-Xylene | 2.59 |
| n-Decane | 2.44 |
| m,p-Ethyltoluenes | 2.35 |
| Ethylbenzene | 2.23 |
| n-Hexane | 2.00 |
| Trichloroethylene | 1.85 |
| 2-Methylpentane | 1.83 |
| Methylene chloride | 1.80 |
| n-Undecane | 1.68 |
| Acetone | 1.60 |
| 1,1,1-Trichloroethane | 1.48 |
| Methylcyclohexane | 1.40 |
| n-Heptane | 1.35 |
| 1,3,5-Trimethylbenzene | 1.31 |
| 3-Methylpentane | 1.27 |
| o-Ethyltoluene | 1.16 |
| n-Butylacetone | 1.20 |
| Methylisobutylketone | 1.01 |
| Celloacetate | 1.00 |
| 2,2,4-Trimethylpentane | 0.99 |
| n-Octane | 0.96 |
| A methyloctane | 0.91 |
| n-Butanol | 0.95 |
| Unknown | 0.83 |
| n-Dodecane | 0.72 |
| 1,2,3-Trimethylbenzene | 0.75 |
| 2,3-Dimethylbutane | 0.67 |
| n-Propylbenzene | 0.57 |
| iso-Octane | 0.56 |
| Cyclopentane | 0.53 |
| Styrene | 0.50 |
| 3-Methylhexane | 0.50 |
| iso-Octane | 0.48 |
| n-Pentane | 0.48 |
| i-Butylacetate | 0.40 |
| Methylcyclopentane | 0.37 |
| Perchloroethylene | 0.36 |
| i-Butanol | 0.35 |
| Cyclohexane | 0.34 |
| i-Propylbenzene | 0.33 |
| $C_6$ cycloparaffins | 0.28 |
| i-Pentane | 0.25 |
| n-Tridecane | 0.20 |
| iso-Octane | 0.19 |
| n-Tetradecane | 0.12 |
| Benzene | 0.04 |
| n-Butane | 0.01 |
| i-Butane | <0.01 |

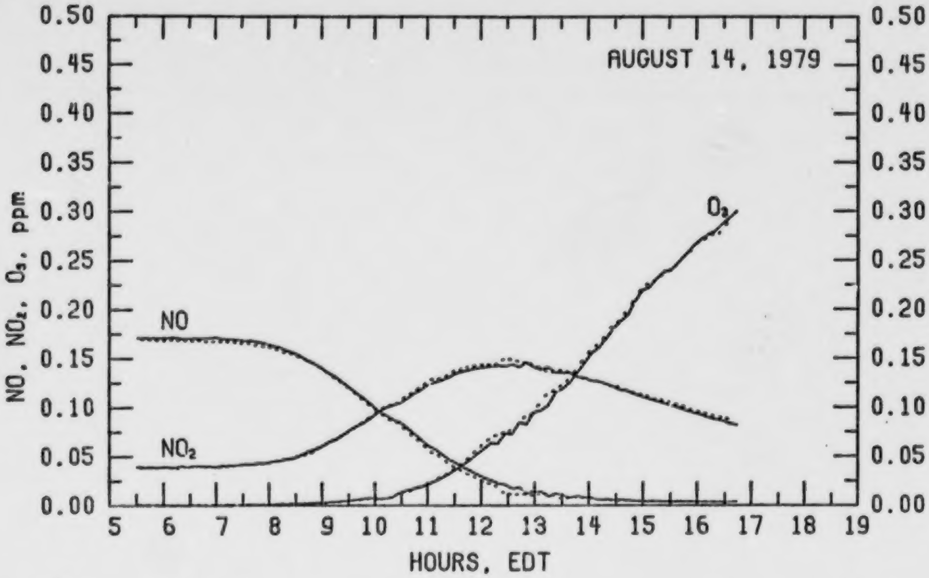

Figure 41. Experimental data for mix (with Sydney Solvent), mix-cellosolve run. Initial HC: (——) 1.12 ppmC mix, 70.7% paraffins, 29.2% olefin with 0.48 ppmC Sydney Solvent, 0.00 ppmC cellosolve mix; (---) 1.12 ppmC mix, 70.7% paraffins, 29.2% olefin with 0.24 ppmC Sydney Solvent, 0.035 ppmC cellosolve, 0.035 ppmC b-cellosolve.

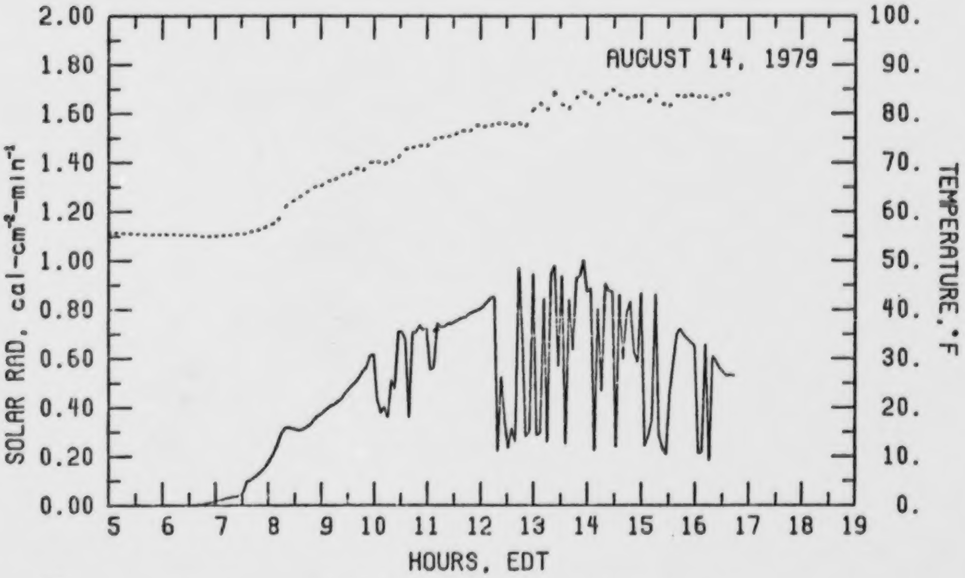

Figure 42. Total solar radiation and temperature data for August 14, 1979.

## SECTION 8

# OTHER SELECTED STUDIES AND COMPARISONS

### EFFECT OF DYNAMIC OPERATING CONDITIONS ON OZONE FORMATION

In a typical urban environment, reactant material is usually emitted throughout the day. The volume into which the reactants are mixed determines the concentration of precursors available for $O_3$ formation. Static smog chamber experiments on the other hand, start with all the mass present initially.

The UNC dual chamber has been used to compare static experiments with those in which the same mass was added to the same volume, but ramp-injected slowly over a 12 hour time period (0600-1800 EDT). In these experiments, propylene, a 60:40 mixture of n-butane:propylene, and the UNC mix (acetylene, 5 paraffins, 6 olefins) were each used as a hydrocarbon. All static experiments had a $NO_2$ to $NO_x$ initial ratio of 0.2. On the ramp side, NO and HC were injected each minute. Between 5 and 10% of the NO was oxidized to $NO_2$ at injection.

Figure 43 and 44 illustrate some typical results. (Solid lines are static, dashed lines ramp). Table 27 summarizes the conditions and results. In general, the $O_3$ profiles in the static and ramp-injected runs are very similar. The ramp side usually forms $O_3$ earlier and is higher in $O_3$ until afternoon when the static side usually overtakes and slightly passes the ramped $O_3$. The $O_3$ maximum, or $O_3$ at 1900 EDT in the ramped run, is usually about 90% of the static $O_3$ unless cloud conditions in the late afternoon influenced the final $O_3$ (these have a slightly lower percentage). In two runs, the ramped side formed more $O_3$. This was apparently because of a low NO injection rate, resulting in less total NO and a shift in the HC-to-$NO_x$ ratio on the ramped side, compared to the matching static run.

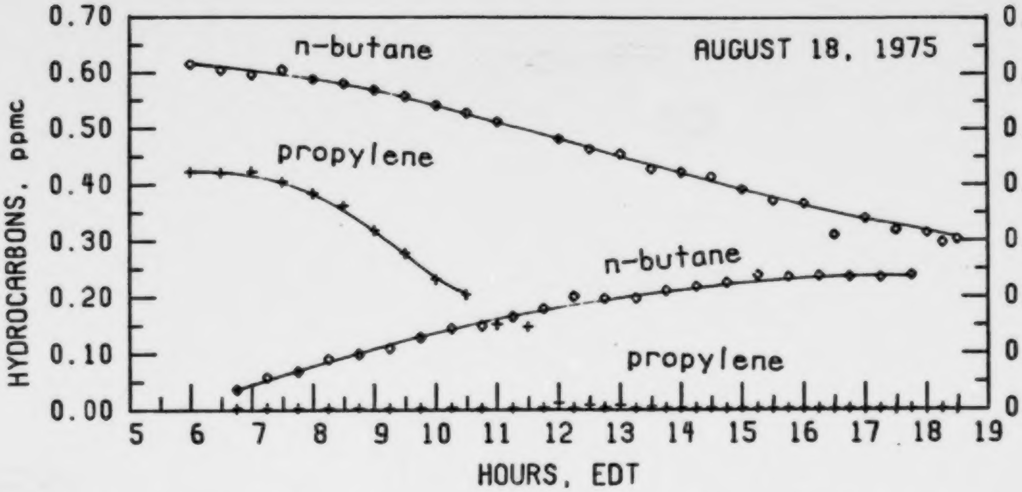

Figure 43. Static (—) and Ramp injection (--) dual run in UNC outdoor smog chamber. Initial conditions at 0545 in static side (—): NO, 0.29 ppm; $NO_2$, 0.07 ppm; $n\text{-}C_4H_{10}$, 0.60 ppmC; $C_3H_6$, 0.40 ppmC. Ramp side (--) would achieve: NO, 0.36 ppm; $n\text{-}C_4H_{10}$, 0.60 ppmC; $C_3H_6$, 0.40 ppmC at 1800 hours if reaction occurred.

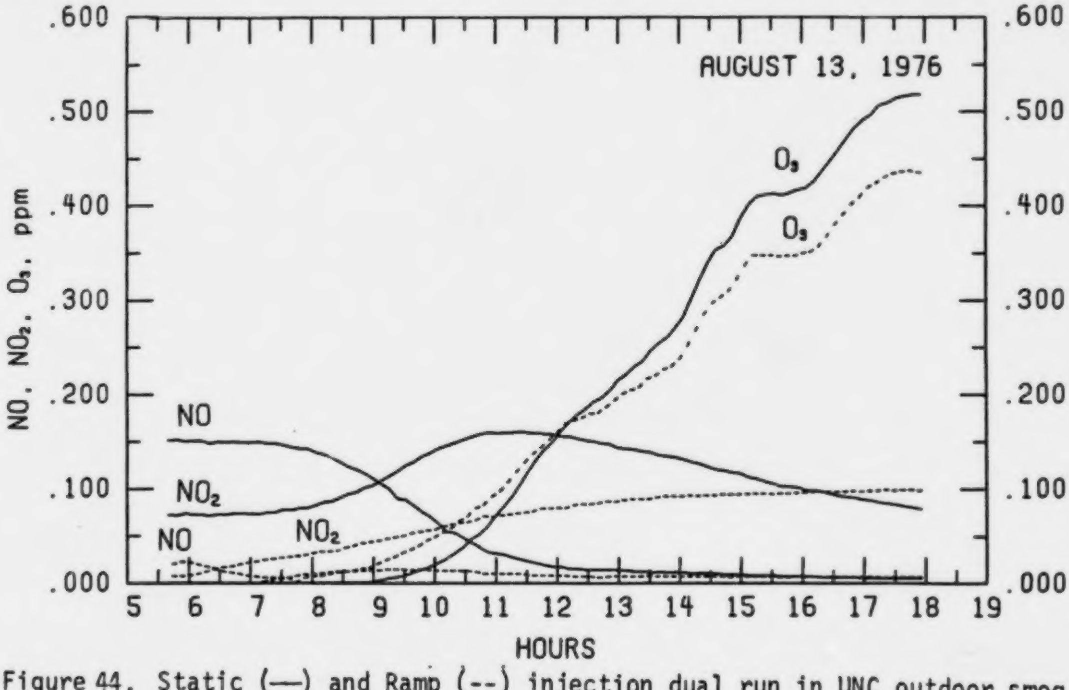

Figure 44. Static (—) and Ramp (--) injection dual run in UNC outdoor smog chamber. Initial conditions at 0540 in static side: NO, 0.151 ppm; $NO_2$, 0.072 ppm; 1.93 ppmC urban hydrocarbon mix. Ramp side (--) would achieve: NO, 0.22 ppm; 1.93 ppmC urban hydrocarbon mix at 1800 hours if no reaction occurred.

## TABLE 27. OZONE FORMATION IN STATIC AND RAMP INJECTED OUTDOOR SMOG CHAMBER EXPERIMENTS

| Date | Precursor Conditions[a] $NO_x$ | HC | cmp[b] | $HC/NO_x$ ppmC/ppm | $O_3$ max, ppm static | ramp | ramp/static % |
|---|---|---|---|---|---|---|---|
| 8/16/75 | 0.37 | 0.98 | P | 2.65 | 0.68 | 0.48 | 71 |
| 8/17/75 | 0.36 | 1.00 | B/P | 2.78 | 0.28 | 0.25 | 89 |
| 8/18/75 | 0.36 | 1.00 | B/P | 2.78 | 0.18 | 0.16 | 89 |
| 8/4/76 | 0.35 | 0.97 | M | 2.70 | 0.05 | 0.05 | 100 |
| 8/5/76 | 0.31 | 1.93 | M | 6.23 | 0.24 | 0.32[c] | 133 |
| 8/6/76 | 0.24 | 0.97 | M | 4.04 | 0.17 | 0.29[c] | 171 |
| 8/12/76 | 0.24 | 1.93 | M | 8.04 | 0.72 | 0.65 | 90 |
| 8/13/76 | 0.24 | 1.93 | M | 8.04 | 0.49 | 0.41 | 84 |
| 8/24/75 | 0.38 | 4.00 | M | 10.53 | 0.57 | 0.46 | 81 |
| 8/30/76 | 0.36 | 4.56 | M | 12.00 | 0.74 | 0.65 | 88 |

---

[a] initial values for static experiments established at 0540 EDT and values that would have existed at 1800 EDT in ramp injected experiments if no reaction occurred.

[b] P, propylene; B/P, 60% n-butane-40% propylene by carbon; M, synthetic urban mixture of acetylene, paraffins, and olefins.

[c] NO injection rate for ramped side lower than required to give final $NO_x$ value

The $NO_x$ and HC profiles in these runs are quite different from their static counterparts, not converging until near the end of the run. This convergence implies approximately the same total mass reacted over the same time period.

Another experiment simulated a highly simplified urban condition. It was assumed that an air parcel moved along a trajectory over a uniform emissions surface from 0600 to 1200 EDT. At 1200 EDT the parcel left the emissions surface. During its movement over the surface from 0900 to 1200 EDT, the mixing height doubled in a linear manner. Therefore, in the absence of reaction, the concentration of precursors in the air parcel would increase linearly from 0600 to 0900, and then, the concentration (mass/volume) would remain constant while an additional 3 hours of emissions was added to a volume that was doubled in 3 hours.

This run was compared to a static run which started with the same mass as would be present, *in the absence of reaction*, at the end of the dynamic run (and also at 0900 EDT). The run was accomplished by ramp injecting NO and HC into a static chamber from 0600 to 0900 EDT, and then diluting the chamber by 50% while continuing to inject NO and HC at a rate equal to the mass lost by dilution, assuming no reaction. The results are shown in Figures 45-48. Except for $O_3$ at the very end of the run and the ramp NO and HC injection, there is *almost no difference* in the profiles.

For these unique dynamic conditions we were able to approximate the smog profiles of a static system. Much of this work was published in the 1976 Proceedings of the International Conference on Oxidants.[64] In the following run season much more complex dilution and injection schemes were used. This was done to simulate in the chamber the atmospheric events occurring in an air parcel characterized during the 1973 Los Angeles Reactive Pollutant Program (LARPP). The analysis and results of this very complex smog chamber simulation were published in an EPA report[65] and other publications by Feigley et al.[66,67].

## COMPARISON RUNS BETWEEN UNC AND RESEARCH TRIANGLE INSTITUTE OUTDOOR CHAMBERS

To test the performance of two different types of outdoor smog chambers, located at two sites and using independently calibrated instruments, a single set of target initial conditions for propane and $NO_x$ were run in the UNC dual chamber (UNC-RED and UNC-BLUE) and the four Research Triangle Institute (RTI) cylindrical chambers on the same day. The target initial conditions were: 4.00 ppmV propane, obtained from common commercial LP gas tanks, and 0.20 ppm $NO_x$, to be 20% $NO_2$. The chambers were operated statically and a second and third day of irradiation were to occur with no further injections or dilution (except by sampling). Furthermore, bag samples from the chambers were exchanged for cross-analysis of hydrocarbon concentration. Data were obtained approximately every hour from strip charts at RTI and every 4 minutes by the computer-based data acquisition system at UNC.

The profiles for NO, $NO_2$, and $O_3$ in the six chambers are shown in Figures 49, 50, and 51. Summary information for the six runs over the

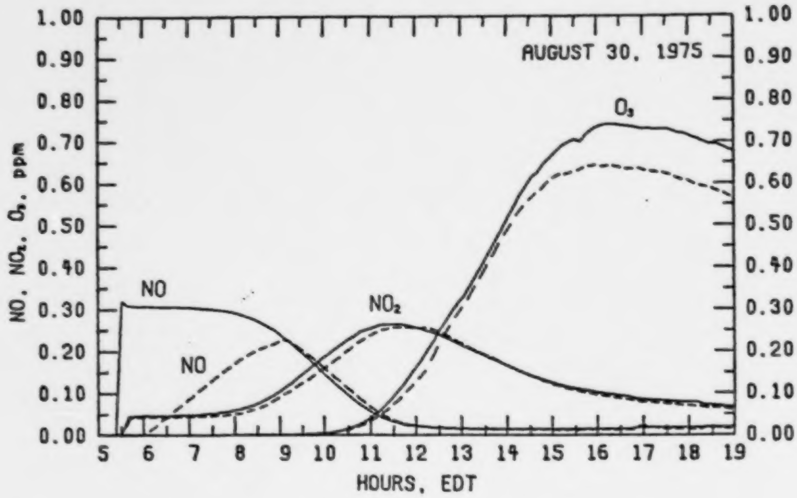

Figure 45. Static (—) and Ramp injection (0600-0900) with 50% dilution (0900-1200) and continued ramp injection (0900-1200) at rate equal to mass removal by dilution if no reaction (--). Initial conditions in static side: NO, 0.31 ppm; $NO_2$, 0.05 ppm; urban hydrocarbon mix, 4.56 ppmC. An initial condition of 0.05 ppm $NO_2$ was established in ramp side (--). NO and six injected in (--) so as to achieve same condition at 0900.

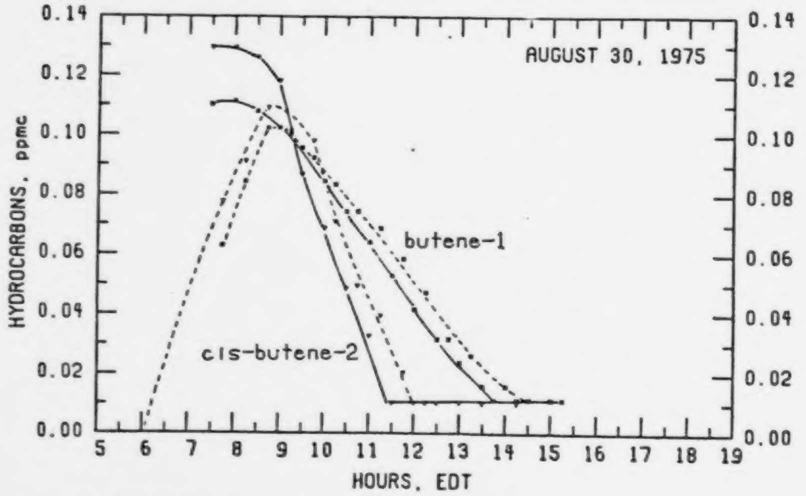

Figure 46. Selected hydrocarbon compounds in urban hydrocarbon mix for static (—) and ramp injection (--) dual run in UNC outdoor smog chamber.

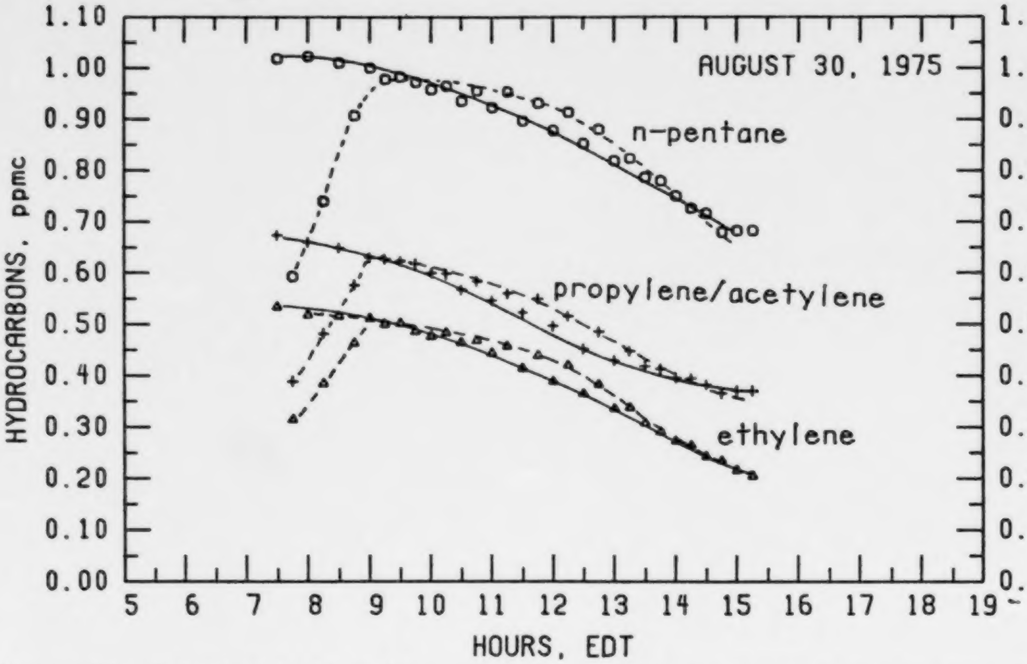

Figure 47. Selected hydrocarbon compounds in urban hydrocarbon mix for static (—) and ramp injection (--) dual run in UNC outdoor smog chamber.

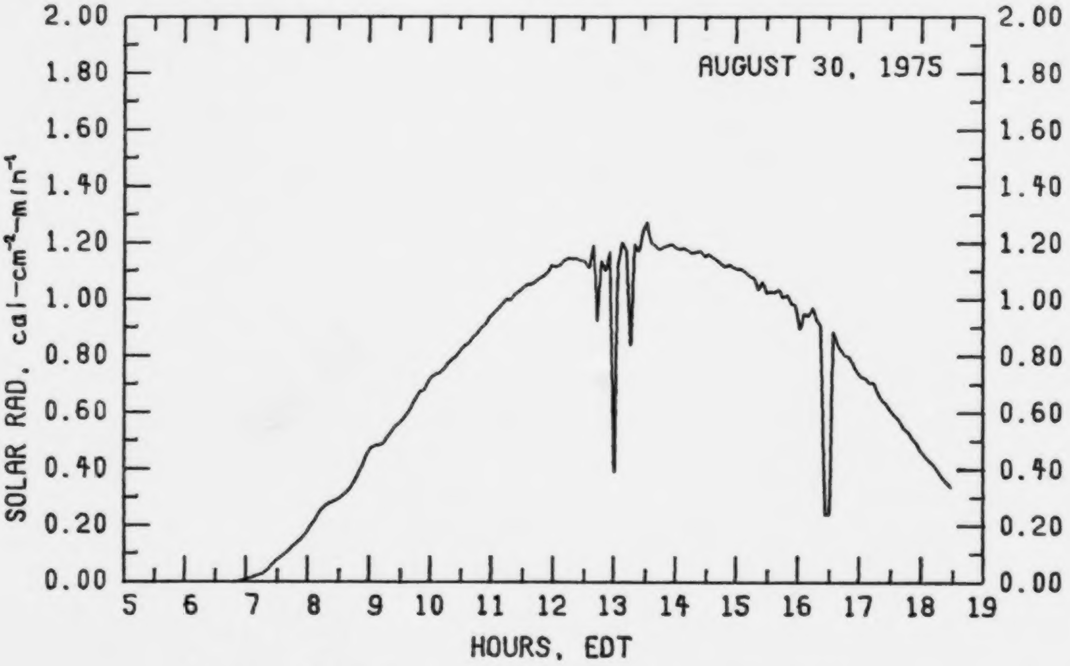

Figure 48. Solar radiation for August 30, 1975.

three day period is given in Table 28. The agreement is remarkable, not only in absolute magnitudes of concentrations, but also in the timing of events. The RTI chambers are slightly faster in reaching NO-$NO_2$ crossover, but the time of $NO_2$ maximum and $O_3$ maximum are very close in all six chambers. A more detailed presentation of this study has been prepared by Wright et al.[68]

TABLE 28. Summary Data September 20-22, 1976

Joint RTI & UNC

Propane $NO_x$ Run

| Chamber | Initial $NO_x$ ppm | Initial NO ppm | % $NO_2$ | ppmv Initial Hydrocarbon UNC GC | UNC THC | RTI | EST cross over time | 1st day $O_3$ max | 2nd day $O_3$ max | 3rd day $O_3$ max |
|---|---|---|---|---|---|---|---|---|---|---|
| UNC RED | 0.220 | 0.165 | 25 | 4.61 | 4.48 | 4.39 | 0916 | 0.224 | 0.252 | 0.272 |
| UNC BLUE | 0.211 | 0.158 | 25 | 4.27 | 3.93 | 4.08 | 0920 | 0.200 | 0.270 | 0.253 |
| UNC aerosol | | | | 1.31 | 1.37 | 1.09 | | | | |
| RTI #1 | 0.196 | 0.159 | 18 | 3.73 | 3.53 | 3.40 | 0904 | 0.180 | 0.26 | - |
| RTI #2 | 0.201 | 0.164 | 18 | 4.06 | 3.99 | 3.69 | 0841 | 0.240 | 0.34 | - |
| RTI #3 | 0.197 | 0.155 | 21 | 3.86 | 3.92 | 3.76 | 0856 | 0.17 | 0.21 | - |
| RTI #4 | 0.194 | 0.157 | 14 | 4.12 | 3.92 | 3.92 | 0907 | 0.20 | 0.25 | - |
| RTI #4* | - | - | -- | 3.83 | 3.67 | - | - | - | - | |

* Hydrocarbons in this bag only measured by UNC

Using slightly different simulated urban hydrocarbon mixes and $NO_x$, the two sets of chambers also yield approximately the same maximum $O_3$, even for experiments not conducted on the same day.

Such agreement between chambers of different design, different surface to volume ratios, different operating modes, and different operators should help improve the reputation of smog chambers as investigative tools in atmospheric chemistry. The reader may also refer to Appendix D, which shows the degree of chamber reproducibility in the UNC chamber over a period of 7 years.

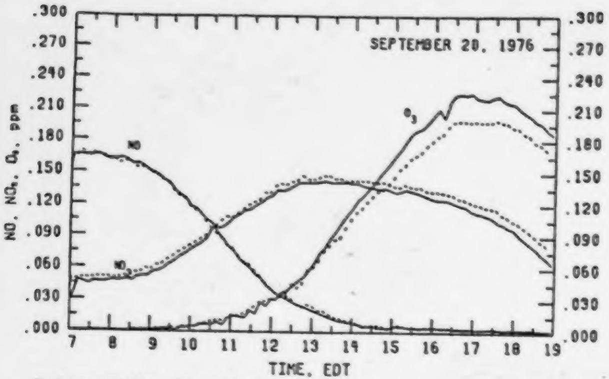

Figure 49. NO, $NO_2$, and $O_3$ profiles in matched dual propane run in UNC outdoor chamber. See Table 27 for initial conditions.

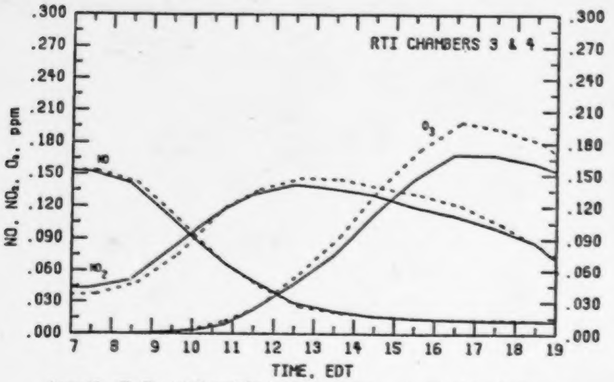

Figure 50. NO, $NO_2$, and $O_3$ profiles in matched propane run in RTI outdoor chambers. See Table 27 for initial conditions.

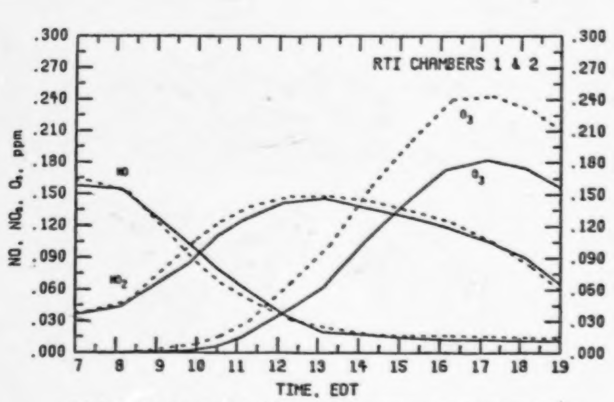

Figure 51. NO, $NO_2$, and $O_3$ profiles in matched propane runs in RTI outdoor chambers. See Table 27 for initial conditions.

## SELECTED CHAMBER CHARACTERIZATION RESULTS

One of the major difficulties one has to address in the use of a smog chamber is the characterization of chamber walls and the extent to which the walls influence chemical behavior during an experiment. It was noted during the course of the research project that for certain conditions freshly injected formaldehyde would disappear from the gas phase at an inordinately high rate. During other experiments which were conducted on overcast days we sometimes observed an increase of $NO_2$ in the chamber.

### Formaldehyde Wall Losses

In many of the formaldehyde-$NO_x$ smog experiments conducted during 1977 and 1978 it was observed that formaldehyde would start to decay immediately after vaporization of injected solid paraformaldehyde and then reappear a few hours later. It was hypothesized that formaldehyde was being lost to cool, humid chamber walls and that when temperatures increased, the formaldehyde on the walls revaporized along with any existing wall moisture. An example of this behavior is shown in the formaldehyde traces for May 18, 1977 and September 8, 1978 (Figure 52). Formaldehyde data for both of these runs were taken with a GC-methanizer technique. This method is discussed in Section 9.

If the above hypothesis was correct, drying the chamber air prior to injection of formaldehyde would reduce if not eliminate the wall loss problem. For a select number of runs, clean chamber air was dried by recirculating it past the cooling coils of an air conditioner. In one such run, clean air in the dried side was recirculated and dried for approximately 2 1/2 hours prior to a 1.2 ppm formaldehyde injection. The other side was not dried but received the same injection of 1.12 ppm HCHO. The formaldehyde, dew point, and temperature plots for both sides of this experiment are shown in Figure 52.

The side which was dried prior to injection had a very stable formaldehyde trace and concentrations did not change until sunrise. The other side exhibited immediate loss and subsequent reappearance of formaldehyde which was reminiscent of the May 18, 1977 run. The dew point stayed at $60^{\circ}F$ in the dried side for the entire day while in the wet side the dew point followed the diurnal rise in temperature. The fact

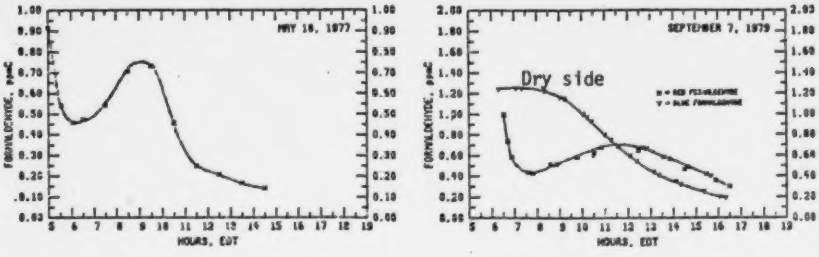

Chamber not dried

Humid vs. dry chamber

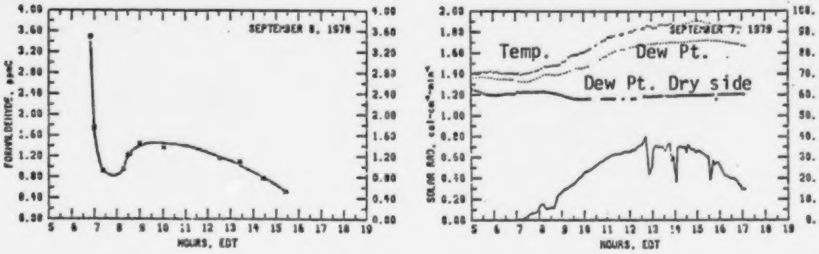

Chamber not dried

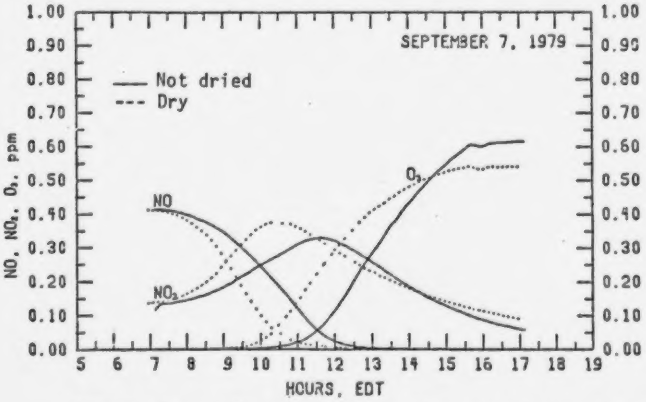

Effect of removing wall moisture in matched HCHO-$NO_x$ run

Figure 52. Wall moisture effects on gas phase formaldehyde systems.

that the dew point increased significantly in the wet side means that condensed moisture was being vaporized into the gas phase. It is hypothesized that the extent of drying required to eliminate the wall losses of formaldehyde is that amount which strips off existing water condensation from the interior surfaces of the chamber.

In comparing the behavior of the wet and dry sides on September 7, 1979, it seems clear that removing condensation from interior walls does have a strong effect on the NO, $NO_2$ and $O_3$ timing of the run. The dry side is an hour faster to crossover and starts making $O_3$ much sooner. This is because much of the morning formaldehyde has been lost to the walls in the wet side and is not available for reaction until it revaporizes. Surprisingly, the wet side $O_3$ maximum was actually higher than in the dry side. Inspection of the formaldehyde traces shows that formaldehyde concentrations in the wet side at 1430 EDT were substantially higher than in the dried side. This "extra" formaldehyde most likely increased the radical flux in the afternoon, resulting in more $O_3$. Finally, note that a very early morning leak developed in one of the ethylene tank fittings in an adjacent facility; this caused an initial morning ethylene contamination of 90 ppbC in the wet side and 40 ppbC in the dried side. The ethylene difference in the two sides will have some impact on the $O_3$ maxima and the magnitude of this effect could potentially be sorted out by modeling both sides of this experiment. Ethylene can be used in the modeling of these experiments to monitor OH.

Under separate funding, many high quality formaldehyde experiments have been run and these have been made available to EPA and modelers at SAI and Environmental Research and Technology. To further illustrate the effects of drying, chemical profiles from a number of these runs are shown in Figures 53a and 53b. Formaldehyde data for the 1979 runs were taken with an automated colorimetric system purchased from CEA Corporation. This is also discussed in Section 9.

## Potential Nitrogen Recycling

In each data season, there have been a few runs in which total [$NO_2$] increased during the run or even before injections in the background air. This $NO_2$ increase did occur in some 1977 runs, but the magnitude was not

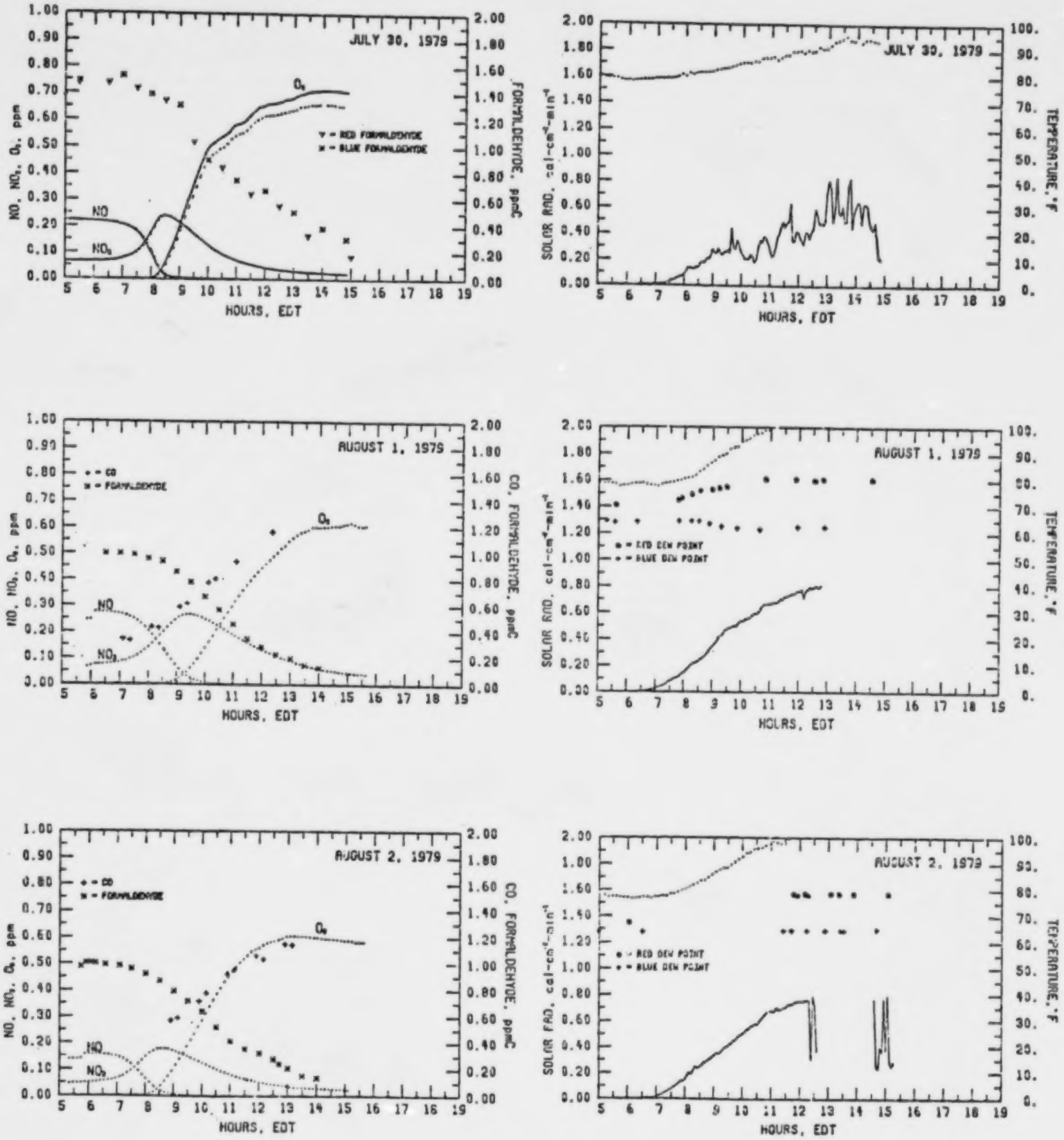

Figure 53a. 1979 UNC formaldehyde-$NO_x$ runs. 1979 TSR data are low by as much as 45% at the peak and another year's profile should be usedto model these data.

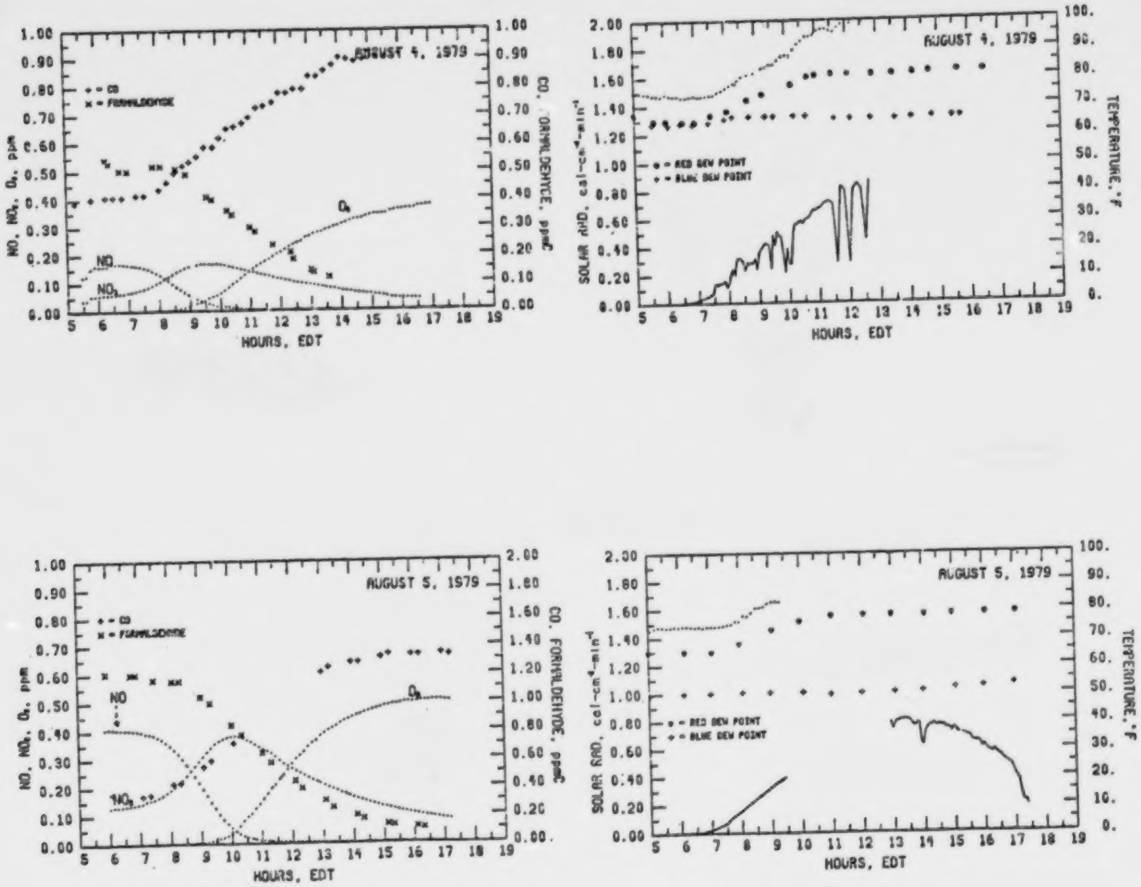

Figure 53b. UNC 1979 formaldehyde-$NO_x$ runs.

great. Instrument drift coupled with possible leaks from old solenoids into the injection manifold were assumed explanations. A check of the old solenoid values on high concentration tanks and back calculations indicated that the solenoids would have had to have leak rates in excess of 30 cc per minute to account for the observed $NO_2$ build-up. On occasion leaks were found, but leakage measured was 5 cc per minute. An improved "fail-safe" injection system was installed early in 1978 making it impossible for tanks to leak into the injection manifold. In 1978, a "wet" year, the $NO_2$ "build-up" problem occurred in more than twenty runs. An analysis of these runs and other runs in which no build-up was seen was made to see if chamber history or other chemical or physical characteristics could be associated with $NO_2$ "build-up". Our observations suggest there is a strong correlation between certain weather conditions and this increasing $NO_x$ phenomenon. It seems that $NO_2$ off-gased from the wall when temperatures were warm compared to previous days, when the purge air had a very high relative humidity, and when conditions were overcast. A detailed analysis of all of the runs which exhibited early morning $NO_2$ bleed showed that morning temperatures ranged between 69-72$^{o}$F (see Figure 54). Fifteen of the 25 days had relative humidities which exceeded 96%. On those days, as cloud cover increased from less than 30% to greater than 80%, the average $NO_2$ bleed increased from almost 0.017 ppm to almost 0.06 ppm. It would therefore seem that there is a unique association between $NO_2$ bleed, temperature, humidity and sky cover.

To test for high humidity effects several experiments were conducted in which one side of the chamber was dried using molecular sieve drying trays. A goal was to reduce early morning $NO_2$ off-gasing and perhaps prevent nitric acid absorbing on the walls during the run. In the seven runs where one side was dried, no $NO_2$ off-gasing was observed in the dried side. In the other side $NO_2$ off-gasing was observed if the weather conditions were conducive to this type of problem.

Near the end of the 1978 season one side of the chamber was entirely "mopped down" with distilled water. The wash water obtained from this cleaning process was analyzed and found to contain large amounts of nitrate. A matched initial conditions run was conducted the next day

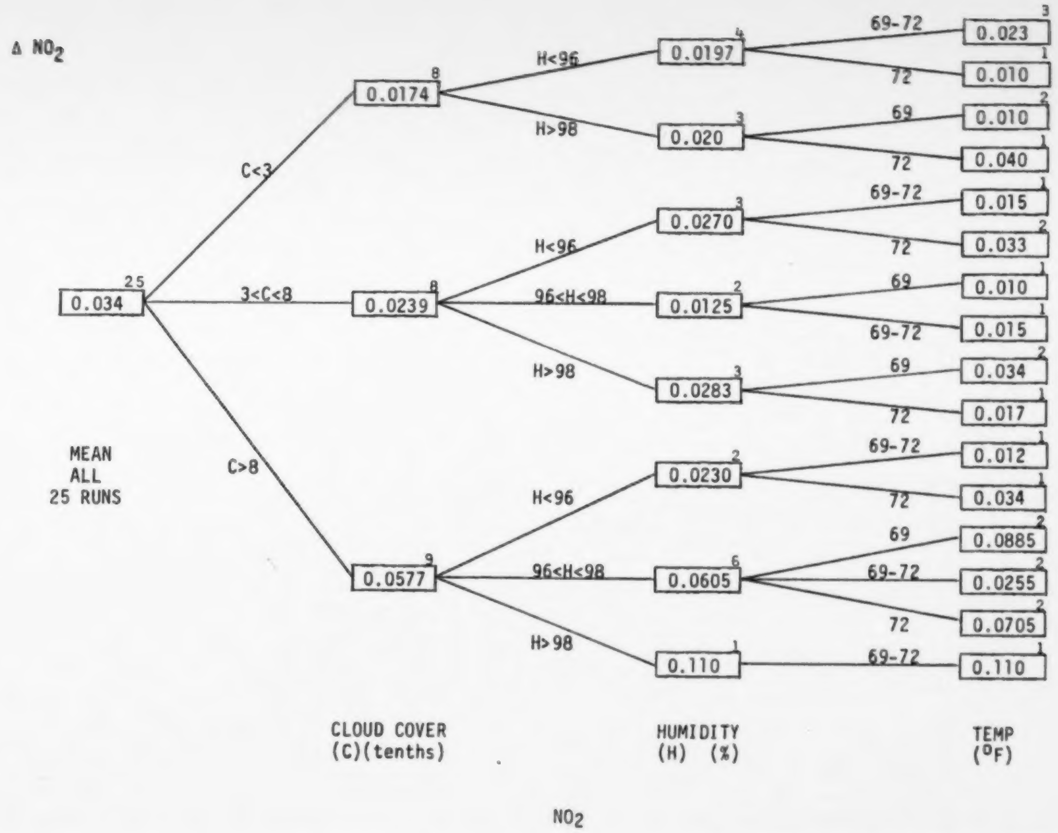
Δ NO$_2$
MEAN
ALL
25 RUNS
25
0.034
C<3
3<C<8
C>8
8
0.0174
8
0.0239
9
0.0577
H<96
H>98
H<96
96<H<98
H>98
H<96
96<H<98
H>98
4
0.0197
3
0.020
3
0.0270
2
0.0125
3
0.0283
2
0.0230
6
0.0605
1
0.110
69-72
72
69
72
69-72
72
69
69-72
69
72
69-72
72
69
69-72
72
69-72
3
0.023
1
0.010
2
0.010
1
0.040
1
0.015
2
0.033
1
0.010
1
0.015
2
0.034
1
0.017
1
0.012
1
0.034
2
0.0885
2
0.0255
2
0.0705
1
0.110
CLOUD COVER
(C)(tenths)
HUMIDITY
(H) (%)
TEMP
(°F)
NO$_2$

Figure 54. Mean NO$_2$ morning bleed (ppm) of all runs with morning NO$_2$ bleed broken down by cloud cover, humidity and temperature. Number of cases indicated in numbers over boxes.

without "drying" either side. The two sides did not behave the same in the morning. $NO_2$ did not increase in the washed side but did increase in the other side. $HNO_3$ did off-gas on the washed side before injection; $HNO_3$ formation was observed in the gas phase but only at 40-50 ppb, the rest apparently went to walls.

It is reasonable to assume that the observed nitrate on the chamber walls resulted from the loss of a gas phase nitrogen specie (or species) to the chamber surfaces. The generally low level of observed gas phase nitric acid and model predictions of the nitric acid that should be generated from chamber photochemical systems strongly suggest that nitric acid is lost from the gas phase. Once on the walls it would be expected that nitric acid would impart a certain wall acidity level. The level of acidity will depend on the amount of $HNO_3$ lost to the walls, and the amount of condensation on the interior walls of the chamber.

A recent analysis by Ross[69] attempted to characterize equilibrium for $NO_x$ species vs. acidity in aerosol droplets. Estimated equilibrium profiles for NO, $NO_2$, $HONO_2$, $HNO_3$, etc. are shown in Figure 55 and reactions for species involved in this equilibrium are shown below in Reactions 37-43. It is noted in Figure 55 that sulfuric acid is used to create aerosol acidities. On the chamber walls the high-self ionization potential of nitric acid should provide needed hydronium ions from the dissociation of nitric acid.

If the equilibrium diagrams in Figure 55 represent the relative $NO_x$ species equilibrium on the chamber walls, then it may be inferred that the above noted physical conditions could give rise to wall acidities which promote the release of $NO_2$. In all of the chamber systems which show $NO_2$ bleed we have never observed an increase in NO. It may be that acidity is never so weak that observed NO is released. This is probably because there is a maximum amount of water that the walls can hold. According to Figure 55, as drying of the chamber walls takes place, acidity in the condensed phase should increase and the nitrogen species in the water droplets will become more concentrated. Ultimately, the higher acidity should inhibit the release of $NO_2$ and HONO from the liquid phase. This is very consistent with the previously mentioned dry vs. wet experiments in which the major effect of drying was to reduce $NO_2$ bleed.

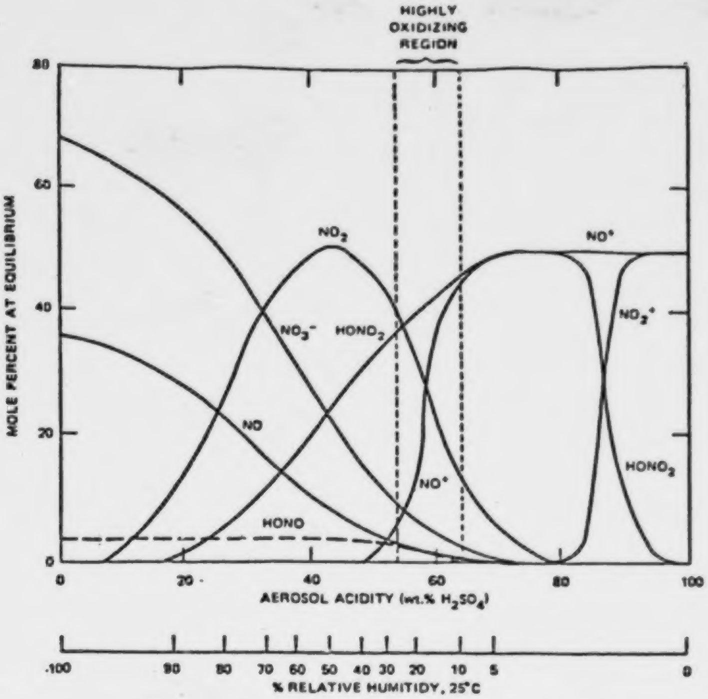

Figure 55. ESTIMATED EQUILIBRIUM PROFILES FOR $NO_x$ SPECIES VERSUS AEROSOL ACIDITY

Established for an initial condition of $NO_2$ in equilibrium with $H_2SO_4$

$$HONO_2 + H_2O \rightleftarrows H_3O^+ + NO_3^- \qquad (37)$$

$$HONO + H_2O \rightleftarrows H_3O^+ + NO_2^- \qquad (38)$$

$$H^+ + HONO_2 \rightleftarrows (H_2ONO_2)^+ \rightleftarrows H_2O + NO_2^+ \qquad (39)$$

$$H^+ + HONO \rightleftarrows (H_2ONO)^+ \rightleftarrows H_2O + NO^+ \qquad (40)$$

$$4\ HONO \rightleftarrows 2\ H_2O + 2\ NO + 2\ NO_2 \qquad NO_2 \rightleftarrows N_2O_4 \qquad (41)$$

$$N_2O_4 + H_2O \rightarrow HONO + H^+ + NO_3^- \qquad (42)$$

$$NO^+ + HONO \rightleftarrows H^+ + \begin{array}{c} N_2O_3 \\ \uparrow\downarrow \\ NO + NO_2 \end{array} \qquad (43)$$

Equilibrium reactions for $NO_x$ species in the liquid phase

During smog chamber runs when nitric acid was typically observed it was usually at very low concentrations. Often nitric acid would begin to appear as theoretically predicted (after NO is nearly consumed) and then decrease to zero. Many times when the chamber was being purged, low concentrations of nitric acid would appear and remain into the night. Sometimes $HNO_3$ appeared after closing the vent doors but before injections were made. On one occasion, on the second day of a three day run (November 3-5, 1978), 0.17 ppm nitric acid and 0.19 ppm $NO_2$ off-gassed by the morning of the second day (Figure 56). The nitric acid appeared at 2200 EDT on the first day and reached the maximum at 0900 EDT on the second day. $NO_2$ appeared at 0300 EDT on the second day and reached maximum at 1045 EDT the same day (nitric acid = 0.06 ppm at this time). These processes began in the dark. The total nitrogen concentration reached a maximum value of 0.25 ppm (1000 EDT on the second day), half of the initial $NO_x$ of the run. Nitric acid disappeared by 0200 EDT on the third day while $NO_2$ maintained a minimum concentration of 0.02 ppm all night. Nitric acid and $NO_2$ reappeared on the third day at concentrations of about 0.04 ppm. The temperature at 1900 EDT on November 3 was approximately $54^0$ and at 0600 EDT on November 4 was approximately $56^0$. Since the chamber was closed during this period it may be conjectured that when nitric acid began to off-gas at approximately 2200 EDT, the wall acidities were fairly high (since this is the region in which $HONO_2$ can be liberated from the liquid phase). As $HNO_3$ was released during the evening and early morning, presumably the wall moisture acidity would decrease to the point where the walls would off-gas $NO_2$. Also, since temperatures increased slightly during this time, water may have evaporated, setting up a delicate balance which maintained the wall acidity in the "$NO_2$ off-gasing region" for a sustained period of time.

It must be stressed that the kinds of meteorological conditions which give rise to $NO_2$ and $HNO_3$ bleed are not very desirable for smog chamber runs. Most of the experiments selected for modeling or other comparison purposes are conducted during better outdoor conditions when these effects are minimized or eliminated. Analyses of these problems, with the associated meteorological data and chamber run history are

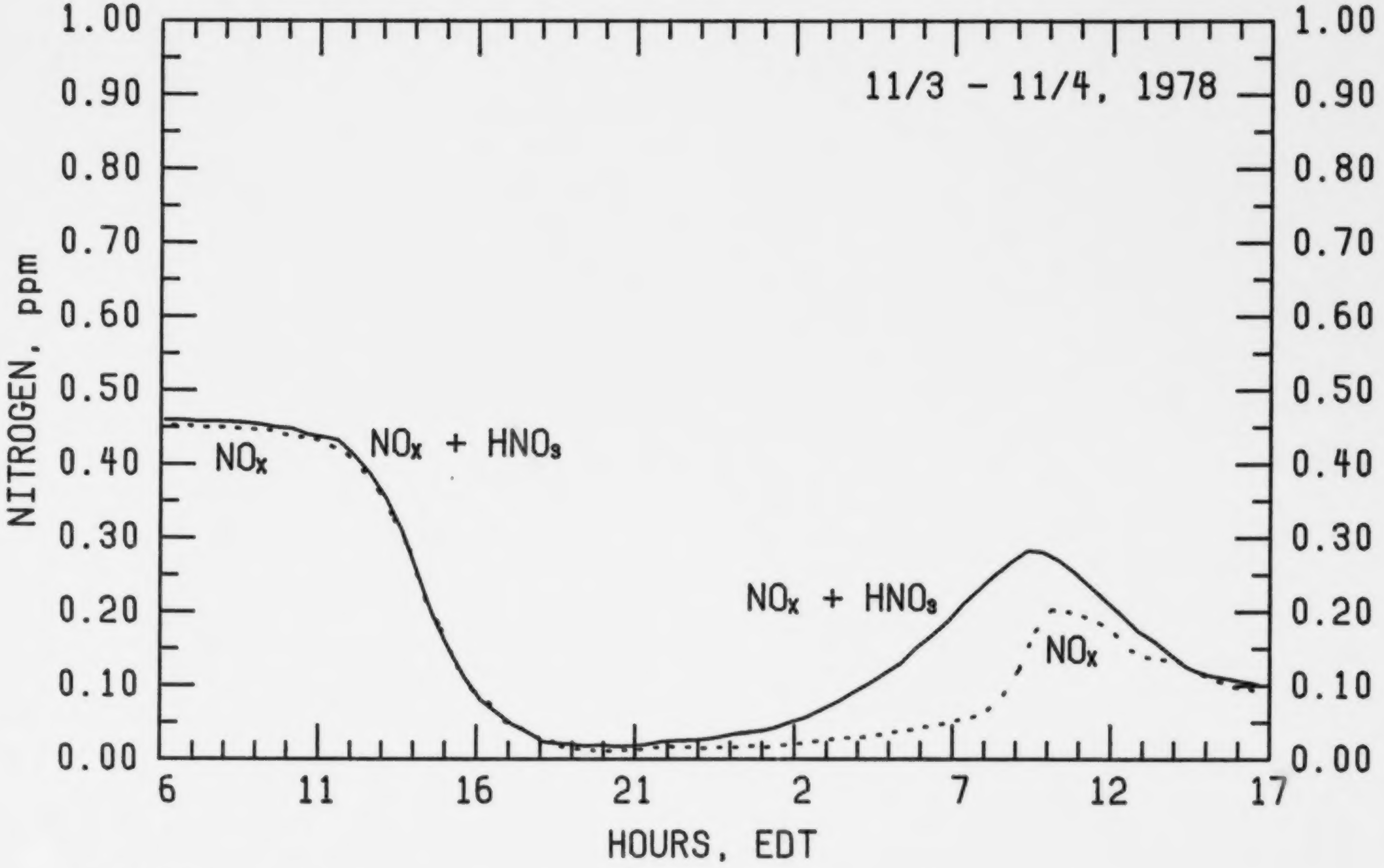

FIGURE 56. Molybedenum catalyst-chemiluminescence method for $HNO_3$ recording showing $HNO_3$ and $NO_2$ appearing on second day of a three day ethylene/$NO_x$ run.

continuing. The above observations do suggest that there is a heterogeneous process for recycling nitric acid into $NO_2$ under selected conditions.

## CHARACTERIZATION OF SELECTED SINGLE HYDROCARBON-$NO_x$ CHAMBER RUNS FOR MODELING STUDIES.

A small portion of our research during this project was devoted to generating single hydrocarbon-$NO_x$ runs which would aid outdoor photochemical modeling efforts. Five of these runs have been worked up in detail and will be presented below. These as well as many other related experiments have been analyzed and modeled by Sexton in "The Role of Nitrogen Containing Compounds in Several Organic Smog Systems".[70] In addition, approximately 100 different modeling experiments have been conducted under separate funding. Most of these runs include detailed product information and have been made available to EPA. Dr. Marcia Dodge at EPA, Research Triangle Park, North Carolina should be contacted for further information.

### August 8, 1977 Propylene Run

This matched dual run illustrates the degree of reproducibility (Figure 57) between the two chamber halves. Major product information is fairly complete except for CO.

The temperature and solar radiation profiles for this day are shown in Figure 57. The initial outside and inside chamber temperatures were about 75°F at 0500 EDT. By 1000 EDT the outside temperature was 84°F while inside the chamber it was almost 90°F. The chamber temperature peaked at about 101°F at 1450. The solar radiation curve shows a clear morning; at 1200 EDT the first evidence of clouds can be seen. By this time $NO_2$ had already peaked and $O_3$ production was well under way.

Comparison of Saltzman $NO_2$ and chemiluminescent $NO_2$ (Figure 57) which shows interference in the chemiluminescent $NO_2$, suggests that our chemiluminescent meter does not respond 100% to PAN. This is clearly indicated by the October 22, 1977 data and to a lesser extent by the July 18, 1977 data (these are discussed below). The early morning, 0500 to 0600, $NO_2$ resulted from the 0430 NO injection. Some of the NO was oxidized thermally at high concentration during injection, and some was

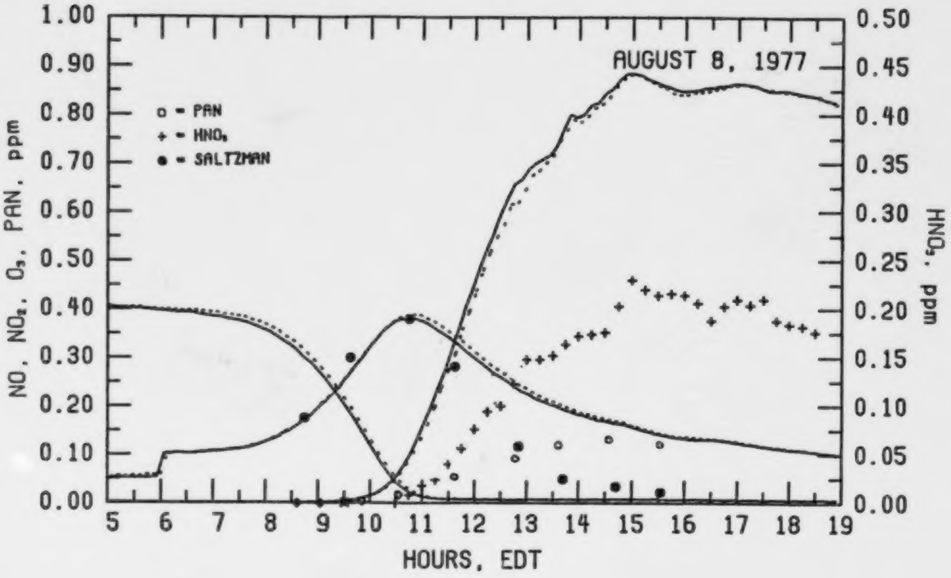

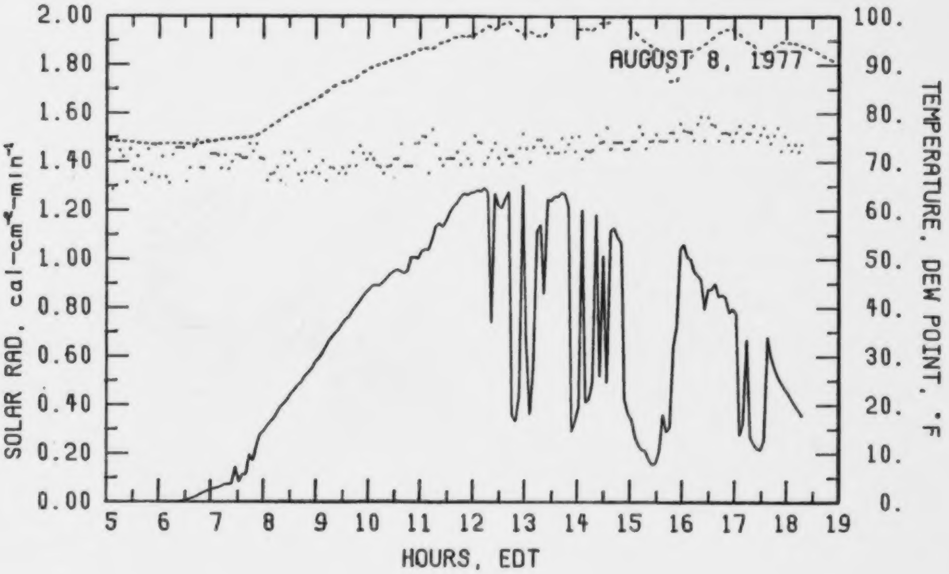

Figure 57. August 8, 1977, 1.5 ppmC propylene and 0.5 ppm $NO_x$ run.

oxidized by titrating the NO with the early morning ambient air $O_3$ in the chamber from overnight purging. The $NO_2$ injection occurred at 0600 EDT.

This run is somewhat unique in that very high concentrations of nitric acid were measured in the gas phase. Although auxiliary chamber drying did not take place on this day, the ambient conditions were such that at 0500 EDT the chamber dew point was 70°F compared to the ambient chamber temperature which was 75°F. The chamber dew point remained constant during this entire run at approximately 70-73°F; this indicates that no additional condensed water was in the chamber during the run (Figure 57). Hence it is reasonable that most of the nitric acid formed from the reaction of $NO_2$ and OH stayed in the gas phase.

The nitrogen balance for this run is shown in Figure 58. Little PAN or $HNO_3$ is formed until NO is almost completely removed. One fine detail to remember for later discussion is the slight increase in nitrogen measured between 1030 and 1130 EDT, just as NO is nearly consumed. At 1500 EDT, the total nitrogen, adjusted for dilution, would be 0.468 ppm. Our measurements show that approximately 26% was PAN, 39% $HNO_3$, and 8.6% $NO_2$. This leaves 26% which we were unable to measure. PAN decreased slightly after this time while $HNO_3$ increased.

Figure 58 also shows the carbon containing species time profiles. The side which had a slightly larger initial propylene (0.06 ppmC) was a slightly faster run. Propylene was consumed to below the detection limit; both acetaldehyde and HCHO exhibited a clear maximum and decline. PAN also showed a maximum and slight decline. In the carbon balance shown in Figure 58, CO has been estimated according to CO measured in other propylene/$NO_x$ runs with similar concentrations.

## October 22, 1977 Propylene Run

This run used a relatively high concentration of propylene (3.7 ppmC) and 0.5 ppm $NO_x$ (Figure 59a). Sunrise occurred at 0730 EDT, and the day was cool, with a starting temperature of about 0.5°C (33°F) and a maximum in the chamber of 24°C (75°F). This run had a high propylene/$NO_x$ ratio in a cooler environment and shows the effects of increasing the $[HC]/[NO_x]$ ratio under cooler temperatures. The

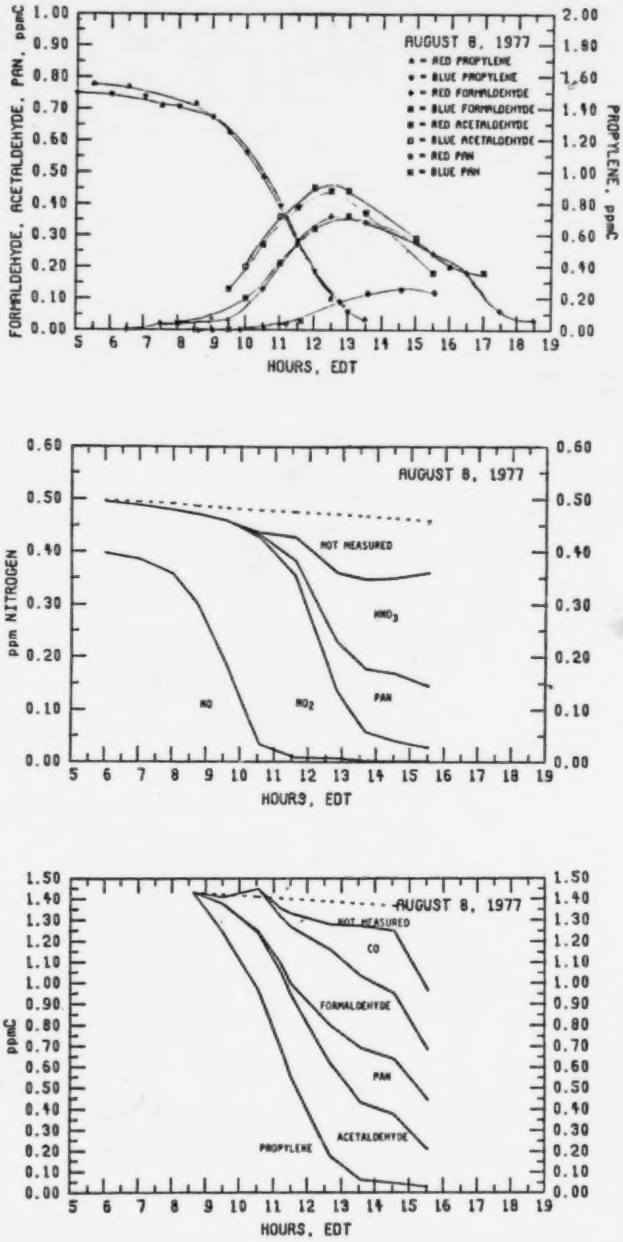

Figure 58. Product, nitrogen, and carbon balance for October 8, 1977, 1.5 ppmC propylene, 0.5 ppm $NO_x$ run.

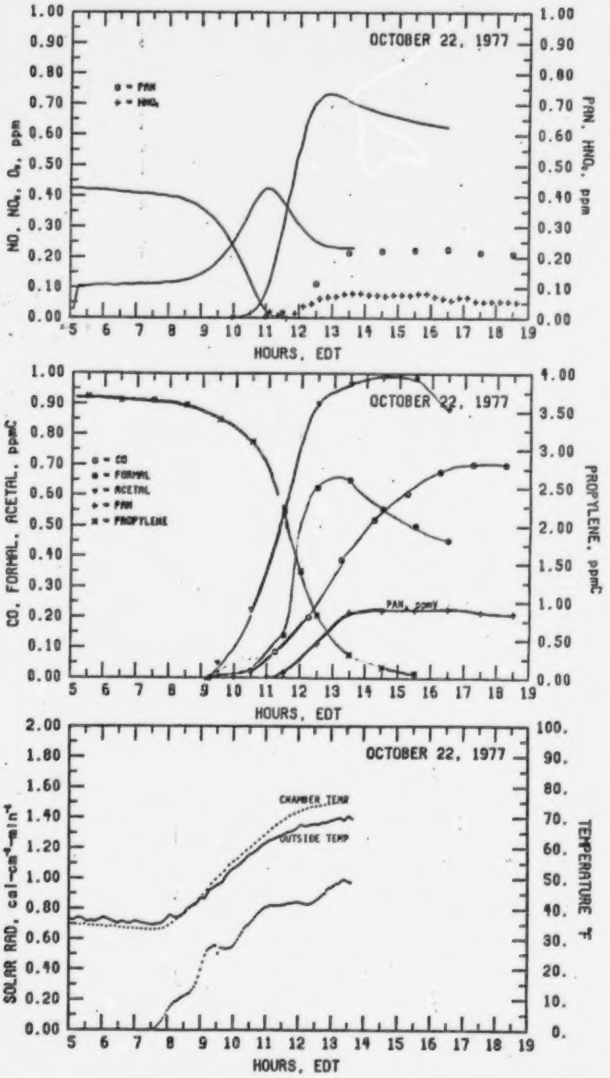

Figure 59a. Experimental data for October 22, 1977.

reactions of propylene produce the acyl radical necessary for PAN formation. By increasing the initial propylene concentration, a greater potential for PAN production was expected; the longer half-life of PAN at cooler temperatures also indicates a further increase in the potential for producing PAN. Since the formation of PAN effectively reduces the nitrogen involved in producing $O_3$, this experiment should also show the effect of increased PAN formation on the maximum $O_3$ concentration produced. $NO_2$ Saltzman data are missing from this run, but from other similar runs which included these data, we have assumed: 1) that the chemiluminescent $NO_2$ values are valid until just after $NO_2$ maximum, 2) that the meter's response is about 100% to PAN, and 3) that the roll-over in the $O_3$ curve is close to a point at which $NO_2$ is essentially consumed. These assumptions allow completion of the nitrogen balance (Figure 59b). The only part of the curve that would be affected by these assumptions is the slope of the line from $NO_2$ maximum to total $NO_2$ consumption. Figure 59a shows that, unlike the August 8 run, higher propylene and cooler temperatures lead to a much higher PAN and less $HNO_3$. At 1430 EDT the measured $HNO_3$ and PAN were 0.077 ppm and 0.213 ppm, indicating a PAN/$HNO_3$ ratio of 2.77. At this time, the concentrations of PAN and $HNO_3$ represent 60% of the initial nitrogen. This may indicate the presence of other unmeasured product nitrogen compounds, or more likely, nitric acid loss to the chamber walls.

Under separate funding this experiment was repeated a year later on October 21, 1978. Both of these runs had similar dew point, temperature and solar radiation; it is not surprising that the chemical behavior of both systems would be similar. The agreement, however, is so close that when the pollutant profiles were overlayed from these two days, they were almost indistinguishable (Figure 60). The run on October 21, 1978 is also noteworthy because the other chamber side had the same initial chemical conditions except that the background air prior to injection was dried down by recirculation over molecular sieve drying trays. The effects of drying during this experiment and its impact on the associated PNA chemistry have already been discussed in Section 5.

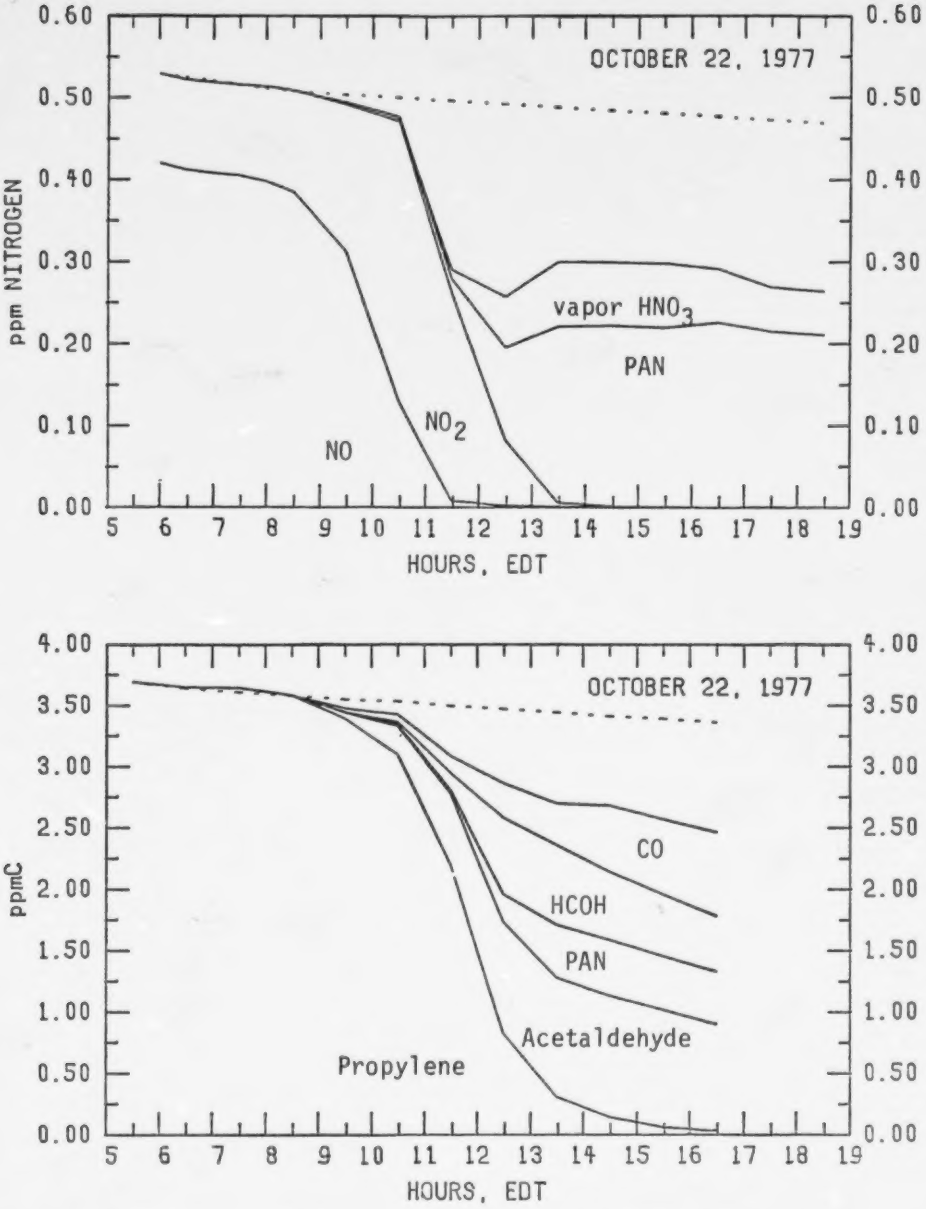

Figure 59b. Nitrogen and carbon balances for October 22, 1977 propylene $NO_x$-run.

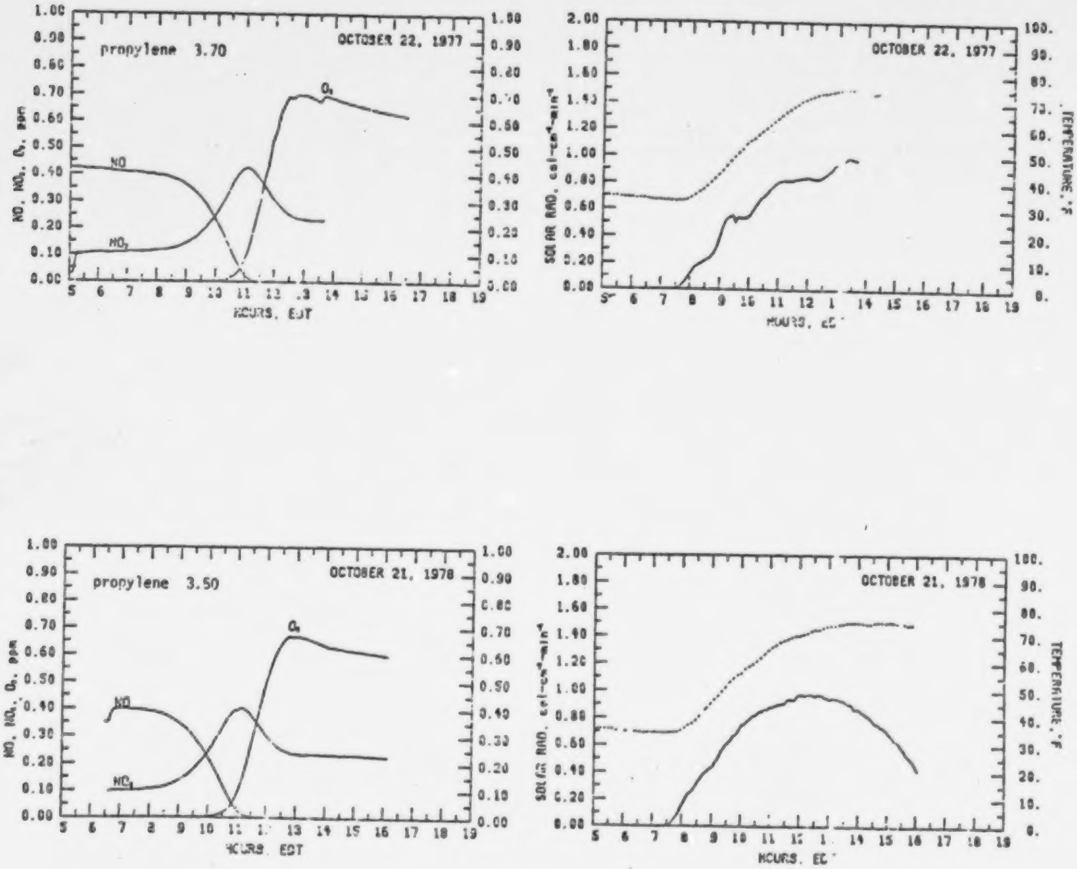

Figure 60. Similar propylene runs (~3.6 ppmC) conducted one year apart in UNC chamber, October 22, 1977 and October 21, 1978.

July 18, 1977 Formaldehyde/Acetaldehyde Run

This run was a side-to-side comparison of formaldehyde (HCHO) and acetaldehyde at similar initial carbon concentrations (Figure 61). Formaldehyde/$NO_x$ systems can produce OH (necessary for $HNO_3$ formation) but not the acyl radical. Therefore, only $HNO_3$ would be expected in a formaldehyde/$NO_x$ system. The acetaldehyde-$NO_x$ system however can produce the acyl radical and therefore would have a large PAN formation potential. July 18 was a hot day. The outside temperature at 0530 EDT was 24°C (75°F); by 1000 EDT it was over 32°C (90°F); the maximum chamber temperature was 48°C (100°F). Predawn inspection of the chamber indicated no visible condensation on either the interior or exterior of the chamber film; no dew was present on the grass at the research site. The morning sun was very good, but some cumulus clouds developed in the afternoon. The initial conditions were 1.27 ppm HCHO, 0.38 ppm NO, and 0.14 ppm $NO_2$ in the HCHO/$NO_x$ side. The acetaldehyde side had 0.49 ppm acetaldehyde and the same initial amounts of NO and $NO_2$. The $HNO_3$ analyzer was sampling on the formaldehyde side for most of the run. Only a few readings were obtained late in the acetaldehyde run (1530 to 1630 EDT, Figure 61). Also since PAN would not form appreciably in the HCHO run, the PAN analyzer sampled air mostly from the acetaldehyde side. Only a few PAN readings were obtained in the HCHO side late in the run to illustrate that the "carry-over" from one sample to the next was very small. (See data points at 1530 and 1645 EDT, Figure 61).

The morning conversion of NO to $NO_2$ until crossover is not substantially different in either the formaldehyde or acetaldehyde. This is similar to the behavior previously noted when HCHO was added to one side and acetaldehyde added to the other side of a matched mix-$NO_x$ system. As the run continues, the HCHO side loses $NO_x$ at a much faster rate than the acetaldehyde system. According to the nitric acid measurements, however, this species is not present in significant amounts in the gas phase. As illustrated by Figure 61, analytical measurements are unable to account for at least 80% (0.38 ppm out of 0.47 ppm) of the nitrogen in the HCHO system. Figure 61 also shows that, in the acetaldehyde system, the measurements account for about 57% (0.29 ppm out of 0.505 ppm) of the nitrogen, but it appears that if the extent of

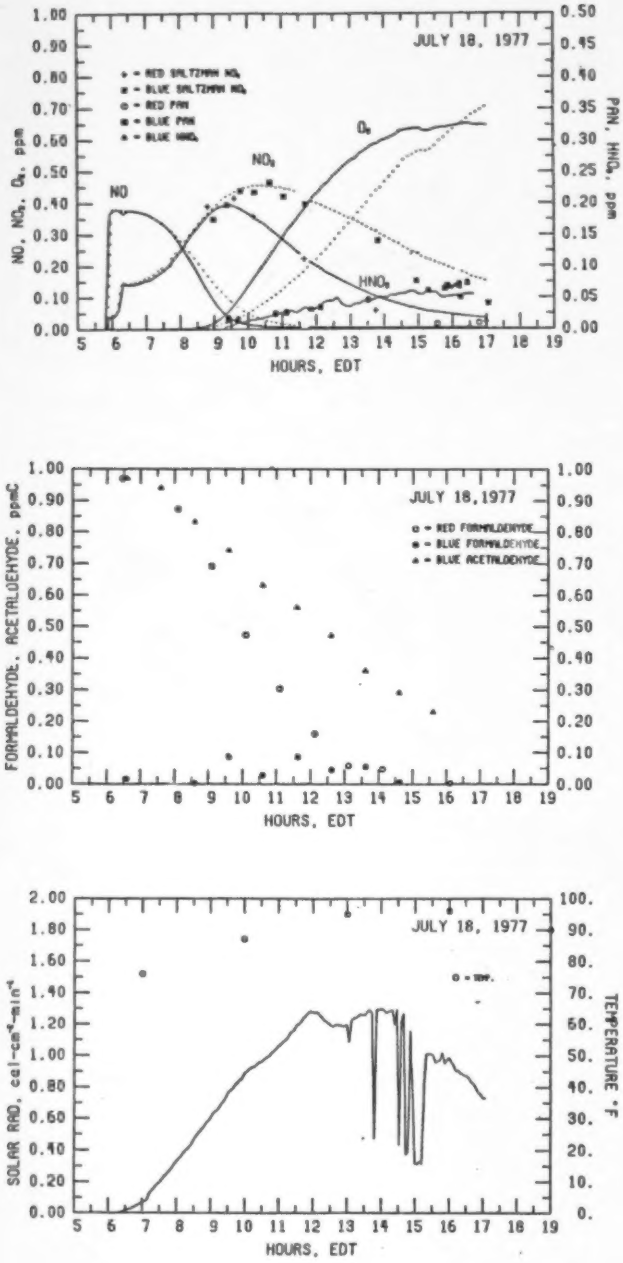

Figure 61. Data for July 18, 1977 aldehyde-$NO_x$ smog experiment.

reaction was greater (i.e. complete $NO_x$ removal), the amount accounted for would have been considerably less. Further, both systems had about the same amount of measured $HNO_3$ late in the run.

## June 3, 1977 Propylene + Formaldehyde/Propylene Run

The two runs on this day (Figure 62) were designed to investigate the effects of adding excess formaldehyde to a propylene-$NO_x$ system. It was suspected that if enough formaldehyde was added, the formaldehyde would substantially increase the OH concentration. Some of this extra OH would react with $NO_2$ and cause more $HNO_3$ to be produced. This in turn would show up as a net loss of $NO_x$ which would in theory reduce the $O_3$ potential of the smog system. Approximately 1.7 ppmC of propylene was added to both sides. The red chamber then received an additional 0.6 ppm of formaldehyde.

The morning was overcast but cleared quickly with only a few clouds for a short time near noon. At sunrise the temperature was about $16^oC$ ($60^oF$); the maximum was about $32^oC$ ($90^oF$) at 1500 EDT. A nitrogen balance is not presented here because neither PAN nor $HNO_3$ data is available. Saltzman $NO_2$ data were obtained.

It can be seen that extra radicals from the formaldehyde caused $NO_2$ maximum to be reached, and $O_3$ production to be initiated one hour sooner than in the propylene-only side. Also, the Saltzman data show that the $NO_2$ was removed very much faster than in the propylene-only side. Further, even though the formaldehyde side is faster (reaching $O_3$ maximum sooner than the propylene-only side), the $O_3$ maximum concentration is actually less than the side with propylene only, because the formaldehyde-propylene side ran out of $NO_2$.

## July 15, 1977 Propylene + Acetaldehyde/Propylene Run

This run consisted of equal concentrations of propylene and $NO_x$ in each side with acetaldehyde added to one side. The experiment was designed to observe the effects of the extra acyl radicals from acetaldehyde on the ratio of PAN to $HNO_3$ formed. It was generally a clear, hot day with no clouds appearing until approximately 1330 EDT, after $O_3$ concentrations were already high.

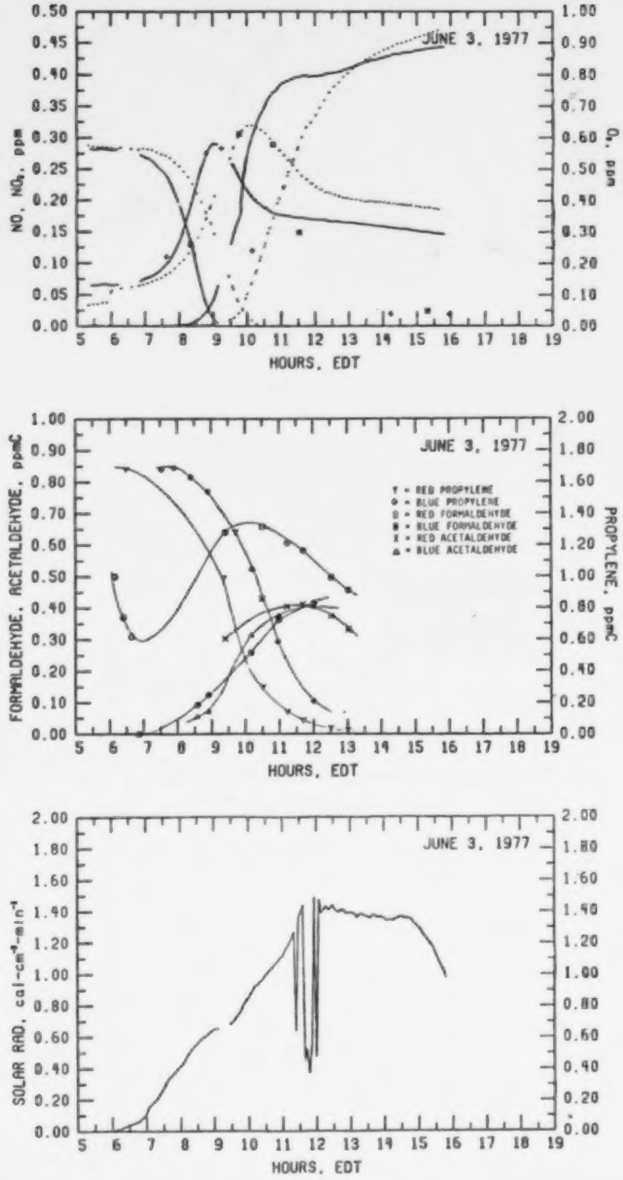

Figure 62. Smog chamber data for June 3, 1977 matched propylene-NO$_x$ run in which one side had an additional injection of 0.6 ppm formaldehyde.

The $HNO_3$ analyzer was used on the side with acetaldehyde. PAN and Saltzman $NO_2$ were measured on both sides. It can be seen in Figure 63 that the addition of acetaldehyde to this propylene/$NO_x$ system increases the effective conversion rate of NO to $NO_2$ and remarkably increases the amount of $O_3$ produced (more than the instrument range). Also, the distribution of the nitrogen end-products in Figure 61 shows a large percentage in the form of PAN (ratio 3.2/1 PAN/$HNO_3$).

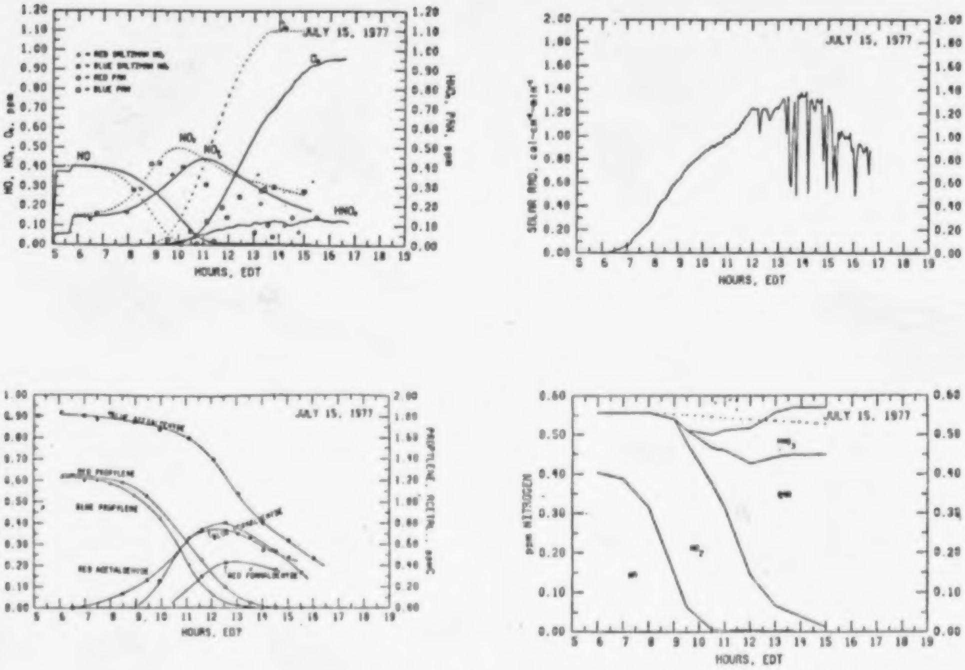

Figure 63. Effect of extra acetaldehyde on a propylene/$NO_x$ chamber run.

# SECTION 9

# DESCRIPTION OF MEASUREMENT TECHNIQUES IMPLEMENTED DURING THIS PROJECT

## AUTOMATIC $C_1$-$C_{10}$ CHROMATOGRAPH

It has been previously documented that the reference method for the measurement of ambient nonmethane hydrocarbons does have certain operating difficulties and is limited in its use as a research tool. For these reasons an automatic gas chromatograph was developed to perform routine analysis of selected $C_1$-$C_8$ hydrocarbons. The design criteria were the following:

1. perform automatic injection, separation, and analysis of $C_1$-$C_8$ compounds in less than 30 minutes
2. require no preconcentration of the air sample and operate isothermally
3. have a sensitivity of 10 ppbC for each species on the chromatograph

The instrument was built using a Carle Model 211 Chromatograph and flame ionization detector (FID). An automatic six-port sample valve and two six-port automatic switching valves shunt the sample to the appropriate column. These valves are activated by a 30 minute programmable valve controller. Three chromatographic columns perform the analytical separation. An additional 2' x 1/8" column of carbowax 400 was installed just before the flame detector to give column bleed balance and prevent excess baseline displacement after valve switches.

The columns are:

| | | |
|---|---|---|
| Column No. 1 | 6' x 1/8" Carbowax 1540 + 5 % Apeizon L on Supelcoport 80/100 mesh support | separates $C_6$-$C_8$ paraffins, olefins and aromatics |
| Column No. 2 | 6' x 1/8" N-octane/Poracil C 100/120 mesh (baked at $240^{\circ}$C for 2 hrs.) + 2' x 1/8" 20% Apeizon L on Supelcoport 80/100 mesh | separates $C_4$ & $C_5$ olefins and some $C_6$ paraffins |
| Column No. 3 | 2' x 1/8" FL alumina treated with 5% NaCl | separates $C_1$-$C_3$ |

The column configurations for each valve position are shown in Figure 64. The indicated restrictors are adjustable S.S. 1/16" Nupro needle valves and are used to match the pressure drop across various columns as these columns are switched in and out of the flow circuit. Automatic injection is made with all three columns in series. One and one half minutes are required for the individual compounds to become distributed into the proper columns. Since column 1 is the first to be encountered, $C_6$-$C_8$ are retained, while $C_1$-$C_5$ pass on to column 2. Methane is the only compound which actually moves to column 3 during this time. After this first 1.5 minutes with the columns in series, a valve switch removes column 2 and 3 from the flow path and permits the compounds in column 1 to elute into the FID. The system remains in this configuration for 5.5 minutes so that $C_6$-$C_{10}$ paraffins and toluene can be measured. We can also extend this time to 14 minutes to pick up $\alpha$-pinene or xylenes. A second valve switch then briefly (1 minute) places columns 1, 2, and 3 back in series so that methane and ethylene can be detected. During this period, propane and propylene move from column 2 to column 3 but do not elute before the third valve switch. This switch removes column 3 and leaves columns 1 and 2 in series with the detector. Butenes, pentanes and pentenes then elute from column 2. Finally with only 2.5 minutes remaining in the 15 minute cycle, the columns are placed back in series so that propane, propylene and acetylene can be measured. Chromatograms of the UNC mix are shown in Figure 65.

The system described has been in continuous operation at the University of North Carolina Smog Chamber Facility for more than 5 years. The operating sensitivity can be as low as 7 to 15 ppbC (at a signal to

INJECT

Col 1,2,3,
in Series

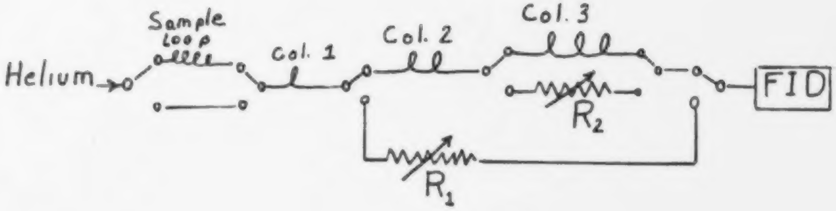
Sample loop
Col. 1
Col. 2
Col. 3
Helium
FID
R2
R1

First Valve Switch
Col. 1 in Series
with FID

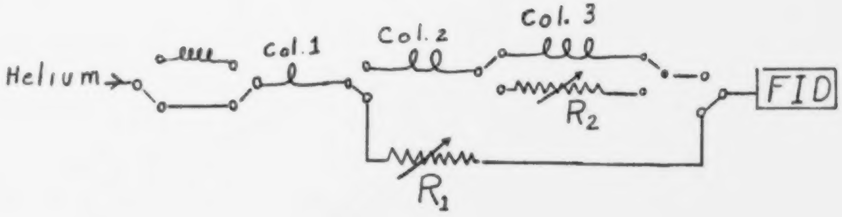
Col. 1
Col. 2
Col. 3
Helium
FID
R2
R1

Third Valve Switch
Col. 1 & 2 in Series

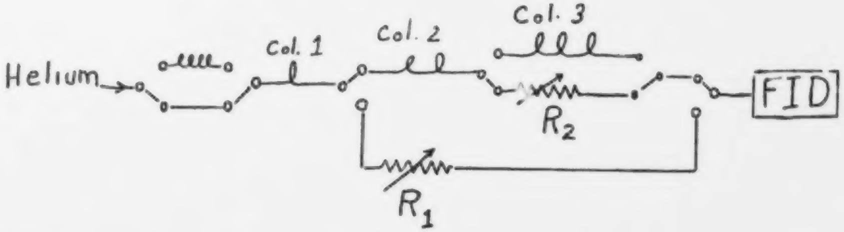
Col. 1
Col. 2
Col. 3
Helium
FID
R2
R1

Figure 64. Column and Valve Configurations for $C_1$-$C_{10}$ Automatic Carle Chromatograph.

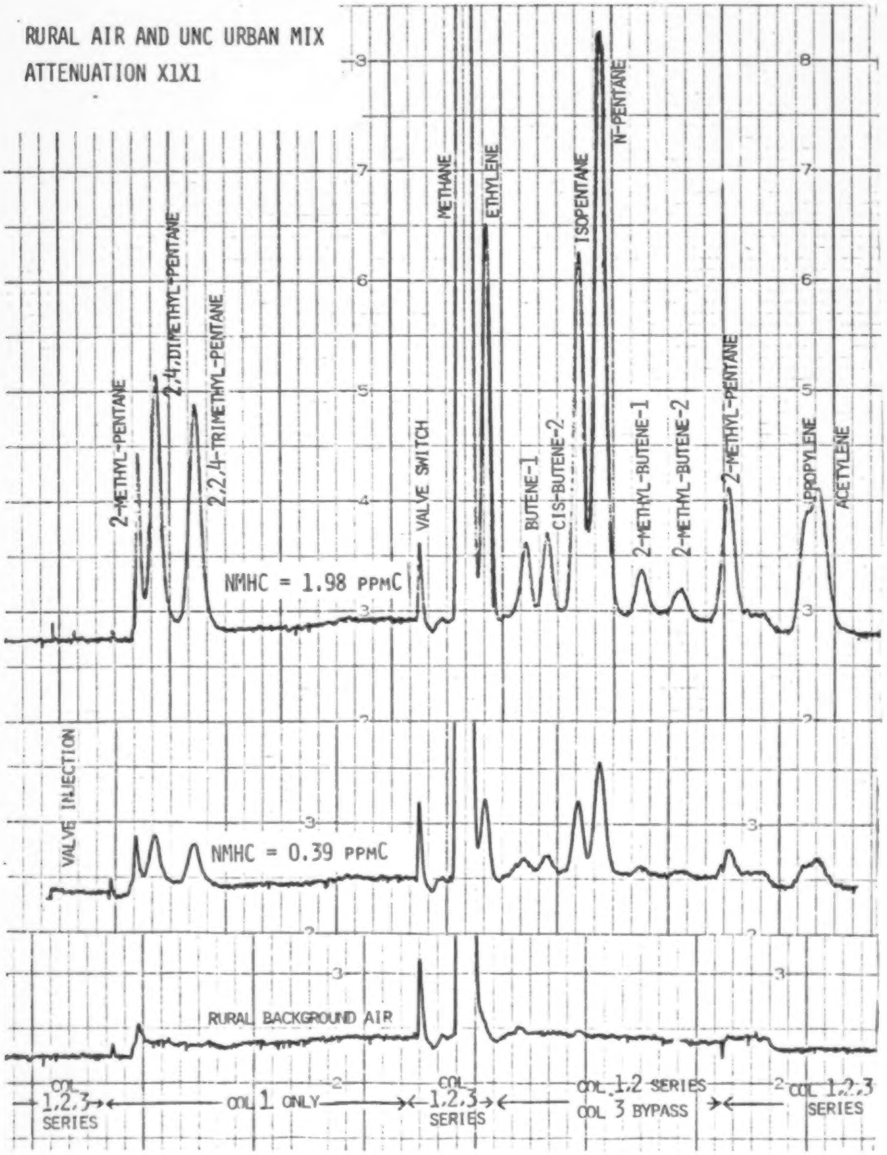

Figure 65. Chromatogram of UNC urban type hydrocarbon mixture on Carle 211 chromatograph.

noise ratio of 2) on the most sensitive scale. This is based on the known distribution of hydrocarbon species in the UNC atmospheric urban mix and individual calibrations of typical compounds (Figure 66). To obtain this sensitivity, a 5 cc gas sample loop was substituted for the original 2 cc loop. In doing this, however, the separation of acetylene from propylene and ethylene from ethane was reduced. Routine calibration of the instrument is usually performed the day before and during the day of the smog chamber run. We have estimated that the accuracy of this method for most hydrocarbons is between 5 and 10%.

The versatility of the system permits us to automatically run sytems with, for example, propylene and butane on one day, mix vs. ethylene and toluene on the second and isoprene and -pinene on the third without any changes in the instrument operating conditions. Critical operating conditions are given below:

Carle Model 211 Analytical GC
Detector - FID sensitivity 0.016 coulombs/gram carbon
detectability minimum $2.5 \times 10^{-12}$ g/sec
Electrometer sensitivity - $1 \times 10^{-12}$ amps
Sample valve - 6 port, 5 groove, mini volume Carle valve
Series-bypass valves - 6 port, 2 groove, mini volume Carle valve
Carle Model 100 valve minder
Valve actuators - automatic bidirectional Carle valve actuator motors
He flow = 33 cc/min
$H_2$ flow = 40 cc/min
Air flow = 350 cc/min
Oven = $64^{o}$C thermal

## AUTOMATED FORMALDEHYDE-ACETALDEHYDE CHROMATOGRAPH

In 1976 an automated gas chromatographic system to measure formaldehyde and acetaldehyde was built by Carle Instruments for UNC. This instrument automatically injected a 2 cc air sample onto an 11', 1/8" S.S. Porapak Q precolumn (isothermal oven at $73^{o}$F). Light hydrocarbons pass directly through to the flame detector, while formaldehyde, propylene, methanol and acetaldehyde are retained. As soon as the light hydrocarbons are passed, the precolumn is placed in series with a 2', 1/8"

CONCENTRATIONS OF INDIVIDUAL SPECIES IN
0.39 PPMC NMHC UNC MIX

| | COMPOUND | CONCENTRATION (PPMC) |
|---|---|---|
| 1 | 2-METHYLPENTENE | 0.035 |
| 2 | 2,4-DIMETHYLPENTENE | 0.039 |
| 3 | 2,2,4-TRIMETHYLPENTANE | 0.040 |
| 4 | ETHYLENE | 0.042 |
| 5 | BUTENE-1 | 0.010 |
| 6 | BUTENE-2 | 0.013 |
| 7 | ISOPENTANE | 0.053 |
| 8 | N-PENTANE | 0.092 |
| 9 | 2-METHYLBUTENE-1 | 0.008 |
| 10 | 2-METHYLBUTENE-2 | 0.007 |
| 11 | PROPYLENE/ACETYLENE | 0.047 |

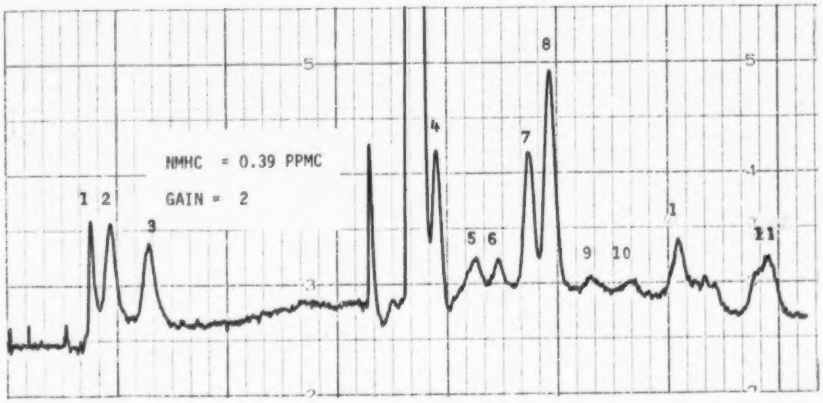

Figure 66. Maximum sensitivity of Carle chromatograph on attenuation of X1 and gain of 2.

S.S. Porapak Q analytical column. The contents of the second Porapak column flow directly into a $400^{o}F$ Ni catalyst methanizer before they reach the detector. In the methanizer, formaldehyde is converted to methane and measured as methane in the flame detector. Thirty minutes are required for an analysis. We have encountered some background interference in the region of the chromatogram where formaldehyde is eluted and currently this defines the lower limit of detectability for the formaldehyde.

Column Modifications

Various means were used to reduce the water ghost peak interference on Porapak Q. This peak most probably results from a displacement of impurities in the Porapak Q by water in the air sample. We observed a strong reduction in the interference when dry formaldehyde air samples were used. As vapor phase water was added back in, the interference would grow. After long periods of purging at high temperatures we were able to maintain a column which did exhibit reasonable separation between the ghost and formaldehyde peaks (Figure 67). The instrument was operated in this fashion from May-December 1977 with almost no maintenance. Impurities in a helium carrier tank installed in January 1978 resulted in deterioration of the analytical 11' x 1/8" S.S. Porapak Q precolumn. Attempts to use glass or Ni alloy columns with Porapak QS have met with marginal success; the instrument was used during 1978 with a significant loss in sensitivity.

In 1979 an inert solid support (Teflon 6) with a partition liquid phase (5% Carbowax 20 M plus 5% Triton 305) was used in a 12' x 1/8" glass column. This column would separate formaldehyde but we found significant memory problems with this system and have used it primarily to measure $C_2$-$C_5$ carbonyls.

FORMALDEHYDE DETECTION BY AUTOMATED COLORIMETRY

In June of 1979 UNC purchased an automated colorimetric formaldehyde system from CEA Corporation (Westwood, NJ). This system employs the reverse West and Gaeke technique and hence requires a constant supply of wet chemicals. Highly purified pararosanaline is essential (we have

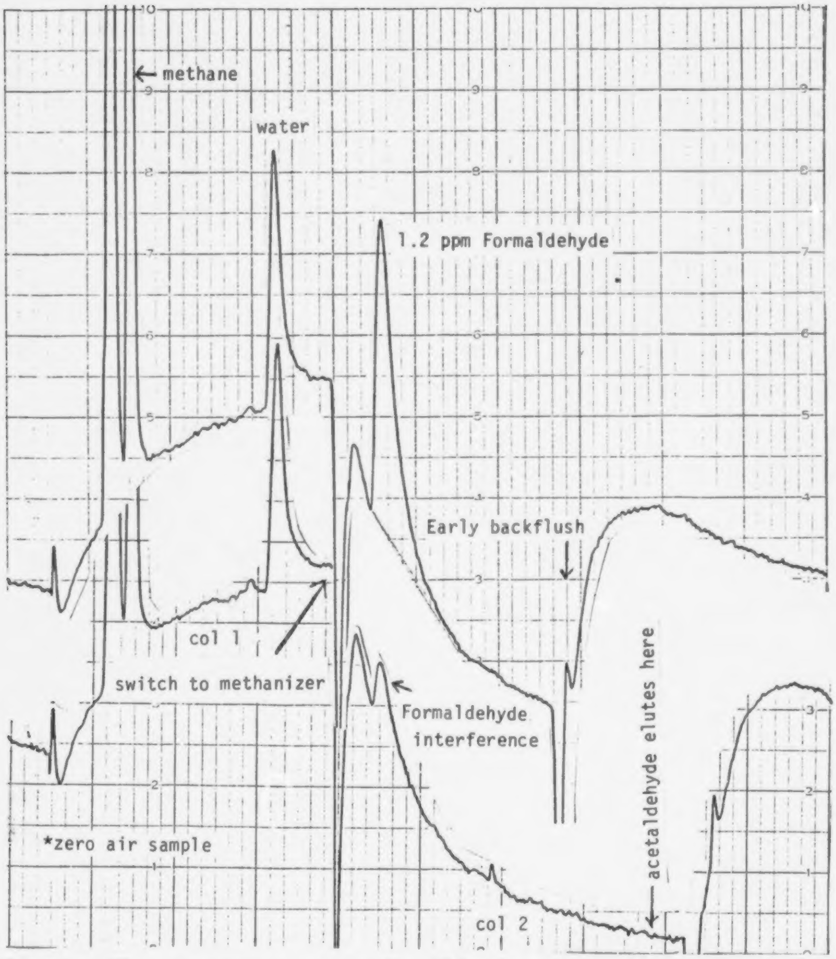

Figure 67. Response of Carle 211 GC with methanizer to 1.2 ppm formaldehyde and zero air with 1.5 ppm methane; oven=73$^{o}$C, He=67 cc/min, $H_2$=80 cc/min, recorder 1 mV fs, atten=X1, range =X1, col 1=11' x 1/8" S.S. PorapackQ, 40:60 mesh, col 2=2'x1/8" PorapackQ, 40:60 mesh.

purchased it directly from CEA). The other compounds, mercuric chloride, sodium chloride, and sodium sulfite, need to be reagent grade. A flow diagram of the system is shown in Figure 68.

Liquid standards can be prepared from 37% formalin solution and diluted in the same sodium tetra mecurate (TMC) used in the instrument. These are then added directly through the TMC feed tube. A dynamically generated HCHO airstream using a formaldehyde permeation tube (Metronics Corporation, Santa Clara, California) was used to supply known levels of gas phase formaldehyde. In addition, calibration samples of formaldehyde were prepared in the chamber. The chamber is usually dried to a dew point of 60% and known quantities of solid paraformaldehyde are then injected.

During the 3 month 1979 data season we found this system showed less than a 10% change in response to known formaldehyde samples. Using the original solutions recommended by CEA we observed a 5% positive interference from acetaldehyde in the concentration range of 0.1-1 ppmV. In 1979 experiments where acetaldehyde was generated, the HCHO data were adjusted to subtract out the positive acetaldehyde interference. In 1980 CEA recommended a 6-fold reduction in the concentration of TMC and sulfite. In addition, sulfite and TMC were to be introduced separately instead of premixing these two solutions. This increased the lifetime of the TMC from 1 day to 2 weeks. Newly mixed sulfite solution and dilute pararosanaline are still required every 24 hours. The less concentrated reagents did not cause a loss in sensitivity of this system and minimized the acetaldehyde interference to 1%. We did however notice a deterioration in precision from calibration to calibration. This was especially true after new tubes were added to the peristaltic pump. Finally, the system that we have been using can exhibit a 30-50% zero drift over a 3-4 hour period. This drift does not affect the span response but requires frequent zero samples. Later, an auto zero valve was installed at the intake of our heated sample manifold. Examples of the system's response to 1.2 and 0.5 ppmC formaldehyde air samples are shown in Figure 69.

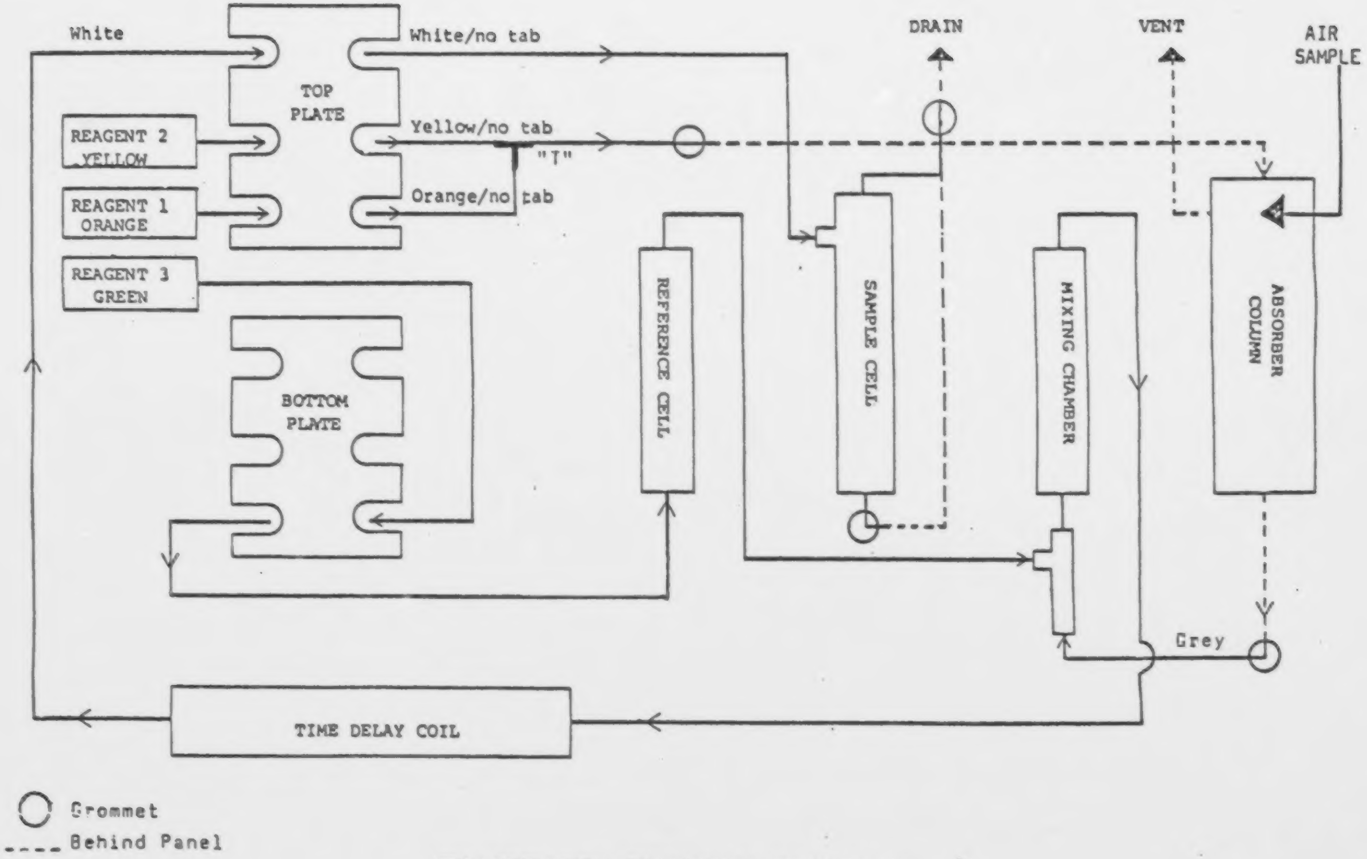
White
TOP PLATE
White/no tab
REAGENT 2 YELLOW
Yellow/no tab
"T"
REAGENT 1 ORANGE
Orange/no tab
REAGENT 3 GREEN
BOTTOM PLATE
DRAIN
VENT
AIR SAMPLE
REFERENCE CELL
SAMPLE CELL
MIXING CHAMBER
ABSORBER COLUMN
Grey
TIME DELAY COIL
Grommet
Behind Panel

FLOW SCHEMATIC - FORMALDEHYDE (HCHO) IN AIR

Figure 68. Solution flow diagram for CEA automated formaldehyde instrument.

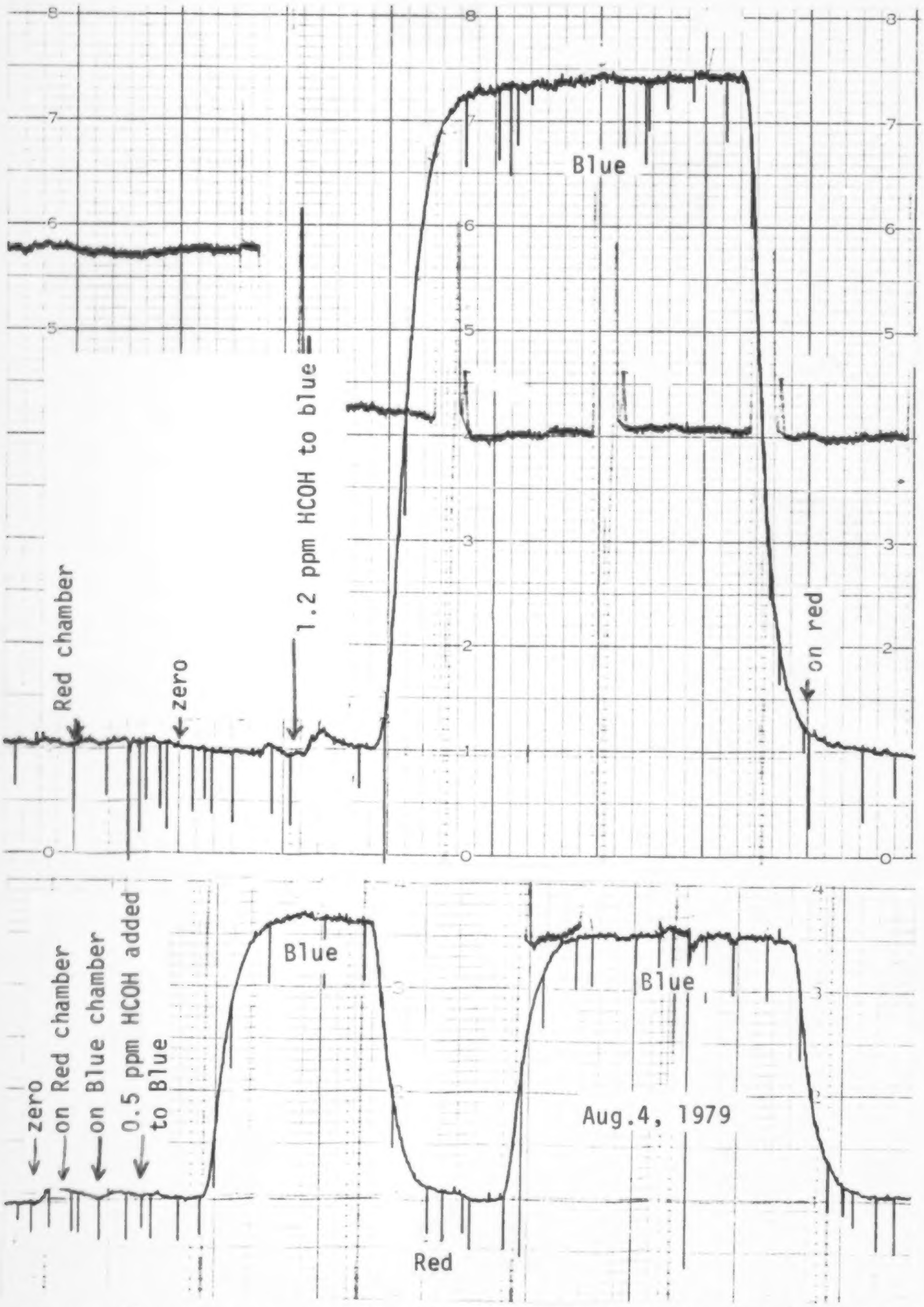

Figure 69. Response of CEA auto formaldehyde instrument to 0.5 and 1.2 ppm of HCOH injected in dry UNC chambers on August 4, 1979 and August 5, 1979.

## DINITROPHENYLHYDRAZONE PROCEDURE FOR CARBONYL ANALYSIS

The analysis of $C_1$-$C_8$ carbonyl species in ambient air by reaction with 2,4 dinitrophenylhydrazone (DNPH) and subsequent reverse phase high pressure liquid chromatography of the hydrazone derivatives has been reported by Kuwata et al.[3] This procedure is fairly specific and can also be used to measure dicarbonyls. The reaction of DNPH with acetaldehyde is shown below.

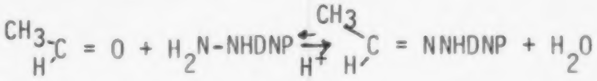

$$\begin{matrix}CH_3\\H\end{matrix}\!\!>C = O + H_2N\text{-}NHDNP \underset{H^+}{\rightleftarrows} \begin{matrix}CH_3\\H\end{matrix}\!\!>C = NNHDNP + H_2O$$

Ambient aldehydes are usually sampled with an impinger arrangement into an absorbing reagent which contains acidified DNPH. Two extractions of the absorbing sample with chloroform, a wash with 2N HCl, and then distilled water, and finally sample concentration to a solid is required. Hull[4] recently proposed a modified bubbler absorbing reagent so that direct HPLC analysis on the absorbing liquid is possible. The absorbing reagent is prepared by dissolving 0.25 g of purified DNPH in one liter of HPLC grade acetonitrile (ACN). This is followed by the addition of 0.2 ml of $H_2SO_4$. Two ml of absorbing reagent in a Mae West type bubbler and a sample flow rate of 0.5 l/min are recommended. In addition the impinger base is placed in ice to reduce ACN evaporation. Hull[4,5] has indicated that excessive water in the air sample can reverse the equilibrium for ketones in the above noted hydrazine reaction and that condensed water in the asorbing reagent from ambient moisture should be limited to 50 $\mu$l/ml. Aldehydes are not affected by water. Outdoor chamber humidities can easily range between 20,000 and 30,000 ppm. This has limited us to a 2-4 liter air sample.

Analysis was performed on a Varian 5010 HPLC with a Varian micropak MCH-10 reverse phase, 30 cm, 9mm column and a fixed 254 nm detector. Initially the system was isocratically run at a 60:40 ACN:$H_2O$ mixture and a solution flow of 1.6 ml/min. High concentration liquid standards in the gas phase equivalent range of 2-6 ppmV were prepared by direct dilution of 5 $\mu$l of authentic knowns into 100 ml of acetonitrile. Five to twenty $\mu$l of this solution were then added to 2 ml of DNPH absorbing reagent. The final DNPH samples were heated in 2 ml Supelco reaction vials at 80$^{o}$C for 45 minutes. Comparisons with gas phase calibration samples are currently being made.

A sample chromatogram of a mixture of aldehydes, ketones and dicarbonyls is shown in Figure 70. It has been observed that retention times on our system can vary significantly from day to day. It is therefore essential to run frequent calibration mixtures. Preliminary tests in our laboratory show that 45 minutes of heating is required to complete the derivation process for compounds that elute as late as biacetyl. Heating beyond this time did not increase chromatographic responses. $C_1$-$C_3$ carbonyls seem to require only 15 minutes. Liquid calibration samples which have been heated initially for 3 hours and then stored at room temperature appear to be stable with little deterioration for periods up to 1 month. Similar samples which are heated every three days were not as stable over the same time period.

Ambient bubbler samples should be stored at 50$^{o}$F or less until they are analyzed. The chromatograms from chamber samples which were stored at room temperature for 2 months exhibited many spurious peaks; quantification of compounds of interest was not possible. It is important that bubbler samples be analyzed as soon as possible.

Hull[4] has suggested that a 360 nm detector be used to eliminate possible interferences of benzene and toluene in the $C_1$-$C_3$ aldehyde region. Although the absorption of benzene and toluene is 1/25 of the hydrazones at 254 nm, it is felt that further quantification of this potential interference is necessary.

In our system we have noticed an increased interference from the 2,4 dinitrophenylhydrazone peak into the formaldehyde-hydrazone elution region. We are not sure if this is due to a deterioration in the DNPH solution or the HPLC analytical column. When formaldehyde is of specific interest we have shifted to an isocratic 55:45 mixture of ACN:$H_2O$ to provide better separation of the formaldehyde and DNPH isomers.

## PAN ANALYSIS

PAN measurements reported during 1977-78 were made on a 1/8" x 36" glass column packed with 10% Carbowax 600 on Gas Chrom G (60-80 mesh) and detected with a Varian 940 electron capture detector.[50] Both the column

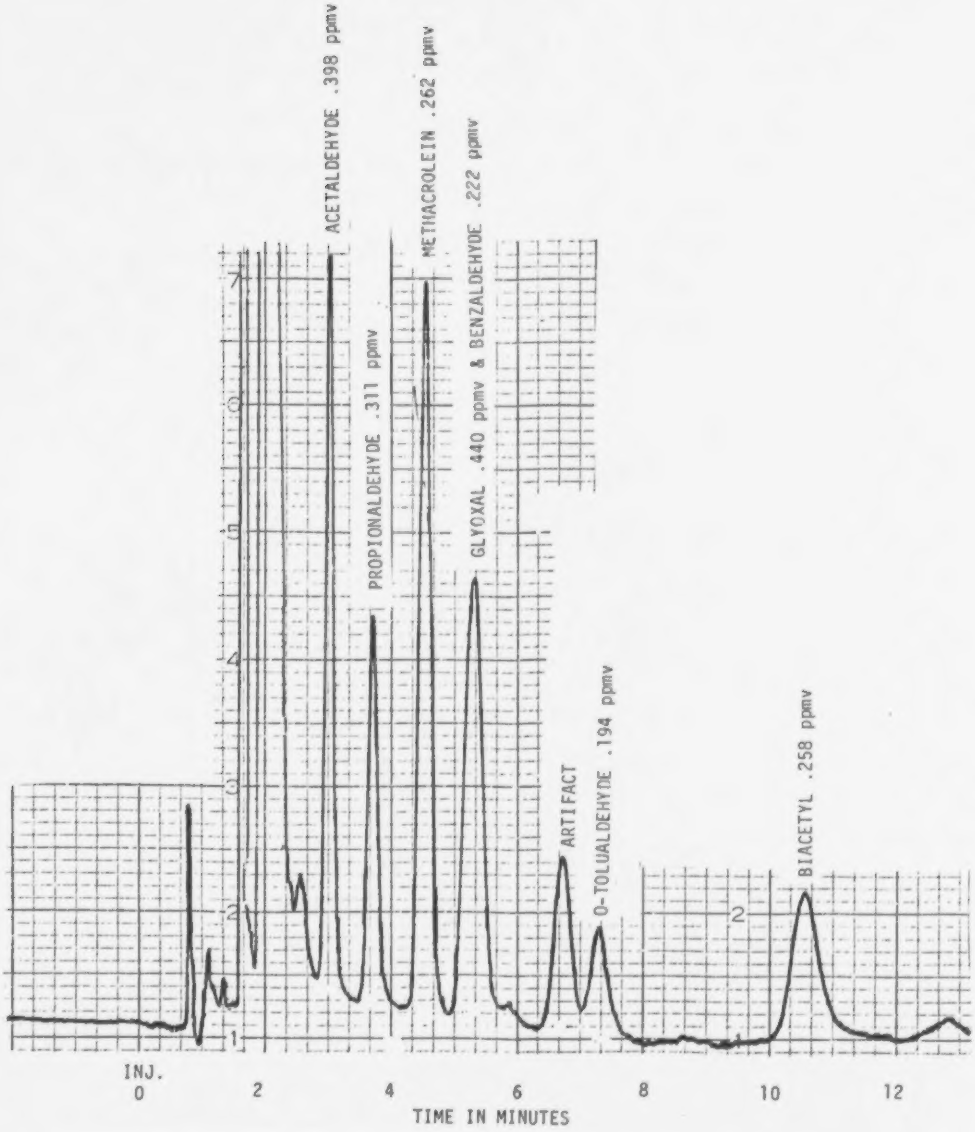

Figure 70. An example of the response of the HPLC with DNPH method.

and the detector were held at room temperature, and 5% methane-argon was used as the carrier gas. The system was originally set up for UNC by EPA project officer Mr. Bruce Gay, Jr. Shortly after location at the UNC research facility a 6-port auto sample valve was installed so that unattended sample injection could be performed. With a standing current of $20\times 10^{-9}$ amps we found good response linearly between 0.01 ppmV and 0.5 ppmV of PAN. Above 0.5 ppmV the signal became slightly nonlinear with concentration. In 1978 a pulse frequency electron capture detector was purchased from Analog Technology Corporation. This detector seemed to give a linear response over the range of 0.01 to 12 ppmV of PAN. The response of both of these systems to 0.12 ppmV of PAN is shown in Figure 71.

## PAN CALIBRATION

From June 1977 to August 1978, high concentration PAN samples (2-17 ppm) in Teflon bags were generated and standardized at ETP-RTP in a 15$\mu$m pathlength IR spectrometer and then transported 25 miles in unairconditioned vehicles to the UNC smog chamber facility. These bags were then immediately diluted (0.1-0.5 ppm) and PAN response factors were established based on the original calibration and associated dilution. Generally there was a difference between the calibration values developed from the 1977 and 1978 PAN calibration bags. Decomposition during transportation, dilution problems, initial calibration by IR, and ambient column temperature fluctuations were among the possible causes for these differences.

From late November 1977 to July 1978, electron capture PAN data were usually 40-50% higher than the afternoon chemiluminescence $NO_2$ concentrations in propylene-$NO_x$ smog systems that completely consumed $NO_2$. August to mid-October 1978 electron capture PAN concentrations from similar type propylene-$NO_2$ systems were only 65-70% of the afternoon chemiluminescence $NO_2$. In these types of smog systems it has been clearly demonstrated that very low concentrations of NO and $NO_2$ are present in the afternoon; also the UNC $NO_x$ meter has been tested for response to nitric acid and has exhibited none. Hence the rather large

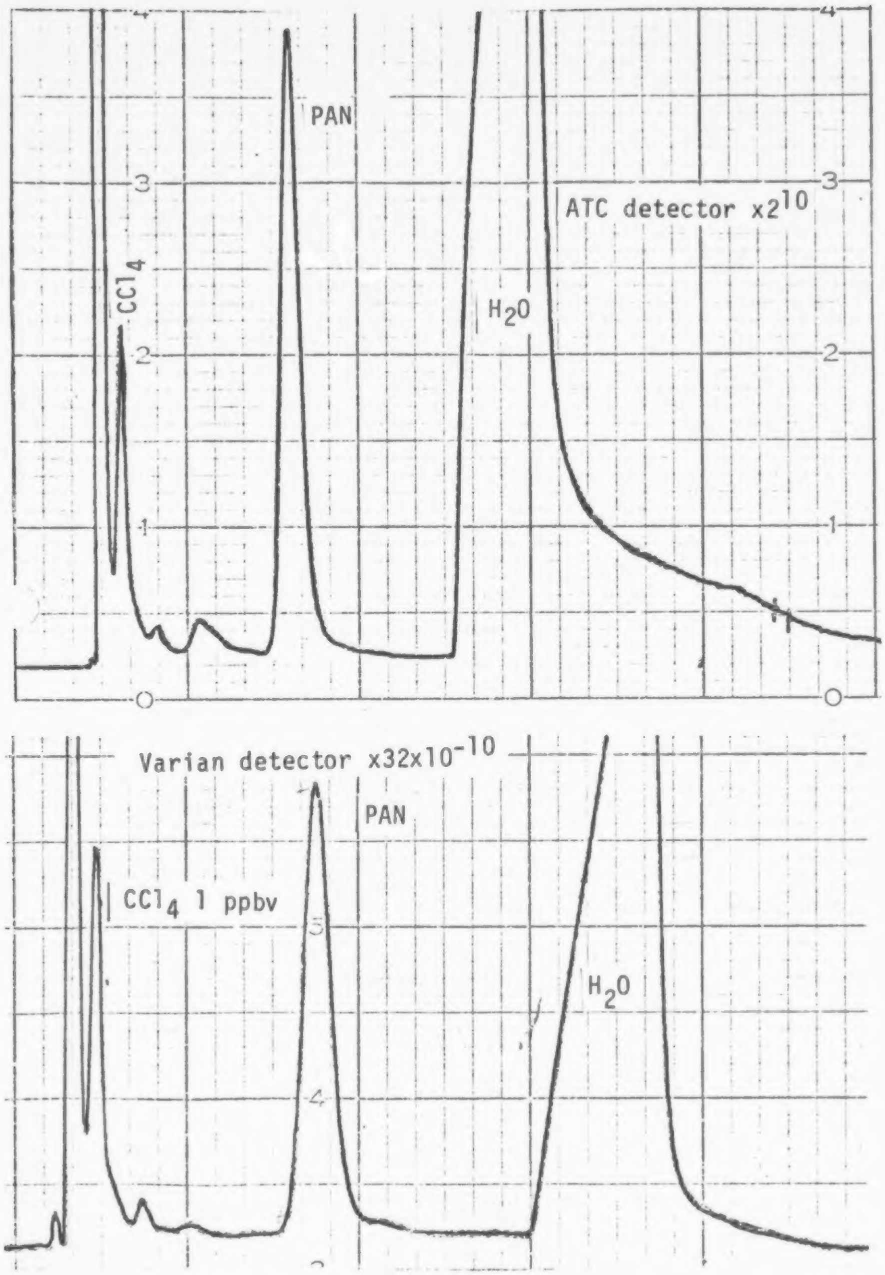

Figure 71. Response of two UNC electron capture detectors to 0.12 ppmv PAN May 1978.

afternoon chemiluminescence $NO_2$ readings from these smog systems are considered to be almost entirely a "chemiluminescent PAN response".

By mid-October 1978, UNC implemented a wet chemical modified Saltzman procedure developed by Stephens and Price[71]. The calibration values derived from this method gave PAN concentrations which were 0-30% lower than the "chemiluminescent PAN response". In 1979 high concentration pure PAN samples were prepared from an irradiated biacetyl-$NO_2$ bag system using a large preparation column and a liquid nitrogen freeze-out concentrator system. The diluted purified PAN was then measured with a calibrated EPA chemiluminescence $NO_x$ analyzer and a calibrated PAN analyzer similar to the one used at UNC. Both EPA units gave the same concentration response. This PAN bag was then immediately transported to UNC in an air conditioned car and measured on the calibrated UNC chemiluminescence $NO_x$ meter and UNC PAN monitor. The UNC $NO_x$ meter gave the same reading as the EPA $NO_x$ and PAN monitors. This strongly suggests that both the EPA and UNC $NO_x$ monitors have a 100% response to PAN. Since that time UNC has generated high concentrations of PAN and purified the PAN by the EPA method described above. The pure PAN samples were standardized with the UNC chemiluminescence $NO_x$ meter and this was used to calibrate the UNC PAN meter. Thus the 1979 UNC PAN concentrations have been directly linked or keyed to "chemiluminescence PAN readings". To make the 1977 and 1978 PAN data set consistent with the 1979 data set, 1977 and 1978 PAN values were compared with the many propylene-$NO_x$ smog systems which had gone to completion and had given a stable afternoon "chemiluminescent PAN" concentration.

Ideally, we have found the best way to generate calibration samples of PAN is by the above cryogenic procedure. If this is not possible we would recommend that 4 ppmC + 0.5 ppm of propylene and $NO_x$ (40% $NO_2$) be irradiated outdoors for 3-4 hours during the mid-morning and the early afternoon. With a calibrated chemiluminescent $NO_x$ meter, follow the NO and $NO_2$ concentration beyond the $NO_2$ peak until $NO_2$ stabilizes as shown in many of the smog chamber runs in Figures 18, 57 and 59a. This system should generate from 0.15 to 0.25 ppmV of PAN.

## ALKYLNITRATES

$C_1$-$C_5$ alkylnitrates can be detected on the same system that is used to measure PAN. Calibration samples (Figure 72) ethyl, isopropyl, propyl, and butylnitrates were performed by carefully injecting microliter volumes of the authentic samples into the outdoor chambers and applying the appropriate dilution and temperature factors. Calibration factors for compounds for which we did not have authentic samples (like sec-butylnitrate and isopentylnitrate) were estimated from the ECD response of n-butylnitrate. An uncertainty of ±40% was then assigned to these compounds.

## MODIFIED MAST OZONE METER FOR MONITORING $HNO_3$

A modified Mast model 724-2 ozone meter as described by Miller and Spicer (1975)[72] was used to continuously monitor gaseous nitric acid. The analyzer consists of a sample conditioning procedure and a microcoulomb cell utilizing a reagent adapted for sensing acids rather than oxidants.

The reagent contains KI and $KIO_3$ which reacts with acids:

$$HX + H_2O \rightarrow H_3O^+ + X^-$$

$$6\ H_3O^+ + IO_3^- + 5\ I^- \rightarrow 3\ I_2 + 9\ H_2O$$

At the cathode of the cell, a thin layer of $H_2$ (g) is produced by a polarization current: $2\ e^- + 2\ H^+ \rightarrow H_2$. When the voltage is first applied across the cell, the hydrogen layer builds to a maximum and the polarization current ceases. When $I_2$ is produced from the acid sampled, it reacts with the $H_2$: $H_2 + I_2 \rightarrow 2\ HI$. The removal of $H_2$ causes a repolarization current to reestablish equilibrium. Therefore, the current is directly proportional to the mass of acid sampled per unit time.

Figure 73 shows the general design of the sensor (microcoulomb) cell. The chemical solution for detecting acids is pumped at a constant rate into the cell. It then flows in a fine film down the electrode support E,

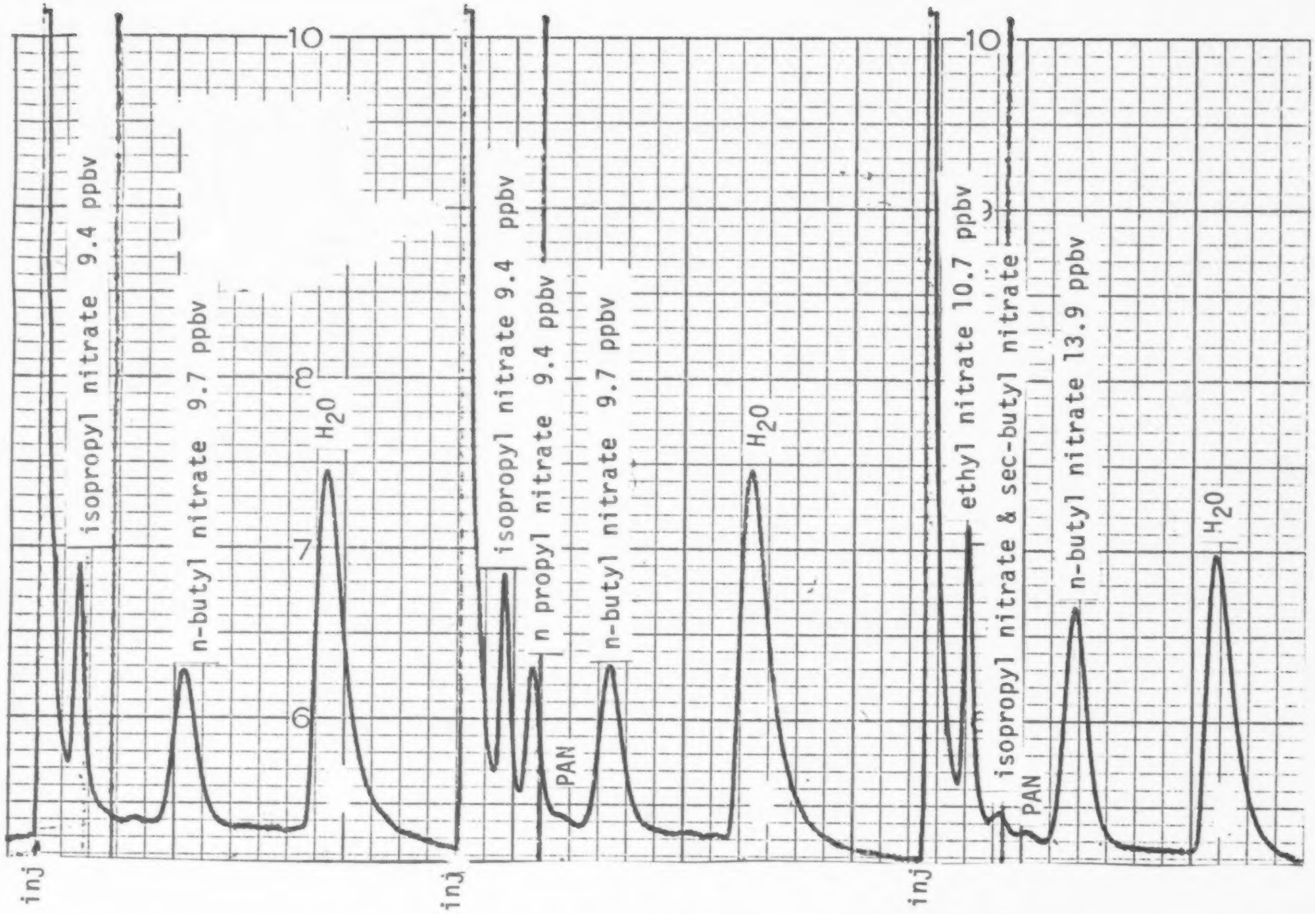

Figure 72. Detection of alkylnitrates with automated PAN GC, Varian 940 ECD. $N_2$ flow = 5 cc/min, oven and detector at 24.5$^{o}$C, standing current on $32x10^{-9}$ amps = 91% of full scale, chart = .1"/min, atten.= $x32x10^{-10}$ amps.

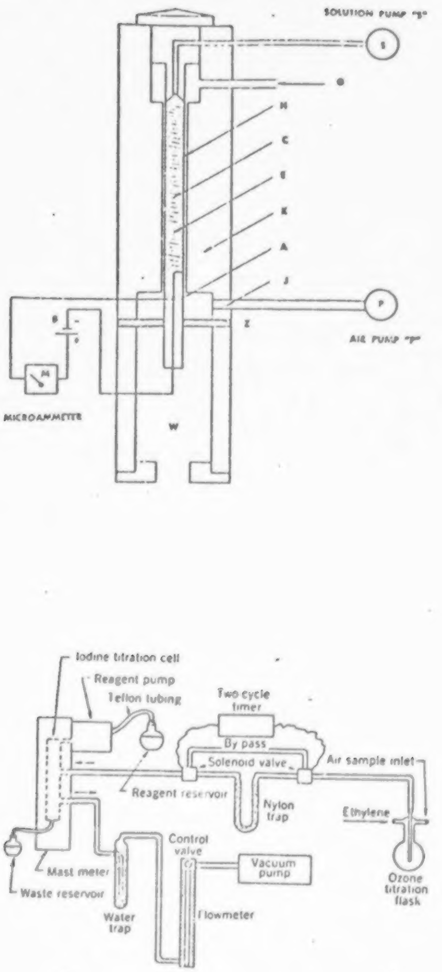
SOLUTION PUMP "S"
S
G
H
C
E
K
A
J
P
Z
AIR PUMP "P"
B
M
MICROAMMETER
W
Iodine titration cell
Reagent pump
Teflon tubing
Two cycle timer
By pass
Solenoid valve
Air sample inlet
Reagent reservoir
Nylon trap
Ethylene
Control valve
Vacuum pump
Mast meter
Waste reservoir
Water trap
Flowmeter
Ozone titration flask

FIGURE 73. Schematics of Mast electrochemical cell and configuration of entire microcoulombmetric instrument for measurement of gaseous $HNO_3$.

(which contains many turns of a cathode wire C, and a single turn of a wire anode A) and is allowed to flow into a waste reservoir W. An air sample is pulled into the cell and comes into contact with the solution film on the electrode support. A small potential is applied across the cell and the resultant current flow is converted to voltage by a current-to-voltage operational amplifier circuit. The method has a sensitivity to $HNO_3$ of about 5-10 ppb.

Note that this system will respond to $O_3$ and $NO_2$. Therefore, a sample pretreatment titration with ethylene is necessary to remove $O_3$. The sample is then alternately switched either through a nylon wool filter or around the nylon filter. The nylon wool filter selectively removes nitric acid without removing $NO_2$. The difference in the resultant voltage from the analyzer is proportional to the amount of gaseous nitric acid. A sample trace is shown in Figure 74.

Miller and Spicer (1975)[72] discussed several discouraging observations while calibrating the modified Mast nitric acid analyzer: 1) the acid will significantly absorb then desorb from new Teflon sampling tubing, 2) at low to moderate humidities nitric acid persists in the gas phase, but at somewhat higher humidities the acid seems to initially cluster as aerosols as indicated by a condensation nuclei counter, and 3) because of a "memory effect", at least five minutes are required for alternate cycles.

## CHEMILUMINESCENCE METHOD FOR NITRIC ACID MONITORING

Several research groups had reported various responses of commercial chemiluminescent $NO_x$ analyzers to $HNO_3$, ranging from 0% to 100% response. The reason for this wide range was due to the different types of catalyst used to reduce $NO_2$ to NO. Joseph and Spicer (1978)[73] reported on a method to measure nitric acid utilizing chemiluminescence and a molybdenum catalyst system. They used the same nylon wool filtering arrangement that was used on the modified Mast analyzer. It was found that the method responded 100% to $HNO_3$ and compared well with the Mast system which had previously been successfully compared with a Fourier transform spectroscopy-infrared system.

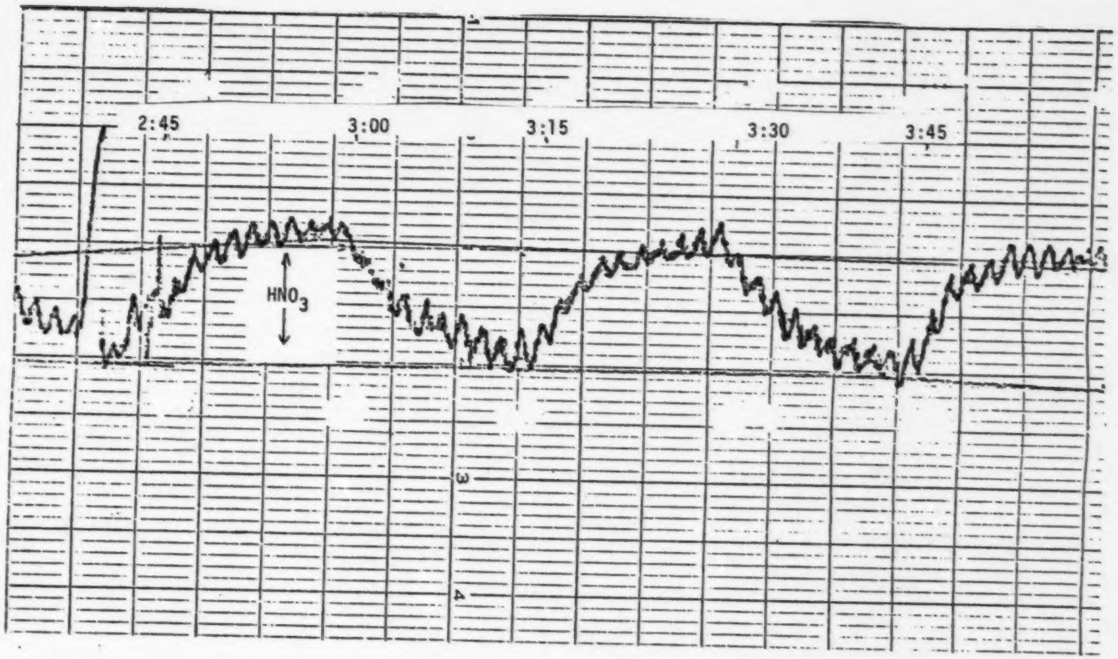

Figure 74. Example of signal trace from modified Mast microcoulombmetric method for gaseous $HNO_3$ monitoring.

A molybdenum catalyst converter was purchased in 1978 by UNC and connected in series with the sample line leading directly to the photomultiplier tube of a Bendix chemiluminescent $NO_x$ monitor. A switching nylon wool filter arrangement was used similar to that used in the Mast nitric analyzer. To minimize possible sample line losses, the molybdenum catalyst was placed directly under the chamber with the nylon filter system on the inlet. Less than 24 inches of sample line was exposed to $HNO_3$. The sample air in the line from the catalyst to the NO converter (~30 feet) contained only NO. This system produced a trace similar to the Mast system: the output alternating between total nitrogen and total nitrogen minus $HNO_3$. A sample trace is shown in Figure 75.

## CALIBRATION OF NITRIC ACID ANALYZERS

Calibration was at first attempted (1977) by carefully measuring the response of the analyzer to $NO_2$ and $O_3$ (no ethylene used). Response factors of 2, 20 and 10 microamperes per ppm for $NO_2$, $O_3$ and $HNO_3$ were reported by Miller and Spicer[72]. $HNO_3$ was therefore "calibrated" by observing the response of the analyzer to $NO_2$ and $O_3$, and then scaling with the relative $HNO_3$ response factor reported by Miller and Spicer. This, of course, was not a direct calibration technique, and it was necessary to assume that the reported response factors were accurate. Spicer and Miller (1976)[74] suggested that the analyzer be calibrated with static test concentrations in Teflon bags. These were generated from purified nitric acid which was prepared under a high vacuum. During the initial check-out of the UNC Mast system, the instrument was allowed to sample from a Teflon bag in which enough concentrated $HNO_3$ was injected to obtain a 0.2 ppm concentration. No nitric acid was measured. The bag was heated and still no nitric acid was observed. Finally enough nitric acid was injected to produce a 20 ppm concentration. The analyzer did respond, taking almost 60 minutes to reach a maximum response of 0.8 ppm. When taken off the bag and allowed to sample room air, about fifteen minutes were needed for the response to drop to zero. It was concluded that a static bag calibration source was unsatisfactory because nitric acid has a tendency to absorb and desorb from "clean" Teflon. Previously, Gantner[75] had used HCl gas to calibrate the Mast $HNO_3$ system. Known

TYPING GUIDE SHEET
BEGIN FIRST LINE OF TEXT HERE
CENTER OF PAGE
TOP OF IMAGE AREA
DROPPED HEAD; BEGIN SECTIONS HERE
BEGIN LAST LINE OF TEXT
BOTTOM OF IMAGE AREA; OUTSIDE DIMENSION FOR TABLES AND ILLUSTRATIONS
3/8"
PAGE NUMBER
EPA-287 (Cin.)
(4-76)

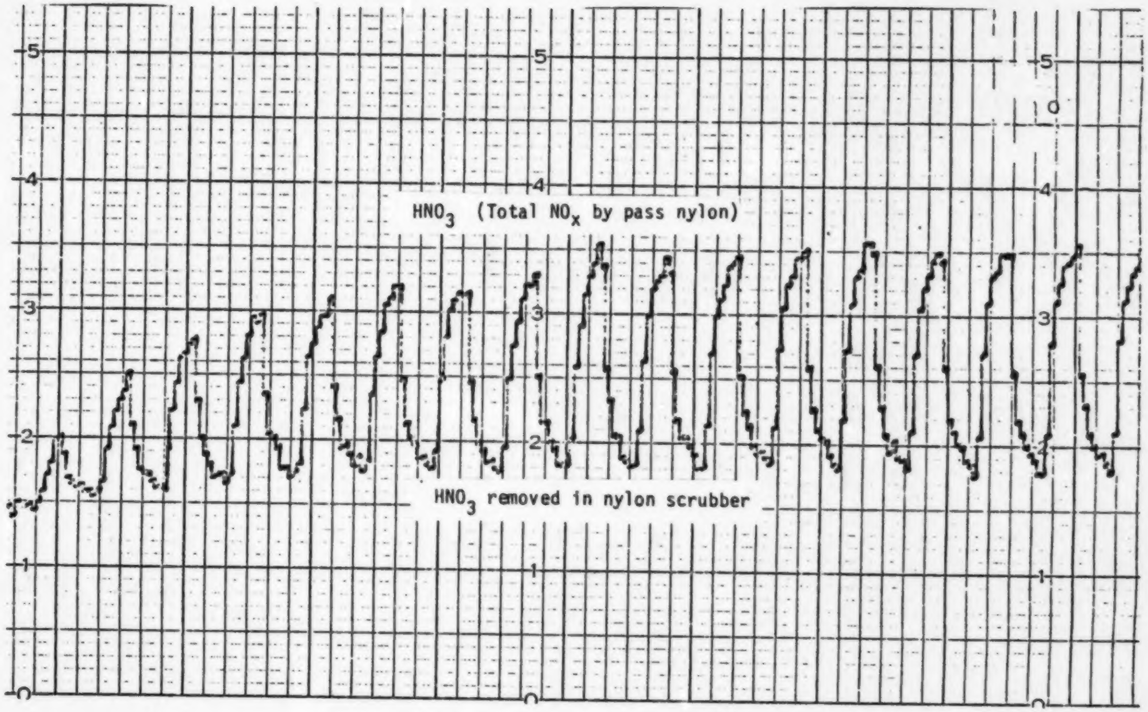

Figure 75. Example of signal trace from molybdenum catalyst chemiluminescence method for gaseous $HNO_3$ monitoring.

TYPING GUIDE SHEET
BEGIN FIRST LINE OF TEXT HERE
CENTER OF PAGE
TOP OF IMAGE AREA
DROPPED HEAD, BEGIN SECTIONS HERE

concentrations of HCl were also difficult to maintain in a bag system, presumably because of similar wall problems.

It was concluded that a continuous source of $HNO_3$ would be necessary to minimize these effects by allowing equilibrium of the surfaces involved thereby insuring an accurate response and calibration to $HNO_3$. A generator was assembled using a diffusion method, described by Nelson (1977).[76] The design is relatively simple (Figure 76). It employs a Teflon sealed flask containing concentrated $HNO_3$ and a capillary tube. The exposed end of the capillary tube conducts vapor phase nitric acid between the generator flask and a mixing chamber. Experimentation led to a capillary size, temperature and flow producing an acceptable range of $HNO_3$ concentrations. A 6 cm x 0.5 mm capillary diffused at a rate (30-40$^{\circ}$C) such that a one to four liter per minute flow rate would yield 0.35 to 0.45 ppm of nitric acid. The generator was insulated and temperature controlled.

The generator was calibrated by utilizing the Spicer bubbler technique (1977)[77] for nitric acid. This method utilizes the chromotropic acid reagent for analysis of nitrates developed by West (1966).[78] A fritted bubbler was filled with 10 ml of 0.03 M NaOH and used to collect a portion of the output of the generator, while the Mast or chemiluminescence system monitored the generator simultaneously. The Mast system would agree well as long as it was "acting" properly. The calibration curve used for the bubbler analysis is shown in Figure 77. To insure that either nitric acid analyzer was working properly, the generator was kept near the analyzer, even when the instrument was under the chamber.

## ANALYSIS AND CALIBRATION OF $H_2O_2$

In 1977 gas phase hydrogen peroxide data were taken at UNC by colorimetric analysis using titanium tetrachloride solution[79] and applying Lambert-Beers law to concentrations obtained from standards. The lowest concentration that can be measured accurately with this technique is 10 ppb hydrogen peroxide. More recently Kok et al.[80] (1978) have developed a chemiluminescent method for the determination of hydrogen peroxide with a reported sensitivity to concentrations as low as 0.5 ppb. Since ambient hydrogen peroxide concentrations and the

BEGIN LAST LINE OF TEXT
BOTTOM OF IMAGE AREA OUTSIDE DIMENSION FOR TABLES AND ILLUSTRATIONS
3/8"

PAGE NUMBER
EPA-287 (Cin.)
(4-76)

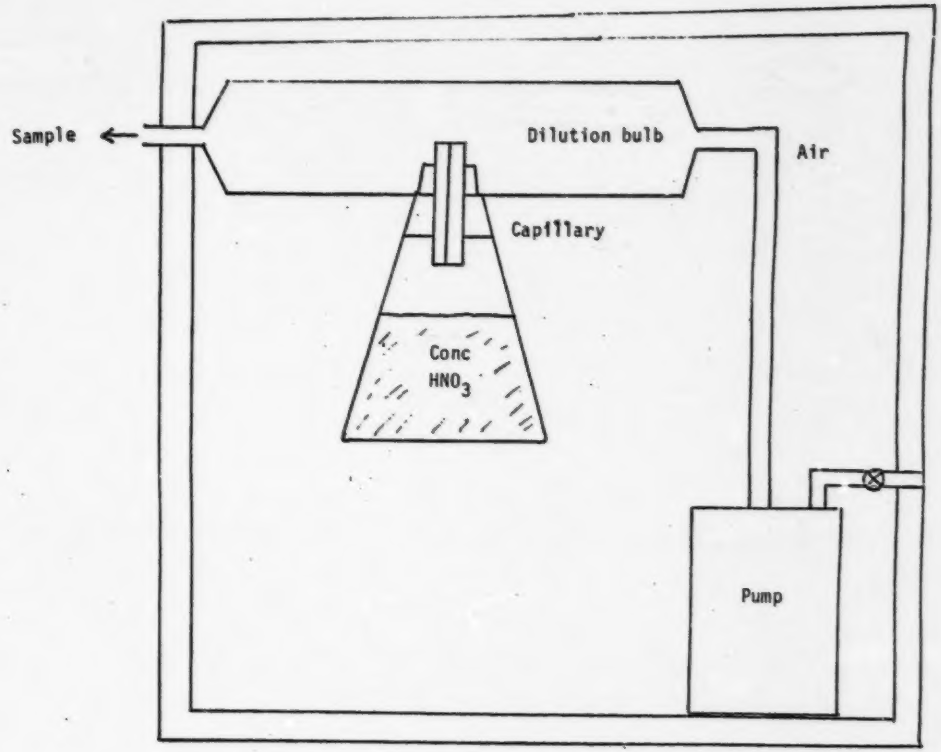
Sample
Dilution bulb
Air
Capillary
Conc
$HNO_3$
Pump

Figure 76. Schematic of gaseous $HNO_3$ generator.

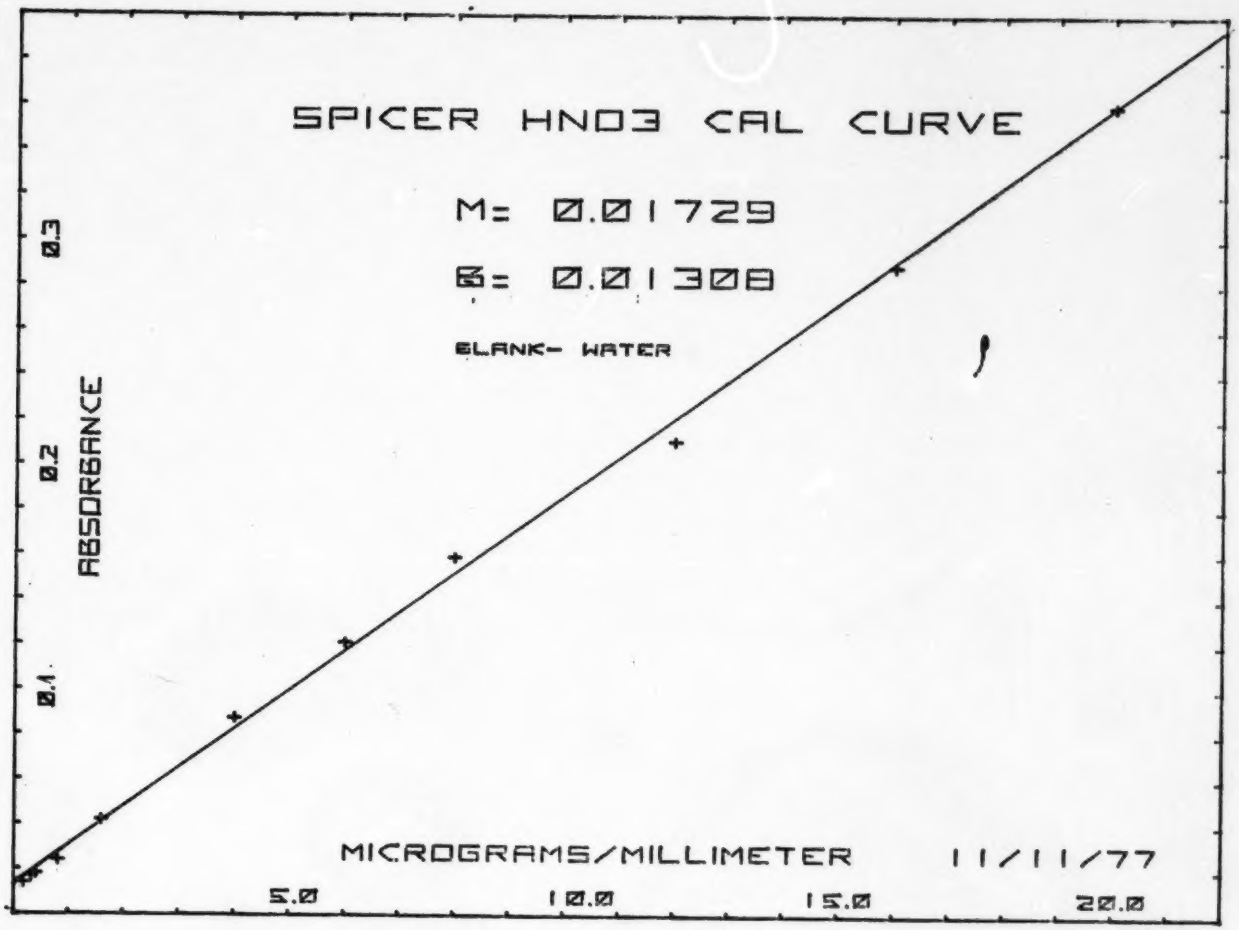

Figure 77. Calibration curve for Spicer method of $HNO_3$ analysis.

concentrations developed from photochemical smog in ambient atmospheres are found to be less than 25 ppb, this technique provides an extremely useful method for quantifying hydrogen peroxide production in our experiments.

Implementation of this technique was done in close collaboration with Messrs. Bruce Gay, Jr. and George Namie at the EPA Environmental Research Lab at EPA. Samples were collected by bubbling air through a midget impinger (in an ice bath) for approximately 10 minutes at about 2 liters per minute. This sample solution is mixed with alkaline (12.8 pH) luminol solution and copper (II) nitrate-sodium hydroxide solution in a small glass spiral reaction vessel at a constant flow rate provided by a technicon peristaltic pump. The luminol is oxidized, light is emitted and the light is detected by a photomultiplier tube.

We have standardized fresh 0.1% hydrogen peroxide solution by two titration methods: 1) $KMnO_4$ reduction titration, 2) standard iodometric titration with KI. Note that the second titration is extremely slow and it is necessary to wait about one hour between mixing the $H_2O_2$ and KI solutions and titrating. These two methods are in good relative agreement. Serial dilutions with hydrogen peroxide-free water indicate that low concentrations of hydrogen peroxide can be prepared with reasonable certainty from higher concentration hydrogen peroxide samples. We have observed an extremely linear response from less than 1 ppb to 100 ppb.

Our present ability to detect ppb levels of dry calibration samples of $H_2O_2$ (dew pt $0^oF$) is indicated in Figure 78. We have noted a significant positive $O_3$ interference to this method when $O_3$ values exceeded 0.1 ppm in the sample air. This interference was reproduced at EPA when a comparison between the EPA and UNC systems was made at EPA. Dr. Kok indicated that perhaps this interference was due to impure luminol.

Attempts to inject high concentrations (0.1-1 ppm) of $H_2O_2$ and measure these levels in the chambers werenot successful. Extreme chamber drying appears to be necessary to maintain $H_2O_2$ in the gas phase. During smog chamber runs in which $H_2O_2$ was monitored, concentrations as high as 5 ppb were observed.

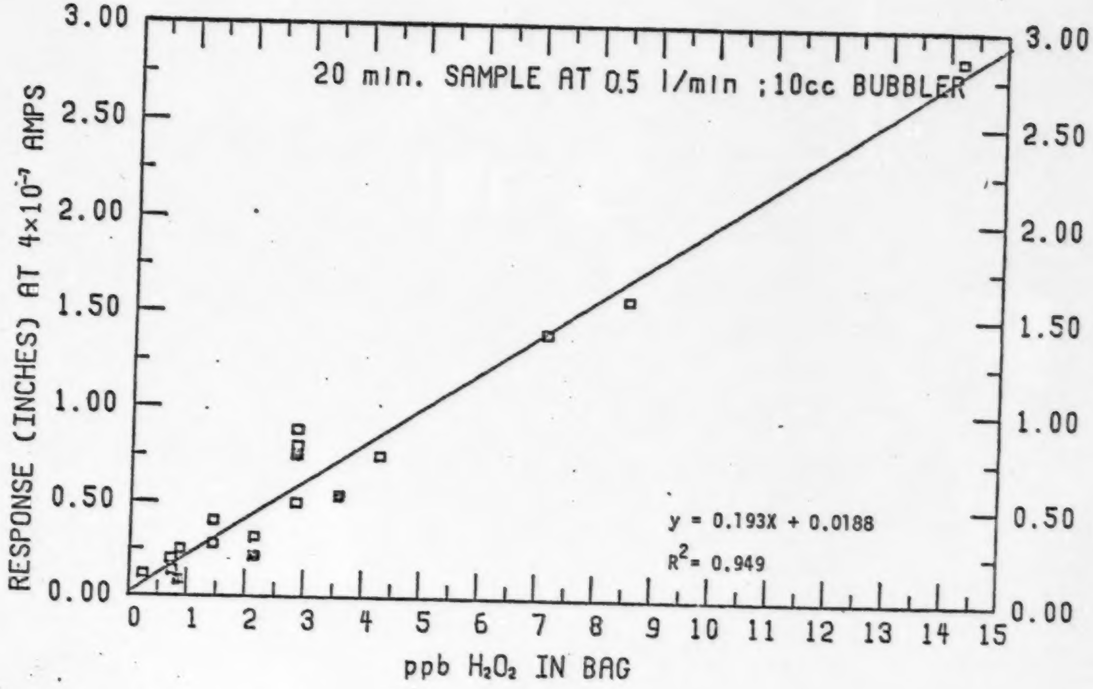

Figure 78. Response of $H_2O_2$ instrument to standard concentrations of $H_2O_2$ in dry air.

BEGIN FIRST LINE OF TEXT HERE
TYPING GUIDE SHEET
CENTER OF PAGE
TOP OF IMAGE AREA
DROPPED HEAD BEGIN SECTIONS HERE

## REFERENCES

1. Jeffries, H. E., D. L. Fox and R. M. Kamens, "Photochemical Conversion of NO to NO$_2$ by Hydrocarbons in an Outdoor Chamber", Journal of Air Pollution Control Association, 6, p. 480, 1976.

2. Jeffries, H. E., K. G. Sexton and C. N. Salmi, "Effects of Chemistry and Meteorology on Ozone Control Calculations Using Simple Trajectory Models and EKMA Procedure", Draft Report, U. S. Environmental Protection Agency, Office of Air Quality Planning and Standards, Durham, NC, December, 1978.

3. Kuwata, K., M. Uebori and Y. Ytamaski, "Determination of Aliphatic and Aromatic Aldehydes in Polluted Airs as Their 2,4-Dinitrophenylhydrazones by High Pressure Liquid Chromatography", J. Chromatographic Science, 17, p. 264, 1979.

4. Hull, L. A., "Procedures for 2,4-Dinitrophenylhydrazone Aldehyde-Ketone Air Analysis", Prepared for U. S. Environmental Protection Agency, Gas Kinetics and Photochemistry Branch, Research Triangle Park, NC, June 1980.

5. Kuntz, P., W. Lonneman, G. Namie and L. A. Hull, "Rapid Determination of Aldehydes in Air Analysis", Analytical Letters, 13, (16), pp. 1409-1415, 1980.

6. Jeffries, H. E., D. L. Fox and R. M. Kamens, "Outdoor Smog Chamber Studies: Effects of Hydrocarbon Reductions on Nitrogen Dioxide", EPA-65/3-75-011, U. S. Environmental Protection Agency, Research Triangle Park, NC, 1975.

7. Saeger, M., "An Experimental Determination of Specific Photolysis Rate of Nitrogen Dioxide", Masters Thesis, Department of Environmental Sciences and Engineering, University of North Carolina, Chapel Hill, NC, 1977.

8. Jeffries, H. E., J. E. Sickles, M. Saeger and M. A. Carpenter, "Experimental Determination of the Specific Photolysis Rate of Nitrogen Dioxide", Draft Final Report, EPA Grant #R805726, Bruce Gay, Jr., Project Officer, U. S. Environmental Protection Agency, Research Triangle Park, NC, April 30, 1981.

BEGIN LAST LINE OF TEXT
BOTTOM OF IMAGE AREA; OUTSIDE DIMENSION FOR TABLES AND ILLUSTRATIONS
3/8"

EPA-287 (Cin.)
(4-76)

TYPING GUIDE SHEET
BEGIN FIRST LINE OF TEXT HERE
CENTER OF PAGE
TOP OF IMAGE AREA
DROPPED HEAD: BEGIN SECTIONS HERE

9. Fox, D. L., R. M. Kamens and H. E. Jeffries, "Photochemical Smog Systems: Effect of Dilution on Ozone Formation", Science, 18, (8), June, 1975.

10. Sickles, J. E., L. A. Ripperton, L. A. Eaton and R. S. Wright, "Oxidant Precursor Relationships under Pollutant Transport Conditions", Outdoor Smog Chamber Study, Vol. 1, EPA-600/3-79-078A, U. S. Environmental Protection Agency, Research Triangle Park, NC, 1978.

11. Niki, H., Private Communication reported by: Gay, B. W., and J. J. Bufalini, "Nitric Acid and the Nitrogen Balance of Irradiated Hydrocarbons in the Presence of Oxides of Nitrogen", Environmental Science and Technology, 5, p. 422, 1971.

12. NASA "Chlorofluoromethanes and the Stratosphere", R. D. Hudson, Ed., NASA Reference Publication 1010, Chapter 1. Recommendations of the Laboratory Measurements Committee for the NASA Chlorofluoromethane Assessment, August, 1977.

13. Chameides, W. L., "The Photochemical Role of Tropospheric Nitrogen Oxides", Geophysical Research Letters, 5, p. 17, 1978.

14. Cox, R. A., "Trace Gas Photochemistry in the Troposphere", Journal of Photochemistry, 9,p. 85, 1978.

15. Fishman, J., "Recent Advances in the Chemical Kinetics of the Atmosphere and Effects on Chemical Pollution Estimates", Journal of Photochemistry, 9, p. 317, 1978.

16. Howard, C. J., "Kinetics of the Reaction of $HO_2$ with NO", Geophysical Research Letters, 4, p. 437, 1977.

17. Hendry, D. G. and R. Kenley, "Generation of Peroxy Radicals from Peroxy Nitrates ($RO_2NO_2$): Decomposition of Peroxyacyl Nitrates", Journal of the American Chemical Society, 9, p. 3198, 1977.

18. Cox, R. A., and M. J. Roffey, "Thermal Decomposition of Peroxyacetyl-Nitrate in the Presence of Nitric Oxide", Environmental Science and Technology, 11, p. 900, 1977.

19. Niki, H., P. D. Maker, C.M. Savage and L. P. Breitenbach, "Fourier Transform IR Spectroscopic Observation of Pernitric Acid Via HOO + $NO_2 \rightarrow HO_2NO_2$", Chemical Physics Letters, 45, p. 564, 1977.

20. Graham, R. A., A. M. Winer and J. N. Pitts, Jr., "Temperature Dependence of the Unimolecular Decomposition of Pernitric Acid and Its Atmopsheric Implications", Chemical Physics Letters, 51, p. 215, 1977.

6-1/2"
BEGIN LAST LINE OF TEXT
BOTTOM OF IMAGE AREA, OUTSIDE DIMENSION FOR TABLES AND ILLUSTRATIONS
3/8"

EPA-287 (Cin.)
(4-76)

21. Simonaitis, R. and J. Heichlen, "Reactions of $HO_2$ with NO and $NO_2$ and of OH with NO", Journal of Physical Chemistry, 80, p. 1, 1976.

22. Hanst, P. L. and B. W. Gay, Jr., "Photochemical Reactions Among Formaldehyde, Chlorine, and $NO_2$", Environmental Science and Technology, 11, p. 1105, 1977.

23. Levine, S. Z., W. M. Uselman, W. H. Chan, J. G. Calvert and J. H. Shaw, "The Kinetics and Mechanism of the $HO_2$-$NO_2$ Reactions: The Significance of Peroxynitric Acid Formation in Photochemical Smog", Chemical Physics Letters, 48, p. 528, 1977.

24. Baldwin, A. C., J. R. Barker, D. M. Golden and D. G. Hendry, "Photochemical Smog: Rate Parameter Estimates and Computer Simulations", Journal of Physical Chemistry, 81, p. 2483, 1977.

25. Uselman, W. M., S. Z. Levine, W. H. Chan, J. G. Calvert and J. H. Shaw, "The Kinetics of the Decay of Gaseous Peroxynitric Acid", Chemical Physics Letters, 58, p. 437, 1978.

26. Cox, R. A. and R. G. Derwent, "Kinetics of the Reaction of $HO_2$ with Nitric Oxide and $NO_2$", Journal of Photochemistry, 4, p. 139, 1975.

27. Chan, W. H., R. J. Nordstrom, J. G. Calvert and J. H. Shaw, "Kinetic Study of HONO Formation and Decay Reactions in Gaseous Mixtures of HONO, NO, $NO_2$, $H_2O$, and $N_2$", Environmental Science and Technology, 10, p. 674, 1976.

28. Demerjian, K. L., J. A. Kerr and J. G. Calvert, "The Mechanism of Photochemical Smog Formation", in Advances in Environmental Science and Technology, 4(1) (J. N. Pitts, Jr. and R. L. Metcalf, Ed.) John Wiley and Sons, New York, 1974.

29. Cox, R. A. and R. G. Derwent, "The Ultra-violet Absorption Spectrum of Gaseous Nitrous Acid", Journal of Photochemistry, 6, p. 23, 1976-1977.

30. Stockwell, W. R. and J. G. Calvert, "The Near UV Absorption Spectrum of Gaseous HONO and $N_2O_3$", Journal of Photochemistry, 8, p. 193, 1978.

31. Niki, H., P. D. Maker, C. M. Savage and L. P. Breitenbach, "FTIR Spectroscopic Observation of Peroxyalkyl Nitrates Formed Via ROO + $NO_2 \rightarrow ROONO_2$", Chemical Physics Letters, 55, p. 289, 1978.

32. Hamilton, E. J., "The Dependence on $H_2O$ and on $NH_3$ of the Kinetics of the Self-Reaction of $HO_2$ in the Gas-Phase Formation of $HO_2 \cdot H_2O$ and $\cdot HO_2\ NH_3$ Complexes", International Journal of Chemical Kinetics, 9, p. 875, 1977.

TYPING GUIDE SHEET
BEGIN FIRST LINE OF TEXT HERE
CENTER OF PAGE
TOP OF IMAGE AREA
DROPPED HEAD; BEGIN SECTIONS HERE
BOTTOM OF IMAGE AREA; OUTSIDE DIMENSION FOR TABLES AND ILLUSTRATIONS
BEGIN LAST LINE OF TEXT
3/8"
PAGE NUMBER
EPA-287 (Cin.)
(4-76)

TYPING GUIDE SHEET

33. Westberg, H. and M. Holdren, Quarterly Report. U. S. Environmental Protection Agency Research Grant No. R800670, Research Triangle Park, NC, 1976.

34. Zimmerman, P. R.," Procedures for Conducting Hydrocarbon Emission Inventories of Biogenic Sources and Some Results of Recent Investigation." Presented at U. S. Environmental Protection Agency Workshop on Emissions Inventory Factors, Raleigh, NC, 1977.

35. Zimmerman, P. R.," Response to Questions Raised by EPA-GKPB Review of NEDS Draft Final Report and Preliminary Florida Emissions Inventory Special Report. U. S. Environmental Protection Agency Contract No. DU-77-C063, Washington State University, Pullman, WA, 1978.

36. Lonneman, W. A., R. L. Seila and J. J. Bufalini, "Ambient Air Hydrocarbon Concentrations in Florida", Environmental Science and Technology, 12, pp. 459-463, 1978.

37. Lonneman, W. A. and J. J. Bufalini, Letter to the Editor. Environmental Science and Technology, 13, pp. 236-239, 1979.

38. Sandberg, J. S., M. J. Basso and B. A. Okin, "Winter Rain and Summer Ozone: A Predictive Relationship", Science, 200, pp 1051-1054, 1978.

39. Miller, P. R., J. N. Pitts and A. M. Winer,"Factors in Summer Ozone Production in the San Francisco Air Basin," Science, 203, pp. 81-82, 1979.

40. Arnts, R. R. and B. W. Gay, Jr.,"Photochemistry of Some Naturally Emitted Hydrocarbons," EPA-600/3-79-081, Research Triangle Park, NC, 1979.

41. Dodge, M. , Personal communication to H. E. Jeffries, 1979.

42. Kamens, R. M., H. E. Jeffries, M. W. Gery, R. W. Wiener and K. G. Sexton, "The Impact of Natural Hydrocarbons on Urban Smog Formation in the UNC Outdoor Smog Chamber", EPA Symposium on Atmospheric Biogenic Hydrocarbons, Research Triangle Park, NC, 1980.

43. Jeffries, H. E. and R. M. Kamens, "Modeling Observed Hydrocarbon Mixture Reactivity Effects", in U. S. Environmental Protection Agency Grant Proposal, Grant #R807762-01, 1980.

44. Hull, L., "Terpene Ozonolysis Products", EPA Symposium on Atmospheric Biogenic Hydrocarbon, Research Triangle Park, NC, 1980.

45. Ripperton, L. A., H. E. Jeffries and O. White, "Formation of Aerosols by Reaction of Ozone with Selected Hydrocarbons, Advances in Chemistry Series, 13, p. 219-231, 1972.

EPA-287 (Cin.)
(4-76)

46. Fox, D. L., J. E. Sickles, M. R. Kuhlman, P. C. Reist and W. E. Wilson,"Design and Operating Parameters for a Large Ambient Aerosol Chamber," Journal of Air Pollution Control Association, 25, p. 1049-1053, 1975.

47. Kamens, R. M., Smog chamber experiments: Unpublished data, 1980.

48. Schuck, E. A. and G. J. Doyle, "Photooxidation of Hydrocarbons in Mixtures Containing Oxides of Nitrogen and Sulfur Oxides", Report Number 29, Air Pollution Foundation, San Marino, CA, 1959.

49. Jeffries, H. E., D. L. Fox and R. M. Kamens, "Outdoor Smog Chamber Studies Effects of Hydrocarbon Reductions on Nitrogen Dioxide", EPA-65/3-75-011, U. S. Environmental Protection Agency, Research Triangle Park, NC, 1975.

50. Lonneman, W. A., "PAN Measurement in Dry and Humid Atmospheres", Environmental Science and Technology, 11(2) pp. 194-6, 1977.

51. Kamens, R. M., H. E. Jeffries, M. W. Gery, R. W. Wiener, K. G. Sexton, and G. B. Howe, "The Impact of α-pinene on Urban Smog Formation: An Outdoor Chamber Study", Atmospheric Environment, 15(6) p. 969, 1981.

52. Preparation of Ethereal Alcoholic Solutions of Diazomethane, Aldrich Technical Information, September 1975.

53. Lonneman, W. A., "Ozone and Hydrocarbon Measurements in Recent Oxidant Transport Studies", Proceedings of International Conference on Photochemical Oxidant Pollution and Its Control, EPA-600/3-77-001, U. S. Environmental Protection Agency, Research Triangle Park, NC, 1977.

54. Dodge, M. C. and R. R. Arnts, "A New Mechanism for the Reaction of Ozone with Olefins", International Journal of Chemical Kinetics, XI, pp. 399-410, 1979.

55. Niki, H., P. D. Maker, C. M. Savage and L. P Breitenbach, "A FTIR Study of a Transitory Product in the Gas-Phase Ozone-Ethylene Reaction", Journal Physical Chemistry, 85(8), pp. 1024-1027, 1981.

56. Su, F., J. G. Calvert and J. H. Shaw, "A FTIR Spectroscopic Study of the Ozone-Ethene Reaction Mechanism in $O_2$ Rich Mixtures", Journal of Physical Chemistry, 84, pp. 239-246, 1980.

57. Herron, J. V. and R. E. Huie, "Stopped Flow Studies of the Mechanism of Ozone-Alkene Reactions in the Gas Phase Ethylene", Journal of the American Chemistry Society, 99(6), pp. 5430-5435, 1977.

BEGIN FIRST LINE OF TEXT HERE
TYPING GUIDE SHEET
CENTER OF PAGE
TOP OF IMAGE AREA
DROPPED HEAD; BEGIN SECTIONS HERE

58. Adeniji, S. A., J. A. Kerr and M. R. Williams, "Rate Constant for Ozone-Alkene Reaction under Atmospheric Conditions", International Journal of Chemical Kinetics, XIII, pp. 209-217, 1981.

59. Durbin, P. A., T. A. Hecht and G. Z. Whitten, "Mathematical Modeling of Simulated Photochemical Smog, Final Report", EPA Contract #68-02-0500, Systems Application Inc., 1975.

60. Bass, A. M., et al., "Temperature Dependent Absorption Cross Sections for Formaldehyde ($CH_2O$): The Effect of Formaldehyde on Stratospheric Chlorine Chemistry", In press, Planetary and Space Science.

61. Jeffries, H. E., "Part II: The Issue of Hydrocarbon Reactivity, A Critical Review", In Analysis of Evidence and Viewpoints --International Conference on Oxidants 1976, EPA-600/3-77-114, 1977.

62. Dodge, M. C., "Effect of Selected Parameters on Predictions of a Photochemical Model", EPA-600/3-77-048, U. S. Environmental Protection Agency, Research Triangle Park, NC, 1977.

63. Jeffries, H. E. and K. G. Sexton, "Comparison of Nitrogen Transformation Processes in Various Photochemical Kinetic Models", University of North Carolina, Chapel Hill, NC, 1979.

64. Jeffries, H. E., R. M. Kamens, D. L. Fox, and B. Dimitriades, "Outdoor Smog Chamber Studies: Effect of Diurnal Light, Dilution, and Continuous Emission on Oxidant Precursor Relationships", in International Conference on Photochemical Oxidant Pollution and Its Control, Proceedings: Vol. 2, EPA-600/3-77-001b, January, 1977.

65. Feigley, C. E., H. E. Jeffries and M. A. Carpenter, "Smog Chamber Validation Using Lagrangian Atmospheric Data", EPA-600/3-79-050, May 1979.

66. Feigley, C. E. and H. E. Jeffries, "Analysis of Processes Affecting Oxidant Precursors in the Los Angeles Reactive Pollutant Program (LARPP) Operation 33", Atmospheric Environment, 13(10), pp. 1369-1384, 1979.

67. Feigley, C. E., H. E. Jeffries and R. M. Kamens, "An Experimental Simulation of Los Angeles Reactive Pollutant Program (LARPP) Operation 33, Part I & II, Submitted to Atmospheric Environment, 1981.

68. Wright, R. S., R. M. Kamens, J. E. Sickles, H. E. Jeffries and W. C. Eaton, "Comparison Between Two Outdoor Chamber Facilities: Matched Experiments", Journal of Air Pollution Control Association, 28(3), pp. 248-250, 1978.

BOTTOM OF IMAGE AREA OUTSIDE DIMENSION FOR TABLES AND ILLUSTRATIONS
BEGIN LAST LINE OF TEXT
3/8"

EPA-287 (Cin.)
(4-76)

69. Ross, D., Grant Proposal from SRI Submitted to Harold M. Barms, Environmental Protection Agency, Research Triangle Park, NC, 1979.

70. Sexton, K. G., "The Role of Nitrogen Containing Compounds in Several Organic Smog Systems", Masters Thesis, Department of Environmental Sciences and Engineering, University of North Carolina, Chapel Hill, NC, 1979.

71. Stephens, E. and M. A. Price, Paper presented at 8th Conference on Methods in Air Pollution and Industrial Hygiene Studies, Oakland, CA, February 1977.

72. Miller, D. F. and C. W. Spicer, "Measurement of Nitric Acid in Smog", *Journal of the Air Pollution Control Association*, *25*, p. 940, 1975.

73. Joseph, D. W. and C. W. Spicer, "A Chemiluminescence Method for Atmospheric Monitoring of Nitric Acid and Nitrogen Oxides", *Analytical Chemistry*, *50*, p. 1400, 1978.

74. Spicer, C. W. and D. F. Miller, "Nitrogen Balance in Smog Chamber Studies", *Journal of the Air Pollution Control Association*, *26*, p. 45, 1976.

75. Gantner, B. A., "Fate of Oxides Nitrogen in Outdoor Smog Chamber", Masters Thesis, Department of Environmental Sciences and Engineering, University of North Carolina, Chapel Hill, NC, 1975.

76. Nelson, G. O., *Controlled Test Atmospheres: Principles and Techniques*, Ann Arbor Science Publishers, Inc. 247 pp., 1971.

77. Spicer, C. W., "The Fate of Nitrogen Oxides in the Atmopshere", In *Advances in Environmental Science and Technology*, *7*, p. 163, (J. N. Pitts, Jr. and R. L. Metcalf, Ed.) John Wiley and Sons, New York. 520 pp., 1977.

78. West, P. and T. P. Ramachandran, "Spectrophotometric Determination of Nitrate Using Chromotropic Acid", *Analytic Chimiea Acta*, *35*, p. 317, 1966.

79. Pile, W. and I. Johann, "The Determination of Smallest Amounts of Hydrogen Peroxide in the Air", *International Journal Environmental Analytical Chemistry*, *3*, pp. 257-270, 1974.

80. Kok, G. L., T. P. Holler, M. B. Lopez, H. A. Nachtrieb and M. Yuan, "Chemiluminescent Method for Determination of Hydrogen Peroxide in Ambient Atmosphere",*Environmental Science and Technology*, *12*(9), pp. 1072-1076, 1978.

BEGIN FIRST LINE OF TEXT HERE
TYPING GUIDE SHEET
CENTER OF PAGE
TOP OF IMAGE AREA
DROPPED HEAD: BEGIN SECTIONS HERE

## Appendix A

## CHAMBER AND FACILITY DESCRIPTION

### Description

Location. The site is approximately 32 kilometers from the University of North Carolina at Chapel Hill. It is in Chatham County, North Carolina and is approximately 10 kilometers from the small town of Pittsboro. Chatham County is one of the most rural, least industrialized counties in North Carolina and is heavily wooded. The background concentrations of $NO_x$ and nonmethane hydrocarbons are usually less than 5 ppb and less than 80 ppbC. More importantly, the air exhibits very low reactivity in the chamber.

Materials. The chamber surfaces are FEP Teflon$^R$. The film's transmission in the UV and visible regions of the solar spectrum is excellent, and it has only a few absorption bands in the IR, a property necessary to reduce the "greenhouse effect". It has a very low permeability for most chemical species and can be heat sealed to form large durable panels. For this application its worst property is its ability to hold a static charge for long periods of time. Type A film, 0.13 mm thick is used.

Physical Design. Inlet and outlet doors, stirring fans, manifolds and other fittings are inserted through a solid floor. The sides are free for light entry. The floor of the chamber is elevated approximately 1.2 m to allow for easy access under the chamber.

The design is an A-frame 9.14 m wide, 12.10 m long and 6.10 m high at the peak on a plywood floor 1.22 m above the ground. Wooden beams, 5.08 cm by 20.32 cm, located on edge at 99.1 cm centers form an exterior framework on top of the plywood floor. Continuous 16.46 m lengths of film are attached to the inside by aluminum u-channels, screwed firmly to the wooden beams thus compressing the film against the external support. See Figures 1 and 2.

One piece, heat sealed Teflon film panels are used in such places as the triangular end panels and floors. The floor-to-side seals are achieved by a 0.61 m overlap of side panel film over floor panel film. A rubber strip under the film and an aluminum strip over top of the film complete the seal. All other seals are Teflon-to-Teflon under pressure of the aluminum u

BEGIN LAST LINE OF TEXT
BOTTOM OF IMAGE AREA OUTSIDE DIMENSION FOR TABLES AND ILLUSTRATIONS
3/8"

PAGE NUMBER
EPA-287 (Cin.)
(4-76)

BEGIN FIRST LINE OF TEXT HERE

TYPING GUIDE SHEET

CENTER OF PAGE

TOP OF IMAGE AREA

DROPPED HEAD; BEGIN SECTIONS HERE

Reproduced from best available copy.

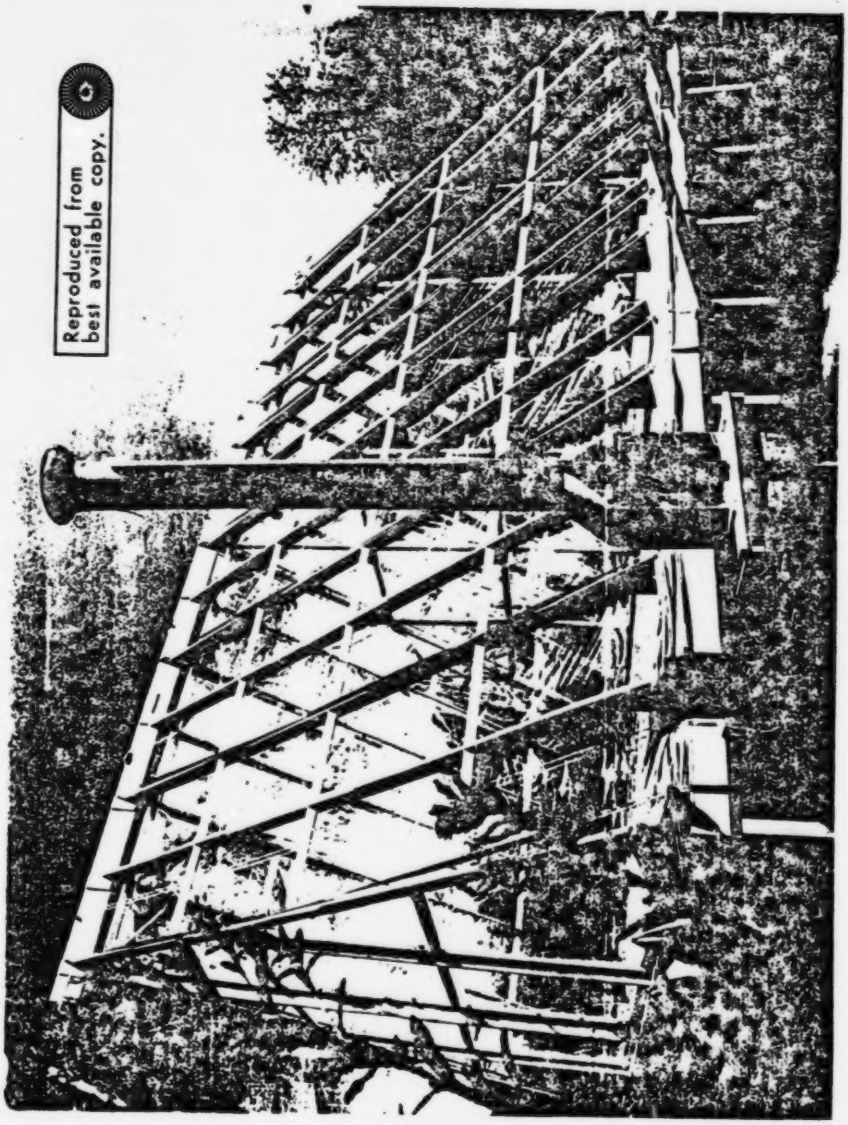

Figure 1: The University of North Carolina Outdoor Smog Chamber. (Courtesy of the Greensboro Daily News)

BEGIN LAST LINE OF TEXT

BOTTOM OF IMAGE AREA; OUTSIDE DIMENSION FOR TABLES AND ILLUSTRATIONS

3/8"

EPA-287 (Cin.)
(4-76)

TYPING GUIDE SHEET
BEGIN FIRST LINE OF TEXT HERE
CENTER OF PAGE
TOP OF IMAGE AREA
DROPPED HEAD. BEGIN SECTIONS HERE

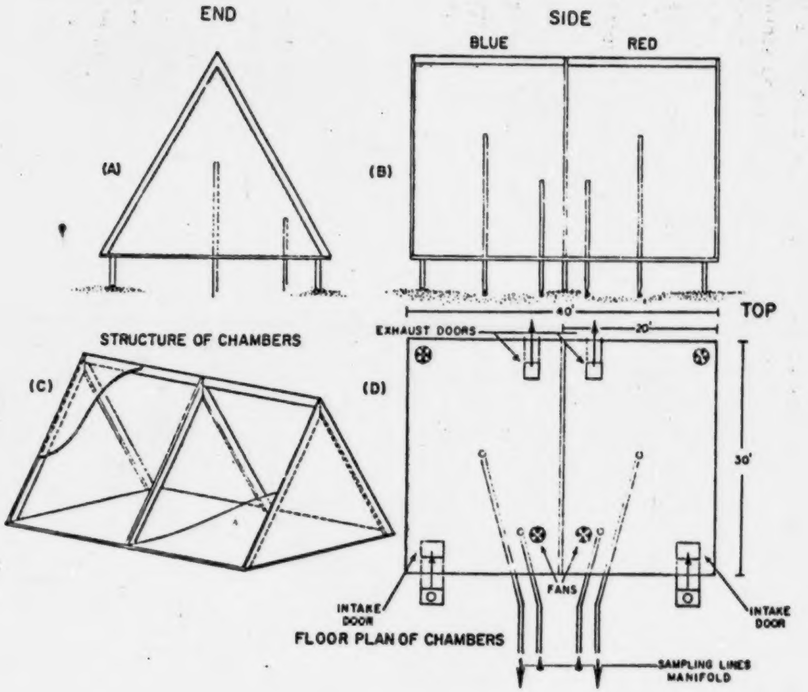
END
(A)
SIDE
BLUE
RED
(B)
STRUCTURE OF CHAMBERS
(C)
TOP
40'
20'
30'
EXHAUST DOORS
(D)
FANS
INTAKE DOOR
INTAKE DOOR
FLOOR PLAN OF CHAMBERS
SAMPLING LINES MANIFOLD

Figure 2. Schematic of UNC Outdoor Smog Chamber

BEGIN LAST LINE OF TEXT
BOTTOM OF IMAGE AREA: OUTSIDE DIMENSION FOR TABLES AND ILLUSTRATIONS
3/8"

PAGE NUMBER
EPA-287 (Cin.)
(4-76)

BEGIN FIRST LINE OF TEXT HERE
TYPING GUIDE SHEET
CENTER OF PAGE
TOP OF IMAGE AREA
DROPPED HEAD; BEGIN SECTIONS HERE

channel. A single unsupported heat sealed Teflon panel similar to the end panels is used to separate the chamber into two halves of equal volume. It is sealed to the floor and side panels in the same manner as described above. Aluminum foil is placed under the film on the floor to reflect the light and heat backup through the chamber. This is necessary to reduce solar heating of the air to a value that is within normal urban environments and to compensate for transmission losses through the Teflon film.

Orientation. The chamber is oriented with its long axis approximately north to south. The actual long axis orientation is along a 27° - 207° true heading. The orientation with respect to the sunrise and sunset at different times of the year and the altitude of the sun at noon for different times of the year are illustrated in Figures 3 and 4.

Air Handling Systems. There are four air handling systems in each half of the chamber, one for exhausting, one for sampling, one for recirculating through dehumidifiers, and one for mixing. The exhaust system consists of two intake stacks, 0.61 m x 0.91 m intake doors, 0.61 m x 0.61 m exhaust doors, and an exhaust blower. The exhaust blower is a dual blower on a single shaft driven by a 1.5 horsepower motor. Air enters the system through the two 5.49 m high by 30.5 cm diameter stacks. This system is designed to permit rapid exhausting of chamber contents and replacement with ambient air. The filling rate is 7190 l/min. The chamber can be flushed with a 99.6% decay of initial contents in 2 hours.

The second air handling or manifold system is for sampling and injection of pollutant materails into the chamber halves. To insure representative sampling, a 3.17 cm I.D. glass manifold runs from a point 1.83 m above the floor in the center of each chamber half down through the floor and over to a sampling laboratory. The sampling volume required by all the instruments does not exceed 5 l/min but to reduce losses due to long resident times it is necessary to have higher flows in the manifold. The flow rate in the manifold is 60 lpm. The manfold system is wrapped with a controlled heating tape to maintain the sample slightly warmer than the chamber temperature. To avoid the necessity of makeup air, the sampling manifold is a closed loop. Squirrel cage blowers with housings and fans that are Teflon coated are used to circulate air through the manifolds. The unused sample air is then returned through a 3.17 cm I.D. glass manifold to the chamber. These return manifolds provide a convenient method for injecting the initial reactants. There is also a special heated Teflon manifold for formaldehyde sampling.

BEGIN LAST LINE OF TEXT
BOTTOM OF IMAGE AREA, OUTSIDE DIMENSION FOR TABLES AND ILLUSTRATIONS
3/8"

PAGE NUMBER
EPA-287 (Cin.)
(4-76)

TYPING GUIDE SHEET
BEGIN FIRST LINE OF TEXT HERE
CENTER OF PAGE
TOP OF IMAGE AREA
DROPPED HEAD: BEGIN SECTIONS HERE

Inside each chamber half are two mixing fans located in opposite corners. These provide circulation and mixing of the chamber contents. The fans are 50.8 cm diameter cast aluminum units that are FEP Teflon coated. They operate in a horizontal position, 0.76 m above the floor on 2.54 cm diameter Teflon coated steel shafts that extend through the chamber floor. Under the floor, 1/4 horsepower, 1750 rpm motors provide power through a belt and pulley system to each fan. Each fan operates at approximately 31.15 $m^3$/min.

Laboratory. The laboratory is adjacent to the chamber. It is a 3.66 m W x 15.24 m L x 3.05 m H wooden structure oriented perpendicular to the chamber and 3.66 m away from it to avoid any shadowing. The first 5.49 m nearest the chamber contain the instrumentation, manifolds, and calibration systems. The next 5.49 m contain the data acquisition computer system and the operations area. The last 4.27 m of the laboratory is a utility area with running water and storage facilities. Gas tanks necessary to operate the instruments and perform calibration are located in a 1.22 m x 1.83 m room completely closed-off from, but attached to the laboratory. The injection system gas tanks and valves are housed in a second 1.52 m x 1.52 m well-insulated, heated room adjacent to the end of the laboratory nearest the chamber.

Injection System. Pollutants are injected into the chamber sides via the return side of the sampling manifolds. The return manifolds enter the chamber sides under one of the mixing fans. The injection process uses gas cylinders containing pollutants at high concentrations (1000-10,000 ppm range), two stage, stainless steel diaphragm regulators, on-off solenoid valves, and a precision needle valve. The flow rate of injected material into the manifolds is established by a 5 millisecond response time mass flow meter. The total injection volume is accurately controlled as a function of the time the solenoid valve is open. The open time of each solenoid valve is controlled by the computer system on command. Conditions can be varied sufficiently to have the injection time range from a few seconds for each component to 1-2 hours for a programmed injection used to simulate the buildup of pollutants in urban areas.

Data Acquisition System. A computer based data acquisition and control system (DAS) is used to acquire, process, and record data for the chamber instrument system. The complete system is shown schematically in Figure 5.

Output signals from each instrument are wired to a crossbar scanner (or analog signal multiplexer). Under control of programs in the computer, the

BOTTOM OF IMAGE AREA, OUTSIDE DIMENSION FOR TABLES AND ILLUSTRATIONS
BEGIN LAST LINE OF TEXT
3/8"

PAGE NUMBER
EPA-287 (Cin.)
(4-76)

BEGIN FIRST LINE OF TEXT HERE
TYPING GUIDE SHEET
CENTER OF PAGE
TOP OF IMAGE AREA
DROPPED HEAD: BEGIN SECTIONS HERE

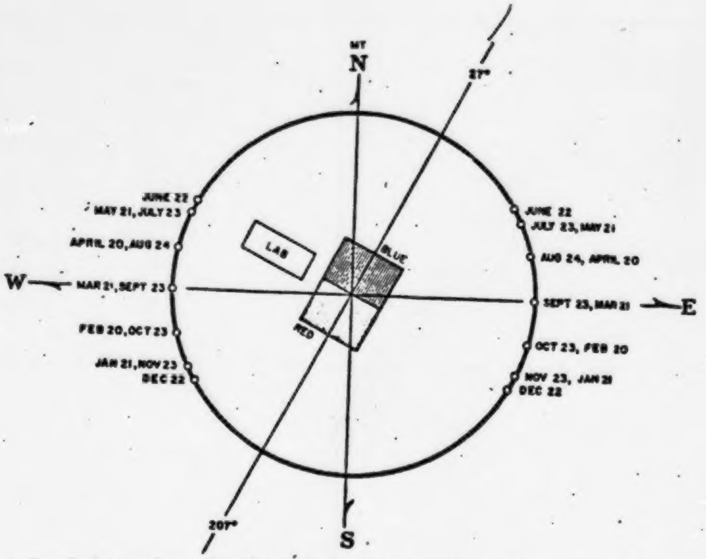
MT
N
27°
JUNE 22
MAY 21, JULY 23
APRIL 20, AUG 24
W
MAR 21, SEPT 23
FEB 20, OCT 23
JAN 21, NOV 23
DEC 22
LAB
BLUE
RED
JUNE 22
JULY 23, MAY 21
AUG 24, APRIL 20
SEPT 23, MAR 21
E
OCT 23, FEB 20
NOV 23, JAN 21
DEC 22
207°
S

Figure 3. Orientation of UNC outdoor smog chamber with respect to seasonal sunrise and sunset positions.

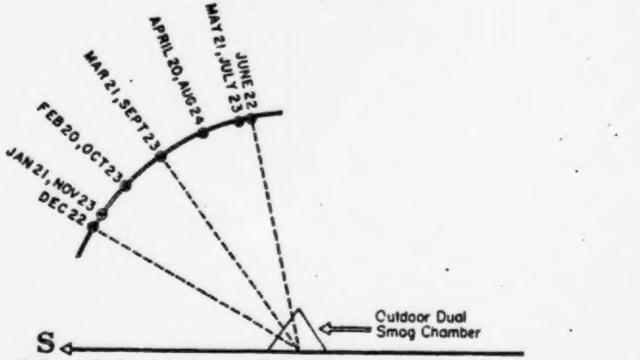
JUNE 22
MAY 21, JULY 23
APRIL 20, AUG 24
MAR 21, SEPT 23
FEB 20, OCT 23
JAN 21, NOV 23
DEC 22
Outdoor Dual Smog Chamber
S

Figure 4. Solar altitude and zenith angle at noon at the UNC outdoor smog chamber for each month.

BEGIN LAST LINE OF TEXT
BOTTOM OF IMAGE AREA; OUTSIDE DIMENSION FOR TABLES AND ILLUSTRATIONS
3/8"

PAGE NUMBER
EPA-287 (Cin.)
(4-76)

TYPING GUIDE SHEET
BEGIN FIRST LINE OF TEXT HERE
DROPPED HEAD; BEGIN SECTIONS HERE
CENTER OF PAGE
TOP OF IMAGE AREA
BEGIN LAST LINE OF TEXT
3/8"
BOTTOM OF IMAGE AREA; OUTSIDE DIMENSION FOR TABLES AND ILLUSTRATIONS

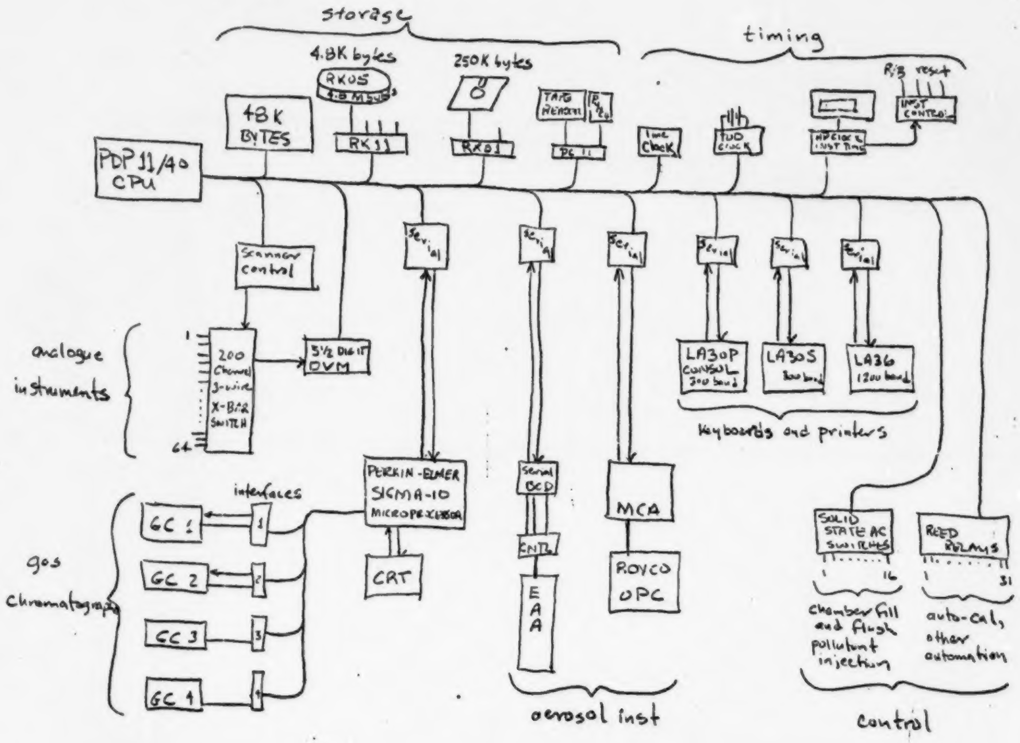
storage
timing
4.8K bytes
RK05
4.8 M bytes
250K bytes
48K BYTES
RK11
RX01
TAPE READER
PC11
line Clock
TOD CLOCK
HP CLOCK & INST TIME
R/B reset
INST CONTROL
PDP 11/40 CPU
Scanner control
Serial
Serial
Serial
Serial
Serial
Serial
Serial
analogue instruments
1
200 Channel 3-wire X-BAR SWITCH
64
5½ DIGIT DVM
LA30P CONSOL 300 baud
LA30S 300 baud
LA36 1200 baud
keyboards and printers
PERKIN-ELMER SIGMA-10 MICROPROCESSOR
CRT
interfaces
1
2
3
4
GC 1
GC 2
GC 3
GC 4
gas chromatographs
Serial BCD
CNTL
EAA
MCA
ROYCO OPC
aerosol inst
SOLID STATE AC SWITCHES
1
16
REED RELAYS
1
31
chamber fill and flush pollutant injection
auto-cal, other automation
control

Figure 5. Data Acquisition and Control System

Reproduced from best available copy.

EPA-287 (Cin.)
(4-76)

BEGIN FIRST LINE OF TEXT HERE
TYPING GUIDE SHEET
CENTER OF PAGE
TOP OF IMAGE AREA
DROPPED HEAD, BEGIN SECTIONS HERE

scanner connects the selected signal leads to the input of the digital voltmeter. The digital voltmeter, which has excellent noise and spurious signal suppression and can measure a 1 volt signal with a resolution of 10 microvolts, is triggered to acquire a reading and to supply the binary coded decimal, 5-1/2 digit number to the computer. The computer proccesses the information and then commands the scanner to move to the next channel and repeat the process. The data processing will be described in a later chapter. The timing of the computer processes is under the control of a digital date and time-of-day clock which signals event times to the computer. Another digital timer operates Teflon solenoid valves on the inlet of each instrument to connect the instruments to one chamber half during a given cycle of data acquisition.

This system provides fully automatic acquisitions and processing of data during a run and provides the operator with immediate, full data in physical units. Given this information about what is happening, the operator can then concentrate on what he wants to do. It also allows the massive amount of information generated during a run to be processed in a more effectual manner after the run is over.

## Experimental Method and Procedures

Instrumentation. The instruments are located in a temperature-controlled laboratory adjacent to the chamber. Gas instruments include equipment for measuring alkanes, alkenes, aromatics, aldehydes, phenols, nitric oxide, nitrogen dioxide, ozone, PAN, $HNO_3$, alkyl nitrates, $H_2O_2$, total hydrocarbons (THC), methane, and CO. Standard meteorological instruments are used to measure solar radiation, ultra-violet radiation, air temperature, and dew point. A Perkin Elmer Sigma 10 processor-based charomatograph integration system is used to acquire data and control the gas chromatographic (GC) methods. Table 1 lists the instrument models and their characteristics.

At the sample inlet of each gas instrument is a three way Teflon ac solenoid valve. Since there are two intake manifolds (one for each chamber half), air from either manifold can be drawn through the three-way valve and into the instrument. In this manner timesharing of one instrument between the two chamber halves is possible.

BEGIN LAST LINE OF TEXT
BOTTOM OF IMAGE AREA; OUTSIDE DIMENSION FOR TABLES AND ILLUSTRATIONS
3/8"

EPA-287 (Cin.)
(4-76)

Standard Calibration Procedures. The techniques used to calibrate the continuous monitoring instruments closely follow the procedures set forth by EPA, although other methods are used as needed (see Table 2). $NO_2$ and $O_3$ calibrations are interlocked via the gas phase titration procedure. A Dasibi (Model #1008-AH) UV absorption ozone photometer is utilized as a primary calibration standard. A certified commercial cyclinder of NO is also used for comparison and checking.

The GC analysis for specific hydrocarbons is calibrated with: (1) an NBS traceable high pressure cylinders containg ppmC levels of six representative $C_2$-$C_8$ alkanes and alkenes and (2) low static (chamber) concentrations prepared by injection of known amounts of aromatic hydrocarbons, aromatic aldehydes, and phenols. Acetaldehyde, propionaldehyde, and MEK are calibrated with carefully prepared bag and chamber samples. Carbon monoxide, THC, $CH_4$ are also calibrated with an NBS traceable calibration cylinder of these gases. Formaldehyde is calibrated with : 1) liquid samples prepared by dilution of calibrated 37% HCHO, and 2) static samples prepared in the chamber from carefully weighed and vaporized samples of paraformaldehyde, and comparison with the chromotropic acid bubbler method.

The PAN analyzer is calibrated by comparing the response of the GC and the $NO_2$ chemiluminescence analyzer to samples of pure PAN. It has been shown that the chemiluminescence $NO_x$ analyzer responds 100% to PAN. PAN is produced photochemically from biacetyl and $NO_2$ and then concentrated and purified, with a gas chromatographic technique.

Several alkyl nitrates have been identified and have been calibrated with static calibration samples prepared in the chamber by injecting microliter quantities of pure liquids. We plan to improve calibration with a dynamic system with either permeation tubes or a capillary diffusion device.

As with $O_3$ it is not possible to prepare or store nitric acid vapors in a container for later calibration use. A dynamic source of $HNO_3$ is used and is calibrated by a bubbler-colorimetric procedure. From this we have determined that our chemiluminescence $NO_2$ analyzer with a molybdenum convector has a 100% response to $HNO_3$. The convertor is located directly under the chamber floor so that sample line losses can be minimized. The $H_2O_2$ method is calibrated with liquid standards prepared from serial dilutions of a $KMnO_4$ standardized stocked solution of $H_2O_2$.

TYPING GUIDE SHEET

Table 1. Instrument Characteristics

| Substance | Method | Manufac. & Model | MDC | Range | Mode | Time Shared |
|---|---|---|---|---|---|---|
| $O_3$ | Chemiluminescence | Bendix 8002 | 0.001 | 0-2 | Continuous | Yes |
| NO, $NO_x$, $NO_2$ | Chemiluminescence | Bendix 8101-B | 0.005 | 0-1 | Cyclic-30 sec each | Yes |
| HC's alkenes<br>alkanes<br>aromatics | GC-FI<br>Automated, programmable,<br>Multiple column | Carle 211 | 0.005-0.010 | 0-100 | Cyclic 15 or 30 min | Yes |
| THC<br>CO<br>$CH_4$ | GC-FI<br>Automated<br>Multiple column | Beckman 6800 | 0.010 | 0-30 | Cyclic 5 min or 15 min | Yes |
| HCHO | Automated<br>Colorimetric<br>(reverse West-Gaeke) | CEA 555 | 0.01 | 0-2 | Continuous | Yes |
| Acetaldehyde<br>Propionaldehyde<br>MEK | GC-FI | Carle 211M | 0.02-0.05<br>0.1<br>0.07 | 0-100 | Cyclic 30 min | Yes |
| Aromatics HC<br>aromatic aldehydes<br>phenols | GC-FI | Perkin Elmer 900 | -0.010 | 0-100 | Manual | Yes |
| PAN | GC-EC | Analog Tech. Corp.<br>140 A EC<br>Var. Freq. pulsed bias detector | 0.0004 | 0-1 | Cyclic | Yes |
| Alkyl nitrates | GC-EC | Varian Aerograph<br>DC biased EC<br>Model 940 | 0.0003-0.0008 | 0-1 | Cyclic | Yes |
| $HNO_3$ | Chemiluminescence<br>Molybdenum converter<br>Nylon scrubber | Bendix 8101-B<br>TECO Molybdenum Converter | 0.003 | 0-1 | Cyclic 15 min | No |
| $H_2O_2$ | Bubbler-Man<br>Automated<br>Chemilum. analysis | | 0.0001 | 0-1 | Manual | Yes |
| Temp | Thermistor | YSI | 0.2 F | 20-110°F | Continuous | No |
| TSR | Pyranometer | Eppley Black & White | 7.5 mv/cal/$cm^2$-min | 0-2 cal/$cm^2$-min | Continuous | NO |
| UV | Pyranometer | Eppley UV | 0.2 mv/cal/$cm^2$-min | 0-0.1 cal/$cm^2$-min | Continuous | No |
| Dew Point | Cooled mirror & conductivity | EG&G 880<br>Gen. Eastern 600 | 0.1°F | -40°F-120°F | Continuous | Yes |

EPA-287 (in.)
(4-70)

BEGIN FIRST LINE OF TEXT HERE
TYPING GUIDE SHEET
CENTER OF PAGE
TOP OF IMAGE AREA
DROPPED HEAD: BEGIN SECTIONS HERE

Standard Operating Procedure. Most experiments are initiated early in the morning by the site computer which has been programmed the night before to carry out a detailed set of commands. Prior to an experimental run, the chamber is automatically purged overnight with background ambient air. Several hours before dawn the DAS begins recording measurements of the background concentration. Single instruments are timeshared on an alternating four minute cycle between the two sides. The chamber intake and exhaust doors are sealed and the initial concentrations of reactants of interest are injected before sunrise. The computer selects the proper tank and calculates the correct time to achieve the desired initial concentrations. Injections are normally short "slug" injections; most experiments have initial hydrocarbon, NO, and $NO_2$. Monitoring of the chemical and physical species mentioned earlier continues usually until 1800 EDT when the experiment is terminated. The computer then performs several close-down procedures: turning off certain instruments, opening chamber vent doors, and turning on the exhaust fan to purge the chamber. Instructions for another experiment can then be programmed.

Variations of the standard operating procedures include: 1) changing humidity before the experiment, 2) injecting pollutants slowly during the experiment, 3) diluting the chamber(s) during the experiment to simulate mixing height profiles, 4) transfer of contents of one chamber side to the other, and injecting initial conditions into the chamber containing part or all of the product of a day-old experiment. Most pollutants are injected from high concentration gas cylinders (10,000 ppm) which can be controlled by the computer. Some pollutants are liquids with vapor pressure too low to have high vapor concentration (cylinder ) prepared. These are injected manually. Carefully measured samples are heated in a U-tube in which warm zero air is passed through to the return manifold. Automated liquid injectors will be installed soon.

## DATA TREATMENT PROCEDURES

General. Figure 8 is the flowchart of the processes used to treat the data collected. The processes are divided into those that occur during a run, those performed immediately after a run, and those that are done later. The operations are carried out on three different computers, and the Broomall plotter. The PDP 11/40 is at the computer site and is responsible for

BOTTOM OF IMAGE AREA, OUTSIDE DIMENSION FOR TABLES AND ILLUSTRATIONS
BEGIN LAST LINE OF TEXT
3/8"

PAGE NUMBER
EPA-287 (Cin.)
(4-76)

TYPING GUIDE SHEET
BEGIN FIRST LINE OF TEXT HERE
DROPPED HEAD: BEGIN SECTIONS HERE
CENTER OF PAGE
TOP OF IMAGE AREA
BEGIN LAST LINE OF TEXT
BOTTOM OF IMAGE AREA, OUTSIDE DIMENSION FOR TABLES AND ILLUSTRATIONS
3/8"

Table 2. Calibration Sources for Gases

| Species | Source | Calibration Method | References |
|---|---|---|---|
| $O_3$ | UV-Quartz<br>$O_3$ generator | UV Photometry<br>Dasibi Model #1008-AH | EPA |
| NO | Cylinder | Certified Commercial analysis<br>$O_3$ UV photometry transfer via Gas Phase titration | EPA |
| $NO_2$ | Oxidation of NO | Gas Phase Titration | EPA |
| $CH_4$<br>CO<br>THC | Cylinder | Certified commercial analysis | EPA |
| HC's | Cylinder | Certified commercial analysis | EPA |
| HCHO | paraformaldehyde & 37% HCHO | Prepared static calibration standards<br>Verified with chromotropic acid bubbler technique | |
| Ace<br>Propionaldehyde<br>MEK | | Prepared static calibration standards | |
| Aromatics | | Prepared static calibration standards | |
| PAN | PAN purified | Reference method and transfer standard | Winer, A. et. al. ES&T 8 1116 (1974) |
| Alkyl nitrates | Alkyl nitrates | Prepared static calibration standards | |
| $HNO_3$ | $HNO_3$ (gaseous) | Dynamic source (gas) calibrated by colorimetric (chromotropic acid) bubbler method | Spicer, C, Adv. Envr. Sci. & Tech. 7 (163) 197 |
| $H_2O_2$ | $H_2O_2$ | Liquid standards and iodometric analysis | |

EPA-287 (Cin.)
(4-76)

TYPING GUIDE SHEET
BEGIN FIRST LINE OF TEXT HERE
CENTER OF PAGE
TOP OF IMAGE AREA
DROPPED HEAD: BEGIN SECTIONS HERE

```
 RUN DX1:DATRAN
SPECIFY OPTIONS DESIRED (AS option,option,option <CR>):   GAS
INJECTION TANK VALUES AS OF: 27-SEP-79
GAS      CONC(PPMC)    FLOW(L/MIN)
NO         10700.          6.
NO2        20500.         10.
PROPYL     21396.         10.
UNCMIX     10471.         10.
ETHYL1      2028.         10.
N2       1000000.         10.
AUTOMX     10487.         10.
ACETAL      4110.         10.
BUTAN1     92400.         10.
BUTPPL     11456.         10.
CO        100000.         10.
PROPAN     22068.         10.
ETHYL2     20663.         10.
BUTAN2     20760.         10.
SOURCE FILE NAME?   FEB1
DATE OF RUN (AS dd-MMM-yy):   1-FEB-80
ERRORS ARE FLAGGED BY [NN]

 [THIS IS AN ACTUAL EXAMPLE RUN]
 IMMED VENT; CLR CHARTS;
 AT 3:30 SET CHARTS; OSC 35 ON 45 SEC EVERY 15 MIN; [CO]
 AT 3:50 CLOSE;
 AT 3:59 SET 6; [CARLE 1 AND 2]
 AT 4:00 UNTIL 19:20 START DVM;
 AT 5:00 INJECT NO 13 TO 400 PPBC IN BOTH PURGE;
 AT 5:10 INJECT UNCMIX 10 TO 4 PPMC IN BOTH PURGE;
                                            ^
    [ 1]         WARNING- INJECTION TOO LONG, BEING SPLIT
    [ 2]         WARNING- INJECTION TOO LONG, BEING SPLIT

 AT 5:30 INJECT NO2 12 TO 100 PPBC IN BOTH PURGE;
 AT 19:20 VENT; HALT;
 RSTART 0:00 VENT; CLR CHARTS;
 RSTART 3:30 SET CHARTS; CLOSE;
 RSTART 3:30 MOD 1 OSC 35 ON 45 SEC EVERY 15 MIN;
 RSTART 4:00 START DVM;
 !
```

Figure 6. Sample Command File

BEGIN LAST LINE OF TEXT
BOTTOM OF IMAGE AREA OUTSIDE DIMENSION FOR TABLES AND ILLUSTRATIONS
3/8"
PAGE NUMBER
EPA-287 (Cin.)
(4-76)

acquiring the data. Shown in Figure 5 is the configuration of the control and data acquisition system, which was described earlier. The PDP 11/03, the IBM 370/360 and the Broomall plotter are on campus grounds, and complete the data treatment procedure.

During Run. DATCOL and DATRAN are written in assembly language and PASCAL. DATCOL performs several functions, such as accepting instructions from the keyboard and interpreting a command file (optional) which prepares the chamber, makes injections, turns on the necessary instruments, and finally purges the chamber and turns off the instrumentation at the end of the experiment. Command files can be written in an English text (easily readable) style. An example is shown in Figure 6. A program DATRAN translates this file into a file which DATCOL can interpret (Figure 7). DATCOL also controls the data acquisition process, and records:

1) the instrument analog outputs;
2) the GC files produced by the Perkin Elmer Sigma 10 GC integrator and processor;
3) the adjustment file (computer readable instructions for data adjustment); and
4) the comments files, all on the RK05 hard disk.

It also maintains status information to restart and continue an experiment after a power failure.

The operator has a choice with DATCOL, of either 1) having the data printed during the whole experiment; 2) printing data for only select times during the experiment; 3) having earlier data printed; or 4) not printing data at all.

The operator can also, at any time during the experiment, enter through the keyboard information such as calibration corrections for any instrument or that an instrument is not functional and for what time interval this information applies. This type of information is entered by DATCOL into an Adjustment file. This file can be read and interpreted by other computers and can be directly applied to correcting and processing data later. The operator can at any time also enter general comments through the keyboard which DATCOL stores in a comment file. Such information when transferred along with the digital data greatly aids in processing.

Strip charts are operated for almost every instrument as a back-up to the computer.

BEGIN FIRST LINE OF TEXT HERE
TYPING GUIDE SHEET
CENTER OF PAGE
TOP OF IMAGE AREA
DROPPED HEAD, BEGIN SECTIONS HERE

Reproduced from best available copy.

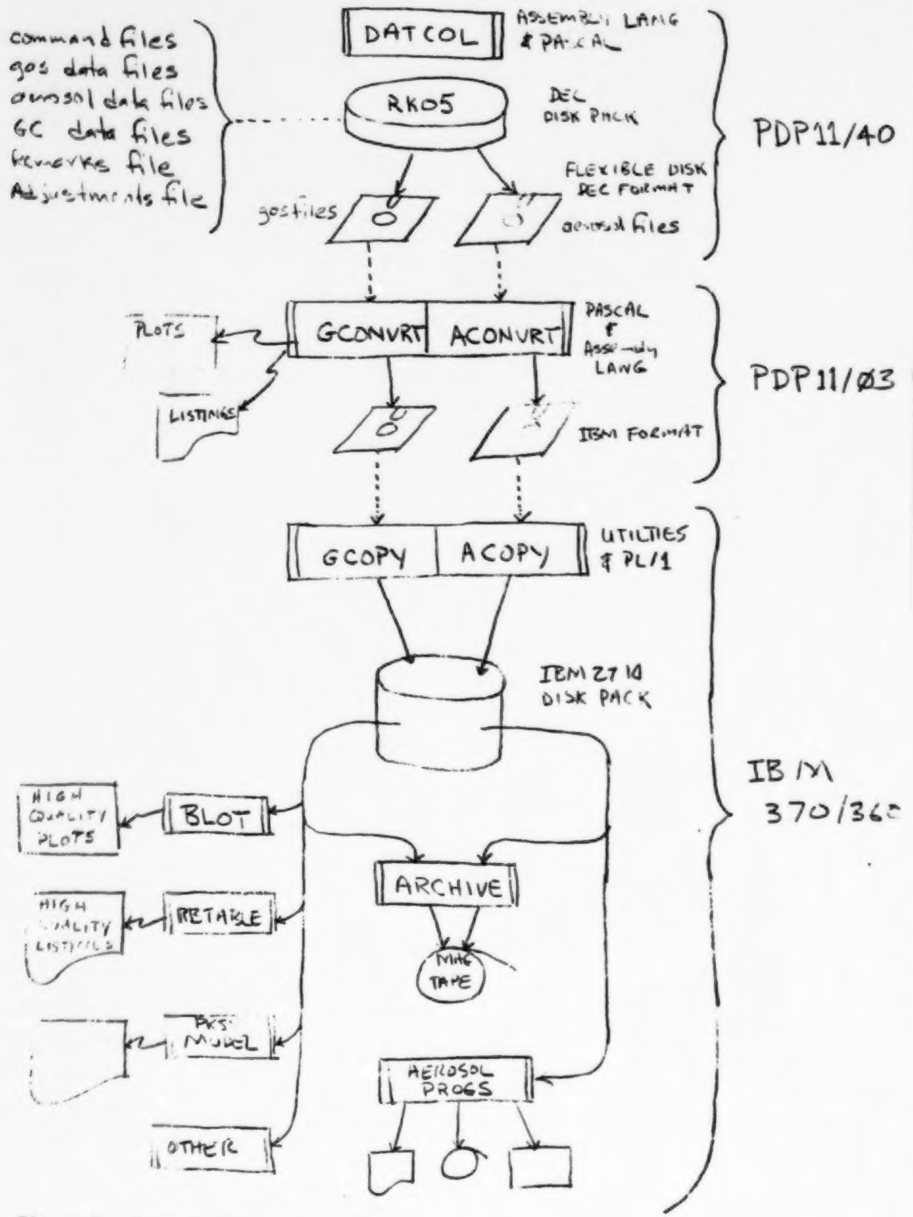
DATCOL
ASSEMBLY LANG & PASCAL
command files
gas data files
aerosol data files
GC data files
remarks file
Adjustments file
RK05
DEC DISK PACK
PDP11/40
FLEXIBLE DISK DEC FORMAT
gasfiles
aerosol files
PLOTS
GCONVRT
ACONVRT
PASCAL & Assembly LANG
PDP11/03
LISTINGS
IBM FORMAT
GCOPY
ACOPY
UTILITIES & PL/1
IBM 2710 DISK PACK
IBM 370/365
HIGH QUALITY PLOTS
BLOT
HIGH QUALITY LISTINGS
RETABLE
ARCHIVE
MAG TAPE
PBS MODEL
AEROSOL PROGS
OTHER

Figure 8. Data Treatment Process

BOTTOM OF IMAGE AREA OUTSIDE DIMENSION FOR TABLES AND ILLUSTRATIONS
BEGIN LAST LINE OF TEXT
3/8"

PAGE NUMBER
EPA-287 (Cin.)
(4-76)

Reproduced from best available copy.

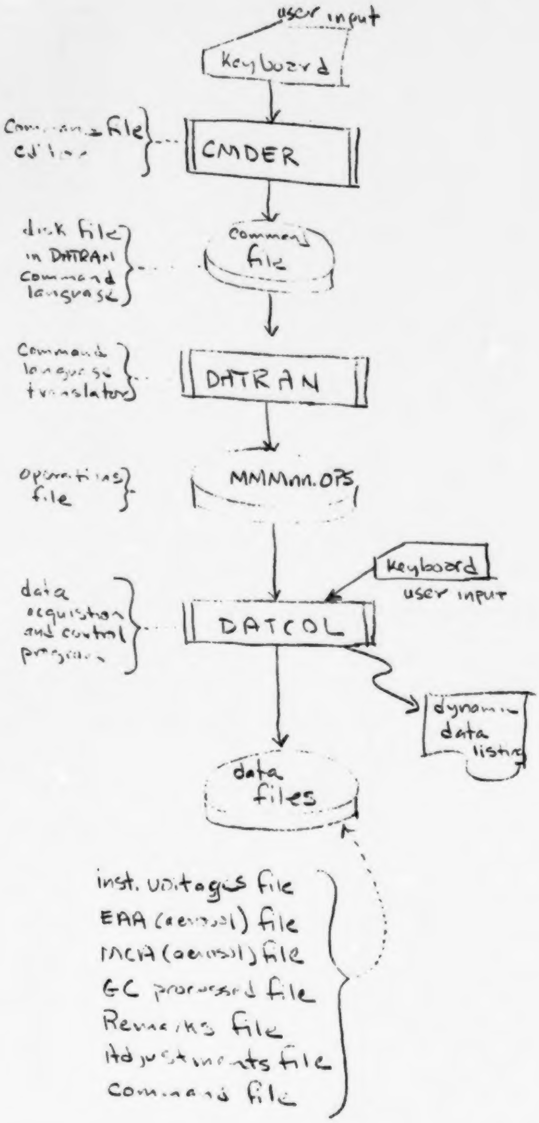
user input
Keyboard
Command file editor
CMDER
disk file in DATRAN command language
command file
Command language translator
DATRAN
Operations file
MMMnn.OPS
Keyboard
user input
data acquisition and control program
DATCOL
dynamic data listing
data files
inst. voltages file
EAA (aerosol) file
MCA (aerosol) file
GC processed file
Remarks file
Adjustments file
Command file

Figure 7. Data Acquisition Process

EPA Form 2350-4 (4-80)
(PREVIOUSLY EPA FORM 287)
TYPING GUIDE SHEET

After run. After a run, the contents of the hard disk are transferred to two floppy disks with RK2DX (a program) (Figure 8). In this way data is then transferred to the university computers quickly.

The data is converted to IBM EBCDIC character set on a PDP 11/03 using GCONVRT. GCONVRT can also be used to generate plots and listings of the data. The general comments file is examined. The Adjustment file can be used at this point to eliminate or correct appropriate data before the conversion to IBM form. These translated floppies can then be read by the IBM 370/360, whereby data is transferred to an IBM 2714 disk pack, using GCOPY.

Once the corrected and verified data is on the IBM disk pack, various programs can be run to present and utilize the data in several ways. The data is archived on magnetic tape. The data can be fed directly to a plotting program (BPLOT) which generates high quality plots on the Broomall plotter. RBTABLE takes the data off the disk pack and generates high quality listings. Finally the data can be compared with the simulation of the experiment generated by the PKSS (Photochemical Kinetics Simulation System).

TYPING GUIDE SHEET
BEGIN FIRST LINE OF TEXT HERE
CENTER OF PAGE
TOP OF IMAGE AREA
DROPPED HEAD: BEGIN SECTIONS HERE

# APPENDIX B

## COMPUTER SIMULATION OF CHEMICAL MECHANISMS

The development of a suitable photochemical smog mechanism relies heavily on chemical kinetics data. New data are constantly being obtained. Often much discussion concerns the rates of a few key reactions involved in a recycling process critical in the mechanism, with opinions commonly differing by factors of percent to orders of magnitude on the values of these constants. New kinetics data has affected nearly every aspect of the atmospheric nitrogen chemistry. Several aspects of the mechanism though are fairly well established. The general mechanism used in simulation of the previously presented experiments follows. All rate constants have units of $min^{-1}$ or $ppm^{-1}min^{-1}$.

Inorganic reactions

The most important reactions involving NO and $NO_2$ are:

| | |
|---|---|
| $NO_2 \xrightarrow{hv} NO + O$ | $\Phi K_a$ |
| $O + O_2 + M \rightarrow O_3 + M$ | $8.1 \times 10^5 exp(5-1x10^2/T)$ |
| $O_3 + NO \rightarrow NO_2 + O_2$ | $3.1 \times 10^3 exp(-1.45x10^3\ T)$ |
| $NO_2 + O \rightarrow NO$ | $1.38 \times 10^4$ |

Ozone and $NO_2$ react to start a sequence involving other nitrogen oxides:

| | |
|---|---|
| $O_3 + NO_2 \rightarrow NO_3$ | $1.77 \times 10^2 exp(-2.45x10^3/T)$ |
| $NO_3 + NO \rightarrow 2\ NO_2$ | $2.8 \times 10^4$ |
| $NO_3 + NO_2 \rightarrow N_2O_5$ | $2.19 \times 10^2 exp(8.61x10^2/T)$ |
| $NO_3 \xrightarrow{hv} NO_2 + O$ | $1.25 \times \Phi Ka$ |
| $N_2O_5 \rightarrow NO_3 + NO_2$ | $7.4 \times 10^{15} exp(-1.0x10^4/T)$ |
| $N_2O_5 \xrightarrow{H_2O} 2HNO_3$ | $1.5 \times 10^{-5} x[H_2O]$ |

BOTTOM OF IMAGE AREA OUTSIDE DIMENSION FOR TABLES AND ILLUSTRATIONS
BEGIN LAST LINE OF TEXT

EPA-287 (Cin.)
(4-76)

BEGIN FIRST LINE OF TEXT HERE
TYPING GUIDE SHEET
CENTER OF PAGE
TOP OF IMAGE AREA
DROPPED HEAD: BEGIN SECTIONS HERE

And further:

| | |
|---|---|
| $2\ CH_3CH_2CH(OH)O_2 \rightarrow 2\ CH_3CHO + 2\ HCHO + 2\ HO_2$ | 500 |
| $2\ CH_3CH(OH)O_2 \rightarrow 4\ HCHO + 2\ HO_2$ | 500 |

The hydroxyperoxy radical also oxidizes NO to $NO_2$ and forms aldehydes and $HO_2$:

| | |
|---|---|
| $CH_3CH_2CH(OH)O_2 + NO \rightarrow NO_2 + CH_3CHO + HCHO + HO_2$ | 12,000 |
| $CH_3CH(OH)O_2 + NO \rightarrow NO_2 + 2\ HCHO + HO_2$ | 12,000 |

The radical also reacts with $NO_2$ to form an $RO_2NO_2$ type compound which decomposes back to $NO_2$ and the radical:

| | |
|---|---|
| $CH_3CH_2CH(OH)O_2 + NO_2 \rightarrow CH_3CH_2CH(OH)O_2NO_2$ | 1750 |
| $CH_3CH(OH)O_2 + NO_2 \rightarrow CH_3CH(OH)O_2NO_2$ | 1750 |
| $CH_3CH_2CH(OH)O_2NO_2 \rightarrow CH_3CH_2CH(OH)O_2 + NO_2$ | $3 \times 10^{17} \times \exp(-1.17 \times 10^4/T)$ |
| $CH_3CH(OH)O_2NO_2 \rightarrow CH_3CH(OH)O_2 + NO_2$ | $3 \times 10^{17} \times \exp(-1.17 \times 10^4/T)$ |

The ozone reaction with the alkenes involves several "hot" intermediates including dioxirane. The details have been previously discussed in the isoprene-$O_3$ portion of section 6 and will not be discussed here. The following stoichiometry is as used in the mechanism for computer simulation:

| | |
|---|---|
| $O_3 + C_3H_6 \rightarrow CH_3CHO + 0.2\ HO_2 + 0.70\ CO$ | $4.5 \times \exp(-1.9 \times 10^3/T)$ |
| $O_3 + C_3H_6 \rightarrow HCHO + 0.2\ CH_3\dot{C}HOO\cdot + 0.8\ [\text{acetic acid}]^*$ | $4.5 \times \exp(-1.9 \times 10^3/T)$ |
| $[\text{acetic acid}]^* \rightarrow 0.68\ OH + 0.17\ HCHO$ | $3 \times 10^3$ |
| $[\text{acetic acid}]^* \rightarrow 1.53\ COO + 1.19\ HO_2 + 0.85\ CO$ | $3 \times 10^3$ |
| $O_3 + C_2H_4 \rightarrow HCHO + 0.2\ HO_2 + 0.70\ CO$ | $1.33 \times 10^4 \times \exp(-2.6 \times 10^3/T)$ |

BOTTOM OF IMAGE AREA; OUTSIDE DIMENSION FOR TABLES AND ILLUSTRATIONS
BEGIN LAST LINE OF TEXT
3/8"

EPA-287 (Cin.)
(4-76)

BEGIN FIRST LINE OF TEXT HERE
TYPING GUIDE SHEET
CENTER OF PAGE
TOP OF IMAGE AREA
DROPPED HEAD; BEGIN SECTIONS HERE

Ozone itself photolyzes, forming OH and $HO_2$:

| | |
|---|---|
| $O_3 \xrightarrow{hv} 0.11\ O1D + 0.89\ O$ | $4.0 \times 10^{-2} \times \Phi Ka$ |
| $O1D \rightarrow O$ | 430 |
| $O1D \xrightarrow{H_2O} 2\ OH$ | $3.4 \times 10^{-3} \times [H_2O]$ |
| $O_3 + OH \rightarrow HO_2$ | $2.4 \times 10^3$ exp*$-1.0 \times 10^3/T)$ |
| $O_3 + HO_2 \rightarrow OH$ | $1.5 \times 10^2 \exp(-1.25 \times 10^3/T)$ |

OH and $HO_2$ form several important inorganic compounds.

| | |
|---|---|
| $OH + NO \rightarrow HNO_2$ | $3.9 \times 10^2 \exp(1.1 \times 10^3/T)$ |
| $HNO_2 \xrightarrow{hv} NO + OH$ | $0.38 \times \Phi Ka$ |
| $OH + NO_2 \rightarrow HNO_3$ | $1.4 \times 10^4$ |
| $OH + HNO_3 \rightarrow NO_3$ | $8.9 \times 10^2 \exp(-4 \times 10^2/T)$ |
| $HO_2 + NO \rightarrow NO_2 + OH$ | $1.2 \times 10^4$ |
| $HO_2 + NO_2 \rightarrow HO_2NO_2$ | $7.0 \times 10^3$ or $0.96 \times ([H_2O]-4{,}000$ ppm) |
| $HO_2NO_2 \rightarrow HO_2 + NO_2$ | $3.0 \times 10^{17} \exp(-1.17 \times 10^4/T)$ |
| $HO_2 + NO_3 \rightarrow HNO_3$ | $2.5 \times 10^3$ |
| $HO_2 + HO_2 \rightarrow H_2O_2$ | $4.9 \times 10^4 \exp(-5.4 \times 10^2/T)$ |
| $H_2O_2 \xrightarrow{hv} OH$ | $3.5 \times 10^{-3} \times \Phi Ka$ |
| $OH + CO \rightarrow HO_2$ | $4.4 \times 10^2$ |

## Organic reactions

The principle organics modeled in this project were propylene ($C_3H_6$), ethylene ($C_2H_4$), acetaldehyde ($CH_3CHO$), and formaldehyde (HCHO).

Ethylene and propylene are attacked principally by OH and $O_3$. OH yields the hydroxyperoxy radical:

| | |
|---|---|
| $OH + C_3H_6 \rightarrow CH_3CH_2CH(OH)O_2$ | $6.06 \times 10^3 \exp(5.4 \times 10^2/T)$ |
| $OH + C_2H_4 \rightarrow CH_3CH(OH)O_2$ | $3.25 \times 10^3 \exp(3.85 \times 10^2/T)$ |

BEGIN LAST LINE OF TEXT
BOTTOM OF IMAGE AREA, OUTSIDE DIMENSION FOR TABLES AND ILLUSTRATIONS

PAGE NUMBER
EPA-287 (Cin.)
(4-76)

TYPING GUIDE SHEET

Both aldehydes photolyze:

| | |
|---|---|
| $HCHO \rightarrow CO + 0.58\ HO_2$ | $0.01 \times Ka$ |
| $CH_3CHO \xrightarrow{h\nu} CO + HO_2 + CH_3OO$ | $1.0\times10^{13}\exp(-1.073\times10^4/T) \times Ka$ |

OH also reacts with the aldehydes:

| | |
|---|---|
| $OH + HCHO \rightarrow HO_2 + CO$ | 14,000 |
| $OH + CH_3CHO \rightarrow CH_3COO_2$ | 24,000 |

The peroxyacetyl radical oxidizes NO to $NO_2$ and forms the methyl peroxy radical, and reacts with $NO_2$ to form peroxyacetyl nitrate (PAN) which is thermally unstable:

| | |
|---|---|
| $CH_3COO_2 + NO \rightarrow NO_2 + CH_3O_2$ | 4,900 |
| $CH_3COO_2 + NO_2 \rightarrow CH_3OO_2NO_2$ | 1,545 |
| $CH_3OO_2NO_2 \rightarrow CH_3COO_2 + NO_2$ | $1.2 \times 10^{18} \times \exp(-1.35\times10^4/T)$ |

The methyl peroxy radical also oxidizes NO and forms a $RO_2NO_2$ type compound.

| | |
|---|---|
| $CH_3OO + NO \rightarrow NO_2 + HCHO + HO_2$ | 9,600 |
| $CH_3OO + NO \rightarrow HCHO + HNO_2$ | 24,000 |
| $CH_3OO + NO_2 \rightarrow CH_3OONO_2$ | 1,750 |
| $CH_3OONO_2 \rightarrow CH_3OO + NO_2$ | $3 \times 10^{17} \times \exp(-1.17\times10^4/T)$ |

The Criegee biradical formed from $O_3$ attack on propylene also reacts with NO and $NO_2$:

| | |
|---|---|
| $CH_3\dot{C}HOO\cdot + NO \rightarrow NO_2 + CH_3CHO$ | 2,000 |
| $CH_3\dot{C}HOO\cdot + NO_2 \rightarrow NO_3 + CH_3CHO$ | 700 |

EPA-287 (Cin.)
(4-76)

# Appendix C

## Water Effect Experiments

The results of October 21, 1978 (Figure C) have already been presented. This experiment was used to develop the water dependent PNA mechanism. Note from Table C that the dried side (always Blue in these experiments) produced an $O_3$ maximum 11% higher than the wet side as well as a higher $NO_2$ maximum. The dried side was also 9 minutes faster to crossover, 17 minutes fster to $NO_2$ maximum and 12 minutes faster to $O_3$ maximum. Dew point and temperature at time of $O_3$ maximum are listed in Table C.

June 29, 1979 was a high [propylene]/[$NO_x$] experiment with initial conditions similar to October 21, 1978. The major difference is the warmer weather and "summer light". Although, the dew points for each side were relatively higher than in the October run significant drying was achieved. The temperatures on this day were also higher and therefore the PNA decomposition rate on each side was very high. As stated before, these circumstances tended to minimize the effect of PNA formation in this experiment. Consequently, this experiment was perfectly matched.

October 26, 1979 was a modification of the regular type of "dry-down" experiment. Using a fine misting device, about 400 ml of distilled water was sprayed on the walls inside the chamber in the Red side before injections were made. The water did not run down the sides of the chamber. The addition of water was made to increase the difference in dew point and to further test the PNA theory. The temperature on this day was also somewhat cooler than the October 21, 1978 experiment and initial propylene was higher, 4.8 ppmC. The dried side produced a 41% higher $O_3$ maximum concentration than the misted side. The dried side $O_3$ maximum on October 26 was also 10.3% higher than that of October 21, 1978. The dried side was faster in converting NO to $NO_2$ and as expected had a higher $NO_2$ maximum. This experiment seems to agree with the general theory. Looking at the misted side however, one sees that the $O_3$ maximum was lower than expected. This might have been caused by heterogeneous processes on the misted surface, such as HCHO wall absorption. Since the walls remained wet during this entire run, formaldehyde was never revaporized and hence a significant radical source was lost during this entire run.

October 29, 1979 was a regular dry down experiment with ethylene. The dry side produced a 24% higher $O_3$ maximum, a slightly higher $NO_2$ maximum; and was faster to reach crossover (11 minutes), $NO_2$ maximum (21 minutes) and $O_3$ maximum (24 minutes).

October 31, 1979 was generally a repeat of October 29, 1979, although the drying was much better. The dry side of this run produced a 7.3% higher $O_3$ maximum and a higher $O_2$ maximum. The Blue side however was slower. We have no clear explanation for these results.

November 8, 1979, a matched ethylene experiment, had one side misted while the other side received extensive drying. Unfortunately the wet side lacks $O_3$ data until late in the afternoon. The dry side produced twice the $O_3$ but since it was such a cloudy day the misted side became severely light limited. A higher $NO_2$ maximum was also observed on the dry side of this run. Time to $NO_2$ maximum was the same on the two sides, but time to crossover was later on the dry side by 21 minutes.

October 16, 1979 was a regular "dry-down" experient with propylene. The weather conditions were fair and dry, so that although drying had taken place on one side, the other side was not very humid. The dry side had a slightly higher $O_3$ maximum and both sides had the same $NO_2$ maximum and time to $O_3$ maximum. The minimum difference observed is thought to be caused by the low moisture concentration of the undried side. Although the differences in the water concentrations on each side were great (high kwet/kdry), the absolute value of kwet was low because the air was very dry and therefore relatively little PNA was formed.

## Table C. Critical Data for Humid VS. Dry Runs

| Date | Run Type | $[NO_2]_o$ |  | $[NO_x]_o$ |  | $[HC]_o$ ppmC |  | $[D.P.]_F$ |  | $[T°]_i$ | $[T°]_f$ | Time Cross |  | $[NO_2]$ Max |  | Time $NO_2$ Max |  | $[O_3]$ max |  | Time $O_3$ max |  | Sun |
|---|---|---|---|---|---|---|---|---|---|---|---|---|---|---|---|---|---|---|---|---|---|---|
|  |  | Blue | Red | Blue | Red | Blue | Red | Blue | Red |  |  | Blue | Red | Blue | Red | Blue | Red | Blue | Red | Blue | Red |  |
| 10/21/78 | Match propylene<br>Blue dried | 0.110 | 0.111 | 0.503 | 0.505 | 3.45 | 3.48 | 43 | 58 | 34.7 | 72.4 | 9:41 | 9:50 | 0.484 | 0.461 | 10:48 | 11:05 | +11%<br>0.745 | 0.670 | 12:30 | 12:42 | 90% |
| 6/29/79 | Match propylene<br>Blue dried | 0.085 | 0.094 | 0.458 | 0.464 | 3.504 | 3.553 | 57 | 69 | 58 | 79.2 | 8:32 | 8:31 | 0.396 | 0.387 | 9:26 | 9:24 | 0.891 | 0.893 | 13:35 | 12:32 | 23% |
| 10/16/79 | Match propylene<br>Blue dried | 0.085 | 0.083 | 0.371 | 0.371 | 3.126 | 3.172 | 32 | 48 | 40.8 | 74.5 | 9:55 | 9:46 | 0.341 | 0.342 | 10:58 | 10:52 | +1.9%<br>0.822 | 0.807 | 13:01 | 12:47 | 80% |
| 10/26/79 | Match propylene<br>Blue dried<br>Red misted | 0.091 | 0.092 | 0.494 | 0.496 | 4.765 | 4.839 | 28 | 56 | 35 | 61 | 9:54 | 10:00 | 0.472 | 0.452 | 10:43 | 10:59 | +41%<br>0.822 | 0.582 | 12:14 | 12:24 | 100% |
| 10/29/79 | Match ethylene<br>Blue dried | 0.087 | 0.086 | 0.476 | 0.474 | 3.189 | 3.212 | 58.5 | 68.4 | 44 | 75 | 10:47 | 10:58 | 0.411 | 0.403 | 12:06 | 12:27 | +24%<br>0.760 | 0.613 | 14:25 | 14:59 | 55% |
| 10/31/79 | Match ethylene<br>Blue dried | 0.097 | 0.098 | 0.497 | 0.498 | 3.706 | 3.743 | 28 | 62.5 | 50 | 72 | 11:08 | 10:49 | 0.43 | 0.416 | 12:26 | 12:19 | +7.3%<br>0.887 | 0.827 | 3:30 | 3:02 | Clear |
| 11/8/79 | Match ethylene<br>Blue dried<br>Red misted | 0.096 | 0.097 | 0.492 | 0.494 | 3.818 | 3.79 | 27.4 | 47.6 | 31.2 | 60.3 | 12:03 | 11:42 | 0.387 | 0.356 | 14:34 | 14:34 | +>100%<br>0.31 | 0.15 | 16:23 |  | Cloudy |

a. All dewpoints and temperatures are in °F.

b. $[D.P.]_F$ is dew point at $O_3$ maximum.

c. $[T°]_i$ and $[T°]_f$ are temperatures at time of sunrise and $O_3$ maximum

d. "Misted" means ~400 ml of distilled water added to inside of vertical walls of undried side.

e. 11/8/79 run - $O_3$ data missing until end of run on Red side. $O_3$ max concentration is estimated.

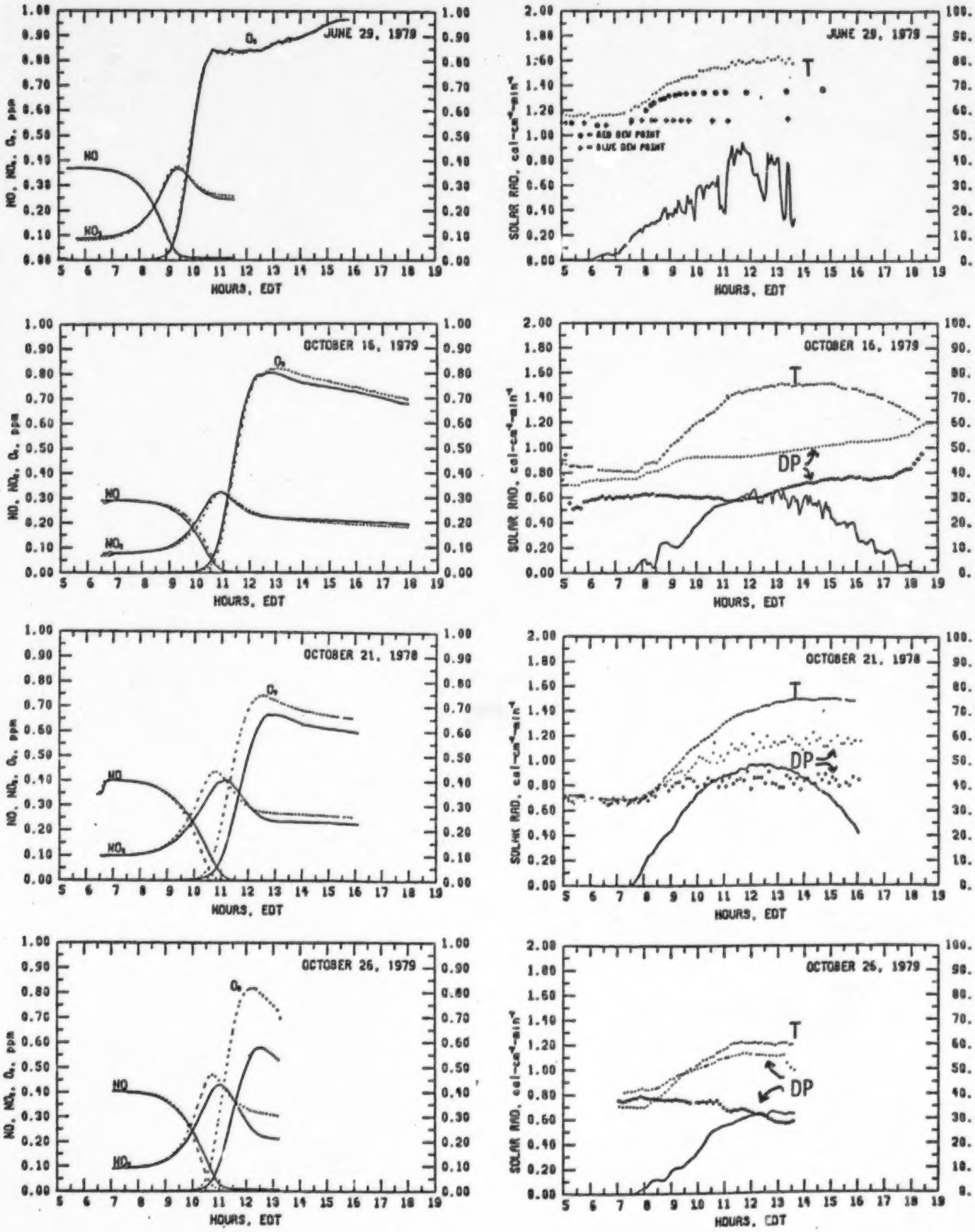

Figure C1. UNC smog chamber water effect experiments.

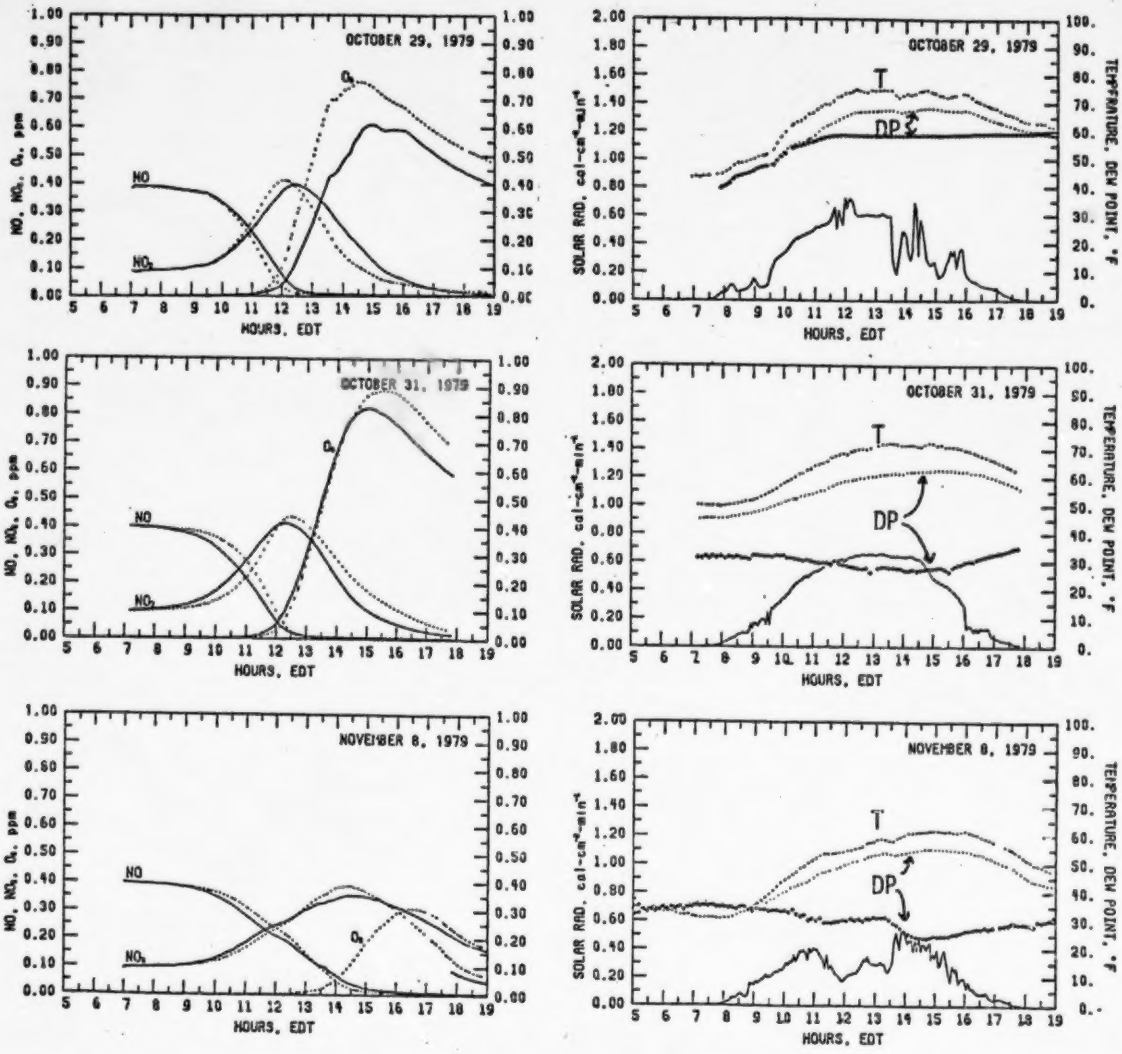

Figure C2. UNC smog chamber water effect experiments.

# Appendix D

## Reproducibility of 2 UNC Chambers

During the course of a run season 3 or 4 matched runs are conducted in both chambers. This involves the slug injection of the same concentration of a given hydrocarbon or hydrocarbon mixture and the same NO and $NO_2$. Figures D1 - D3 show some of these systems from the past 6 years; almost no chemical difference can be discerned between the two chamber sides.

In 1977 and 1978, a set of runs with similar initial conditions were repeated to observe differences in behavior that might occur from seasonal changes. Several 1.5 ppmC propylene/0.5 ppm $NO_x$ and 1.5 ppmC ethylene/0.5 ppm $NO_x$ runs are shown in Figures D4 and D5. Inspection of Figure D4 shows these experiments to cover 3 summer months and two consecutive years. In general, there is reasonable agreement between these runs. The August 8, 1977 propylene run is about 1 hour slower than the other propylene runs, although magnitudes of concentrations are similar. Our own modeling indicates that using ~3 ppb initial HONO for August 8 and ~5 ppb initial HONO for August 9, 1977 produces good fits for both days with a propylene model.

Figure D6 contains two high concentration propylene/$NO_x$ runs (~3.6 ppmC + 0.5 ppm). Both were conducted on October 21 and 22 in the same chamber side almost one year apart. It is rather remarkable, however, that both runs experienced the same dew point, temperature and solar radiation profiles; it is not surprising that these experiments would agree. The agreement however, is so close that when the pollutant profiles were overlapped they were almost indistinguishable.

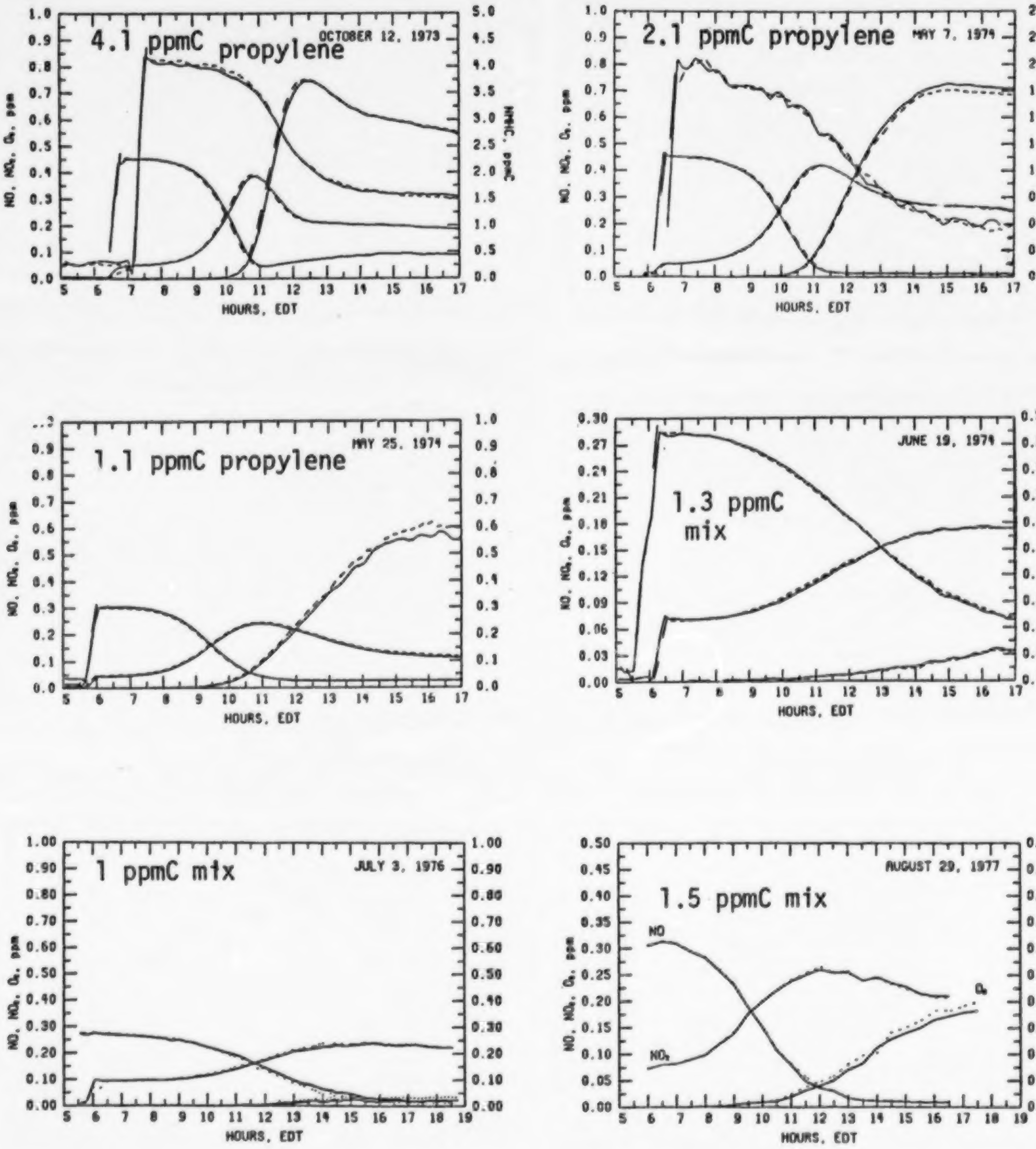

Figure D1. Similar Chemical Conditions in Both Halves of UNC Chamber 1973-77, — Red Side, ··· Blue Side

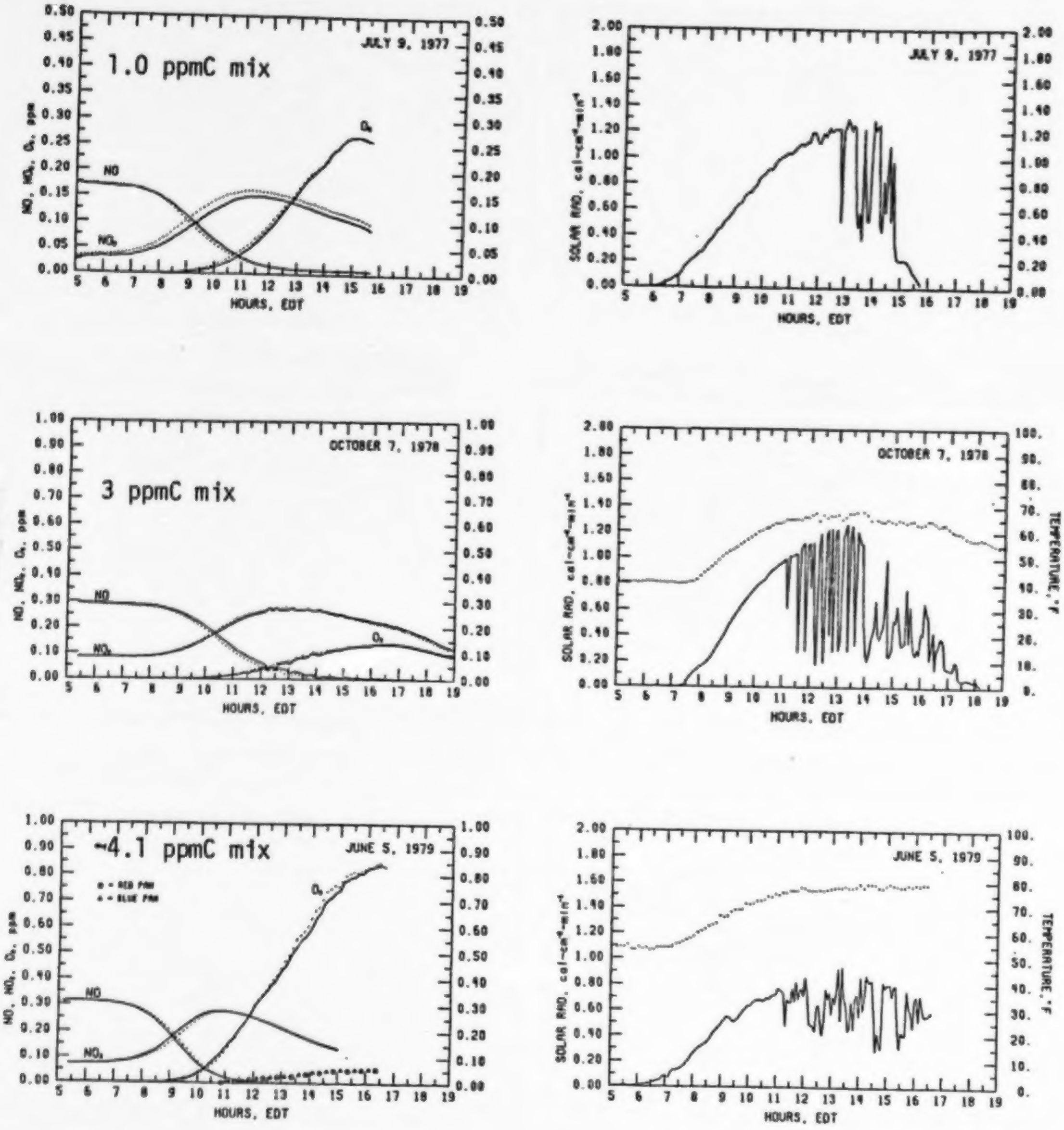

Figure D2. Similar Chemical Conditions in Both Sides of UNC Chamber 1977-79.

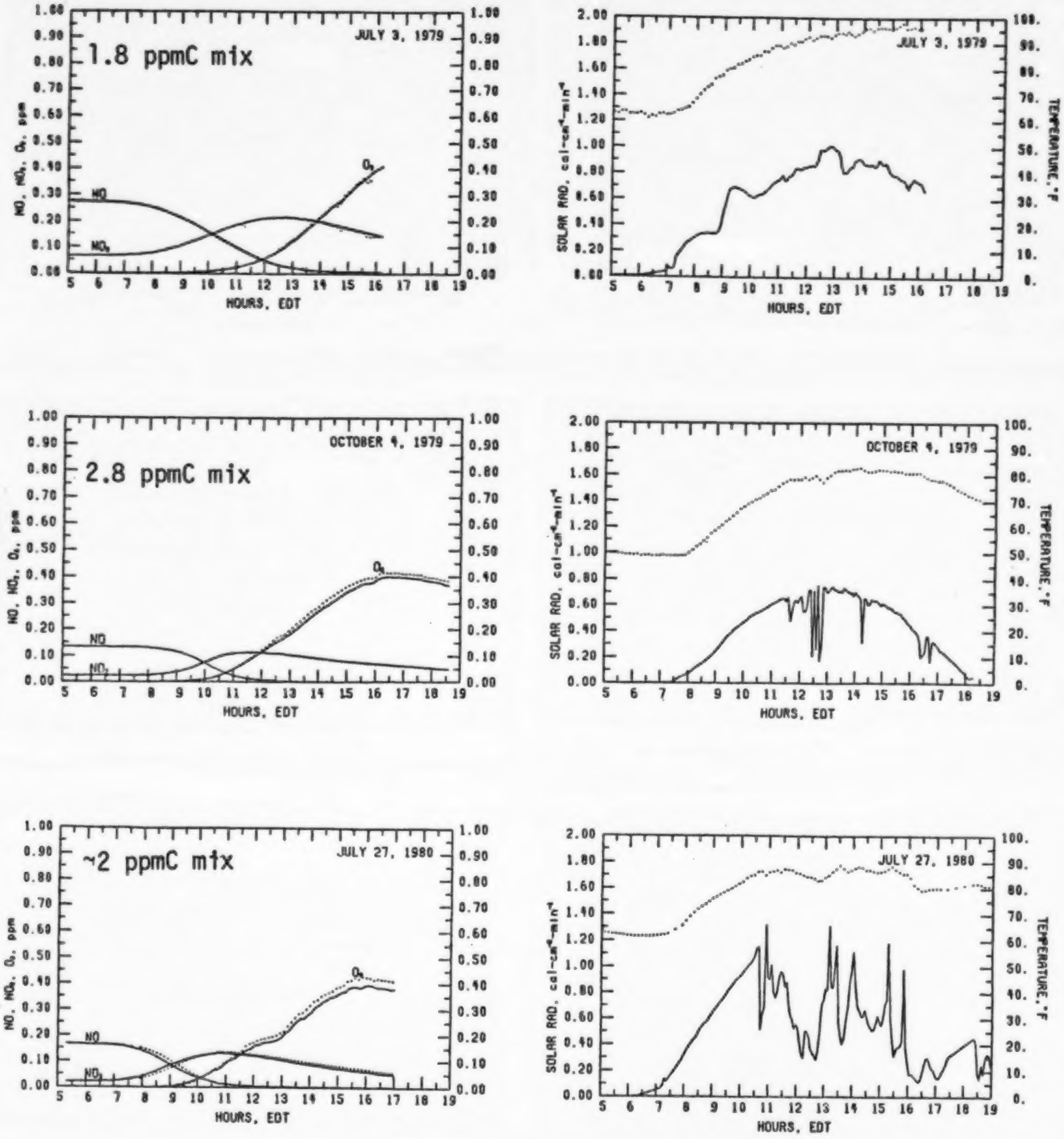

Figure D3. Similar Chemical Conditions in Both Halves of UNC Chamber 1979-80.

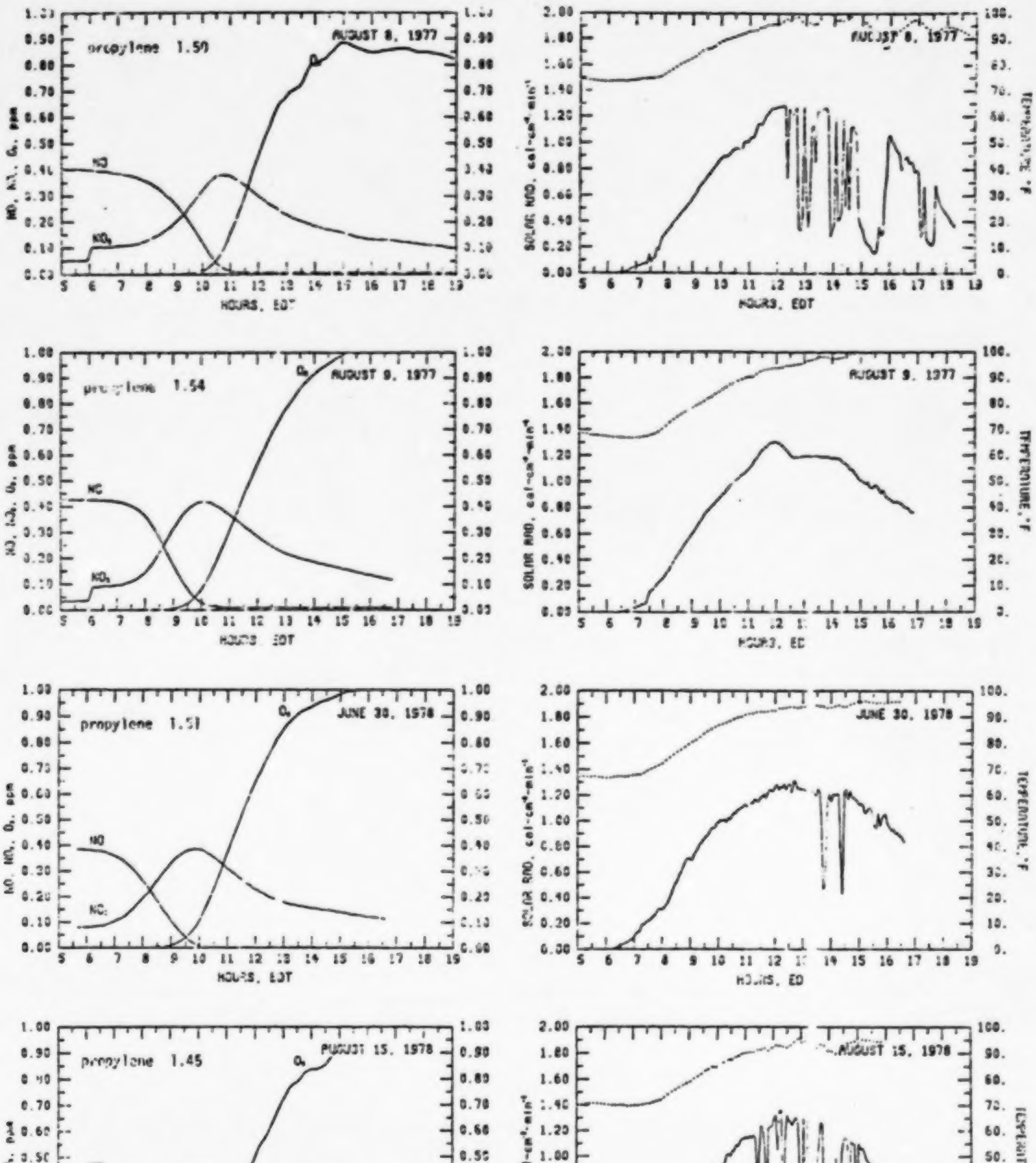

Reproduced from best available copy.

Figure D4. 1.5 ppmC propylene and 0.5 ppm $NO_x$ runs in UNC chamber.

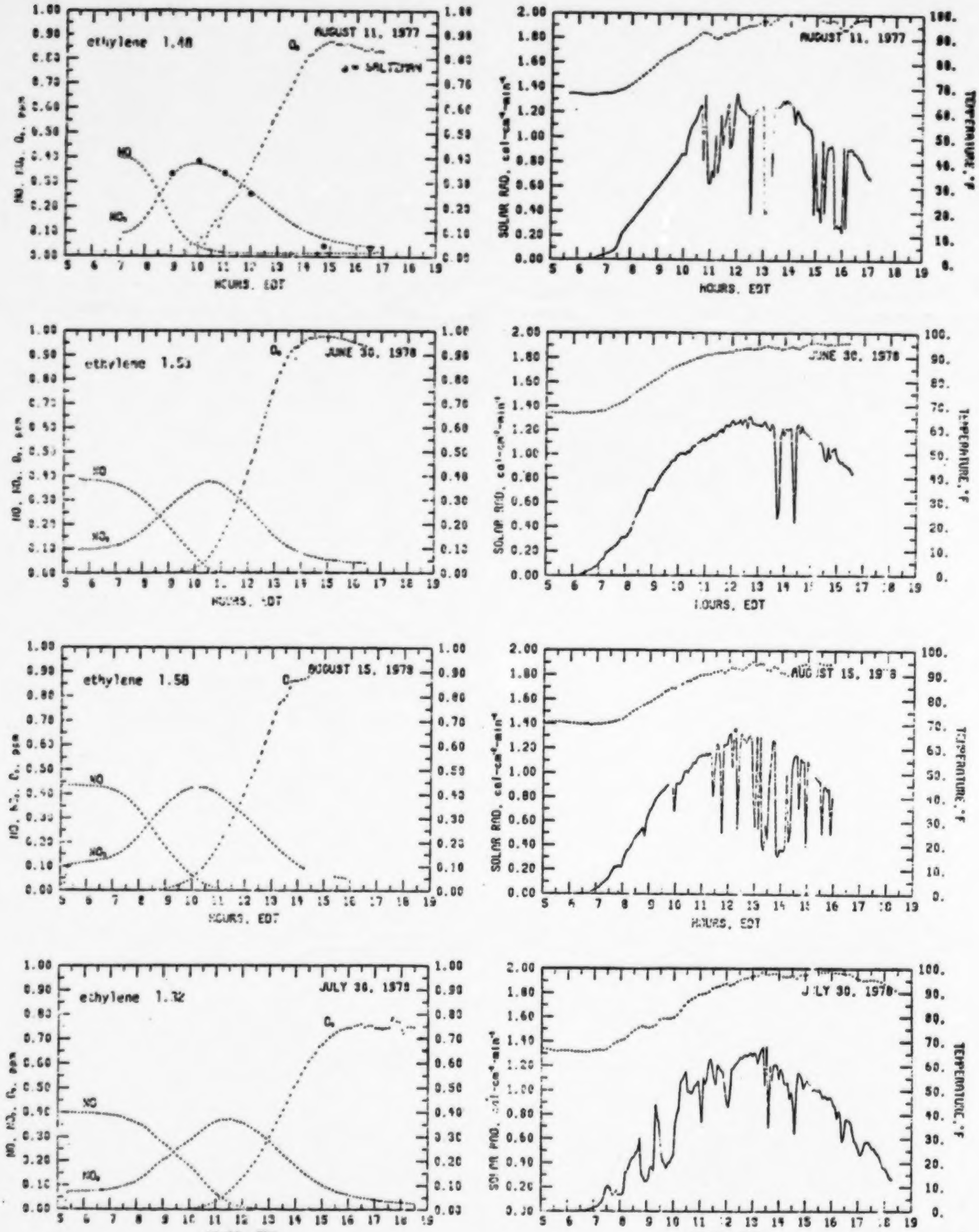

Reproduced from best available copy.

Figure D5.1.5 ppmC Ethylene and 0.5 ppm $NO_x$ runs in UNC chamber.

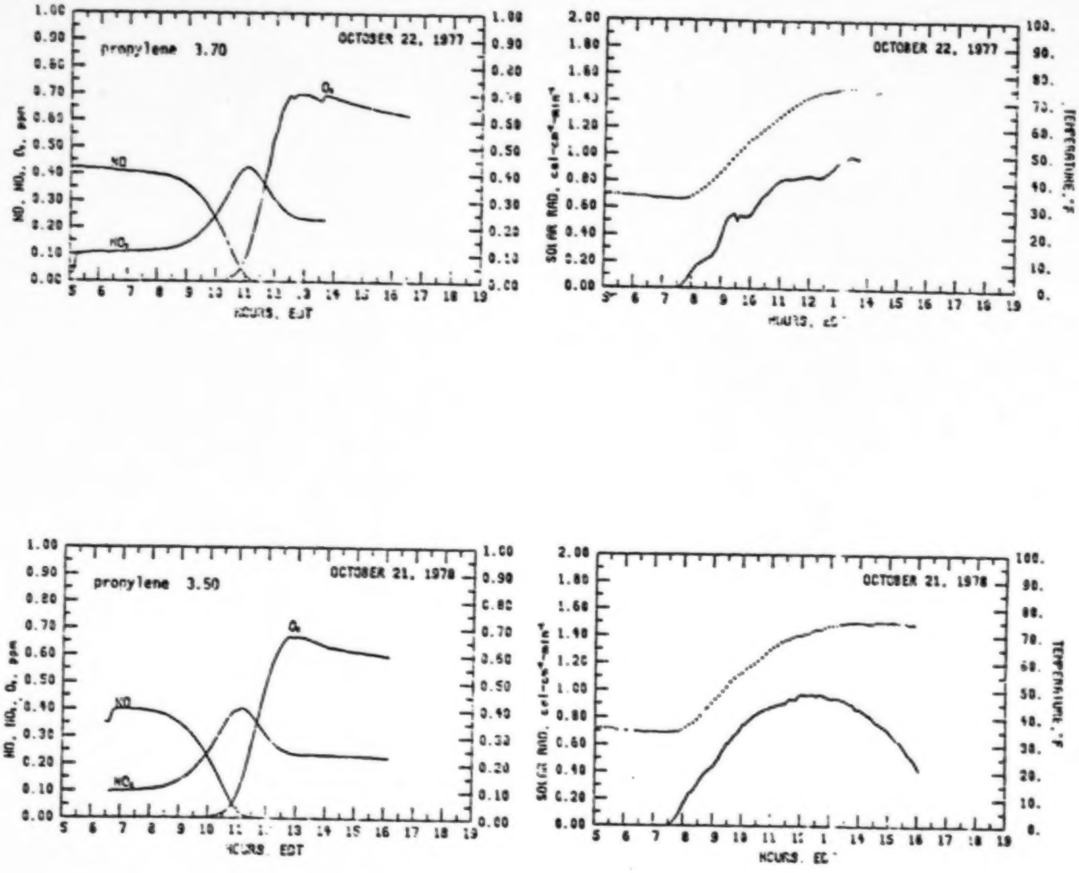

Figure D6. Similar propylene runs (~3.6 ppmC) conducted one year apart in UNC chamber, October 22, 1978.